



University
of Glasgow

Hamilton, Hazel Jean (2019) *The Leish niche: the secretome of Leishmania and its role in parasite virulence*. PhD thesis.

<https://theses.gla.ac.uk/41158/>

Copyright and moral rights for this work are retained by the author

A copy can be downloaded for personal non-commercial research or study, without prior permission or charge

This work cannot be reproduced or quoted extensively from without first obtaining permission in writing from the author

The content must not be changed in any way or sold commercially in any format or medium without the formal permission of the author

When referring to this work, full bibliographic details including the author, title, awarding institution and date of the thesis must be given

Enlighten: Theses

<https://theses.gla.ac.uk/>
research-enlighten@glasgow.ac.uk



The Leish Niche: The secretome of *Leishmania* and its role in parasite virulence

Hazel Jean Hamilton

BSc (Hons), MRes

Submitted in fulfilment of the requirement for the
Degree of Doctor of Philosophy

Institute of Infection, Immunity and Inflammation

College of Medical, Veterinary and Life Sciences

University of Glasgow

April 2019

Abstract

Leishmaniasis is a neglected tropical parasitic disease that causes several debilitating manifestations. No commercially available vaccine exists against this disease, and treatment strategies are far from ideal with the emergence of resistance, coupled with toxic side effects of many of the drugs available. Rational drug design relies on knowledge of the cell biology of the parasite and the interplay between the parasite and its hosts. Production of secreted proteins, the secretome, has become a known strategy for parasite invasion and persistence in host cells, however, host-parasite interaction is still not well defined. Virulence factors secreted by the parasite mediate the host-parasite interaction and create a niche permissive for parasite proliferation. They therefore represent potential therapeutic targets and vaccine candidates.

Here, the use of secretomics was implemented to investigate these virulence factors. Parasite conditioned culture supernatant, containing the secretome, was characterised by morphological, immunochemical and proteomic analyses. Here, we optimised and extended current methods and applied them to the medically relevant amastigote stage. Method development and validation was implemented to extract a reproducible secretome *in vitro*. Induction of cell stress was managed and cell viability maintained to minimise interference of intracellular proteins.

A total of 256 proteins were reproducibly identified in the secretome of promastigotes and 36 proteins were reproducibly identified in the secretome of amastigotes. Analysis of their protein abundance index (emPAI) allowed comparison of the relative abundance of proteins and functions of the secretome throughout the parasite life cycle. Differences in the putative functions of nutrient salvage, protease production and antioxidant activity were observed. Analyses reveal that many proteins lack a signal peptide and as such are thought to be released by nonclassical secretion mechanisms. Several exosome-associated proteins and membrane proteins were also detected in the secretome, suggesting the occurrence of secretion by exosomes or microvesicles.

Extended comparative analyses between the secretome of parasites with differing phenotypes allowed us to infer functionality of the secretome in the parasite's

survival but also variations within the same species which result in differing disease outcomes. Dysregulation in the secretion of various proteins in attenuated parasites implicates these proteins in the virulence of the parasite. An increase in the secretion of pro-inflammatory mediators and destructive proteases by parasites isolated from patients with chronic cutaneous leishmaniasis compared to those from patients with self-healing lesions, indicates the role of the parasite in the chronicity of cutaneous leishmaniasis.

Here, we demonstrate an applicable method for the study of the *Leishmania mexicana* promastigote and amastigote secretome. Results suggest that the secretome plays a role in disease progression and virulence. Proteomic analyses of the secretome, like this study presented here, provide crucial information on the host:parasite interaction for the identification of therapeutic targets and potential vaccine candidates for the provision of safer treatments and new vaccines for eradication of this disease.

Table of Contents

Abstract	II
List of Tables.....	VIII
List of Figures	IX
Conference Proceedings	XI
Acknowledgements	XII
Author's Declaration	XIII
Abbreviations.....	XIV
Chapter 1 Introduction	16
1.1 Leishmaniasis	17
1.1.1 Diagnosis, treatment and vaccination.....	19
1.2 The <i>Leishmania</i> parasite	21
1.3 Mechanisms of <i>Leishmania</i> parasite survival	22
1.3.1 Promastigote survival in the sand fly vector	22
1.3.2 During transmission from vector to host.....	24
1.3.3 Entry to the phagolysosome and differentiation	25
1.3.4 Amastigote survival	28
1.4 Protein secretion	32
1.4.1 Trypanosomatid secretion	33
1.5 Proteomics	36
1.5.1 Gel-based proteomics	36
1.5.2 Gel-free proteomics	37
1.5.3 Quantitative MS-based proteomics	39
1.5.4 Secretomics	40
1.6 Summary and Aims	44
Chapter 2 Materials & Methods	45
2.1 Materials.....	46
2.2 Parasite culture	46
2.3 Alamar blue assay	47
2.4 Secreted protein isolation	47
2.5 Whole cell protein lysate collection.....	48
2.6 Protein assay.....	49
2.7 1D SDS-PAGE	49
2.8 Western blotting.....	50
2.9 2D electrophoresis	50
2.9.1 Gel casting using the Ettan DALT system	50
2.9.2 Difference gel electrophoresis (DiGE) sample preparation	51
2.9.3 Isoelectric focussing (1st dimension).....	51

2.9.4	Molecular weight separation, SDS-PAGE (2 nd dimension)	52
2.9.5	Gel imaging	52
2.10	Spot Picking and Processing	53
2.11	Trypsin digestion	53
2.12	TMT™ Labelling	54
2.13	Peptide/protein identification by nLC-ESI-MS/MS	55
2.14	Mascot	56
2.15	Following TMT labelling	57
2.16	Analyses of the <i>L. mexicana</i> secretome	57
Chapter 3	Method development for <i>Leishmania</i> secretomics	58
3.1	Introduction	59
3.1.1	Axenic cell culture in secretomic studies.....	59
3.1.2	Isolating the secretome of <i>Leishmania</i>	62
3.2	Aims and hypotheses.....	65
3.3	Results	66
3.3.1	Evaluation of media for secretome collection	66
3.3.2	Cell viability is monitored during secretome isolation	68
3.3.3	Supernatant recovery and concentration.....	69
3.3.4	Amastigote secreted proteins are degraded by proteolysis	71
3.3.5	Protein quantitation	73
3.3.6	Identification of secretome proteins by mass spectrometry.....	74
3.3.7	Validation of the secretome by comparison to lysate	84
3.4	Discussion.....	87
3.4.1	Axenic culture systems are advantageous for secretome studies.....	87
3.4.2	Secretion and isolation processes.....	88
3.4.3	Overcoming challenges of secretome extraction	89
3.4.4	Protein identification and validation.....	91
3.5	Summary.....	93
Chapter 4	Characterisation and comparison of the <i>L. mexicana</i> promastigote and amastigote secretome	95
4.1	Introduction	96
4.1.1	Secreted proteins play a key role in the virulence of parasites.....	96
4.1.2	Parasites can alter their secretome to adapt to different environments and stresses	97
4.1.3	Secreted proteins are major drug targets and vaccine candidates ...	98
4.2	Aims and Hypotheses	101
4.3	Results	102
4.3.1	Promastigote and amastigote secretomes display visually distinct electrophoretic profiles	102

4.3.2	Amastigote secretome has different physical properties compared to the promastigote secretome.....	104
4.3.3	Mass spectrometry of culture supernatant reveals the <i>L. mexicana</i> secretome	106
4.3.4	Comparative analyses of the predicted properties of <i>Leishmania</i> secreted proteins.....	118
4.3.5	Validation and experimentation using Western Blot	121
4.4	Discussion.....	123
4.4.1	The <i>Leishmania</i> secretome	123
4.4.2	Comparison of promastigote and amastigote secretome	126
4.4.3	Predicted functions and categories of secreted proteins	129
4.5	Summary.....	136
Chapter 5	Application of secretomics to <i>Leishmania</i> parasites with differing phenotypes.....	137
5.1	Introduction.....	138
5.1.1	Quantitative Proteomics Methods.....	138
5.1.2	Quantitative proteomics data analysis	141
5.1.3	Attenuated <i>L. mexicana</i> parasites and clinical isolates of <i>L. panamensis</i>	144
5.2	Aims and hypotheses.....	146
5.3	Results	147
5.3.1	Growth and morphology of <i>L. mexicana</i> wild type and attenuated parasites.....	147
5.3.2	Secretome collection and visualisation from <i>L. mexicana</i> wild type and attenuated parasites.....	150
5.3.3	Quantitative analysis of the <i>L. mexicana</i> WT and attenuated parasite secretome using isobaric peptide tagging	154
5.3.4	Secreted protein identities and quantitation are validated by immunodetection	162
5.3.5	Secretome collection and visualisation from <i>L. panamensis</i> parasites causing chronic and self-healing disease	163
5.3.6	Quantitative analysis of the <i>L. panamensis</i> secretome using isobaric peptide tagging	167
5.4	Discussion.....	173
5.4.1	Quantitative analysis using isobaric tags	173
5.4.2	Statistical testing for analysis of quantitative proteomic data.....	173
5.4.3	<i>L. mexicana</i> attenuated parasites display delayed progression through the life cycle.....	174
5.4.4	Comparative analysis of the secretome of <i>L. mexicana</i> wild type and attenuated parasites.....	175
5.4.5	<i>L. panamensis</i> secretome	178
5.5	Summary.....	179

Chapter 6	Concluding Remarks	181
6.1	Change in environmental niche is accompanied by life cycle progression and alterations to protein secretion	181
6.2	Changes in secretion are associated with virulence	182
6.3	Further analyses of the secretome as a whole.....	183
6.4	Proposal of protein candidates for further analyses	184
Appendices	186
List of References	188

List of Tables

Table 1-1 Species of <i>Leishmania</i> affecting humans and their principal disease manifestation.	17
Table 1-2 Anti-leishmanial drug therapies.	20
Table 2-1 Detergent compatible (DC) Protein Assay (BioRad) recommended concentrations and reagent volumes.	49
Table 3-1 Methods employed for collection of the secretome from <i>Leishmania</i> spp.	63
Table 3-2 Protease inhibitors added to the <i>L. mexicana</i> secretome.	72
Table 3-3 Estimated secreted protein yield from <i>L. mexicana</i>	74
Table 3-4 Summary of <i>L. mexicana</i> promastigote secretome identifications by LC-MS/MS	76
Table 3-5 Summary of <i>L. mexicana</i> amastigote secretome identifications by LC-MS/MS	76
Table 3-6 <i>L. mexicana</i> promastigote secretome identifications from method development.	77
Table 3-7 Secreted proteins from <i>L. mexicana</i> amastigotes.	81
Table 3-8 Identifications from MS analysis of serum-free base medium.	83
Table 3-9 Spectral query that was matched to the mass and fragmentation of two different peptides.	92
Table 4-1 Proteins from the insoluble component of the <i>L. mexicana</i> amastigote secretome.	105
Table 4-2 Secreted proteins of <i>L. mexicana promastigotes</i>	107
Table 4-3 Secreted proteins of <i>L. mexicana</i> amastigotes.	116
Table 4-4 Predicted molecular properties of proteins secreted from <i>L. mexicana</i> promastigotes and amastigotes.	119
Table 4-5 Molecular chaperone proteins present in the <i>L. mexicana</i> promastigote and amastigote secretome.	134
Table 5-1 <i>L. mexicana</i> promastigote secretome proteins significantly up- or down-regulated in attenuated parasites compared to wild-type.	160
Table 5-2 <i>L. mexicana</i> amastigote secretome proteins significantly up- or down-regulated in attenuated parasites compared to wild-type. AmaTMT...	161
Table 5-3 <i>L. panamensis</i> promastigote cell viability <i>in vitro</i>	164
Table 5-4 <i>L. panamensis</i> 25C significant proteins <0.05 pvalue and changing greater than 1.5 fold. Up in chronic.....	172
Table 5-5 <i>L. panamensis</i> 34C significant proteins <0.05 pvalue and changing greater than 1.5 fold Up in chronic.....	172

List of Figures

Figure 1-1 Geographical distribution of new cases of cutaneous and visceral leishmaniasis in 2016.	18
Figure 1-2 The life cycle of <i>Leishmania</i>	22
Figure 1-3 Life cycle of <i>Leishmania</i> in the sand fly vector.	23
Figure 1-4 Eukaryotic classical secretion pathway.	33
Figure 1-5 Eukaryotic non-classical secretion pathways.	33
Figure 1-6 Schematic of secretory and endocytic organelles in <i>Leishmania mexicana</i> promastigotes.	35
Figure 1-7 Schematic of proposed outcomes of <i>Leishmania</i> promastigote exosomal secretion.	43
Figure 3-1 Growth of <i>Leishmania mexicana</i> <i>in vitro</i>	66
Figure 3-2 Viability of <i>L. mexicana</i> during secretome collection.	69
Figure 3-3 Comparison of protein concentration methods for <i>L. mexicana</i> promastigote secretome by SDS-PAGE.	70
Figure 3-4 Secretome collection from <i>L. mexicana</i> axenic amastigotes and promastigotes.	71
Figure 3-5 SDS-PAGE of <i>L. mexicana</i> secretome and lysate.	71
Figure 3-6 <i>L. mexicana</i> promastigote and amastigote secretome compared to cell lysate.	73
Figure 3-7 Venn diagrams illustrating the proteins in common between lysate and secretome protein samples of <i>L. mexicana</i>	84
Figure 3-8 <i>L. mexicana</i> promastigote whole cell proteins versus secretome proteins arranged in order of decreasing abundance.	85
Figure 3-9 <i>L. mexicana</i> amastigote whole cell proteins versus secretome proteins arranged in order of decreasing abundance.	86
Figure 3-10 Flow chart summarising the method implemented for the study of the <i>L. mexicana</i> promastigote and amastigote secretome.	94
Figure 4-1 Secretome from <i>L. mexicana</i> promastigotes and amastigotes.	103
Figure 4-2 2-dimensional SDS-PAGE of <i>L. mexicana</i> protein samples.	103
Figure 4-3 The <i>L. mexicana</i> amastigote secretome contains an insoluble component.	104
Figure 4-4 Staining of glyco-moieties on <i>L. mexicana</i> protein samples.	106
Figure 4-5 Gene ontology (GO) of the promastigote (a) and amastigote (b) secretome.	119
Figure 4-6 Predicted isoelectric point of <i>L. mexicana</i> promastigote and amastigote proteins from the proteome and the secretome.	120
Figure 4-7 Western blots of <i>L. mexicana</i> parasite lysates (a) and secreted proteins (b).	122
Figure 4-8 Venn diagram showing overlapping <i>Leishmania</i> secreted protein identifications.	124
Figure 4-9 Venn diagram showing common identifications between <i>L. mexicana</i> amastigote putatively secreted proteins	125
Figure 5-1 Diagram depicting the structural chemistry of Thermo Scientific Tandem Mass Tags (TMT™)	139
Figure 5-2 Schematic of the quantitative Tandem Mass Tagging (TMT™) process from sample preparation to mass spectrometry analysis.	140
Figure 5-3 Proteome Discoverer™ Software processing and consensus workflows.	142

Figure 5-4	Virulence of <i>L. mexicana</i> wild type (WT) and attenuated (H-line) parasites and efficacy of the H-line as a vaccine in mice.	144
Figure 5-5	Growth of wild type and attenuated <i>L. mexicana</i> promastigotes and amastigotes <i>in vitro</i>	148
Figure 5-6	Measurements of <i>L. mexicana</i> wild type (WT) and attenuated (H) parasites during axenic growth.	149
Figure 5-7	Densitometry profile plots of the <i>L. mexicana</i> promastigote secretome.	151
Figure 5-8	Densitometry profile plots of the <i>L. mexicana</i> amastigote secretome.	152
Figure 5-9	<i>L. mexicana</i> secretome proteins separated by 2-dimensional electrophoresis.	153
Figure 5-10	Cluster dendrogram of <i>L. mexicana</i> promastigote quantitative secretome data.	154
Figure 5-11	Heat map of quantitative differences between secreted proteins of <i>L. mexicana</i> promastigote wild type and attenuated cell lines.	155
Figure 5-12	Volcano plots of 6-plex TMT™ quantitation of <i>L. mexicana</i> promastigote secretome from wild type (WT) and attenuated (H) parasites.	156
Figure 5-13	Cluster dendrogram of <i>L. mexicana</i> amastigote quantitative secretome data	157
Figure 5-14	Heat map of quantitative differences between secreted proteins of <i>L. mexicana</i> amastigote wild type and attenuated cell lines.	158
Figure 5-15	Volcano plots of 6-plex TMT™ quantitation of <i>L. mexicana</i> amastigote secretome from wild type (WT) and attenuated (H) parasites.	159
Figure 5-16	Western blots of <i>L. mexicana</i> secreted proteins paired with quantitation values from the same samples analysed by LC-MS/MS.	163
Figure 5-17	<i>L. panamensis</i> cell lysate proteome and secretome comparison	165
Figure 5-18	SDS-PAGE separation of <i>L. panamensis</i> promastigote secretome.	165
Figure 5-19	Lane profiling of <i>L. panamensis</i> 25°C secretome.	166
Figure 5-20	Lane profiling of <i>L. panamensis</i> 34°C secretome.	166
Figure 5-21	Cluster dendrogram of <i>L. panamensis</i> promastigote quantitative 25°C secretome data comparing replicates collected from self-healing parasites and from chronic parasites.	167
Figure 5-22	Heat map of quantitative differences between secreted proteins of <i>L. panamensis</i> parasites causing self-healing and chronic disease, collected at 25°C.	168
Figure 5-23	Cluster dendrogram of <i>L. panamensis</i> promastigote quantitative 34°C secretome data comparing replicates collected from self-healing parasites and from chronic parasites.	168
Figure 5-24	Heat map of quantitative differences between secreted proteins of <i>L. panamensis</i> parasites causing self-healing and chronic disease, collected at 34°C.	169
Figure 5-25	Volcano plots of 6-plex TMT™ quantitation of <i>L. panamensis</i> promastigote secretome collected from Chronic (Chr) and Self-healing (SH) disease-causing parasites at 25°C.	170
Figure 5-26	Volcano plots of 6-plex TMT™ quantitation of <i>L. panamensis</i> promastigote secretome collected from Chronic (Chr) and Self-healing (SH) disease-causing parasites at 34°C.	171
Figure 5-27	Pie chart indicating the percentage of the <i>L. mexicana</i> promastigote secretome with certain activity or location associations.	176

Conference Proceedings

Parts of this thesis have been presented at the following national and international conferences and meetings:

- ❖ CIDEOMICS Symposium: Omic Technologies for Research on Infectious Diseases, Cali, Colombia, 2017 [Oral Presentation]

- ❖ British Society for Proteome Research Conference, Glasgow, UK, 2016 [Poster]

- ❖ British Society for Parasitology, Trypanosomiasis and Leishmaniasis Seminar, České Budějovice, Czech Republic, 2016 [Poster]

- ❖ EMBO 10th European Advanced Proteomics Workshop, Brixen, Italy, 2016 [Poster]

- ❖ 47th Parasite Metabolism Microsymposium, Glasgow, UK, 2015 [Oral Presentation]

Acknowledgements

My initial thanks go to my supervisory team, Dr Richard J. Burchmore and Dr Karl E.V. Burgess, and my assessors Dr Richard McCulloch and Dr Donal Wall for their insightful comments, support and encouragement.

Special thanks go to my primary supervisor Richard Burchmore. Thank you for your supervision and guidance throughout this PhD project. I have enjoyed being part of your team, and I thank you for supporting me through everything.

I would also like to thank numerous others for their technical support, help and encouragement. I couldn't have got to this stage without each of you. In no particular order I thank: Daniel Harris, Najad Zaki, Abdulbaset Kabli, Snezhana Akpunarlieva, Stefan Weidt, Jeni Haggarty, Suzanne McGill, Christina Naula, Aruna Prakash.

Thank you to the other research groups of level 6 of the GBRC, where I carried out my research. Thank you to the Doctoral Training Centre in Technologies at the Interface between Engineering, Physical Sciences & Life Sciences, and to my funders: Biotechnology and Biological Sciences Research Council (BBSRC) and the Engineering and Physical sciences Research Councils (EPSRC). My thanks also go to our collaborators at CIDEIM, Dr Maria Adelaida Gómez and her team.

I would like to thank my Dad, William Hamilton and my brother Ross Hamilton. I wouldn't have reached this stage without you. We have been through some hard times recently, but your love and support has kept me going and got me to where I am now.

A special thanks to my partner Laurence Stipetic. You have always been there through the good and the bad, and I can always rely on you. Thank you for truly being my rock, I don't think I would even have a thesis without your constant support and encouragement, as well as snacks and coffees and discussions.

To the Hamilton and Stevenson family, the Stipetic family and all my friends that I have not had the chance to name, thank you so much for all your support.

Dedication

I dedicate this thesis to my mum, Elaine Hamilton. Sadly, I lost you during this time. You watched me start and grow, and I wish you could be here to see me finish. You always believed in me and although I missed your physical support, I knew you would have always been in my corner. I love you always.

Author's Declaration

I declare that, except where explicit reference is made to the contribution of others, that this thesis is the result of my own work and has not been submitted for any other degree at the University of Glasgow or any other institution.

Signature:

Printed name: Hazel Jean Hamilton

Abbreviations

°C	Degrees Celsius
µg	Microgram
µl	Microlitre
µm	Micrometre
µM	Micromolar
2-DE	2-dimensional electrophoresis
ACN	Acetonitrile
AmB	Amphotericin B
AP-1	Activator protein-1
APCs	Antigen Presenting Cells
ATCC	American Type Culture Collection
BSA	Bovine serum albumin
C	Carbon
C3b	Complement component 3 subunit
C3bi	Inactive complement subcomponent C3b
cHOM	Complete HOMEM – HOMEM medium (GE Healthcare) + 10% HiFBS
CL	Cutaneous leishmaniasis
CO ₂	Carbon dioxide
cSDM	Complete Schneider's Drosophila Medium (Gibco) + 20% HiFBS + mM Haemin, pH 5.5
Cy3, Cy5, Cy2	Cyanine dyes
Da/ kDa	Dalton/ kilodalton
DB	Database
DCs	Dendritic cells
DiGE	Difference gel electrophoresis
DiMe	Stable isotope dimethyl labelling
DMSO	Dimethyl sulfoxide
DNA	Deoxyribonucleic acid
DTT	Dichloro-diphenyl-trichloroethane
ECL	Enhanced chemiluminescence
ECM	Extra-cellular matrix
EDTA	Ethylenediaminetetraacetic acid
EF	Elongation factor
EF1A	Elongation factor-1 alpha
ELISA	Enzyme-linked immunosorbent assay
empAI	Exponentially modified protein abundance index
ENO	Enolase
ESI	Electrospray ionisation
FASP	Filter-aided sample preparation
FC	Fold-change
FDR	False discovery rate
g	gram
GO	Gene Ontology
GP63	Glycoprotein-63/ leishmanolysin
GPIs	Glycosylinositol phospholipids
h	Hour
H	Hydrogen
HCl	Hydrochloric acid
HiFBS	Heat Inactivated Foetal Bovine Serum (Gibco)
HOMEM	Haemoflagellate minimal essential medium
HSP	Heat shock protein
ICAT	Isotope-coded affinity tags
ID	Identifiers
IL	Interleukin
iNOS	Inducible Nitric Oxide Synthase
iTRAQ	Isotope tags for relative and absolute quantification
JAK	Janus tyrosine kinase

KMP-11	Kinetoplastid membrane protein-11
L	Litre
LC-MS/MS	Liquid chromatography coupled to tandem mass spectrometry
LFQ	Label-free quantitation
LFQ	Label-free quantification
Log	Logarithm
LPG	Lipophosphoglycan
M	Molar
m/z	Mass to charge ratio
MCL	Mucocutaneous leishmaniasis
mg	Milligram
MHC	Major histocompatibility complex
ml	Millilitre
mM	Millimolar
mm	Millilitre
mRNA	Messenger RNA
MS	Mass spectrometry
MudPIT	Multidimensional Protein Identification Technology
MW	Molecular weight
MWCO	Molecular weight cut-off
N	Nitrogen
NO	Nitric oxide
O	Oxygen
PBS	Phosphate-buffered saline
PBS-T	PBS-Tween 20
PFR	Paraflagellar rod
pI	Isoelectric point
ROS	Reactive oxygen species
SCX	Strong Cation exchange
SDS	Sodium dodecyl sulphate
SDS-PAGE	Sodium dodecyl sulphate polyacrylamide gel electrophoresis
sfHOM	Serum free HOMEM
sfSDM	Schneider's Drosophila Medium, pH 5.5
SILAC	Stable isotope labelling with amino acids in cell culture
SOD	Superoxide dismutase
spp.	species
STAT	Signal transducer and activator of transcription factor
TFA	Trifluoroacetic acid
Th1	T helper 1 type
Th2	T helper 2 type
TMT	Tandem mass tags
VL	Visceral leishmaniasis
WT	Wild type
x g	times gravity

Chapter 1 Introduction

1.1 Leishmaniasis

The leishmaniasis are a group of debilitating and often disfiguring diseases that are classed as ‘Neglected Tropical Diseases’, a term encompassing a group of infectious diseases affecting some of the world’s poorest tropical and subtropical areas (Utzinger et al. 2012). Leishmaniasis is caused by protozoan parasites of the genus *Leishmania*, of which over 20 species are known to infect and cause disease in humans (W.H.O. 2010). The differing species of *Leishmania* dictate the nature and severity of the disease, causing three main manifestations of the disease: visceral leishmaniasis (VL), cutaneous leishmaniasis (CL) and mucocutaneous leishmaniasis (MCL). The manifestations are not exclusive to, but most commonly caused by the species listed in Table 1-1 (W.H.O. 2010). CL affects the highest numbers of people and is characterised by localised open or closed skin lesions that can sometimes spread over the entire body and cause diffuse/disseminated CL. MCL leads to disfiguring destruction of the mucous membranes of the nose, mouth, and throat cavities. VL results in anaemia, weight loss, swelling of the spleen and liver, and is almost always fatal if left untreated (Utzinger et al. 2012).

Table 1-1 Species of *Leishmania* affecting humans and their principal disease manifestation. List compiled in WHO Expert Committee report on Control of the Leishmaniasis (2010) (W.H.O. 2010).

Figure has been removed due to Copyright restrictions.

a

Figure has been removed due to Copyright restrictions.

b

Figure has been removed due to Copyright restrictions.

Figure 1-1 Geographical distribution of new cases of cutaneous and visceral leishmaniasis in 2016. (a) Cases of cutaneous leishmaniasis, (b) Cases of visceral leishmaniasis. WHO Leishmaniasis update 2018 (W.H.O. 2018).

The leishmaniasis are widespread globally, with cutaneous leishmaniasis (CL) endemic in 87 countries (Figure 1-1a), and visceral leishmaniasis (VL) endemic in 75 countries (Figure 1-1b) (W.H.O. 2018). In a recent comprehensive report on leishmaniasis from the World Health Organisation, over 200,000 new cases of CL were reported in 2016, and over 22,000 new cases of VL were reported in 2016 (W.H.O. 2018). However, notification of incidence only occurred in 57 of the 87 CL-affected countries in 2015 (W.H.O. 2017), increasing marginally to 62 out of 87

reporting in 2016 (W.H.O. 2018). And 54 of the 75 VL-endemic countries reported in 2015 (W.H.O. 2017) and 2016 (W.H.O. 2018). It is therefore highly likely that the number of cases of leishmaniasis is severely under-reported. In addition, many leishmaniasis cases are either asymptomatic or misdiagnosed, and outbreaks which occur in zones of extreme conflict or in remote rural areas seldom visited by healthcare officials are often unreported. It is therefore estimated that 0.7 to 1.2 million cases of CL and 0.2 to 0.4 million cases of VL occur globally every year, resulting in an estimated 40,000 deaths per year world-wide (Alvar *et al.* 2012).

1.1.1 Diagnosis, treatment and vaccination

Early phase diagnosis of leishmaniasis has proved a challenge for diagnostic approaches as infection can be asymptomatic. This, coupled with geographical and logistical challenges of providing lab-based field diagnostics in remote and challenging environments where this disease is endemic, intensifies the complexity of providing a leishmaniasis diagnosis. Parasitological methods for the diagnosis of CL are highly specific and remain the gold standard over immunological diagnosis, which cannot distinguish between previous and current infections. In parasitological diagnosis, material from lesion biopsies or aspirates is examined by microscopy, by culturing from the sample, or by molecular PCR-based methods. Although the simplest and most applicable in the field, microscopy can be time-consuming and error prone due to insensitivity and operator interpretation. This allows for the possibility of false negative diagnoses as parasites can be scarce at the lesion site. Culture of the parasite is definitive and allows species identification, but this method is limited by the need for significant expertise and laboratory facilities. This limitation also applies to molecular diagnostics. These techniques have the advantage of allowing rapid diagnosis and species identification, particularly where multiple species may be present, but requires access to laboratory infrastructure (W.H.O. 2010).

Treatment of leishmaniasis also faces many problems and there is still no treatment strategy available that does not either incur damaging side effects, or substantial costs. Anti-leishmanial drugs currently available on the market have variable efficacy, are often administered over long treatment regimens, and often come with toxicity and adverse side-effects, summarised in Table 1-2 (de Menezes *et al.*

2015). Furthermore, many anti-leishmanial drugs are expensive, have shown to demonstrate resistance and cannot, with the exception of miltefosine, be administered orally, with the others requiring sterile equipment and trained personnel for safe administration over the course of the long treatment periods. Alternative treatment therapies include the use of controlled release systems, such as liposomes, including a liposomal formulation of amphotericin B (AmB), Ambisome (Davidson *et al.* 1994). However, there are high costs associated with these amendments and liposomal AmB is unstable at room temperature so requires a cold chain. Functionalised carbon nanotubes used as anti-leishmanial drug carriers show good efficacy and low toxicity in tests, but again are associated with high costs and are still under development (Prajapati *et al.* 2011). Thus, there remains the need to identify new targets and treatment therapies to overcome problems such as efficacy, toxicity and resistance. Several leishmaniasis vaccines have been developed and trialled in animal models (Kedzierski *et al.* 2006), of which a small number have begun phase I or II trials in human subjects, namely LEISH-F1 (Nascimento *et al.* 2010), LEISH-F3 (ClinicalTrials.gov 2012) and Leish-111f, which has completed phase I and II trials in humans (Coler *et al.* 2007). However, as yet there are no commercially available vaccines for leishmaniasis in humans.

Table 1-2 Anti-leishmanial drug therapies. Administration route abbreviations: intramuscular (IM), intravenous (IV), intralymphatic (IL). Adapted from de Menezes *et al.* 2015 (de Menezes *et al.* 2015).

Drug	Efficacy	Treatment length	Toxicity and Side effects	Cost	Resistance	Administ. route
Pentavalent antimonials	35-95%	28-30 days	Cardiotoxicity, pancreatitis, nephrotoxicity, hepatotoxicity	High	Common	IM, IV, IL
Amphotericin B	>90%	15-20 days	Nephrotoxicity, infusion complications, hypokalemia, fever	High	Laboratory strains	IV
Liposomal amphotericin B	>97%	Single dose	Infrequent and mild Rigors, chills, nephrotoxicity	Very High	None reported	IV
Miltefosine	60-94%	28 days	Vomiting, diarrhoea, nephrotoxicity, hepatotoxicity, teratogenicity	High	India 2017 (Khanra <i>et al.</i> 2017)	Oral
Paromomycin	46-84%	17 or 21 days dose dependent	nephrotoxicity, ototoxicity, hepatotoxicity	Low	Laboratory strains	IM, topical
Pentamidine	35-96%	Every other day, x4 injections	Pancreatic damage leading to hyperglycemia, hypotension, tachycardia, electrocardiographic changes	High	None reported	IM

1.2 The *Leishmania* parasite

Leishmania have a digenetic life cycle and are spread to the human host by the bite of an insect vector. The vector for these protozoa are sand flies, of the genus *Phlebotomus* for Old World *Leishmania* species such as *L. major* and *L. donovani*, and *Lutzomyia* for New World species such as *L. mexicana* and *L. braziliensis* (Bates 2007). The parasites maintain different morphologies corresponding to their survival in the vector or the host. Figure 1-2 depicts the life cycle of *Leishmania*. When sand flies take a blood meal from an infected host, they ingest amastigotes which differentiate in the midgut of the insect to procyclic promastigotes. Procyclic promastigotes divide in the midgut and migrate to the mouthparts, where differentiation into the infective metacyclic stage occurs. These metacyclic promastigotes are introduced to the human host by the bite of the sand fly and are phagocytosed by macrophages, where they differentiate into the amastigote form in order to survive and multiply by binary fission.

The amastigotes are successful as intracellular parasites due to their ability to resist the host cell defence mechanisms and exploit host cell nutrients and proteins. However, it is unlikely that physical adaptation alone facilitates their survival. We hypothesise that they also secrete factors which manipulate the host cell environment. Other intracellular pathogens such as *Mycobacterium* (Wagner *et al.* 2005), *Legionella* (Manske & Hilbi 2014) and *Coxiella* (Larson *et al.* 2015), have been shown to create pathogen-induced microenvironments in the host cell for their survival. One of the primary mechanisms used by these pathogens is the secretion of proteins to modulate the surrounding environment or modulate host cell signalling. *Mycobacterium spp.* have been shown to induce iron-rich microenvironments, *Legionella* employ a type IV secretion system and translocate hundreds of different effector proteins into host cells, and *Coxiella* secrete effector proteins which integrate into the parasitophorous vacuole (PV) membrane allowing for niche modification (Larson *et al.* 2015; Manske & Hilbi 2014; Wagner *et al.* 2005). The intracellular parasite *Toxoplasma gondii* actively secretes parasite proteins after invasion of the host cell, resulting in modification of the vacuole to render it permeable to small molecules and thus promoting nutrient acquisition (Sibley *et al.* 2013).

Studying the proteins secreted by the parasites at different stages in their life cycle could help to put together a picture of *Leishmania* survival mechanisms and most importantly how these might be targeted to aid parasite clearance and treat infection.

Figure has been removed due to Copyright restrictions.

Figure 1-2 The life cycle of *Leishmania*. Image adapted from Esch & Petersen, 2013 (Esch & Petersen 2013)

1.3 Mechanisms of *Leishmania* parasite survival

1.3.1 Promastigote survival in the sand fly vector

Change of form

Promastigotes change forms to adapt to the stresses of their environment in the vector as they migrate from the midgut to the anterior gut and finally to the mouthparts; nectomonad, leptomonad, and metacyclic, respectively (Figure 1-3). However, these parasites can also modulate their environment to facilitate their survival by secreting proteins and compounds which are thought to influence their niche and allow the establishment of infection and growth within the host (Lambertz *et al.* 2012; Silverman & Reiner 2012).

Figure has been removed due to Copyright restrictions.

Figure 1-3 Life cycle of *Leishmania* in the sand fly vector. Ingestion of amastigotes during a blood meal from an infected mammalian host (1), followed by differentiation to procyclic promastigotes, then nectomonad-form promastigotes which can exit the peritrophic matrix (2, 3, 4). The promastigotes migrate to the thoracic midgut and stomodeal valve (5) where they differentiate into leptomonad forms that can subsequently differentiate to mammalian-infective metacyclics or haptomonad forms which attach to the stomodeal valve (6). Metacyclic promastigotes are transmitted to the mammalian host during a blood meal (7,8). From Sunter & Gull (2017) (Sunter & Gull 2017).

Secretion of proteins for nutritional functions

Promastigotes have been shown to secrete a number of enzymes which are thought to be released in the midgut of the vector to digest large sugars and other nutrients to smaller molecules for uptake. For example, glycosidases such as glucosidase and sucrase which hydrolyse maltose and sucrose into their individual subunits (BLUM & OPPERDOES 1994; Jacobson & Schlein 2001). Promastigotes also release a secreted acid phosphatase (SAP), an enzymatically active filamentous phosphoglycoprotein polymer (Ilg *et al.* 1991). The glycoprotein was found to be secreted via the flagellar pocket (Stierhof *et al.* 1994). The enzyme has broad substrate specificity, and as it is released into the insect midgut, is thought to have a nutritional function (Ilg 2000b).

Secreted proteins with physical roles

Promastigotes also secrete several unusual glycoproteins which have been found to play various roles in parasite pathogenesis. Filamentous proteophosphoglycan (fPPG) (Ilg 2000b; Ilg *et al.* 1996) is the main component of promastigote secretory

gel (PSG) (Rogers *et al.* 2002). PSG, released by the parasites into the sand fly midgut, causes a physical blockage and promotes regurgitation of the parasites into the bite site, and therefore transmission (Bates 2007). A secreted chitinase has also been identified (Joshi *et al.* 2005). Its putative substrate, chitin, is a structural polysaccharide found in arthropods and is one of the main structural components of the peritrophic matrix, a membrane surrounding the food in the insect's midgut (Secundino *et al.* 2005). As such, the enzyme's main roles are thought to be the breakdown of blocks and membranes inside the insect vector and physical egress from the peritrophic matrix (Joshi *et al.* 2005). This then allows migration to the thoracic midgut and further development from there.

1.3.2 During transmission from vector to host

Recruitment and alternative activation of host cells

In addition to promoting regurgitation of parasites, secreted PSG also exacerbates cutaneous infection by other mechanisms. Firstly, PSG causes strong recruitment of macrophages to the site of infection and secondly, it has been shown to stimulate alternative activation of the macrophage (Rogers *et al.* 2009). Alternative activation of macrophages, directing a Th2 immune response, induces macrophage metabolism that is conducive to parasite growth and can also provide essential nutrients to the parasite. Classical activation upregulates production of inducible nitric oxide synthase (iNOS) which produces harmful NO during the conversion of L-arginine to L-citrulline (Cecilio *et al.* 2014). During classical activation, directing a Th1 immune response, expression of arginase is downregulated and as such the metabolism of arginine is shifted towards this iNOS pathway. Conversely, during a Th2 response, the expression of arginase increases which shifts arginine metabolism away from the production of NO, promoting parasite survival and additionally increasing the availability of polyamines to the parasite (McConville & Naderer 2011; Naderer & McConville 2008). Another way the parasite actively contributes to this alternative activation of the macrophage is by secretion of cysteine protease B (CPB) which has been correlated with IL-4 production and subsequent Th2 response (Alexander *et al.* 1998; Denise *et al.* 2003). One of the actions of the CPB enzyme is to cleave CD23 and CD25, IgE and IL-2 receptors respectively, and thus promote a Th2 response (Pollock *et al.* 2003).

Promoting phagocytosis

After injection into the host in the sand fly bite, promastigotes are then taken up by professional phagocytic cells. Phagocytosis is a receptor-mediated process by recognition and binding of pathogens to receptors on the macrophage surface (Flannagan *et al.* 2012). There are many different receptors that mediate the phagocytosis of foreign bodies. Pattern-recognition receptors detect pathogen molecules directly, and opsonic receptors bind foreign bodies via opsonins on the pathogen surface (Flannagan *et al.* 2012). At least three different receptors have been reported to be involved in the phagocytosis of infective promastigotes. These include the first complement receptor CR1, the third complement receptor CR3 and fibronectin receptors (FnRs) (Ueno & Wilson 2012; Wenzel *et al.* 2012). *L. major* promastigotes have been found to be internalised by a CR1-mediated phagocytic process (Wenzel *et al.* 2012), and *L. mexicana*, *L. amazonensis*, *L. donovani*, *L. infantum*, and *L. major* promastigotes via CR3. Additionally, the parasites can be opsonised with fibronectin and the subsequent binding to fibronectin receptors can increase the attachment to the host cell for the engagement of other receptors (Ueno & Wilson 2012). This can be mediated by self-produced factors, such as enolase and SMP-1 secretion, which bind plasminogen, a fibrinolytic protease precursor (Avilán *et al.* 2011; Figuera *et al.* 2013). Furthermore, parasite surface and secreted GP63 cleaves complement protein 3 into C3b, which binds to CR1, and C3b into iC3b, which opsonises the parasite for CR3-mediated uptake (Brittingham *et al.* 1995; Ueno & Wilson 2012).

1.3.3 Entry to the phagolysosome and differentiation

Following internalisation, the newly formed phagosome is subjected to a rapid succession of biochemical changes; a process termed phagosome maturation. This involves a systematic chain of interactions with early endosomes, late endosomes and lysosomes, resulting in the production of an acidic, oxidative and hydrolytic microbicidal compartment (Flannagan *et al.* 2012). Following phagocytosis, *Leishmania* not only survives the microbicidal assault, but differentiates and thrives as its obligate intracellular form, the amastigote. A variety of promastigote extracellular and secreted effectors contribute to the maintenance of infection, allowing it to promote its own intracellular survival, differentiation and subsequent

division. The effectors impede the maturation of the phagosome and delay the formation of the acidic pH and other unfavourable conditions affording the parasite time to differentiate into its more adapted intracellular form, the amastigote.

Delaying phagosome maturation

The first mechanism the promastigote uses to prolong its survival in the phagosome is impairing phagosome fusion with the late endosomal system and lysosomes (Moradin & Descoteaux 2012; Scianimanico *et al.* 1999). *L. donovani* achieves this by f-actin accumulation around the phagosome which provides a physical barrier to vesicular trafficking to the phagosome. This has been shown to be induced by *L. donovani* LPG via retention of Cdc42, F-actin assembly proteins and Rac1 (Holm *et al.* 2001; Lerm *et al.* 2006; Lodge & Descoteaux 2005). Interestingly, f-actin accumulation has not been observed in all *Leishmania* species, like *L. amazonensis* (Courret *et al.* 2002), highlighting the species diversity in survival mechanisms. And while it has been shown that actively inhibiting phagosome-lysosome fusion in *L. mexicana* caused an increase in parasite multiplication, and promoting phagosome-lysosome fusion inhibited parasite growth (Alexander 1981), the parasite driven mechanisms of this stage of promastigote survival have not been elucidated in *L. mexicana*. Additionally, LPG was found not to be essential for *L. mexicana* infection of macrophages suggesting an alternative mechanism for this species (Ilg 2000a). Phagosome maturation is also delayed by impaired regulation of interactions between the PV and late endosomes and lysosomes, due to poor recruitment of Rab7, a small GTPase associated with this regulation (Zhang *et al.* 2009). This could be a consequence of the F-actin barrier around the phagosome, but additionally, promastigote infection of host macrophage results in an up-regulation in host expression of Th2 cytokines, inhibiting a Th1 response, and down-regulation of Rab7 and Rab9 expression in the host cell (Ali *et al.* 2013). The promastigote slows the acidification of the phagolysosome by impairing the recruitment of the vesicular proton-ATPase (v-ATPase) to the phagosome (Moradin & Descoteaux 2012; Vinet *et al.* 2009). The presence of parasite LPG in the phagosome membrane has been shown to exclude Synaptotagmin V (SytV), a regulator of maturation, thereby interfering with the recruitment of v-ATPase to the phagosome (Vinet *et al.* 2009).

Evasion of ROS and NO

Parasites also evade the mechanisms of reactive oxygen species (ROS) and nitric oxide (NO) killing by macrophages. As discussed previously, alternative activation of macrophages towards a Th2-type response downregulates production of iNOS and increases production of L-arginase. This shifts the metabolism of L-arginine away from NO production by iNOS (Rogers *et al.* 2009), a reduction of which encourages parasite survival (Green *et al.* 1990). A mechanism of ROS evasion is failure of NADPH oxidase complex formation in the PV membrane (Lodge *et al.* 2006). In *L. donovani*, this is thought to be due to LPG disruption of PV membrane lipid microdomains by incorporation of LPG into macrophage membrane lipid rafts (Winberg *et al.* 2009). For other *Leishmania* species mechanisms of scavenging or neutralizing intracellular ROS have been described, for example *L. major* methionine sulfoxide reductase A plays an anti-oxidative role (Sansom *et al.* 2013). Parasite superoxide dismutase (SOD) also plays a role in ROS defence as parasites deficient in this enzyme are markedly more sensitive to ROS *in vitro* and display reduced survival *in vivo* (Ghosh *et al.* 2003). SOD also appears to initiate signalling for the differentiation of infective promastigotes to amastigotes, mediated by ROS (Mittra *et al.* 2017). *Leishmania* also express and secrete a number of intrinsic antioxidants including trypanothione reductase, trypanredoxin, peroxidoxin and thioredoxin-like protein (Castro *et al.* 2002, 2017).

Inhibition of macrophage apoptosis

Infection with *Leishmania* appears to actively increase the lifespan of macrophages during infection through release of proteins which influence and inhibit macrophage apoptosis (Moore & Matlashewski 1994). Various mechanisms have been described in different species to explain this effect, but what is clear is that despite the mechanism, this effect is occurring. Release of NdK in *L. amazonensis* prevents ATP-induced cytolysis of the macrophage (Kolli *et al.* 2008); *L. major* produces a human migration inhibitory factor (MIF)-like protein which was shown to inhibit macrophage apoptosis *in vitro* (Kamir *et al.* 2008); *L. infantum* promastigotes and soluble factors from spent media have been shown to inhibit actinomycin D-induced apoptosis in macrophages, but the effectors have not been identified (Lisi *et al.* 2005). In the following cases infection with *Leishmania* has

been demonstrated to inhibit apoptosis in macrophages induced with various compounds, including actinomycin D (Lisi *et al.* 2005; Ruhland *et al.* 2007), camptothecin (Ruhland *et al.* 2007), staurosporine (Akarid *et al.* 2004), and cycloheximide (Donovan *et al.* 2009), but the mechanisms of inhibition are still unknown.

1.3.4 Amastigote survival

Leishmania survives within the microbicidal environment of the macrophage phagolysosome by differentiating into its highly adapted form, the amastigote. Amastigotes are the disease-causing mammalian stage of the parasite life cycle. The amastigote form is rounded with a non-emergent flagellum. In addition to resisting the microbicidal assault of the macrophage, it is evident that the amastigote adapts the niche itself in order to survive (Podinovskaia & Descoteaux 2015). However, the mechanisms responsible for these adaptations to the niche are still poorly understood, but release of specific virulence factors has been elaborated in some studies and is a key area of investigation into the host-parasite interaction.

The adaptations the parasite undergoes to enable its survival in the acidic phagolysosome environment have been investigated. The amastigote stage is optimised to the more acidic environment of the PV lumen, for example they express surface metalloproteinases which have an optimum pH of ~5.5-6.0 (Zilberstein & Shapira 1994) and transport of glucose, and many other nutrients, are optimised to an acidic pH in amastigotes (Burchmore & Barrett 2001; Burchmore & Hart 1995). The parasite cytosol, however, is not acidic. The amastigote maintains a steep transmembrane pH gradient between its cytosol and the PV by expression of stage-specific proton pumps in the plasma membrane (Burchmore & Barrett 2001; Glaser *et al.* 1988; Zilberstein & Shapira 1994).

Evasion of Host Proteases

Serine peptidase inhibitors expressed by *Leishmania* act as virulence factors. Inhibitor of serine peptidase 2 (ISP2) is expressed in *L. major* metacyclics and amastigotes and inhibits a serine peptidase expressed by neutrophils, monocytes and macrophages (Goundry *et al.* 2018). The PV is also rich in hydrolytic enzymes

such as acid phosphatases, trimetaphosphatases A and B, β -glucuronidases, and cathepsins B, D, H and L (Antoine *et al.* 1998). Amastigotes are able to resist host proteases in the PV and have been found to contain high levels of host-derived glycosphingolipids in their plasma membrane, which could potentially act as a physical barrier to the host proteases (McConville & Blackwell 1991). Proteinase GP63 in the parasite membrane protects it from degradation in the phagolysosome, demonstrated by coating liposomes with gp63 resulting in their protection from phagolysosomal degradation (Chaudhuri *et al.* 1989).

Evasion of Nutriprive and Active Nutrient Salvage

In addition to the microbicidal mechanisms above, macrophages deprive the pathogens within the PV of nutrients; this is the nutriprive hypothesis (Appelberg 2006). The parasites are competing with several nutrient transporters, lysosomal transporters which become associated with the PV during phagosome maturation. For example, host transporters gradually deplete iron from endosomes and lysosomes to avoid toxicity, but this too depletes iron availability for the parasite for essential cofactor functions (Huynh & Andrews 2008). The amastigote has many transporters of essential nutrients to overcome this, for example: nucleoside/nucleobase transporters (Dean *et al.* 2014); hexose transporters (Burchmore *et al.* 2003); iron transporters (Huynh & Andrews 2008); amino acid transporters (McConville *et al.* 2007); aquaporins for the transport of water, polyamines, bioppterin, folate etc (Burchmore & Barrett 2001; McConville *et al.* 2007). The parasite can also perform gluconeogenesis and de novo synthesis of inositol and mannose as the supply of hexoses in the PV is poor (Naderer & McConville 2008). *L. amazonensis* was also found to inhibit expression of the mammalian iron exporter ferroportin in macrophages to prevent iron export and promote its own intracellular growth (Ben-Othman *et al.* 2014). Although the mechanism behind this is still unknown, this is an example of an active modification to the phagolysosomal niche that enhances amastigote nutrient salvage.

In addition to possessing a repertoire of nutrient transporters for nutrient salvage from the PV, *Leishmania* parasites have also been shown to secrete several enzymes which are thought to play a role in nutrient salvage. *Leishmania* are unable to synthesise purines *de novo* and as such produce and secrete a nuclease in *L.*

donovani promastigotes, and also express the nuclease in both axenic amastigotes and tissue-derived amastigotes (Joshi & Dwyer 2007). The hypothesis is that this secreted nuclease would hydrolyse nucleic acids from the host to facilitate purine uptake by the parasite by surface-membrane transporters (Joshi & Dwyer 2007). Amastigotes also express several plasma membrane nucleotidases which cleave phosphate from the nucleotides, and are thought to be involved in the salvage of nucleosides (Hassan & Coombs 1987).

A similar mechanism has also been described for a *Leishmania*-secreted lipase. *Leishmania* are opportunistic facultative lipid scavengers, salvaging these macromolecules from their host. The secreted lipase would allow the parasite to break down lipids to salvage fatty acids from both the mammalian and insect host, for use in the synthesis of complex lipids or as substrates for beta oxidation and energy metabolism (Shakarian *et al.* 2010). Fatty acid oxidation can serve as a major source of energy in amastigotes as *Leishmania* can exploit glucose, amino acids or fatty acids as carbon sources (Hart & Coombs 1982). In macrophages, endocytosed lipoproteins are delivered to late endosomal compartments for degradation (Burchmore & Barrett 2001). Cholesterol esters from lipid droplets in the cytoplasm are also delivered to lysosomes by autophagy, so-called lipophagy, where they undergo lipolysis (Singh *et al.* 2009). Lipids are therefore available to amastigotes in the PV from the endocytosis and autophagic systems. Autophagosomes fuse with the endosomal system during autophagy in eukaryotes (Huang *et al.* 2015) and have been shown to fuse with the PV (Schaible *et al.* 1999) which resembles a late endosomal compartment (Russell *et al.* 1992).

As demonstrated by the examples above, the autophagic system in macrophages appears to be a key process in the supply of cytoplasmic nutrients to the PV. Interestingly, autophagy is no longer considered to be a non-selective mechanism, for bulk degradation of the constituents of the cytoplasm. Preferential targeting of cargo for autophagic degradation has now been demonstrated (Weidberg *et al.* 2011). It will be interesting to investigate if, in addition to their secretion of enzymes, amastigotes can enhance or alter this process as a mechanism of 'hand-delivering' nutrients to the PV.

Evading Antigen Presentation

The parasites can interrupt MHC class II antigen presentation by the host cell, by means of sequestering the complexes within the PV by blocking their egress or by internalisation and degradation of the MHC class II molecules (De Souza Leao *et al.* 1995). In addition, other molecules in the antigen presentation pathway are also endocytosed by *L. mexicana* and *L. amazonensis* amastigotes (Antoine *et al.* 1999). In addition to sequestering MHC molecules to evade antigen presentation, *Leishmania* parasites can also actively degrade MHC by secretion of amastigote cysteine proteases. Cysteine protease B (CPB) is activated in the flagellar pocket and released into the PV where it has been shown to degrade MHC Class II molecules (De Souza Leao *et al.* 1995; Mottram *et al.* 2004).

Expansion of the parasitophorous vacuole (PV)

As discussed above, *Leishmania* promastigotes produce and secrete number of glycoconjugates. *L. mexicana* amastigotes also secrete an amastigote-specific proteophosphoglycan (aPPG) into the PV (Ilg *et al.* 1995). This was shown to induce vacuolisation in macrophages, and is therefore thought to be involved in the expansion of the large PVs of the *L. mexicana* complex (Peters *et al.* 1997b). The secreted aPPG has also been shown to activate and therefore locally deplete complement, and so an additional role of the aPPG may be in helping the parasites to avoid complement lysis when released from macrophages (Ilg 2000b; Peters *et al.* 1997b).

Amastigote-mediated evasion of NO killing

L. mexicana amastigotes may prevent increased NO synthesis, usually formed by the conversion of arginine to citrulline and NO, by rapidly depleting the substrate, the host arginine pool, via secretion of a parasite-derived arginase (Gaur *et al.* 2007). Depletion of the substrate prevents the macrophage from synthesising the highly microbicidal molecule NO, thus increasing parasite survival in the PV.

Interference with host signalling

Leishmania subverts the macrophage translation machinery using its cell-surface-expressed and soluble secreted GP63 protease (Jaramillo *et al.* 2011). GP63 has been shown to cleave a serine/threonine kinase that is involved in regulation of a translational repressor molecule, resulting in activation of this translational repressor. This interaction promotes parasite survival and proliferation (Jaramillo *et al.* 2011).

1.4 Protein secretion

Eukaryotes have differing methods of secreting proteins to the cell membrane or extracellular space. The conventional or 'classical' secretory pathway, and other non-classical secretion mechanisms. The classical secretory pathway, summarised in Figure 1-4, is endoplasmic reticulum (ER) and Golgi-dependent. The proteins secreted by this pathway contain an N-terminal or internal secretion-signal peptide which directs them to the ER during the sorting process. Once in the ER, they are trafficked through the ER-Golgi secretory pathway to be released in specially coated vesicles (Nickel & Rabouille 2009). Non-classical protein secretion occurs independently of the Golgi and/or the ER, summarised in Figure 1-5. Four main mechanisms have been proposed for unconventional secretion of soluble cytoplasmic proteins: non-vesicular plasma membrane translocation (Zehe *et al.* 2006), translocation into and release by secretory lysosomes (Andrei *et al.* 2004), microvesicle shedding (MacKenzie *et al.* 2001), and capture of the protein from the cytoplasm during formation of intracellular endosomes, and exosome release thereafter from multivesicular bodies (Nickel & Rabouille 2009). The ESCRT (endosomal sorting complex required for transport) pathway consists of three complexes (ESCRT-I, ESCRT-II, ESCRT-III) and is a key mediator of MVB biogenesis, regulating membrane budding at cell surfaces and at the level of late endosomes (Raposo & Stoorvogel 2013). These evolutionarily conserved proteins assemble into four multiprotein complexes: ESCRT-0, -I, -II, and -III, which associate with accessory proteins (e.g., Alix and VPS4). The ESCRT-0, -I, and -II complexes recognize and sequester ubiquitinated membrane proteins at the endosomal delimiting membrane, whereas the ESCRT-III complex is responsible for membrane budding and actual scission of vesicles (Schmidt & Teis 2012).

Figure has been removed due to Copyright restrictions.

Figure 1-4 Eukaryotic classical secretion pathway. Image adapted from Nickel & Rabouille 2009.

Figure has been removed due to Copyright restrictions.

Figure 1-5 Eukaryotic non-classical secretion pathways. 1. Non-vesicular plasma membrane translocation, 2. Translocation into and release by secretory lysosomes, 3. Microvesicle shedding, 4. Formation of internal vesicles in endosomes and exosome release from multivesicular bodies. Question marks indicate unknown transporter identities. Image adapted from Nickel & Rabouille 2009.

1.4.1 Trypanosomatid secretion

There is evidence for the presence of both classical and non-classical secretion pathways in *Leishmania* (Cuervo *et al.* 2009; Silverman *et al.* 2008; Stierhof *et al.* 1994). The classical secretory pathway appears to be polarised and restricted to a small area of plasma membrane, the flagellar pocket (Figure 1-6), at the anterior

pole of the cell. The majority of uptake and secretion in *Leishmania* is thought to be confined to the flagellar pocket as there is a lack of microtubule attachment to the flagellar pocket membrane whereas the rest of the cell body is supported by closely spaced subpellicular microtubules which are believed to be prohibitive for membrane vesicle fusion or fission. This region is where the classical endocytic /exocytic machinery is found (McConville *et al.* 2002; Overath *et al.* 1997).

Classical secretion is mediated via the endoplasmic reticulum and the Golgi apparatus. The *Leishmania* endoplasmic reticulum (ER) is made up of functionally distinct domains (Figure 1-6), the nuclear envelope (NE), cortical ER and an extension of the ER, the transitional ER (tER). The tER has a ribosome-free membrane facing the Golgi and is thought to be essential in sustaining high levels of lipid and protein transport to the cell surface in rapidly dividing cells (McConville *et al.* 2002). Little is known about the unusual organelle, the lysosome-multivesicular tubule, thought to be a site where the endocytic and secretory pathways converge. The secretion of proteins such as secretory acid phosphatase and GP63 have been shown to be Rab1-mediated in *L. donovani*, a GTPase which localises to the Golgi and facilitates the conventional secretory pathway (Bahl *et al.* 2015).

Non-classical secretion has been proposed for the targeting of hydrophilic acylated surface proteins (HASPs) in *Leishmania*. These proteins have been detected at the flagellar pocket and extracellular plasma membrane of the parasites but lack the classical N-terminal signal sequence for secretion. Although the exact translocation mechanism is unknown, adding the N-terminal region of HASPB to GFP was sufficient to target it to the exterior cell surface and as this domain was found to direct both N-myristoylation and palmitoylation, the protein export was determined to be acylation-dependent (Denny *et al.* 2000; Stegmayer *et al.* 2005). Furthermore, the acylation process, addition of fatty acid moieties such as myristate and palmitate to proteins, was found to be essential for the survival and infectivity of trypanosomatids as genetic knockout of N-myristoyltransferase compromised virulence (Goldston *et al.* 2014).

An exosome-based secretion mechanism has also been suggested in *Leishmania* (Hassani *et al.* 2011; Silverman *et al.* 2008, 2010a). This was initially proposed after

the visualisation of membrane vesicles on the entire surface of the parasite by scanning electron microscopy (SEM), the collection and analysis of which showed that they contained proteins (Hassani *et al.* 2011; Silverman *et al.* 2008). The exocytosis of vesicles from the entire parasite surface, however, was considered unlikely due to the subpellicular corset as mentioned above, and the appearance of these vesicles in the SEM images may be artefactual as a result of sample preparation, or an example of apoptotic blebbing due to cell stress. Despite this, exosomal proteins and intact exosomes have been identified in the spent media of these parasites, indicating that this process is occurring whether from the flagellar pocket or from the entire surface of the parasite. There is additional evidence for the subpellicular microtubules not constituting a barrier to exocytosis. The ER has been shown to associate with the plasma membrane in *Leishmania* which demonstrates passage through the microtubule corset (Pimenta & de Souza 1985). Additionally, other pathogens, for example *Toxoplasma gondii*, have a stable cortical cytoskeleton which was thought to inhibit accessibility to the plasma membrane. However, dense granules have been found to penetrate the cortical skeletal complex to secrete their contents (McConville *et al.* 2002; Ngô *et al.* 2000). Therefore bulk secretion of exosomes may represent another method of *Leishmania* secretion, not previously described or thought to occur (Hassani *et al.* 2011; Silverman *et al.* 2008, 2010a; Silverman & Reiner 2012).

Figure has been removed due to Copyright restrictions.

Figure 1-6 Schematic of secretory and endocytic organelles in *Leishmania mexicana* promastigotes. The nuclear envelope (NE) and cortical endoplasmic reticulum (ER) are connected to the specialised transitional ER (tER). These are in close proximity to the Golgi apparatus (G) and flagellar pocket (fp). Early endosomes (EE) and multivesicular bodies (MVBs) are also pictured, anterior to the highly unusual lysosome-multivesicular tubule (L-MVT) which spans the length of the parasite. Adapted from McConville *et al.* (McConville *et al.* 2002).

1.5 Proteomics

The proteome comprises all proteins encoded by a genome within a cell, tissue or organism. The proteome has additional complexity compared to the genome due to its dynamic nature, responding to change in genetic and environmental factors and cues, intensified by the occurrence of post translational modifications of the proteins themselves. The overarching goal of modern proteomics is to identify and quantify all, or as many as possible, of the proteins associated with a particular state, metabolic snap-shot or dynamic change of an organism or a cell type evoked by a specific environment, chemical treatment, or altered cell phenotype. Moreover, the dynamic range of protein abundance within many proteomes make protein studies even more challenging.

1.5.1 Gel-based proteomics

Traditional proteomic approaches utilise gel-based methods for protein separation and visualisation. Outlined by Laemmli (1970), sodium dodecyl sulphate polyacrylamide gel electrophoresis (SDS-PAGE) is a common method for separating proteins by electrophoresis using a discontinuous polyacrylamide gel as a support medium and sodium dodecyl sulphate (SDS) to denature the proteins. Proteins are separated according to size. Although SDS-PAGE is relatively easy to use and has low cost, it has low resolution, low accuracy and samples of high complexity are unable to be adequately separated.

To overcome the constraints of SDS-PAGE, researchers moved to 2-dimensional gel electrophoresis (2-DE), pioneered by O'Farrell (1975). This technique separates proteins from complex samples based on both their isoelectric points and molecular weights. In the first dimension, proteins are separated by their isoelectric point (pI) by isoelectric focusing (IEF) and in the second dimension they are separated by their molecular weight by SDS-PAGE. After separation, proteins can be visualised, cut out of the gel, and identified by mass spectrometry (MS) following enzymatic processing and chromatography separation. Digestion with trypsin creates peptides that can be replicated *in silico*. For comparative purposes, samples are loaded on separate gels and protein spot patterns and spot intensities are compared visually using 2D gel analysis software. Despite its powerful resolving capabilities, the 2-DE technique lacks reproducibility and is laborious (Delahunty & Yates III 2005).

Additionally, there are several challenges for automatic software-based analysis such as incompletely separated (overlapping) spots, weak spots/noise, running differences between gels, as well as unmatched or undetected spots (Westermeier *et al.* 2008). Nevertheless, many researchers employ 2-DE coupled with MS as a standard protocol of proteomics, where automated in-gel digestion of protein spots is subjected to subsequent identification of the proteins by MS.

To overcome issues with reproducibility and gel to gel variation, difference gel electrophoresis (DiGE) can be employed. Proteins from different samples can be labelled with different size-matched, charge-matched spectrally resolvable fluorescent dyes (e.g. Cy3, Cy5, Cy2) and then mixed, making it possible to directly compare different samples on a single gel. Interesting spots with differential fluorescent intensity between the dyes are cut from a preparative gel, run in parallel to the analytical gel, after staining with Coomassie Blue in order to allow protein identification by MS analysis (Westermeier *et al.* 2008). Limitations of this method include: it is a time-consuming technique, and limited sensitivity, which as a consequence, proteins with a low concentration may fail to be selected for further analysis and subsequently missed (Ünlü' *et al.* 1997). It requires large amounts of protein sample for adequate identification by MS and for required replicates, along with multiple sample preparation steps which can result in loss of sample (Anand *et al.* 2017).

1.5.2 Gel-free proteomics

Gel-free proteomic methods and technologies are typically employed in studies dealing with complex protein samples, where gel approaches are unsuitable for the analysis of low concentrations of proteins within the sample to minimise protein loss. These methods typically employ direct proteolysis of the sample to produce peptides, followed by chromatographic separation coupled with MS analysis of the peptides, without prior in-gel separation.

Shotgun Proteomics

Shotgun proteomics is the untargeted analysis of a proteome, whereby in theory, the entire proteome is sampled and analysed. In shotgun proteomics, the aim is to provide an untargeted analysis of a proteome, following protein digestion into

peptides, which can then be separated using LC and analysed using MS (Matallana-Surget *et al.* 2010). Peptide digestions use proteolytic enzymes, typically trypsin which has high cleavage specificity, cleaving exclusively at arginine and lysine residues, to digest proteins into peptides before MS analysis. This allows a database of protein sequences of the target organism to be experimentally cleaved *in silico*, allowing fragmentation spectra to be matched to expected values. In Multidimensional Protein Identification Technology (MudPIT), complex proteome samples are enzymatically digested with the creation of a large number of peptides which are then separated by 2-dimensional liquid chromatography (LC) before being analysed using MS/MS (Wolters *et al.* 2001).

Liquid Chromatography (LC)

LC is used for separation of peptides following proteolysis. It is employed to reduce complexity in samples as many discrete peptides can have similar molecular masses, producing a single peak of overlapping peptides in the MS spectrum (Karpievitch *et al.* 2010). It also increases the overall dynamic range of the peptides measured. Separation of peptides is typically carried out by reversed phase (RP) chromatography using C18 columns. However, strong cation exchange (SCX) chromatography can be utilised prior to RP to increase the separation of peptides in a 2-dimensional liquid chromatography analysis.

Ionisation and mass spectrometry (MS)

After peptide separation using LC, MS can be used in to determine the accurate mass of the peptides in the fractions, thus creating a peptide mass fingerprint. The initial stage of MS is ionisation. Different methods of ionisation exist with electrospray ionisation (ESI) commonly employed. ESI results in charged molecular ions of peptides in a gas-phase created from highly charged liquid solvent droplets and a high electric field. These ions then pass into the mass spectrometer. Following ionisation, a mass analyser coupled with a detection system, detects charged species and can resolve ions according to their mass to charge ratio. Furthermore, tandem mass spectrometry (MS/MS) can be utilised, whereby ions are formed and analysed in the first instant by mass to charge ratio, but the most abundant precursor ions are then selected and fragmented by collision induced

dissociation or other means and then detected. Peptide sequencing is then possible in comparison to a parent peptide library of known proteins via database searching

1.5.3 Quantitative MS-based proteomics

Quantitative proteomics aims to not only identify proteins in a given proteome but provide quantitative analysis between proteins present. This allows for changes in protein abundance to be studied, for example in response to environmental or genetic changes, such as drug treatment or between different cell phenotypes.

Label-free quantitation is a relatively straightforward method for performing quantitative proteomics as it does not require any labelling of proteins. Consequently, it is more cost-effective and sample preparation is less time consuming than with label-based methods. The quantitation in label-free approaches comes from recording precursor signal intensity or spectral counting, whereby the signal intensity of a peptide precursor ion is measured or the number of fragmentation spectra are counted, respectively (Anand *et al.* 2017; Wong & Cagney 2010). The exponentially modified protein abundance index (emPAI) is a spectral counting quantification method, where, in simplified terms, the number of observed peptides is divided by the number of theoretically observable tryptic peptides for each protein (Ishihama *et al.* 2005). There are many other methods of label-free quantitation, and their strengths lie in their ability to be applied to any proteomics sample. A disadvantage of LFQ is run to run variation as samples are run separately, resulting in low replicate precision. Technical variation in the preparation of samples must be kept to an absolute minimum as there is no sample combination in this method. LFQ also requires more instrument time with the addition of more comparisons, unlike label-based methods which can be multiplexed.

Label-based quantitation approaches involves the incorporation of stable-isotopes into one or more of the samples being investigated. Labels such as ^3H , ^{13}C , ^{15}N and ^{18}O are chemically or metabolically incorporated into peptides or proteins. These isotope labels can then be detected and enable discrimination between labelled and unlabelled proteins. Through calculation of the label ratio, quantitation can be achieved and information regarding protein abundance can be generated.

One approach is Stable Isotope Labelling by Amino acids in Cell culture (SILAC). This approach incorporates stable-isotope-labelled amino acids into the cell culture medium to metabolically label the cells (Ong & Mann 2007). Dimethyl labelled, extracted proteins are digested with trypsin and differentially labelled with formaldehyde or deuterated formaldehyde. Chemical reductive amination of all primary amines, the N-terminus and ϵ -amino groups of L-lysine residues, is performed (Hsu *et al.* 2003). Differentially labelled peptide samples are subsequently combined and analysed by MS/MS. The labelling generates a mass increase of 28 Da and 36 Da in the light- and heavy-labelled peptides, respectively. Since stable isotope dimethyl labelling occurs at the peptide level, and not at the protein level as the SILAC labelling does, the sample preparation is prone to the introduction of more technical errors which could result in possible sample loss and variability. SILAC allows sample combination at the protein level which in theory should provide more precise and reproducible quantitative results. Other label approaches include Isotope-coded affinity tags (ICAT) (Gygi *et al.* 1999), and isobaric tags such as Isotope tags for relative and absolute quantification (iTRAQ) (Ross *et al.* 2004), or tandem mass tags (TMT™) (Thompson *et al.* 2003), whereby peptides are labelled with tags of the same nominal mass which cleave during fragmentation producing reporter ions with differing mass allowing quantitation in in MS/MS spectrum. This approach provides a more accurate quantitative comparison between replicates than other previously described approaches.

1.5.4 Secretomics

Secretomics is the study of all the proteins and small molecules secreted by a cell. The term secretome was first used in the literature in 2000, and was used to describe all the genes in the *Bacillus subtilis* genome which were identified as containing a secretory signal peptide sequence (Tjalsma *et al.* 2000). In the absence of established proteomic methods to study secretomes, they were originally identified by genome-wide searches for secretory-signal peptide sequences. However, this did not take into account those proteins which are secreted by non-classical mechanisms. Additionally, genome-based and mRNA based studies are not always reliable measures of protein expression as there are always discrepancies between the levels of mRNA expression and respective protein expression. This is particularly relevant for *Leishmania* as the regulation of gene

expression in these parasites is largely post-transcriptional (Clayton 2002). Proteomics is therefore considered to be a more representative method of investigating the *Leishmania* secretome. Metabolomics is a complementary technique that could be applied alongside proteomics, to look for different types of secreted molecules and additionally with the possibility of assessing secreted enzyme function. Secretomics is a powerful technique in cancer studies in the search for secreted biomarkers and for investigations of cell-to-cell signalling and the molecular mechanisms of carcinogenesis (Lin *et al.* 2013; Xue *et al.* 2008). Further to this, secretomics is also used to identify secreted virulence factors in the search for drug and vaccine targets for pathogens such as parasites and bacteria (Antelmann *et al.* 2001; Braga *et al.* 2014).

1.5.4.1 Secretomic studies in *Leishmania*

Several secretomic studies have been performed for global analysis of protein secretion in *Leishmania*. These analyses comprise promastigote exoproteomes of *L. donovani* (Silverman *et al.* 2008), *L. braziliensis* (Cuervo *et al.* 2009), *L. mexicana* (Hassani *et al.* 2011) and *L. infantum* (Braga *et al.* 2014; Santarém *et al.* 2013b), performed using exponential phase (Braga *et al.* 2014; Cuervo *et al.* 2009), and stationary phase (Hassani *et al.* 2011; Silverman *et al.* 2008) promastigotes. Relatively few classically secreted proteins were detected in the exoproteome of *Leishmania*, with only ~5% containing a classical secretion signal in *L. braziliensis* (Cuervo *et al.* 2009), 9% in *L. donovani* (Silverman *et al.* 2008), and 6% in the *L. infantum* secretome (Braga *et al.* 2014), demonstrating that alternative secretion mechanisms must be used by the parasites. Known eukaryotic exosomal proteins were also detected from *L. donovani*, which suggests a method of vesicle-based secretion (Silverman *et al.* 2008). A comparative analysis of three of the secretome studies found that the average molecular weight per protein is lower than in the intracellular proteomes. The average isoelectric point of the exoproteomes is also lower than in the proteomes of the parasites (Peysseon *et al.* 2013). Bias towards a lower pI could indicate their increased stability in the acidic conditions of the PV, and their lower molecular weight would facilitate their secretion.

The exoproteomes in all but one of these studies were obtained by a short incubation in serum-free growth media (Braga *et al.* 2014; Cuervo *et al.* 2009;

Hassani *et al.* 2011; Silverman *et al.* 2008). There are inherent problems associated with this method, however. These stressful conditions may modify the secretome and cause a different protein profile as would be seen *in vivo* and may additionally induce cell death and introduce intracellular protein contamination into the culture media. It is therefore essential to minimise these stresses as far as possible by assessing and reducing incubation times in the serum-free media and slowing centrifugation speeds to obtain the cell-free spent media. The studies all attempt to monitor and quantify the amount of cell death in the cultures to exclude any low levels of intracellular proteins contamination from the analysis. This was done by a combination of cell viability monitoring by cell counting or flow cytometry, intracellular marker enzymatic assays, for example using glucose-6-phosphate dehydrogenase (Silverman *et al.* 2008) and exclusion from the proteomic data proteins which fell below a threshold set by the abundant intracellular contaminant histone H2B (Silverman *et al.* 2008).

Global functionality was also assessed in some of the studies, for example by exposing the *L. mexicana* temperature-induced exoproteome to macrophages. This induced cleavage and activation of some host proteins, and also inhibited nitric oxide production (Hassani *et al.* 2011).

1.5.4.2 Secretion of exosomes

As mentioned above, there is compelling evidence for the existence of bulk exosome secretion in *Leishmania* and Trypanosoma species (Atyame Nten *et al.* 2010; Silverman *et al.* 2010a). Hassani *et al.* observed budding of surface exovesicles in response to an increase in temperature from *L. mexicana* promastigotes (Hassani *et al.* 2011). This observation gives rise to a potential function of promastigote exosomes for priming of macrophages after entry to the host in the sand fly bite and the subsequent change in environmental conditions. Secretion of exosomes containing GP63 and EF-1 α by *Leishmania* were found to influence the macrophage response (Silverman & Reiner 2012). The exosomes were shown to directly interact with naïve host cells (Silverman *et al.* 2010a) and have immunomodulatory properties such as promoting enhanced IFN- γ induced IL-10 production to direct macrophage activation towards an infection-promoting profile (Figure 1-7) (Silverman *et al.* 2010a; Silverman & Reiner 2012).

Figure has been removed due to Copyright restrictions.

Figure 1-7 Schematic of proposed outcomes of *Leishmania* promastigote exosomal secretion. Promastigote exosomes containing GP63 and EF1 α play an immunomodulatory role by directing macrophage activation towards an anti-inflammatory response. Image adapted from Silverman & Reiner, 2012(Silverman & Reiner 2012)

1.6 Summary and Aims

To summarise, it is evident that both life cycles stages of *Leishmania* secrete effectors which play many different roles in parasite survival in the host, from immunomodulation, to nutrient salvage, to physical modification of the PV. In many cases, particularly with the amastigote stage, the modulatory effect the parasite has on the host cell has been deduced but the parasite-derived mechanism or effector has not yet been identified and our knowledge of these amastigote-host interactions is still very limited.

In addition to furthering our knowledge on the cell biology of these parasites and their interactions with the mammalian host, particularly in the medically relevant disease-causing stage, studying factors secreted by the pathogen is highly significant, as exogenous factors represent a source of antigens for the development of vaccines, and essential and parasite-specific proteins and pathways are potential targets for drug development.

The overall aim of this project is to identify mechanisms by which *Leishmania* promastigotes and amastigotes might enhance their nutritional environment, their surroundings for survival or augment macrophage signalling by examining the secretion of proteins. Following on from previous secretomics work on promastigotes of *L. donovani*, *L. braziliensis*, *L. mexicana* and *L. infantum* (Braga *et al.* 2014; Cuervo *et al.* 2009; Hassani *et al.* 2011; Santarém *et al.* 2013b; Silverman *et al.* 2008), these methods will be utilised and adapted to define the secretome of axenic amastigotes to begin to understand the mechanisms by which amastigotes may modify their niche within the macrophage by secretion of proteins. The secretome of promastigotes and amastigotes will be isolated to facilitate a comparative analysis which should illustrate the hypothesised differences between the two lifecycle stages due to their inherent differences in environment and target proteins. Furthermore, comparison of the secretome of parasites with differing phenotypes with respect to virulence and disease outcome will shed light on key secreted effectors in parasite pathogenicity.

Chapter 2 Materials & Methods

2.1 Materials

All reagents and chemicals were purchased from Sigma-Aldrich, Dorset, UK, unless stated otherwise.

2.2 Parasite culture

The species and strain of *Leishmania* used in this study was *L. mexicana* M379. For storage, mid log phase promastigotes in culture were cryopreserved 1:1 in 70% heat-inactivated foetal bovine serum (HiFBS) (Life Technologies) / 30% glycerol. Promastigote parasites were recovered and cultures were expanded in haemoflagellate minimal essential medium (HOMEM) (GE Healthcare) supplemented with 10% FBS (cHOM) at 25°C, and maintained in logarithmic phase culture by routine passage every 2-3 days. Axenic amastigotes were cultured in Schneider's Drosophila Medium (Gibco) adjusted to pH 5.5 supplemented with 20% FBS and 3ml of 2.5mg/ml haemin in 50mM NaOH (cSDM). Amastigotes are transformed from promastigotes by placing 1 x 10⁶ cells/ml late log/stationary phase promastigotes in cSDM and incubating at 32°C with 5% CO₂, and were maintained in culture by weekly passage. For experiments using defined growth media (NM, (Nayak *et al.* 2018)), the parasites were washed 3 times to remove residual serum and sub-cultured into the defined growth medium. Parasite growth was monitored by counting using a haemocytometer by diluting 1:1 in 2% formaldehyde, followed by placing 10 µl of the fixed cells on a Neubauer haemocytometer. Following cell counting, a parasite growth curve could be formulated by plotting cell number vs. culture time.

$$\text{Doubling time} = \frac{\text{duration} * \log(2)}{\log(\text{FinalConcentration}) - \log(\text{InitialConcentration})}$$

Parasite viability was assessed by counting before and after 4 h serum-free incubation using the Trypan Blue dye exclusion method as previously described (Cuervo *et al.* 2009). The cells were counted using a haemocytometer, as described above.

2.3 Alamar blue assay

An alamar blue metabolic assay was also employed to quantify the viability of the parasites after incubation in the medias, using a modified transformation assay (Jain *et al.* 2012). Briefly, viable axenic amastigotes were cultured in cSDM and prepared by washing in PBS and sfSDM. The parasites were then split to the same density across four medium types and incubated in a 96-well plate for 4 hours at 32.5°C. After incubation, the amastigotes were recovered from the medias by centrifuging and the medium replaced with cHOM to transform any live amastigotes to promastigotes. The plate was then incubated at 25°C for 48 hours. Parasite viability was evaluated by the addition of 10 µl resazurin dye, followed by incubation for a further 24 hours. Plates were read for standard fluorescence using a PHERAstar FSX microplate reader (BMG Labtech) at 544 nm excitation, 590 nm emission.

2.4 Secreted protein isolation

For secretion assays, ~5-10 x 10⁹ parasites were harvested from two 150 ml late log / stationary phase cultures by centrifugation at 1000 ×g for 10 min in a bench top centrifuge. The parasite pellet was then washed three times to remove residual serum using pre-warmed PBS by centrifuging as above. The parasites were resuspended to a density of 1 x 10⁸ cells/ml in pre-warmed serum-free media and incubated for 4 h at 25°C or 32°C with 5% CO₂ for promastigote and amastigote cultures, respectively. Secreted parasite proteins in the spent culture supernatant were isolated by pelleting the parasites at 700 ×g for 20 min at 4°C in a bench top centrifuge. The supernatant was collected, kept on ice and protease inhibitors were added (E64 10 µM E64, 5 µg/ml Pepstatin A, 2 mM 1,10-phenanthroline, 500 µg/ml Pefabloc, 100 µg/ml leupeptin, 1 mM EDTA). The supernatant was then further clarified by centrifugation at 3200 ×g for 30 min at 4°C in a bench top centrifuge.

The proteins in the supernatant fraction were then concentrated down to 10 ml using Vivaspin® 20 10 kDa MWCO centrifugal filters (Vivaproducts, Littleton, MA, USA), by loading 14 ml at a time and centrifuging at 8000 ×g, 4 °C, in a Heraeus™

Megafuge™ bench top centrifuge with fixed rotor (Thermo Scientific, Waltham, MA, USA) for 45 min and then reloaded.

As an alternative protein concentrating method, a carrier assisted TCA method was utilised. The clarified supernatant was kept on ice and then 10% (w/v) sodium lauroylsarcosinate solution (sarkosyl and dH₂O) was added to a final concentration of 0.1% and mixed by vortexing briefly. Ice cold 100% (w/v) TCA solution (TCA and dH₂O) was then added to a final concentration of 7.5% and incubated on ice for 2 h. Following incubation, the mixed protein-detergent precipitate was centrifuged at 10 000 xg for 10 min, 4 °C using a bench top centrifuge. The supernatant was then removed and the protein pellet washed with tetrahydrofuran by resuspending in 10 ml of ice-cold tetrahydrofuran by vortexing. This wash was then repeated leaving a protein pellet. Finally, the pellet was dissolved in 100 µl 1x laemmli buffer (2% SDS, 10% Glycerol, 62.5 mM Tris-Cl pH 6.8), using bath sonication for 30 min.

Acetone precipitation was performed by addition of four times sample volume of -20°C acetone and incubation at -20°C for >1hr to overnight. The resulting precipitate was pelleted by centrifugation at 10,000 xg for 10 min at 4 °C. The pellet was washed in 80% acetone in dH₂O at -20 °C and pelleted again as above.

2.5 Whole cell protein lysate collection

The cell pellets from the spent media collection are also retained and used to produce whole cell lysate samples. After pelleting and supernatant removal, the cells were washed twice in 1x PBS and collected by centrifugation at 1000 xg for 10 min at 4 °C in a bench top centrifuge. The cells were then lysed by resuspension in 1x laemmli buffer with protease inhibitors (2% SDS, 10% Glycerol, 62.5 mM Tris-Cl pH 6.8, 200 mM DTT, 2 mM 1,10-Phenanthroline, 1 mM EDTA, 10 µM E-64, 500 µg/ml Pefabloc, 100 µg/ml leupeptin, 5 µg/ml Pepstatin A) and probe-sonicated on ice for 1 sec, 3 times. The protein extracts were then clarified by centrifugation at 14,000 xg for 10min at 4 °C using the Heraeus™ centrifuge described above and precipitated in 100% acetone as described above, followed by two washes in 80% acetone and stored at -20 °C .

2.6 Protein assay

For measurement of the secretome protein concentration, the Biorad DC Protein Assay was used in conjunction with the low-concentration assay (Table 2-1), adapted for use with the Nanodrop spectrophotometer.

Protein assay standards ranging from 5-250 $\mu\text{g}/\text{ml}$ protein were made using BSA in 1x RIPA buffer. Only 4 μl of sample or standard are required per assay, which is mixed with a reagent mix and then absorbance measured at 750 nm, from triplicate samples.

Table 2-1 Detergent compatible (DC) Protein Assay (BioRad) recommended concentrations and reagent volumes.

Protein Concentration	Test Tube	Microplate	Nanodrop
High-concentration assay	0.2-1.5 mg/ml protein	0.2-1.5 mg/ml protein	-
	100 μl sample	5 μl sample	-
	500 μl reagent A	25 μl reagent A	-
	4.0 ml reagent B	200 μl reagent B	-
Low-concentration assay	5-250 $\mu\text{g}/\text{ml}$ protein	5-250 $\mu\text{g}/\text{ml}$ protein	5-250 $\mu\text{g}/\text{ml}$ protein
	200 μl sample	20 μl sample	4 μl sample
	100 μl reagent A	10 μl reagent A	2 μl reagent A
	800 μl reagent B	80 μl reagent B	16 μl reagent B

2.7 1D SDS-PAGE

For 1-dimensional gel electrophoresis, protein samples were mixed 1:4 with 4x laemmli sample buffer with protease inhibitors (2% SDS, 10% Glycerol, 62.5 mM Tris-Cl pH 6.8, 200 mM DTT, 2 mM 1,10-Phenanthroline, 1 mM EDTA, 10 μM E-64, 500 $\mu\text{g}/\text{ml}$ Pefabloc, 100 $\mu\text{g}/\text{ml}$ leupeptin, 5 $\mu\text{g}/\text{ml}$ Pepstatin A). Following this, 0.002% bromophenol blue was then added to each sample and the protein samples and molecular weight (MW) marker (New England Biolabs, Ipswich, MA, USA) were then heated to 60°C for 5 min to denature. ~10 μg of protein was then separated by SDS-PAGE using 4-20% gradient polyacrylamide gels (BioRad) run at 40 mA per gel using the Mini-PROTEAN TetraCell system (BioRad). After running, the gels were washed in Milli-Q® deionised water (ddH₂O) to remove residual SDS, and stained with colloidal Coomassie G-250 according to Kang's method for increased sensitivity (Dyballa & Metzger 2009). Coomassie stained gels were imaged using a

G:Box (SynGene, Cambridge, UK) with combined transilluminator and upper white light, and GeneSnap software (SynGene). Or gels were stained using the Pierce™ Silver Stain Kit (Thermo Fisher) according to the manufacturers instructions.

2.8 Western blotting

Antibodies to *Leishmania* HASPB, EF1a and OPB were kindly gifted by Prof. Jeremy Mottram, U of York. Antibodies to *Leishmania* GP63 monoclonal and polyclonal antisera, secretory acid phosphatase and cysteine protease were kindly gifted by Dr Martin Wiese, U of Strathclyde. Antibodies to ENO, GDH and B-Tub KMX were kindly gifted by Prof Michael Barrett and Dr Tansy Hammarton, U of Glasgow.

For Western blot analysis of secreted material, 0.3 µg of secretome in LDS sample buffer (Expedeon) was resolved on 4-20% RunBlue SDS protein gels using a TEO-tricine-based buffer system (RunBlue™, Expedeon). Samples were then transferred to a PVDF membrane and membranes blocked with 5% skimmed milk powder in PBS-T (0.05% Tween 20) prior to probing with primary antibodies. Bound antibody was detected using anti-mouse, anti-sheep or anti-rabbit secondary antibodies conjugated to horseradish peroxidase (Invitrogen). Membranes were imaged using the Pierce™ ECL Plus Substrate (Thermo Fisher) and chemiluminescence imager.

2.9 2D electrophoresis

Here, 2 types of 2D electrophoresis were performed, namely: difference gel electrophoresis (DiGE), for the comparison of two proteomes; and preparative gels.

2.9.1 Gel casting using the Ettan DALT system

To cast the 24 cm acrylamide gel, first the bottom gel plate was treated with a 1:1000 dilution of bind-silane solution (bind-silane in ethanol/acetic acid/dH₂O). The solution is rubbed on the surface of the plate until dry after which the plate is left to further air dry for 1 h. Following drying the plates were polished with 70% ethanol and then left to air dry for 30 mins. Once the plates were dry the plates were placed and aligned together. White guide spots were placed over the spot markers on the inside of the plate.

The acrylamide was prepared in dH₂O and stored at 4°C. All reagents were then mixed and filter sterilised prior to use. To cast the gels, an Ettan DALT gel casting tank was used to cast up to 6 gels at once. Immediately prior to casting, the temed was added to the acrylamide mixture and mixed by inversion. Following this the acrylamide mixture was poured into the casting tank. After pouring the acrylamide, 1ml of water saturated butanol was pipetted in between the plates of all six gels on top of the acrylamide, providing a thin protective layer on top of the gel to level the acrylamide. The gels were then left to polymerise for 2 h after which the tank was dismantled and excess gel was removed from the outside of the plates. Plates containing the gels were kept wet and stored at 4°C prior to using.

2.9.2 Difference gel electrophoresis (DiGE) sample preparation

Samples were initially thawed on ice. To check the pH of the samples was within the alkaline range, required for DiGE to be successful, the Litmus test was performed by placing a small aliquot of sample onto a piece of Litmus paper. For DiGE, 10µl of each sample to 1 µl CyDyes was used to allow for the correct ratio of protein to dye. If the samples were too concentrated they were diluted before use to ~5 µg/µl in rehydration buffer. 50 µg of each sample was therefore added into the appropriate CyDye. Following incubation with the CyDyes, 1 µl of lysine was then added to each tube and incubated for 10 minutes to quench the reaction. Samples were then ready for IPG strip rehydration.

For isoelectric focussing, samples were prepared by placing the sample into a fresh Eppendorf and making up to a total volume of 460 µl with rehydration buffer.

Preparative gels were run simultaneously by adding 250 µg of each protein sample to be separated and compared on one gel, into a fresh Eppendorf and mixed by vortexing (250 µg of protein sample 1 + 250 µg of protein sample 2 = 500 µg of total protein). The total volume was made up to 460 µl with rehydration buffer.

2.9.3 Isoelectric focussing (1st dimension)

IPG strips were stored at -20°C. When required for use the strips were placed in strip coffins where protein samples with rehydration buffer were distributed evenly along the length of the strip. A coffin lid was then placed on top and the coffin was

incubated at room temperature for 30 mins to allow rehydration. After incubation the strips were overlaid with 1 ml of mineral oil (dry strip cover fluid). The coffins containing the strips were then placed in the IPGphor isoelectric focusing unit set to reach a maximum of 80,000 volt/hours. Isoelectric focusing was performed in the dark due to the light sensitivity of some samples. Following isoelectric focussing the strip was removed from the coffin using forceps and blotted to remove excess mineral oil. The strip was washed by dunking in 1x running buffer twice.

To equilibrate the strips following isoelectric focusing, the strips were placed into a strip tube and 10 ml of SEB with DTT (10 mg/ml) was added. The tube was then shaken on its side ensuring complete coverage of the strip at 75 RPM for 15 mins. After equilibration the SEB+DTT was poured off and replaced with 10 ml SEB with IAA (25 mg/ml), and shaken again for 15 mins.

2.9.4 Molecular weight separation, SDS-PAGE (2nd dimension)

For the second dimension, molecular weight separation the IPG strip is placed along the runway of a gel plate containing a cast gel. The strip was then pushed down to make contact with the DALT gel edge. 1 ml of agarose was then used to seal the strip onto the top edge of the gel. Following strip attachment to the gels the gels were placed in the running tank containing 1x running buffer. The gels were run in darkness if samples were light sensitive, as in the case of DiGE samples. The gels were run over night until the dye front reached the bottom of the gel. Following separation, gels were stored moist at 4°C until analysis. If gels were required to be stained and imaged, for example preparative gels, the plates were separated and the gel bound to the bottom plate was placed in fixing solution. Once fixed the gel was stained with either Coomassie or Sypro orange.

2.9.5 Gel imaging

Images of the gels were taken with the Typhoon 9400 Series Variable Mode Imager using the following settings: for Cy3, 532 nm excitation laser and 580 BP 30 emission filter; for Cy5, 633 nm excitation laser and 670 BP 30 emission filter. The resulting images were processed using DeCyder Differential Analysis software v5.0. The experimental design and relationship between samples was assigned in DeCyder.

The protein spots were filtered to include only proteins that demonstrated a significant change in abundance ($p < 0.005$).

2.10 Spot Picking and Processing

Protein spots were selected and automatically picked from the preparative and DiGE gels using the Ettan spot picker (GE Healthcare). Spots were stored in ddH₂O until processing. Following protein spot picking, the dH₂O was removed and the gel pieces were washed in 50 μ l of 100 mM ammonium bicarbonate and then 150 μ l of 50% acetonitrile/100 mM ammonium bicarbonate, each for 1 h, at room temperature, shaking at 120 RPM, on a bench top shaker. After discarding the final wash, the gel pieces were then shrunk by adding 50 μ l of acetonitrile for 10 mins. The solvent was then removed and the gel piece was dried in a vacuum centrifuge (SPD1010 SpeedVac, Thermo Scientific). A vial of trypsin was resuspended in 1 ml of 2 mM ammonium bicarbonate. Sufficient trypsin, 10 μ l at a time, was added to the dried gel pieces in order to rehydrate the gel. Once the gel piece had appeared fully hydrated and swollen to its previous size the digest sample was incubated for 12 h at 37 °C. Following incubation, all liquid from the protein digestion was transferred to a fresh V-bottom 96 well sample plate. To this 20 μ l of 5% formic acid was added to the gel pieces and incubated for 20 mins on a bench top shaker set at 75 RPM. After incubation 40 μ l of acetonitrile was added to the formic acid and incubated once again on the shaker for a further 20 min. after 20 mins all liquid was transferred to a fresh plate. Samples were pooled if previously separated. Samples were then dried down in a vacuum centrifuge as above and stored at -20 °C until analysis.

2.11 Trypsin digestion

The gel-free protein samples were processed for LC-MS/MS analysis using the filter-aided sample preparation (FASP) method (Expedeon). The protein samples solubilised in 1x Laemmli buffer with DTT, were heated at 60 °C for 5 min to denature and reduce the proteins. ~100 μ g of protein was then loaded into a 30 kDa MWCO filter (Microcon YM-30) and centrifuged at 14,000 \times g for 15 min. The proteins are washed and buffer exchanged on the membrane with 200 μ l 8 M urea in 0.1 M Tris-HCl pH 8.5 followed by centrifugation as above. The proteins are then alkylated

by adding 0.05 M iodoacetamide prepared in urea buffer and incubated for 20 min, in the dark. The iodoacetamide is then removed by further centrifugation and washing twice with fresh urea buffer. The proteins are then washed three times in 100µL of 50mM ammonium bicarbonate (ABC) and centrifuged at 14,000 × g for 10 min. Trypsin is then added to the samples at an enzyme-to-protein ratio of 1:100 and digested for 24 h at 37°C. After digestion, the filter units were transferred to new collection tubes and the tryptic peptides recovered by adding 40µl of 50mM ABC followed by centrifugation at 14,000 × g for 10 min. Any filter-bound peptides were washed out by adding 50µl of 10% acetonitrile (CAN) to the unit followed by centrifugation at 14,000 × g for 10 min. This step eliminates the need for desalting of the peptides and the samples can be immediately dried down in the wells of a 96-well plate ready for LC-MS/MS analysis.

2.12 TMT™ Labelling

For multiplex relative quantitation by mass spectrometry, samples were differentially labelled using the TMT Mass Tagging kit from Thermo Scientific, as per the manufacturer's instructions with some modifications. Reagents were prepared by equilibrating to room temperature. 41 µL of anhydrous acetonitrile was added per 0.8 mg of TMT tag reagent and allowed to dissolve for 5 minutes with occasional vortexing. 5% Hydroxylamine HCl was prepared by dissolving 50 mg of hydroxylamine HCl in 1 mL of 100 mM TEAB.

Briefly, equal concentrations of each protein sample were first buffer-exchanged and trypsin digested using the FASP kit from Expedeon as described in section 2.11. The resulting tryptic peptides for each sample were then resuspended in 100 µl 100 mM TEAB and 41 µL of the TMT Label Reagent was added to 25-100 µg of digested sample. The reaction was incubated for 1 hour at room temperature. The reaction was quenched by the addition of 8 µl of 5% hydroxylamine HCl per sample and incubated for a further 15 min. The differentially labelled samples could then be combined and 6 µg of sample mixture dried down using a SpeedVac (Thermo Scientific) for LC-MS/MS analysis. For peptide samples of 25 µg or less, the method was adjusted to resuspend the tryptic peptides in 50 µl of 100 µM TEAB, and 18 µl of TMT Label Reagent was added to the samples.

2.13 Peptide/protein identification by nLC-ESI-MS/MS

Following FASP to create tryptic peptides, samples were analysed using nanoflow HPLC coupled to electrospray tandem mass spectrometry (nLC-ESI-MS/MS). Peptides were solubilized in 0.05 % formic acid and fractionated on a nanoflow uHPLC system (Thermo RSLCnano) before online analysis by electrospray ionisation (ESI) mass spectrometry on an AmaZon ion trap MS/MS (Bruker Daltonics), or the Orbitrap Elite (Thermo Scientific) where specified.

Prior to analysis on the AmaZon Ion Trap, peptide separation was performed on a Pepmap C18 reversed phase column (LC Packings), using a 5 - 85% v/v acetonitrile gradient (in 0.1% v/v formic acid) run over 45 min at a flow rate of 300nl/min. Mass spectrometric (MS) analysis was then performed on the AmaZon Ion Trap using a continuous duty cycle of survey MS scan followed by ten MS/MS analyses of the most abundant peptides, choosing the most intense multiply charged ions with dynamic exclusion for 120s.

Prior to analysis on the Orbitrap Elite, peptides were desalted and concentrated for 4 min on trap column before being transferred to the analytical column using starting solvent conditions (4% solvent B). A water- acetonitrile gradient was used; 4 - 40% v/v solvent B from 12 - 102 min, 40 % to 100% v/v solvent B from 102.1 - 116 min, held at 100 % v/v solvent B 116 - 121 min and re-equilibrated at starting conditions (4 % solvent B) for a total time of 125 min. Solvent A - Water + 0.1% formic acid. Solvent B - 80% acetonitrile + 0.08 % formic acid. A fixed solvent flow rate of 0.3 μ L / min was used for the analytical column. The Orbitrap Elite acquires a high resolution precursor scan at 60,000 RP (over a mass range of m/z 400 - 2000), followed by CID fragmentation and detection of the top 20 precursors in the linear ion trap. Singly charged ions are excluded from selection, while selected precursors are added to a dynamic exclusion list for 180s.

For TMT-labelled samples, peptides were analysed by LC-MS/MS using the Orbitrap Elite. Peptides were desalted and concentrated for 4 mins on the trap column before being transferred to the analytical column using starting solvent conditions (5% solvent B). A water- acetonitrile gradient was used; 5 - 45% v/v solvent B from 4 - 154 min, 45 - 100% v/v solvent B 154 - 154.1 min, held at 100% v/v solvent B

154.1 - 160 min and then re-equilibrated at starting conditions (5% solvent B) for a total time of 165 mins. A fixed solvent flow rate of 0.3 $\mu\text{L}/\text{min}$ was used for the analytical column as before. The Orbitrap Elite acquired a high-resolution precursor scan at 60 000 RP (over a mass range of m/z 380 - 1800) followed by CID fragmentation and detection of the top 3 precursor ions from the MS scan in the linear ion trap. The 3 precursor ions were also subjected to HCD in the HCD collision cell followed by detection in the orbitrap. Singly charged ions are excluded from selection, while selected precursors are added to a dynamic exclusion list for 180s.

2.14 Mascot

The Mascot search engine was then used to search the resulting mass spectra against an in-house *Leishmania* protein database obtained from GeneDB to generate protein identities. Tandem mass spectra were submitted to database searching using the Mascot program (Matrix Science) (Cottrell 2011). Spectra were searched against the *Leishmania mexicana* database LmexicanaMHOMGT2001U1103 from TriTrypDB.org. Search criteria specified for AmaZon Ion Trap: Enzyme, Trypsin; Maximum missed cleavages, 1; Fixed modifications, Carbamidomethyl (C); Variable modifications, Oxidation (M); Peptide mass tolerance, 0.4Da; Fragment mass tolerance, 0.4 Da. Significance threshold set to 0.05. Search criteria specified for Elite Orbitrap: Enzyme, Trypsin; Maximum missed cleavages, 1; Fixed modifications, Carbamidomethyl (C); Variable modifications, Oxidation (M); Peptide mass tolerance, 0.4Da; Fragment mass tolerance, 0.4 Da. Significance threshold set to 0.05.

Only those identifications over the significance threshold of 0.05 and with a protein score of ≥ 30 were included in the protein list and analysis. The protein score is a number calculated by Mascot for every protein match and indicates the confidence of the match. Higher scores therefore indicate a more confident match. The score is formulated from the combined ion scores of each of the mass spectra matched to an amino acid sequence within the protein. These individual ion scores are based on the calculated probability, P , that the observed match between the experimental data and the database sequence is a random event, with a 95% confidence threshold. Peptide matches were excluded from the protein

identification when their p -value exceeded the significance threshold indicated for an FDR of 1%, or 2% where specified.

$-10 * \log_{10}(P)$ Where P is absolute probability.

2.15 Following TMT labelling

Proteome Discoverer™ (Thermo Fisher Scientific) was utilised for processing of the raw MS data to annotate and quantitate the peptides and the reporter tags. A strict FDR of 0.01 was set in the analysis of identified peptides.

2.16 Analyses of the *L. mexicana* secretome

Proteins were categorised by gene ontology (GO) using the annotations found in TriTrypDB (Aslett *et al.* 2010) (<http://tritrypdb.org/tritrypdb/>), and distributed into categories according to their assigned biological function. Proteins for which no annotation was assigned were placed in the unknown category or assigned based on sequence homology to annotated proteins in other *Leishmania* species or based on published data if known. Other predicted features of *Leishmania* proteins such as isoelectric point, molecular weight and transmembrane domains were also exported from the TriTryp Database. The SignalP 4.1 Server found at (<http://www.cbs.dtu.dk/services/SignalP/>) was used to predict the presence of signal peptides. SignalP predicts the presence and location of signal peptide cleavage sites in amino acid sequences from different organisms: Gram-positive prokaryotes, Gram-negative prokaryotes, and eukaryotes. The method incorporates a prediction of cleavage sites and a signal peptide/non-signal peptide prediction based on a combination of several artificial neural networks. Proteins with signal peptides are targeted to the secretory pathway, but are not necessarily secreted (Nielsen 2017). The SecretomeP 2.0 Server found at (<http://www.cbs.dtu.dk/services/SecretomeP/>) was used to predict non-classical secretion, with the scoring cut-off set to mammalian. Non-classically secreted proteins should obtain an NN-score / SecP score exceeding the threshold, but not at the same time be predicted to contain a signal peptide. The recommended thresholds are 0.5 for bacterial sequences and 0.6 for mammalian sequences.

Chapter 3 Method development for *Leishmania* secretomics

3.1 Introduction

Secretomics, as defined in Section 1.5.4 of this thesis, is an expanding area of research which has been applied to many different single and multicellular organisms, and cell types. Secretome studies have been applied to human cells in the study of various cancers with the subsequently derived secretome implicated in various disease pathologies (Lin *et al.* 2013; Makridakis & Vlahou 2010; Xue *et al.* 2008). Furthermore, in studies of pathogenic bacteria and parasites, the secretome has been shown to be involved in pathogenesis and is therefore a promising source of new therapeutic targets (Dwivedi *et al.* 2016; Hakimi & Bougdour 2015; Soni *et al.* 2016; Szempruch *et al.* 2016a). In *Leishmania*, secretome studies have been applied to investigate the host-parasite interaction in the insect vector, and upon parasite entry to the mammalian host, focusing on procyclic (Atayde *et al.* 2015; Braga *et al.* 2014; Cuervo *et al.* 2009; Santarém *et al.* 2013b) and metacyclic (Chenik *et al.* 2006; Hassani *et al.* 2011; Silverman *et al.* 2008) promastigote populations, respectively. There have been no studies to date on the secretome of amastigotes, the intracellular stage that resides in macrophages of the mammalian host.

3.1.1 Axenic cell culture in secretomic studies

Axenic cell culture systems are methods whereby only a single species or strain of cell or organism is present, and mimic as far as possible the *in vivo* environment of the organism (Hine & Martin 2015). These culture systems are particularly useful for creating a controlled environment in which to study intracellular pathogens, such as *Leishmania* amastigotes (Bates *et al.* 1992), free from the host cell. Axenic cell culture is highly amenable to secretome studies as it ensures there is no interference or interaction from different cell types, and allows ease of separating cells from the secretome using separation methods such as centrifugation. The methods used for secretome collection vary greatly between different secretome studies, dependent on the organism or cell type being investigated, discussed below. The methods vary in their starting concentration and number of cells, depending on the secretion yield of the cell type, collection method, concentration method and further processing. There are, however, problems that must be overcome for successful secretome isolation and characterisation.

3.1.1.1 Addition of an undefined supplement in cell culture

Previous secretome studies have highlighted issues with regard to studying the secretome (Chevallet *et al.* 2007). One of the main confounding factors is the addition of serum or other animal products, such as brain: heart infusion, to most culture media. These supplements introduce heterologous and undefined molecules to the extracellular environment such as proteins, electrolytes, lipids and hormones (Stein 2007). While the proteins in the supplements could theoretically be determined before addition to the media and excluded from secretome results during data analysis, they exhibit high batch to batch variation (Stein 2007), thus requiring analysis of every batch which is not feasible for routine secretome analyses. Another dominant issue is the fact that the abundance of specific proteins in these supplements is very high. As much as 6-10 mg/ml total protein has been reported in media supplemented with 10% serum (Broedel Jr. & Papciak 2003). The abundance of these serum proteins may be high enough to mask proteins of interest that are secreted, at a much lower concentration, from the cells under investigation. This is a problem particularly when using techniques such as Data-Dependent Acquisition (DDA) MS analysis to identify the secreted proteins, as this technique is confounded by dynamic range because only the most abundant peptides in each scan are selected for fragmentation and therefore identification (Doerr 2015).

3.1.1.2 Culturing without serum affects cell viability

One solution to these issues would be to remove undefined, protein-rich supplements from the media. However, many cell types cannot be maintained for any significant period of time in a serum-free medium. Suboptimal culture conditions may lead to cell stress, decreased proliferation and cell lysis, in turn altering the secretome and contaminating it with intracellular proteins (Alcolea *et al.* 2016). As such, previous secretome studies have used methodologies where cells are removed from their serum-containing medium, washed and placed into a serum-free medium for a short amount of time. The incubation time varies based on cell type, from 24-96 hours for many mammalian cell lines (Chevallet *et al.* 2007; Makridakis & Vlahou 2010) down to 2-8 hours for *Trypanosoma* and *Leishmania* species (Atyame Nten *et al.* 2010; Braga *et al.* 2014; Cuervo *et al.* 2009; Hassani *et al.* 2011; Silverman *et al.* 2008). For cells or parasites such as nematodes

which can be maintained in a serum-free medium as part of their general culture, samples can be taken at any time point during their culture, with less concern about stress or parasite death which may result in the release of molecules that would not normally be secreted (Hewitson *et al.* 2013; Sotillo *et al.* 2014). For those that can only be incubated for a short time their viability in these suboptimal conditions must be monitored to ensure excessive cell lysis does not contaminate the secretome, and the incubation times adjusted accordingly. However, reducing the time in culture reduces the yield of secreted proteins therefore culture volumes tend to be increased to compensate for this.

Beyond studies like these looking specifically at molecules within the culture supernatant, concerns with the addition of undefined supplements to culture media are far reaching, raising ethical issues and difficulties with reproducibility and standardisation across laboratories. Consequently, there is a great deal of research into the development of defined media (DM) for cell culture (Broedel Jr. & Papciak 2003; Nayak *et al.* 2018; Santarém *et al.* 2013a; van der Valk *et al.* 2010). Many DM are now in use and can be purchased commercially for a variety of cell types, with online databases dedicated to the curation of serum-free alternatives (van der Valk *et al.* 2010, 2018). However, for *Leishmania* and other parasites, developments in DM are very much in their infancy (De Paula Lima *et al.* 2014; Nayak *et al.* 2018; Santarém *et al.* 2013a). For this reason, DM are still not commonly employed in secretome studies.

There are methods designed to retain the use of supplemented culture media whilst avoiding the problem of abundant and undefined serum proteins. Methods employing click chemistry can be used to pull out specifically modified proteins, for example click chemistry of glycoproteins (Kuhn *et al.* 2012), and are used when a known class of secreted proteins are to be investigated. However, these types of methods are not useful for studies aiming to obtain a global coverage of the whole secretome. Other methods of click chemistry using cells labelled with a labelled analogue of a certain metabolite, such as a methionine analogue, are effective at isolating secreted proteins in the presence of serum. However this method relies on the cells being auxotrophic for certain metabolites, and adapting to culture where they must utilise the analogue metabolically and in the case of this particular method, also take up heavy lysine and arginine to allow SILAC labelling (Eichelbaum

& Krijgsveld 2014). And so due to the aim of analysing the full life cycle of *Leishmania* and the potential use of non-culture adapted field strains in this project, labelling with metabolic analogues and isotopes was not used.

3.1.2 Isolating the secretome of *Leishmania*

L. mexicana is suited to secretome analysis due to the ability to cultivate the complete life cycle of this species *in vitro*, culturing the distinct cell morphologies from both the vector and host stages, the promastigote and amastigote, respectively (Bates 1994). Metacyclogenesis in *Leishmania* is induced *in vitro* by low pH and nutrient exhaustion (Bates 2007). Both the metacyclic and procyclic forms generated *in vitro* are morphologically similar to their insect counterparts (Sacks 1989; Debrabant et al. 2004). Axenic amastigotes of *L. mexicana* have been extensively characterised and found to be very similar to lesion-derived amastigotes (Bates 1994; Bates et al. 1992; Gupta et al. 2001). They are characterised by a combination of morphology, for example the presence of amastigote-specific megasomes and non-emergent flagellum; biochemical analyses, to detect increased protease and nuclease activity and decreased protein content and secretory acid phosphatase; and immunochemistry and molecular characterisation, using amastigote-specific antibodies and detection of amastigote-specific gene expression (Gupta et al. 2001). Axenic culture also provides the cell numbers required for studies such as these where large quantities of cells are required to generate enough secreted protein for analysis. It also eliminates the need for host cells, consequently avoiding the complexity of differentiating between host and parasite proteins.

Proposed global secretome collection methods from *Leishmania spp.* are listed in Table 3-1. An important consideration when extracting the *Leishmania* secretome is the growth-phase at which samples are collected. The studies described in Table 3-1 have only sampled promastigotes, at both logarithmic or stationary phases in axenic culture, corresponding to procyclic- or metacyclic-enriched populations, respectively (Burchmore & Hart 1995; Mallinson & Coombs 1989). We aim to extend these analyses to the amastigote stage of the parasite life cycle.

Table 3-1 Methods employed for collection of the secretome from *Leishmania spp.* Abbreviations not included in common abbreviations table: NR – not reported, Ppn – precipitation, dm – defined media, sf – serum free, Leu – leupeptin, AN – antipain, PS – pepstatin, CS – chymostatin, AP – aprotinin, STBI – soya bean trypsin inhibitor, PMSF -phenylmethylsulfonyl fluoride.

<i>Leishmania</i> Species	Wash	Collection medium	Protease inhibitors	Cell density	Incubation time	Centrifugation speeds	Concentration method	Viability monitoring	Identification method	Reference
<i>L. major</i> stationary promastigotes	PBS	sf RPMI	Leu, AN, PS, CS at 2 µg/ml, AP at 16 µg/ml	2 x 10 ⁷ cells/ml Total NR	6 h	4000 x g	Centricon YM-10 filter	Trypan blue /counting	anti-secretome sera + immuno-screening cDNA expression library	(Chenik <i>et al.</i> 2006)
<i>L. donovani</i> stationary promastigotes	HBSS	sf M199 + HEPES + L-glut	SBTI during collection	10 ⁸ cells/ml Total >2x10 ⁹ cells	4-6 h	300 x g	10% TCA OR pyrogallol red Ppn	G6PD assay	SILAC, + LC-MS/MS / IEF + LC-MS/MS	(Silverman <i>et al.</i> 2008)
<i>L. braziliensis</i> log-phase promastigotes	PBS	sf RPMI + HEPES + L-glut	NR	5x10 ⁸ cells/ml Total 2.5x10 ⁹ cells	3 h	2000 x g, 100,000 x g	10% TCA Ppn	Trypan blue /counting	2DE + MALDI-TOF/TOF	(Cuervo <i>et al.</i> 2009)
<i>L. mexicana</i> stationary promastigotes	PBS	sf DMEM or RPMI	NR	10 ⁸ cells/ml Total NR	2-4 h	4000 rpm	15% TCA Ppn OR 10KD filter	PI staining /FACS	LC-MS/MS	(Hassani <i>et al.</i> 2011)
<i>L. infantum</i> log-phase promastigotes	N/A	dm cRPMI (Santarém <i>et al.</i> 2013a)	1mM PMSF	10 ⁶ cells/ml starting inoculum Total NR	24-96 h	Parasite removal speed NR, 0.2 µm filter, 10,000 x g, 100,000 x g	3 KD Ultracel filter + dialysis against PBS	AnnexinV-Cy5 + 7-AAD staining / FACS	1DE + LC-MS/MS	(Santarém <i>et al.</i> 2013b)
<i>L. infantum</i> log-phase promastigotes	sf RPMI	sf RPMI	NR	10 ⁷ cells/ml Total 2.4x10 ⁹ cells	2-8 h	1276 x g	NR	PI staining /FACS	LC-MS/MS	(Braga <i>et al.</i> 2014)
<i>L. major</i> stationary promastigotes	PBS	sf RPMI	NR	10 ⁸ cells/ml Total NR	4 h	3000 rpm, 10,000 rpm, 0.45 µm + 0.20 µm filters	N/A exosome collection only	PI staining /FACS	LC-MS/MS	(Atayde <i>et al.</i> 2015)

A commonly overlooked difficulty with secretome analysis, is that the resulting 'conditioned' culture media will contain a very dilute concentration of secreted proteins. For this reason, many previous studies increased the cell numbers in the secretion medium to increase the yield of secreted material. However, concentration methods must still be employed post-collection of the secretome, such as protein precipitation or molecular weight cut-off (MWCO) filter centrifugation, in order to gain high enough concentrations of protein to be analysed by methods such as gel separation or mass spectrometry. Other factors to be considered include the length of incubation time, methods to monitor cell viability, and the inclusion of protease inhibitors during the collection process.

Having successfully collected the secreted proteins, most studies have then utilised mass spectrometry for protein identification (Atayde *et al.* 2015; Braga *et al.* 2014; Cuervo *et al.* 2009; Hassani *et al.* 2011; Santarém *et al.* 2013b; Silverman *et al.* 2008). There has also been a non-MS-based method for detecting excreted/secreted proteins of *Leishmania*, through the generation of antibodies to stationary culture supernatant, followed by immunoscreening of a cDNA expression library and sequencing of the positive hits to identify the candidate proteins (Chenik *et al.* 2006).

3.2 Aims and hypotheses

As evidenced above, many different methods for secretome collection and variations thereof have been used, and every method has advantages and disadvantages. Here, we aimed to implement and optimise a method for secretome extraction and analysis from *L. mexicana*. We evaluated and adapted current methods for secretome extraction from *Leishmania* promastigotes and applied them to both *L. mexicana* promastigote and amastigote cultures, with the aim that application of these methods would allow us to obtain and characterise the global secretome from both life cycle stages. These analyses could then be used to evaluate and further understand the differences between the promastigote and amastigote life cycle stages and their interactions with the vector and the host.

- We hypothesised that the extracellular proteome of *Leishmania* parasites in axenic culture would differ from the intracellular proteome, and that this could therefore be categorised as the *secretome* fraction.
- We hypothesised that, like promastigotes, amastigotes would secrete proteins in axenic culture, and that previous promastigote secretome collection and analysis methods could be adopted and further optimised for the study of the amastigote secretome.

3.3 Results

3.3.1 Evaluation of media for secretome collection

To establish a viable cell culture of *Leishmania mexicana* M379, *in vitro* methods were employed to culture the cells axenically. Figure 3-1a shows a growth curve for *L. mexicana* WT promastigotes in axenic culture in HOMEM medium with added serum (cHOM), displaying clear logarithmic and stationary growth phases between 0-50 hours and 100-150 hours, respectively. In the logarithmic growth phase the doubling time of the promastigotes was approximately 7.2 hours. Figure 3-1b shows a growth curve for *L. mexicana* axenic amastigotes, cultured in SDM medium with added serum (cSDM), displaying logarithmic growth over the course of 7 days with an average doubling time of 36 hours, a slower growth rate than the promastigote stage.

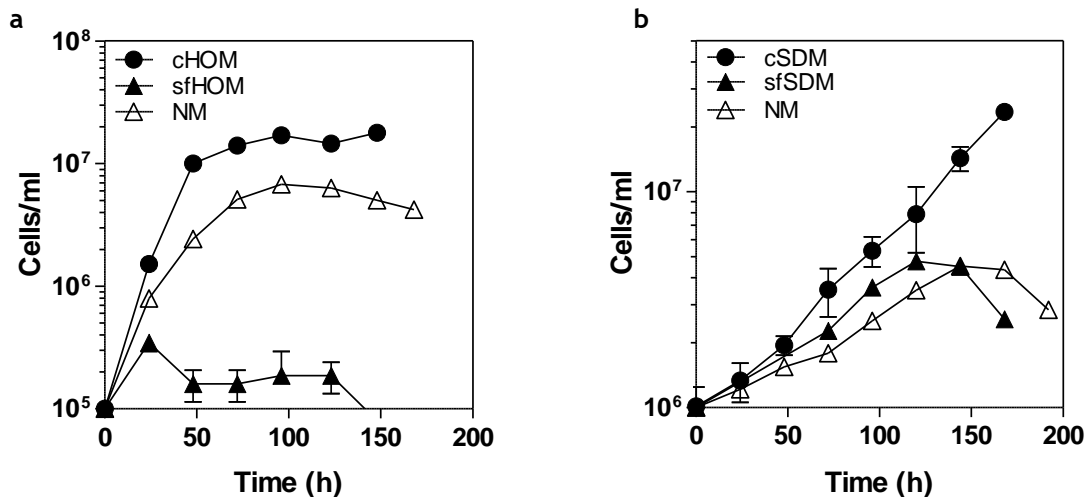


Figure 3-1 Growth of *Leishmania mexicana* *in vitro*. (a) Growth of axenic promastigotes in cHOM (circles), serum-free HOM (filled triangles) or Nayak medium (open triangles), (b) growth of axenic amastigotes in cSDM pH 5.5 (circles), serum-free SDM pH 5.5 (filled triangles) or Nayak medium pH 5.5 (open triangles). Error bars \pm SD, $n=3$.

Due to the undefined nature of the serum added to the culture media and the highly abundant proteins found in it such as albumin, it is necessary to collect the secretome of these cells in a serum free environment. We tested the applicability of two methods to achieve this.

3.3.1.1 Defined media for *L. mexicana*

Similar to the method of Santarém *et al.* (Santarém *et al.* 2013b), we tested the applicability of using a complete defined medium for the culture of *L. mexicana*, which contains all the nutrients required for *in vitro* growth of the parasites without adding serum or any other undefined cell culture products (Nayak *et al.* 2018). Promastigotes grown in cHOM were washed in PBS and transferred to Nayak medium (NM). The promastigotes grew slightly slower in NM than in cHOM (Figure 3-1a), but continued to grow logarithmically with a doubling time of 10.4 hours, reaching a maximum density of 7.5×10^6 cells/ml after 96 hours. Amastigotes did not respond as well to NM, only reaching a maximum density of 4.5×10^6 cells/ml after 144 hours and exhibiting an apparent doubling time of 66.4 hours (Figure 3-1b).

3.3.1.2 Serum-free incubation

In parallel, we also evaluated the frequently used method of using a serum-free media and short incubation to collect the secretome. Parasites were cultured in complete medium (cHOM, cSDM), then washed and transferred to serum-free medium (sfHOM, sfSDM pH 5.5) to investigate their growth and viability prior to secretome collection. No overall growth was observed when promastigotes were cultured in sfHOM, with the small increase in cell number at 24 hours likely to be an artefact of previously dividing cells at the time of transfer (Figure 3-1a). Amastigotes appeared to continue dividing in sfSDM, reaching a maximum density of 4×10^6 cells/ml at 120 hours before dropping (Figure 3-1b). The growth rate during this period was slower than in the cSDM culture with a doubling time of 53.2 hours. Although it appears that the amastigotes were growing in the serum free medium, they only reach a density equivalent to 'two doublings', which is similar to the promastigotes which increased from 1×10^5 to 3.5×10^5 . Therefore again, this may be an artefact of previously dividing cells at the time of transfer, coupled with the amastigotes' slower growth rate and therefore slower response rate.

To allow for a comparison of the protein profiles of the promastigote and amastigote secretome, both samples were obtained by incubation in serum-free base media, Homem or Schneider's Drosophila Medium pH 5.5 for promastigotes or amastigotes, respectively. As with previous studies (Braga *et al.* 2014; Cuervo *et*

al. 2009; Hassani *et al.* 2011; Silverman *et al.* 2008), the incubation time in serum-free media was limited, in this case to 4 hours, to minimise the stress to cells.

3.3.2 Cell viability is monitored during secretome isolation

In order to demonstrate that we have minimised the release of intracellular proteins through cell lysis, any cell death during the 4 hour incubations was monitored and quantified by counting using a cell viability stain, Trypan blue. Figure 3-2a shows that the cell viability of stationary promastigote culture and of amastigote culture is maintained to the same level before and after incubation in serum-free media.

An alamar blue metabolic assay was also employed to quantify the viability of the parasites after incubation in the medias, using a modified transformation assay (Jain *et al.* 2012). Viable axenic amastigotes were cultured in cSDM and prepared by washing off the complete medium and incubating in PBS, cSDM or sfSDM for 4 hours. After incubation, the medium was replaced with cHOM to transform any live amastigotes to promastigotes. Parasite viability was evaluated by the addition of resazurin dye which is metabolised by live parasites to a fluorescent product. Figure 3-2b shows the comparison of the metabolism of viable promastigotes after being incubated in the stated media for 4 hours as amastigotes. The parasites incubated in water showed no fluorescence as there were no viable parasites remaining to metabolise the reagent after the 4 hour incubation. This observation was significantly different from the incubations in PBS, cSDM or sfSDM, and the results in these media showed no statistical difference between them.

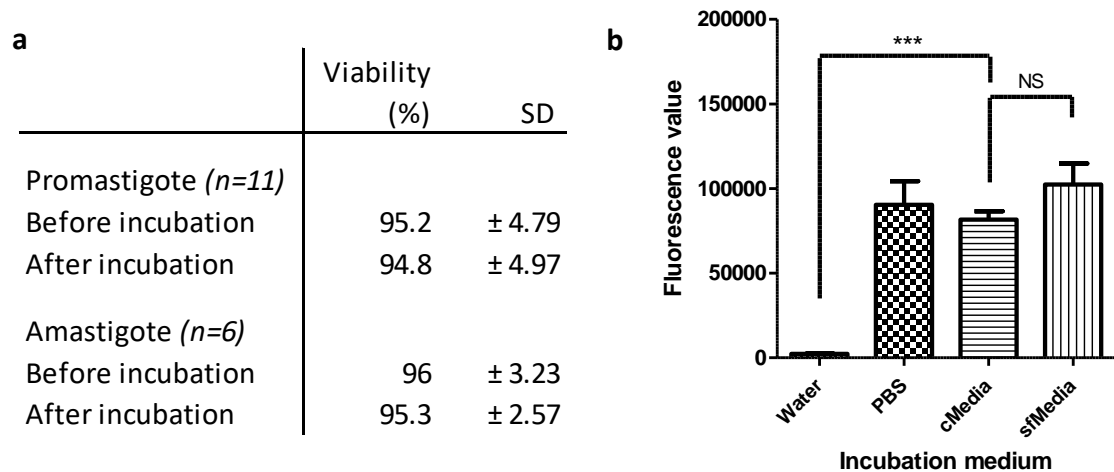


Figure 3-2 Viability of *L. mexicana* during secretome collection. (a) Viability of axenic stationary phase promastigotes and amastigotes before and after 4 h incubation in sfHOM or sfSDM, respectively, measured by counting on a haemocytometer with trypan blue dye exclusion. (b) Viability of amastigotes incubated in various named media and measured using the alamar blue metabolic assay. Error bars +SD (*n*=6). *** $p < 0.0001$, comparison to cMedia, PBS and sfMedia.

3.3.3 Supernatant recovery and concentration

After incubation of the parasites in the secretion media, the parasites were separated from the supernatant using centrifugation, beginning at relatively slow speeds of 700 x g followed by 1000 x g, to separate the intact parasite cells from the supernatant without imposing undue mechanical stress that might result in cell crushing and lysis. Once the cell-free supernatant containing the secretome was isolated, this was subjected to further centrifugation at a higher speed of 3270 x g to remove any cell debris that may be present.

We then sought to optimise the recovery of the proteins from the large volumes of media. Figure 3-3 shows promastigote supernatant samples concentrated using two different precipitation methods, acetone precipitation and a carrier-assisted TCA precipitation using sodium lauryl sarcosinate (TCA-NLS) (Chevallet *et al.* 2007), compared to applying no protein concentration method. Comparing the methods visually by SDS-PAGE and Coomassie staining, greater concentration and recovery of proteins was achieved using acetone precipitation compared to no precipitation, but TCA-NLS provided the greatest concentration and recovery compared to the other approaches. These samples were also compared to a known amount of cell lysate protein (10 µg) to help estimate the amount of protein in the secretome samples. Although incremental improvements were observed, it is clear the secretome recovery is still very low. TCA-NLS precipitation was also applied to the

amastigote secretome (Figure 3-4). Filter concentration with 10 kDa MWCO centrifugal filters was also investigated to provide an alternative method of sample concentration. This method resulted in the greatest recovery of protein (Figure 3-5).

An additional step of including a detergent-based buffer (RIPA buffer) with the filter concentration method was included to lyse any exosomes on the filter, and to promote recovery of any proteins which had stuck to the membrane during concentration (Figure 3-5). This step also functioned to denature the secreted proteins to retain more low MW proteins on the membrane.

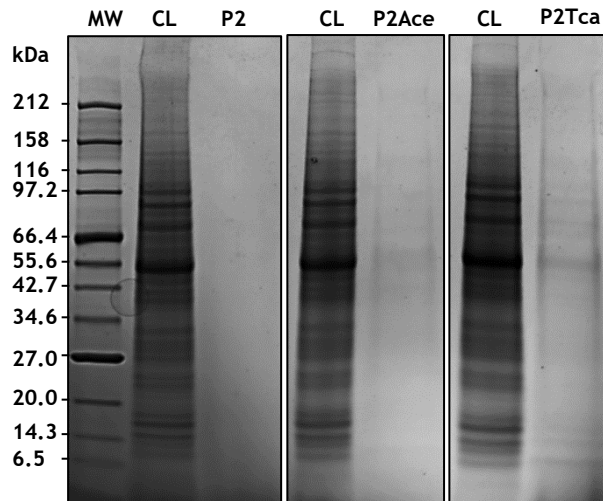


Figure 3-3 Comparison of protein concentration methods for *L. mexicana* promastigote secretome by SDS-PAGE. Three different methods were compared, no concentration (P2) where a sample of the supernatant was applied to the gel, acetone precipitation (P2Ace) and a carrier-assisted TCA precipitation using NLS (P2Tca). These were compared to each other and to 10 μ g of promastigote cell lysate protein (CL). Samples run on 4-20% poly-acrylamide gel with molecular weight marker (MW) P7702 broad range NEB. Stained with colloidal Coomassie G-250 (Dyballa & Metzger 2009).

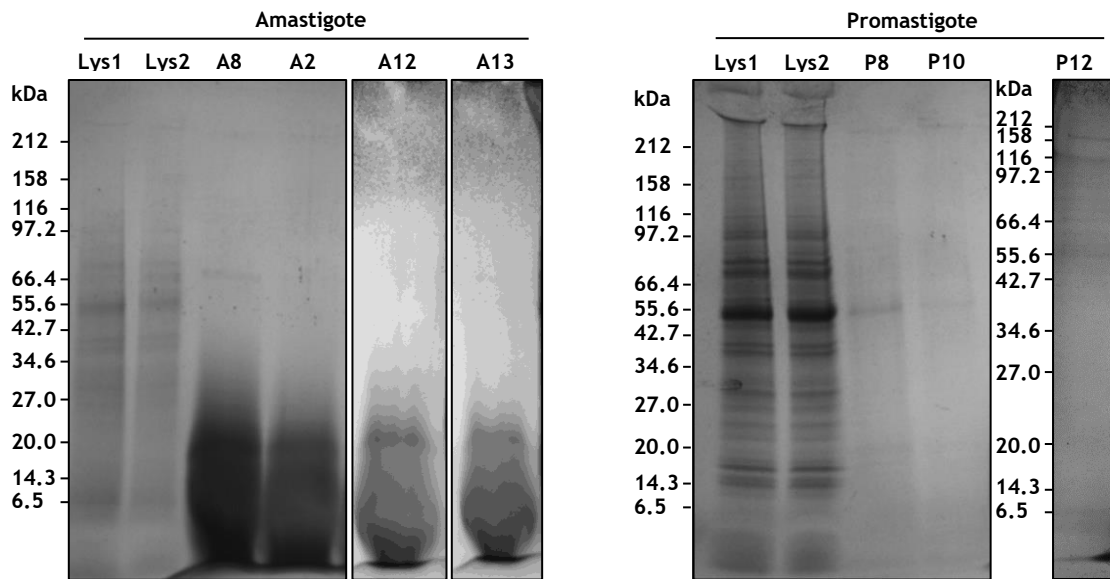


Figure 3-4 Secretome collection from *L. mexicana* axenic amastigotes and promastigotes. Protein extracts from the lysed cells (lys) of both life cycle stages and from the secretome run by 4-20% SDS-PAGE and stained with colloidal Coomassie G-250, samples 1 or 2 indicate two repeats. A2-13 indicate amastigote secretome sample ID's for MS analysis. P8-12 promastigote secretome sample ID's.

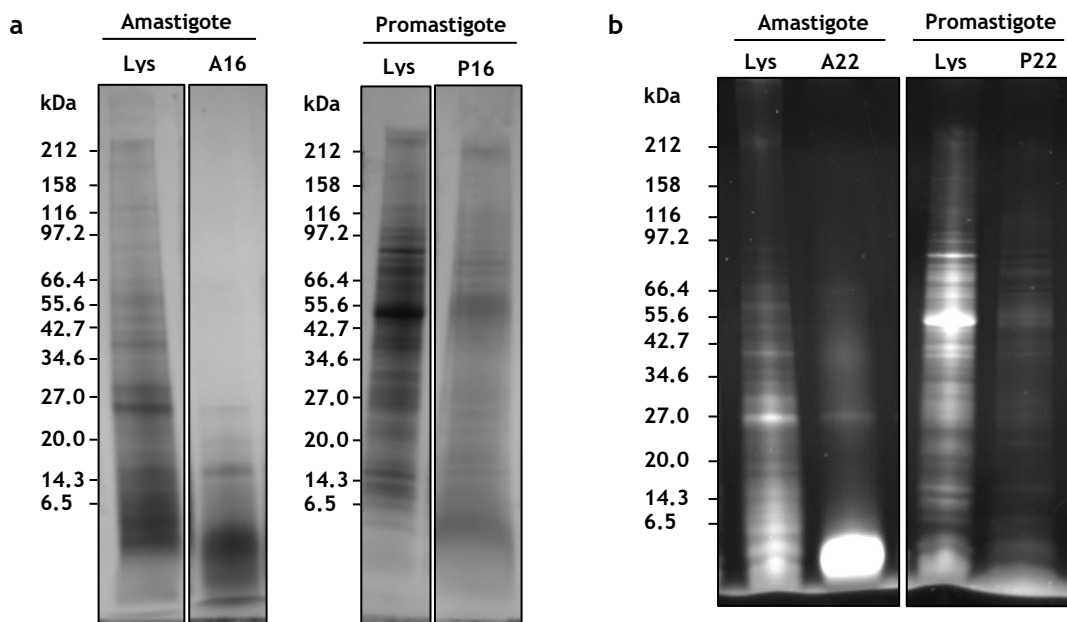


Figure 3-5 SDS-PAGE of *L. mexicana* secretome and lysate. Secretome (A, P) and whole cell extract (Lys) from amastigotes and promastigotes were stained with colloidal Coomassie G-250 (a) and Sypro Orange (b). Secretome samples 16 and 22 were extracted with the addition of a cocktail of protease inhibitors (1 μ M PepstatinA, 0.1 mM Pefabloc, 10 μ M leupeptin, 1 mM 1,10-phenanthroline) and concentrated using 10 kDa MWCO filters.

3.3.4 Amastigote secreted proteins are degraded by proteolysis

After secretome collection from promastigotes and amastigotes, aliquots of both the lysed cell pellets and the secreted protein samples were run side by side to evaluate the profiles of the two fractions. Due to the absence of high molecular

weight proteins in the amastigote secretome samples and an abundance of diffuse low molecular weight material, proteolytic degradation was suspected. To address this, the method was modified to add a cocktail of protease inhibitors to the secretome after parasite removal from the spent media

A cocktail of protease inhibitors (Table 3-2, initial concentration) was added to both the promastigote and amastigote collections (Figure 3-5) (Ambit *et al.* 2011). As a result, there were more higher molecular weight proteins visible in Figure 3-5, and a reduced area of diffuse staining. This was further optimised by adding specific metalloprotease inhibitor EDTA (Woessner 1999) and irreversible cysteine protease inhibitor E64 (Barrett *et al.* 1982) to the cocktail, and increasing the concentrations of the other inhibitors in the amastigote mix. Addition of these protease inhibitors (Table 3-2) after the collection of the secretome improved the detection of high molecular weight bands in amastigote secreted material (Figure 3-6a), and improved the resolution of the promastigote secretome (Figure 3-6b).

Table 3-2 Protease inhibitors added to the *L. mexicana* secretome. The following concentrations of protease inhibitors were added to the secretome after removing the parasites by centrifugation. Pro – promastigotes, Ama – amastigotes.

Inhibitor	Supplier	Initial Conc.	Final Conc. (Pro)	Final Conc. (Ama)
E64	Sigma/E3132	/	10 μ M	50 μ M
Pepstatin A	Sigma/P5318	1 μ M	1 μ M	5 μ M
Pefabloc	Sigma/76307	0.1 mM	0.1 mM	0.5 mM
Leupeptin	Sigma/L2884	10 μ M	10 μ M	50 μ M
1,10-Phenanthroline	Sigma/P9375	1 mM	1 mM	2 mM
EDTA	Sigma/E6758	/	1 mM	2 mM

Improvements in protein visualisation were also observed with the application of SyproOrange staining to the samples (Figure 3-5). The improvements in the collection of both secretomes and from the use of staining using silver stain is evident in Figure 3-6. There is clear defined banding in both secretome samples with distinct banding patterns between the secretome and the lysates, and between promastigote and amastigote samples. There are fewer bands in the amastigote secretome compared to the promastigote secretome.

0.22 μ m filters have previously been used to ensure complete removal of cells from the secretome sample (Atayde *et al.* 2015; Atyame Nten *et al.* 2010; Santarém *et*

al. 2013b). This method was tested to investigate if this would adversely affect the secretome, as future experiments may involve application of the secretome to host cells. However, addition of this step showed some protein loss and therefore was not used in the final method for characterisation of the secretome (Figure 3-6a).

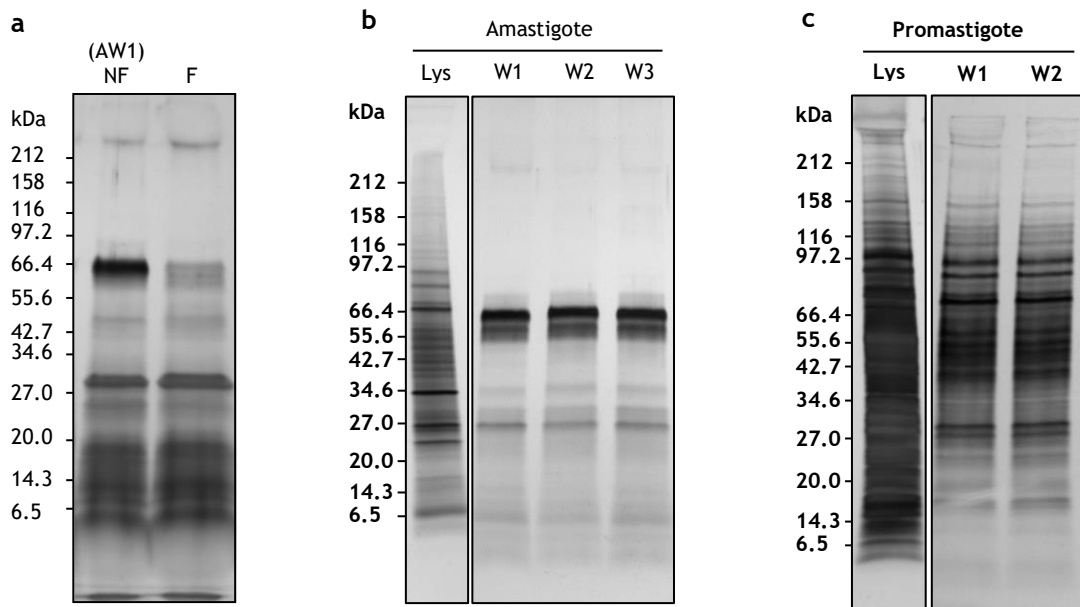


Figure 3-6 *L. mexicana* promastigote and amastigote secretome compared to cell lysate. (a) Amastigote secretome, NF – non-filtered, F – filtered through 0.22 μ M membrane after removal of parasites by centrifugation. (AW1) indicates sample name for MS analysis. (b) Amastigote proteome (Lys) and secretome samples (W1-3). (c) Promastigote proteome (Lys) and secretome (W1-2) samples. Secreted proteins from conditioned axenic culture supernatant separated on 4-20% SDS-PAGE and silver stained. MW marker used was NEB broad range (2-212 kDa). Secretome samples were treated with a cocktail of protease inhibitors specific for promastigotes or amastigotes (Table 3-2) and with RIPA buffer, and concentrated using 10 kDa MWCO centrifugal filters.

The profiles of the secretome and cell lysate were also compared by a 2D-GE analysis. This was performed for both promastigote and amastigote cell lysate and secretome (presented in Chapter 4, Figure 4-2). Visualisation of the differing fractions in higher resolution clearly displays the fundamental differences between the lysate and secretome samples.

3.3.5 Protein quantitation

The low concentration of secreted proteins and their collection in salt- and metabolite-rich culture media presented an additional problem with quantitation of the samples prior to analysis. Two commonly used commercial protein assays, the Bradford assay (BioRad) and the BCA assay (Thermo), were unsuitable for quantitation of the secretome samples. This was due to the addition of detergents

during sample concentration in the case of the Bradford assay, and the presence of free cysteine and other small molecules which interfere with the BCA assay. To combat this, the detergent-compatible (DC) Protein Assay (BioRad) was used which was compatible with all components of the sample. In addition, to avoid using up 10 μ l of the secretome sample per assay replicate in the standard microplate format, which would consume up to 40% of the total sample amount if three replicates were assessed as per the manufacturers' instructions, we implemented the colorimetric nanodrop spectrophotometer method. This was used in combination with the 'low-concentration' protocol of the DC protein assay using standards ranging from 5-250 μ g/ml protein. Only 4 μ l of sample or standard are required per assay, which is mixed with a reagent mix and then absorbance measured at 750 nm, from triplicate samples (Methods 2.6). Unknown protein concentrations in the sample are ascertained by comparison to a standard curve using known protein concentrations. Post extraction of the secretome, we were able to calculate and quantify the protein yield obtained (Table 3-3). Promastigotes were found to secrete approximately five-fold more protein than amastigotes per cell.

Table 3-3 Estimated secreted protein yield from *L. mexicana*. Pro WT – wild type axenic promastigotes, biological replicates 1-3, Ama WT – wild type axenic amastigotes, biological replicates 1-3.

Cell type	Total number of cells	Total yield of secreted protein(μ g)	Yield per 10 ⁸ cells (μ g)
Pro WT 1	3.5 E8	19.5	5.6
Pro WT 2	3.5 E8	22	6.3
Pro WT 3	3.4 E8	12.6	3.7
Ama WT 1	9.92 E8	15.1	1.5
Ama WT 2	7.04 E8	9	1.3
Ama WT 3	9.6 E8	10.2	1.06

3.3.6 Identification of secretome proteins by mass spectrometry

Alongside the development and visual assessment of the method by gel electrophoresis, aliquots of secreted material were also digested with trypsin and the resulting peptides analysed by mass spectrometry to identify the secreted protein components. In early analyses (Figure 3-3; sample P2), secreted material was not sufficiently concentrated and the small aliquot used for mass spectrometry generated very few peptides. These initial analyses resulted in poor protein yields

and identifications. The first MS runs of both the promastigote and amastigote secretome samples yielded significant matches to trypsin only (Table 3-6, Table 3-7). The introduction of the steps described above led to significant improvements in the number of proteins identified with confidence.

After protein concentration with TCA-NLS and increasing the volume of starting culture, the next promastigote secretome analyses P8 and P10 yielded 24 and 23 protein identifications but with high false discovery rates indicating peptide matches with poor confidence. These investigations were improved upon using 10kDa filter concentration and a protease inhibitor cocktail as discussed above, resulting in 32, 15 and 38 confident protein identifications with false discovery rates of <1% and applying a threshold of 30 to the internal Mascot scoring system. The results of these early promastigote analyses are summarised in Table 3-4. After further method development using a combination of filter concentration, improved protease inhibitor cocktail and solubilisation of exosomal proteins and any protein stuck to the filter membrane using detergent, the secretome samples depicted in Figure 3-6 were analysed by mass-spectrometry. From the analysis of the promastigote secretome, 256 proteins were identified over the significance threshold ($P < 0.05$), with a Mascot score exceeding 30 and in at least three replicates, as shown in Chapter 4, Table 4-2.

In parallel, the amastigote collection method was tested and samples of the amastigote secretome were digested with trypsin for mass spectrometry analysis. The total number of protein identifications generated from each amastigote secretome sample are summarised in Table 3-5. Samples A2 - A13, which produced very diffuse LMW stained regions on polyacrylamide gels (Figure 3-4), only generated up to four significant protein identifications. The majority of these were low-scoring hypothetical proteins (Table 3-7). Samples A16 and A22 were generated using filter concentration coupled with the addition of a limited cocktail of protease inhibitors (Figure 3-5), and this resulted in 11 and 19 protein identifications (Table 3-7). Finally, using a combination of filter concentration, a specific cocktail of protease inhibitors and addition of lysis buffer during processing to recover stuck proteins and exosomes, samples AW1 and W1-3 were generated (Figure 3-6) which resulted in the identification of 33 - 39 proteins in the amastigote secretome. Proteins which exceeded significance and scoring thresholds of $P < 0.05$

and 30, respectively, and were present in a minimum of three replicates were included in the final list of amastigote secreted proteins, which totalled 36 proteins (Chapter 4, Table 4-3). Blank serum-free media, HOM and SDM pH 5.5, were also submitted for MS analysis to control for any media additives or contaminants which may influence the results. These analyses resulted in the identification of two peptides matching to porcine trypsin and one peptide matching to a hypothetical *Leishmania* protein, the same protein in both blank samples (Table 3-8), later found to be a spurious match.

Table 3-4 Summary of *L. mexicana* promastigote secretome identifications by LC-MS/MS

Sample ID	Number of significant hits	FDR applied (if known)	Mascot score cut-off	Mass Spec
P2_24	0	/	/	AmaZon Speed
P2_4	0	/	/	AmaZon Speed
p8	24	4.81%	≥30	AmaZon Speed
p10	23	4.73%	≥30	AmaZon Speed
p12	54	4.94%	≥30	AmaZon Speed
p12	32	<1%	≥30	AmaZon Speed
p16	20	4.8%	≥30	AmaZon Speed
p16	15	<1%	≥30	AmaZon Speed
p22	46	5%	≥30	AmaZon Speed
p22	38	<1%	≥30	AmaZon Speed
W1	296	<1%	≥30	Orbitrap Elite
W2	296	<1%	≥30	Orbitrap Elite
W3	247	<1%	≥30	Orbitrap Elite

Table 3-5 Summary of *L. mexicana* amastigote secretome identifications by LC-MS/MS

Sample ID	Number of significant hits	FDR applied (if known)	Mascot score cut-off	Mass Spec
A2	0	/	/	AmaZon Speed
A8	1	/	/	AmaZon Speed
A12	2	/	≥30	AmaZon Speed
A13	4	/	≥30	AmaZon Speed
A16	11	/	≥30	AmaZon Speed
A22	19	/	≥30	AmaZon Speed
AW1	39	<2%	≥30	Orbitrap Elite
W1	33	<1%	≥30	Orbitrap Elite
W2	33	<1%	≥30	Orbitrap Elite
W3	33	<1%	≥30	Orbitrap Elite

Table 3-6 *L. mexicana* promastigote secretome identifications from method development. Secreted proteins identified by LC-MS/MS of tryptic peptides.

Hit #	Accession	Description	Score	Mass	Matches	Sequences	Coverage (%)	emPAI	hits	P2 24h 0 sig
1	LmxM.29.0050	hypothetical protein, conserved	14	87528	0	0				
2	LmxM.36.3260	hypothetical protein, conserved	14	22438	0	0				
1	SWISS-PROT:P00761	Trypsin - Sus scrofa (Pig)	91	25078	5	1		0.13		
Hit #	Accession	Description	Score	Mass	Matches	Sequences	Coverage (%)	emPAI	hits	P2 4h 0 sig
1	LmxM.17.1290	eukaryotic translation initiation factor 3 subunit b	22	81180	0	0	3.1			
2	LmxM.16.0050	hypothetical protein, conserved	14	74109	0	0	1.2			
3	LmxM.07.0240	hypothetical protein, conserved	13	68066	0	0	1.2			
Hit #	Accession	Description	Score	Mass	Matches	Sequences	Coverage (%)	emPAI	24 sig hits	P8 FDR 4.81
1	LmxM.36.6480	histidine secretory acid phosphatase, putative	1270	128157	45	11	10.6	0.37		
2	LmxM.08.1171	hypothetical protein	354	50319	16	6	16.5	0.6		
3	LmxM.13.0280	alpha tubulin	232	61058	10	6	14.4	0.39		
4	LmxM.14.1160	enolase	117	46743	2	2	7	0.16		
5	LmxM.24.0850	triosephosphate isomerase	89	27265	2	1	4.8	0.13		
6	LmxM.09.0910	calmodulin, putative	87	16814	2	1	7.4	0.48		
7	LmxM.09.0891	polyubiquitin, putative	74	14962	1	1	12.5	0.24		
8	LmxM.31.2950	nucleoside diphosphate kinase b	72	16891	3	2	11.9	0.48		
9	LmxM.36.1940	inosine-guanosine transporter	63	54565	2	2	5.2	0.13		
10	LmxM.34.0500	proteophosphoglycan ppg3, putative	56	121456	2	2	1.6	0.06		
11	LmxM.29.2980	glyceraldehyde 3-phosphate dehydrogenase, glycosomal	55	39326	2	1	3.9	0.09		
12	LmxM.23.0200	endoribonuclease L-PSP (pb5), putative	51	17122	2	1	9.8	0.47		
13	LmxM.17.0080	elongation factor 1-alpha	51	49575	1	1	2.4	0.07		
14	LmxM.14.0850	small myristoylated protein-3, putative	50	13055	3	1	8.7	0.28		
15	LmxM.34.2210	kinetoplastid membrane protein-11	49	11271	1	1	9.8	0.33		
16	LmxM.22.1110	dynein heavy chain, cytosolic, putative	46	627131	1	1	0.3	0.01		
17	LmxM.15.1010	glutamate dehydrogenase	44	115208	1	1	1.2	0.03		
18	LmxM.28.2770	heat-shock protein hsp70, putative	41	71482	2	1	1.8	0.05		
19	LmxM.23.0840	hypothetical protein, unknown function	40	57431	1	1	1.5	0.06		
20	LmxM.28.2910	glutamate dehydrogenase, putative	40	49561	1	1	2.4	0.07		
21	LmxM.34.3230	cystathione gamma lyase, putative	39	45102	1	1	2.2	0.08		
22	LmxM.24.0960	hypothetical protein, conserved	38	108178	2	1	0.8	0.03		
23	LmxM.32.0312	heat shock protein 83-1	38	81035	1	1	1.7	0.04		
24	LmxM.32.2540	metallo-peptidase, Clan MA(E) Family M32	38	57378	1	1	2	0.06		

Hit #	Accession	Description	Score	Mass	Matches	Sequences	Coverage (%)	emPAI
1	LmxM.36.6480	histidine secretory acid phosphatase, putative	2097	128157	97	10	8.7	0.3
2	LmxM.08.1171	hypothetical protein	303	50319	13	5	14.4	0.52
3	LmxM.09.0910	calmodulin, putative	238	16814	6	1	7.4	0.42
4	LmxM.13.0280	alpha tubulin	157	61058	6	3	5.7	0.16
5	LmxM.14.1160	enolase	80	46743	1	1	3.5	0.07
6	LmxM.14.0850	small myristoylated protein-3, putative	66	13055	3	1	8.7	0.25
7	LmxM.31.2950	nucleoside diphosphate kinase b	62	16891	2	1	6	0.19
8	LmxM.31.1820	iron superoxide dismutase, putative	58	21994	1	1	7.2	0.14
9	LmxM.24.0850	triosephosphate isomerase	56	27265	1	1	4.8	0.12
10	LmxM.23.0840	hypothetical protein, unknown function	56	57431	3	1	1.5	0.05
11	LmxM.36.1960	phosphomannomutase, putative	53	28231	1	1	4.5	0.11
12	LmxM.17.0080	elongation factor 1-alpha	53	49575	1	1	2.4	0.06
13	LmxM.09.1340	histone H2B	49	11957	1	1	9.3	0.27
14	LmxM.36.1940	inosine-guanosine transporter	49	54565	2	2	3.8	0.12
15	LmxM.34.3230	cystathione gamma lyase, putative	48	45102	2	1	2.9	0.07
16	LmxM.09.0891	polyubiquitin, putative	45	14962	1	1	12.5	0.22
17	LmxM.15.1040	tryparedoxin peroxidase	41	22557	1	1	5.5	0.14
18	LmxM.29.2980	glyceraldehyde 3-phosphate dehydrogenase, glycosomal	38	39326	1	1	3.9	0.08
19	LmxM.34.2210	kinetoplastid membrane protein-11	35	11271	1	1	9.8	0.29
20	LmxM.31.3310	dihydrolipoamide dehydrogenase, putative	35	51083	1	1	2.5	0.06
21	LmxM.30.0010	5-methyl4hydropteroyl3glutamatemethyltransferase putative	34	86681	1	1	1.3	0.04
22	LmxM.26.1420	hypothetical protein, conserved	33	258393	1	1	0.4	0.01
23	LmxM.16.0760	transaldolase, putative	33	37238	1	1	3.6	0.08

P10 FDR 4.73
23 sig hits

Hit #	Accession	Description	Score	Mass	Matches	Sequences	Coverage (%)	emPAI
1	LmxM.36.6480	histidine secretory acid phosphatase, putative	3510	128157	102	10	10	0.3
2	LmxM.13.0280	alpha tubulin	461	61058	20	6	13.3	0.35
3	LmxM.08.1171	hypothetical protein	317	50319	17	8	22.6	0.62
4	LmxM.09.0910	calmodulin, putative	245	16814	6	2	18.8	0.69
5	LmxM.14.1160	enolase	143	46743	5	3	9.1	0.21
6	LmxM.36.1940	inosine-guanosine transporter	139	54565	7	3	8	0.18
7	LmxM.28.2910	glutamate dehydrogenase, putative	125	49561	6	5	15.7	0.36
8	LmxM.23.0840	hypothetical protein, unknown function	116	57431	3	3	6.8	0.17
9	LmxM.32.0312	heat shock protein 83-1	110	81035	4	3	5.6	0.12
10	LmxM.31.1820	iron superoxide dismutase, putative	98	21994	2	1	7.2	0.14
11	LmxM.23.0200	endoribonuclease L-PSP (pb5), putative	96	17122	2	1	9.8	0.19
12	LmxM.28.2770	heat-shock protein hsp70, putative	90	71482	4	3	6.3	0.14
13	LmxM.31.2950	nucleoside diphosphate kinase b	88	16891	2	1	6	0.19
14	LmxM.17.0085	elongation factor 1-alpha	81	45620	4	3	8	0.22

P12 FDR <1%
32 sig hits >30 score

15	LmxM.09.1340	histone H2B	78	11957	3	1	9.3	0.27
16	LmxM.36.2020	chaperonin HSP60, mitochondrial precursor	75	60610	3	2	4.2	0.11
17	LmxM.30.2310	3~-nucleotidase/nuclease	73	41697	1	1	2.9	0.07
18	LmxM.14.0850	small myristoylated protein-3, putative	70	13055	2	2	18.3	0.56
19	LmxM.09.0891	polyubiquitin, putative	70	14962	2	1	12.5	0.21
20	LmxM.29.2980	glyceraldehyde 3-phosphate dehydrogenase, glycosomal	70	39326	2	1	3.9	0.08
21	LmxM.34.3230	cystathione gamma lyase, putative	70	45102	4	2	5.1	0.14
22	LmxM.15.1230	nucleoside transporter 1, putative	68	54462	2	1	2.9	0.06
23	LmxM.16.0760	transaldolase, putative	66	37238	1	1	2.7	0.08
24	LmxM.15.1040	tryparedoxin peroxidase	66	22557	2	2	10.1	0.3
25	LmxM.34.0500	proteophosphoglycan ppg3, putative	62	121456	2	1	0.7	0.03
26	LmxM.25.2010	hypothetical protein, conserved	60	30664	2	1	3.9	0.1
27	LmxM.32.2540	metallo-peptidase, Clan MA(E) Family M32	59	57378	1	1	2.2	0.05
28	LmxM.24.0850	triosephosphate isomerase	59	27265	2	2	10	0.24
29	LmxM.23.1020	hypothetical protein, unknown function	56	12671	2	2	22.2	0.58
30	LmxM.30.1440	hypothetical protein, unknown function	54	49700	1	1	4.2	0.06
31	LmxM.05.0350	trypanothione reductase	54	53710	1	1	2.6	0.06
32	LmxM.11.0630	metallo-peptidase, Clan MF, Family M17	46	57922	1	1	3	0.05

Hit #	Accession	Description	Score	Mass	Matches	Sequences	Coverage (%)	emPAI
1	LmxM.36.6480	histidine secretory acid phosphatase, putative	893	128157	32	6	7	0.15
2	LmxM.09.0910	calmodulin, putative	276	16814	9	3	26.8	1.02
3	LmxM.13.0280	alpha tubulin	182	61058	8	4	8.6	0.22
4	LmxM.14.1160	enolase	76	46743	3	3	11.2	0.21
5	LmxM.34.3230	cystathione gamma lyase, putative	71	45102	2	2	6.1	0.14
6	LmxM.08.1171	hypothetical protein	69	50319	1	1	2.7	0.06
7	LmxM.23.1020	hypothetical protein, unknown function	64	12671	2	1	8.5	0.26
8	LmxM.05.0380	microtubule-associated protein, putative	62	89588	1	1	1.7	0.03
9	LmxM.31.2950	nucleoside diphosphate kinase b	59	16891	1	1	6	0.19
10	LmxM.14.0850	small myristoylated protein-3, putative	59	13055	2	1	9.6	0.56
11	LmxM.15.1160	tryparedoxin peroxidase	57	22538	1	1	7	0.14
12	LmxM.25.2010	hypothetical protein, conserved	56	30664	1	1	3.9	0.1
13	LmxM.16.0760	transaldolase, putative	55	37238	1	1	4.2	0.08
14	LmxM.36.1940	inosine-guanosine transporter	54	54565	1	1	2.6	0.06
15	LmxM.28.2770	heat-shock protein hsp70, putative	52	71482	1	1	2.4	0.04

P16 FDR <2%
15 sig hits >30 score

Hit #	Accession	Description	Score	Mass	Matches	Sequences	Coverage (%)	emPAI
1	LmxM.36.6480	histidine secretory acid phosphatase, putative	1898	128157	68	9	9.4	0.27
2	LmxM.13.0280	alpha tubulin	252	61058	10	5	11.1	0.28
3	LmxM.14.1160	enolase	239	46743	8	5	16.6	0.38
4	LmxM.16.0760	transaldolase, putative	174	37238	8	5	18.5	0.5
5	LmxM.09.0910	calmodulin, putative	171	16814	4	2	18.8	0.42
6	LmxM.23.1020	hypothetical protein, unknown function	151	12671	7	3	30.8	0.98
7	LmxM.34.0500	proteophosphoglycan ppg3, putative	145	121456	8	4	3.5	0.11
8	LmxM.08.1171	hypothetical protein	126	50319	7	5	14.9	0.35
9	LmxM.28.2770	heat-shock protein hsp70, putative	107	71482	3	3	5.8	0.14
10	LmxM.34.3230	cystathione gamma lyase, putative	97	45102	3	2	6.8	0.14
11	LmxM.31.2950	nucleoside diphosphate kinase b	90	16891	4	2	13.9	0.42
12	LmxM.23.0840	hypothetical protein, unknown function	86	57431	2	1	3.4	0.05
13	LmxM.17.0080	elongation factor 1-alpha	85	49575	4	4	10.2	0.28
14	LmxM.31.1820	iron superoxide dismutase, putative	83	21994	1	1	7.2	0.14
15	LmxM.34.0520b	hypothetical protein (pseudogene) (fragment)	78	549866	3	3	0.8	0.02
16	LmxM.23.0200	endoribonuclease L-PSP (pb5), putative	70	17122	1	1	9.8	0.19
17	LmxM.25.2010	hypothetical protein, conserved	69	30664	2	1	3.9	0.1
18	LmxM.29.2980	glyceraldehyde 3-phosphate dehydrogenase, glycosomal	67	39326	1	1	3.9	0.08
19	LmxM.11.0630	metallo-peptidase, Clan MF, Family M17	67	57922	1	1	3	0.05
20	LmxM.24.2060	transketolase, putative	65	72496	1	1	1.6	0.04
21	LmxM.28.2910	glutamate dehydrogenase, putative	64	49561	2	2	6.4	0.13
22	LmxM.23.0110	mannose-1-phosphate guanyltransferase	63	41849	2	1	2.9	0.07
23	LmxM.30.1440	hypothetical protein, unknown function	63	49700	1	1	4.2	0.06
24	LmxM.30.0010	5-methyl4hydropteroyltriglutamate homocysteinemethyltransferase, putative	61	86681	1	1	1.8	0.04
25	LmxM.09.0891	polyubiquitin, putative	58	14962	1	1	12.5	0.21
26	LmxM.30.2020	succinyl-diaminopimelate desuccinylase-like protein	58	51477	1	1	3.2	0.06
27	LmxM.36.6650	2,3-bisphosphoglycerate-independentphosphoglyceratemutase	55	61118	1	1	2.5	0.05
28	LmxM.14.0850	small myristoylated protein-3, putative	54	13055	2	1	8.7	0.25
29	LmxM.26.1570	thimet oligopeptidase, putative	53	77680	1	1	1.6	0.04
30	LmxM.20.1310	small myristoylated protein 1	52	15167	1	1	8.4	0.21
31	LmxM.15.1230	nucleoside transporter 1, putative	51	54462	1	1	2.9	0.06
32	LmxM.32.0312	heat shock protein 83-1	51	81035	1	1	1.7	0.04
33	LmxM.15.1040	tryparedoxin peroxidase	51	22557	2	1	5	0.14
34	LmxM.01.0770	Eukaryotic initiation factor 4A-1	51	51225	1	1	2.2	0.06
35	LmxM.33.0140	malate dehydrogenase	49	33945	1	1	7	0.09
36	LmxM.05.0960	metallo-peptidase, Clan M-, Family M49	47	76027	1	1	1.6	0.04
37	LmxM.36.0180	elongation factor 2	46	94852	1	1	1.8	0.03
38	LmxM.21.1700	proteasome alpha 2 subunit, putative	46	25301	1	1	5.6	0.12

P22 FDR <1%
38 sig hits >30 score

Table 3-7 Secreted proteins from *L. mexicana* amastigotes. Secretome representative of three independent repeats. Where >1 accessions are listed, all peptides matched to these sequences. ^aAccession number from TriTrypDB.org. ^bMascot protein score, derived from the sum of individual probability-based ions scores [$10 \cdot \text{LOG}_{10}(P)$] + corrections, Matrix Science. ^cPredicted protein mass from genome sequence. ^dNumber of spectra matched to peptide sequences in the protein. ^eNumber of different peptide sequences matched. ^f% coverage of the protein sequence. ^gemPAI. P<0.05 significance threshold at level of identity.

Hit #	Accession	Description	Score	Mass	Matches	Sequences	Coverage (%)	emPAI	
1	LmxM.05.1020	hypothetical protein, conserved	21	104936	1	1	1	0.03	0 sig hits
1	P00761	Trypsin - Sus scrofa (Pig).	18	25078	1	1	3.5	0.13	
A2									
1	P00761	Trypsin - Sus scrofa (Pig).	130	25078	9	3	16.5	0.43	1 sig hit
1	LmxM.24.0960	hypothetical protein, conserved	30	108178	1	1	0.8	0.03	
A8									
1	P00761	Trypsin - Sus scrofa (Pig).	44	25078	2	2	7.8	0.27	2 sig hits
1	LmxM.24.0960	hypothetical protein, conserved	39	108178	1	1	0.8	0.03	
2	LmxM.36.5800	hypothetical protein, conserved	31	206526	1	1	0.3	0.01	
A12									
1	P00761	Trypsin - Sus scrofa (Pig).	68	25078	5	1	3.5	0.13	4 sig hits
2	P00924	Enolase 1	48	46830	4	1	1.4	0.07	
1	LmxM.17.0080	elongation factor 1-alpha	61	49575	2	1	1.8	0.06	
2	LmxM.24.0960	hypothetical protein, conserved	36	108178	2	1	0.8	0.03	
3	LmxM.26.1320	hypothetical protein, conserved	36	30638	2	1	2.9	0.1	
4	LmxM.28.2230	cyclin dependent kinase-binding protein, putative	31	99259	1	1	0.7	0.03	
A13									
1	LmxM.09.0891	polyubiquitin, putative	254	14962	8	3	24.2	0.8	11 sig hits
2	LmxM.08.1080	cathepsin L-like protease, putative	200	39285	8	4	15.3	0.36	
3	LmxM.14.0850	small myristoylated protein-3, putative	115	13055	6	2	18.3	0.56	
4	LmxM.23.0200	endoribonuclease L-PSP (pb5), putative	114	17122	4	2	16	0.41	
5	LmxM.09.0910	calmodulin, putative	106	16814	8	3	20.8	0.7	
6	LmxM.24.0850	triosephosphate isomerase	86	27265	3	3	14.7	0.39	
7	LmxM.09.0770	oligopeptidase b	79	84275	2	1	2.3	0.04	
8	LmxM.08_29.1160	tryparedoxin 1, putative	45	16739	2	1	8.3	0.19	
9	LmxM.13.1360	hypothetical protein, conserved	40	91686	1	1	1.6	0.03	
A16									

10	LmxM.36.2840	Flagellar Member 2	34	126576	1	1	0.6	0.02
11	LmxM.34.5320	hypothetical protein, conserved	30	67351	1	1	1.2	0.05

Hit #	Accession	Description	Score	Mass	Matches	Sequences	Coverage (%)	emPAI
1	LmxM.09.0891	polyubiquitin, putative	104	14962	3	2	19.5	0.55
2	LmxM.26.0750	hypothetical protein, conserved	94	185432	3	1	0.8	0.02
3	LmxM.09.0910	calmodulin, putative	92	16814	4	3	27.5	0.8
4	LmxM.08_29.0290	hypothetical protein	43	41544	1	1	2.4	0.08
5	LmxM.34.3240	hypothetical protein, conserved	43	91111	2	1	1	0.04
6	LmxM.21.0825	plectin, putative	41	360915	2	1	0.3	0.01
7	LmxM.20.0160	wd40 repeat domain-containing protein	40	88864	1	1	1	0.04
8	LmxM.08_29.2590	hypothetical protein, conserved	38	73482	1	1	2.5	0.05
9	LmxM.33.2030	hypothetical protein, conserved	38	131098	2	1	0.6	0.03
10	LmxM.08_29.1410	hypothetical protein, unknown function	38	128642	3	2	1	0.05
11	LmxM.09.0770	oligopeptidase b	37	84275	1	1	2.3	0.04
12	LmxM.12.1210	hypothetical protein, conserved	36	103312	2	1	1.1	0.03
13	LmxM.04.1180	hypothetical protein, conserved	36	254100	1	1	0.3	0.01
14	LmxM.07.0960	hypothetical protein, conserved	34	128579	1	1	0.7	0.03
15	LmxM.23.1020	hypothetical protein, unknown function	34	12671	1	1	7.7	0.29
16	LmxM.15.0710	hypothetical protein, conserved	33	364956	2	1	0.3	0.01
17	LmxM.32.0370	hypothetical protein, conserved	32	78370	1	1	0.8	0.04
18	LmxM.36.5200	hypothetical protein, conserved	30	108104	1	1	0.9	0.03
19	LmxM.19.1130	hypothetical protein, conserved	30	620168	1	1	0.2	0.01

A22
19 sig hits

Hit #	Accession	Description	Score	Mass	Matches	Sequences	Coverage (%)	emPAI
1	LmxM.29.2490	heat shock 70-related protein 1, mitochondrial precursor, putative	463	72990	11	6	11	0.47
2	LmxM.08.1030a	hypothetical protein	452	58965	12	6	14.6	0.75
3	LmxM.24.0850	triosephosphate isomerase	372	27265	9	5	25.1	1.36
4	LmxM.09.0891	polyubiquitin, putative	279	14962	9	4	36.7	2.46
5	LmxM.10.0460	GP63, leishmanolysin	203	70995	5	4	7.6	0.3
6	LmxM.28.2770	heat-shock protein hsp70, putative	197	71482	6	4	6.1	0.39
7	LmxM.14.0850	small myristoylated protein-3, putative	161	13055	4	3	19.1	1.89
8	LmxM.06.0030	hypothetical protein, conserved	151	75520	4	2	3.6	0.13
9	LmxM.36.1960	phosphomannomutase, putative	148	28231	3	2	10.5	0.4
10	LmxM.26.0620	10 kDa heat shock protein, putative	136	10695	3	2	26	1.38
11	LmxM.23.0200	endoribonuclease L-PSP (pb5), putative	134	17122	3	2	16	0.73
12	LmxM.36.3210	14-3-3 protein 1, putative	104	29782	3	2	8.5	0.37
13	LmxM.17.0620	hypothetical protein, conserved	99	11466	1	1	19.4	0.5

AW1 FDR<2%
39 sig hits

14	LmxM.36.0970	hypothetical protein, conserved	94	22506	1	1	7.6	0.23
15	LmxM.24.2210	60S ribosomal protein L12, putative	93	17698	2	1	9.1	0.3
16	LmxM.31.1820	iron superoxide dismutase, putative	89	21994	2	1	7.2	0.24
17	LmxM.13.0450	ALBA-domain protein 1	86	13372	2	1	10.7	0.42
18	LmxM.08_29.0820	CPC cysteine peptidase, Clan CA, family C1, Cathepsin B-like	86	38009	2	1	5.6	0.13
19	LmxM.21.1780	40S ribosomal protein S6, putative	85	28302	2	1	6.4	0.18
20	LmxM.36.2020	chaperonin HSP60, mitochondrial precursor	74	60610	2	1	2.1	0.08
21	LmxM.26.2700	6-phosphogluconolactonase	71	28690	1	1	6	0.18
22	LmxM.31.2260	hypothetical protein, conserved	67	20318	2	1	5.9	0.26
23	LmxM.07.1000	RNA binding protein-like protein	65	38691	1	1	3.6	0.13
24	LmxM.28.1200	luminal binding protein 1 (BiP), putative	60	71919	2	1	1.7	0.07
25	LmxM.08_29.1160	tryparedoxin 1, putative	60	16739	6	1	9	1.3
26	LmxM.07.0990	nucleolar RNA-binding protein, putative	53	36307	2	1	2.3	0.14
27	LmxM.15.1040	tryparedoxin peroxidase	52	22557	2	1	5.5	0.23
28	LmxM.32.1750	macrophage migration inhibitory factor-like protein	51	12846	1	1	7.1	0.43
29	LmxM.08.0470	small ubiquitin protein, putative	48	12738	2	1	12.8	0.44
30	LmxM.06.0010	histone H4	48	11436	2	1	10	0.5
31	LmxM.28.0960	40S ribosomal protein S14	48	15667	2	1	9	0.35
32	LmxM.31.2950	nucleoside diphosphate kinase b	47	16891	1	1	6	0.32
33	LmxM.36.0540	ubiquitin-like protein, putative	47	33141	1	1	4.4	0.15
34	LmxM.19.1420	cysteine peptidase A (CPA)	46	39177	1	1	2.5	0.13
35	LmxM.19.1160	hypothetical protein, conserved	43	41571	1	1	2.7	0.12
36	LmxM.14.1100	kinesin K39, putative	43	536483	1	1	0.2	0.01
37	LmxM.34.1300	ubiquitin-conjugating enzyme E2, putative	42	16783	1	1	4.7	0.32
38	LmxM.09.0910	calmodulin, putative	40	16814	1	1	7.4	0.32
39	LmxM.04.1230	actin	40	42350	1	1	2.7	0.12

Table 3-8 Identifications from MS analysis of serum-free base medium. sfHOM – serum-free HOMEM before use for the culture of promastigotes, sfSDM – serum-free Schneider's drosophila medium before use for the culture of amastigotes.

Hit #	Accession	Description	Score	Mass	Matches	Sequences	Coverage (%)	emPAI	
1	LmxM.31.1700	hypothetical protein, conserved	32	90069	1	1	1	0.03	sfHOM only
1	P00761	Trypsin - Sus scrofa (Pig).	82	25078	4	2	7.8	0.27	
Hit #	Accession	Description	Score	Mass	Matches	Sequences	Coverage (%)	emPAI	
1	LmxM.31.1700	hypothetical protein, conserved	29	90069	1	1	1	0.03	sfSDM only
1	P00761	Trypsin - Sus scrofa (Pig).	194	25078	7	2	7.8	0.27	

3.3.7 Validation of the secretome by comparison to lysate

The proteome of the cells was also analysed by LC-MS/MS to experimentally compare the intracellular proteome of the parasites with the secreted proteome. Comparison of the cellular proteome to the secretome shows enrichment of certain proteins in the spent media samples. These distinct protein profiles indicate that the proteins detected in the spent media are unlikely to be artefacts present due to cell lysis during serum-free incubation or processing. There are 67 proteins unique to the promastigote secretome, and 189 proteins in common between the cellular proteome and the secretome of promastigotes (Figure 3-7a). 8 proteins are unique to the amastigote secretome, with 28 proteins in common between the proteome and secretome from amastigotes (Figure 3-7b). However, in order to understand these observations further, the relative abundance of each protein detected in cellular and secreted proteomic analyses were compared. A quantitative measure of protein abundance is the exponentially modified protein abundance index (emPAI) (Ishihama *et al.* 2005). Figure 3-8 and Figure 3-9 correlate the relative abundance of each protein in the proteome and secretome, from promastigote and amastigote respectively, by comparing lists of proteins ranked according to their emPAI. This reveals that the proteins that are in common between the lysate and secretome are not simply those that are most abundant in the lysate, as would be expected if their presence in the secreted sample was due to a degree of cell lysis during sample generation. Additionally, there are many abundant lysate proteins that do not appear in the secretome.

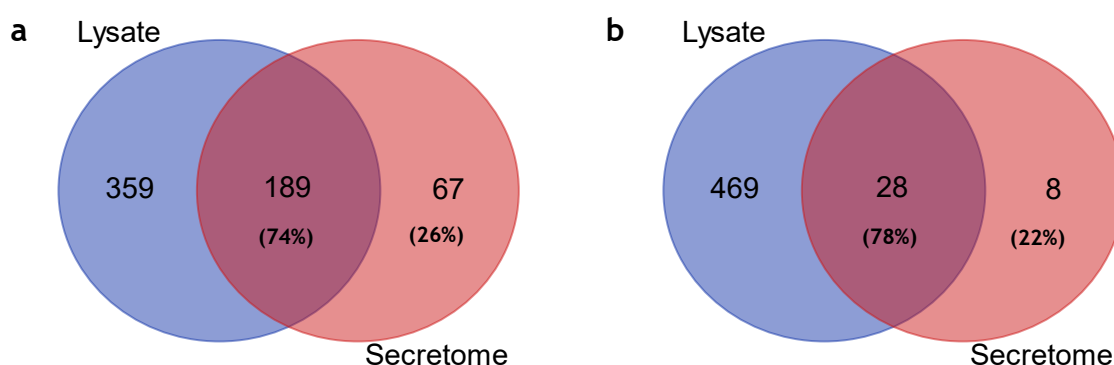


Figure 3-7 Venn diagrams illustrating the proteins in common between lysate and secretome protein samples of *L. mexicana*. (a) promastigote proteome Vs secretome, (b) amastigote proteome Vs secretome (protein descriptions, some redundancies).

<http://bioinformatics.psb.ugent.be/webtools/Venn/>

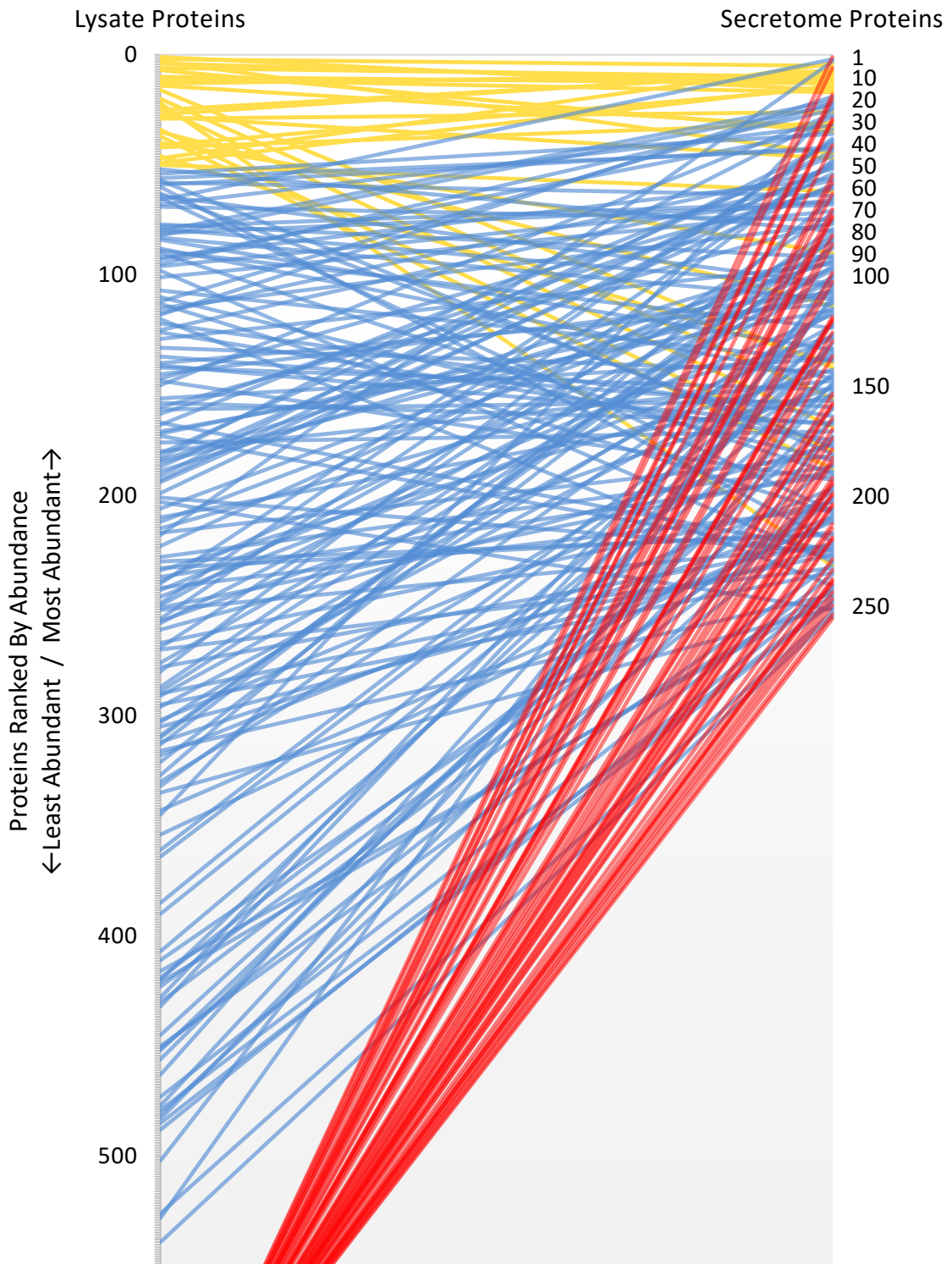


Figure 3-8 *L. mexicana* promastigote whole cell proteins versus secretome proteins arranged in order of decreasing abundance. Tick marks and values from 1 to 548 on the left hand axis denote each protein in the promastigote cell lysate ranked from 1 to 548 in order of decreasing emPAI. Where a line is present, this represents a protein also present in the promastigote secretome. Where there is no line, no corresponding protein was present in the secretome. Proteins identified by LC-MS/MS. Proteins marked by a yellow line are in the top 50 most abundant in the cell lysate, those in blue are enriched in the secretome and less abundant in the lysate. Proteins in red were enriched in the secretome but below the detection limit in the lysate.

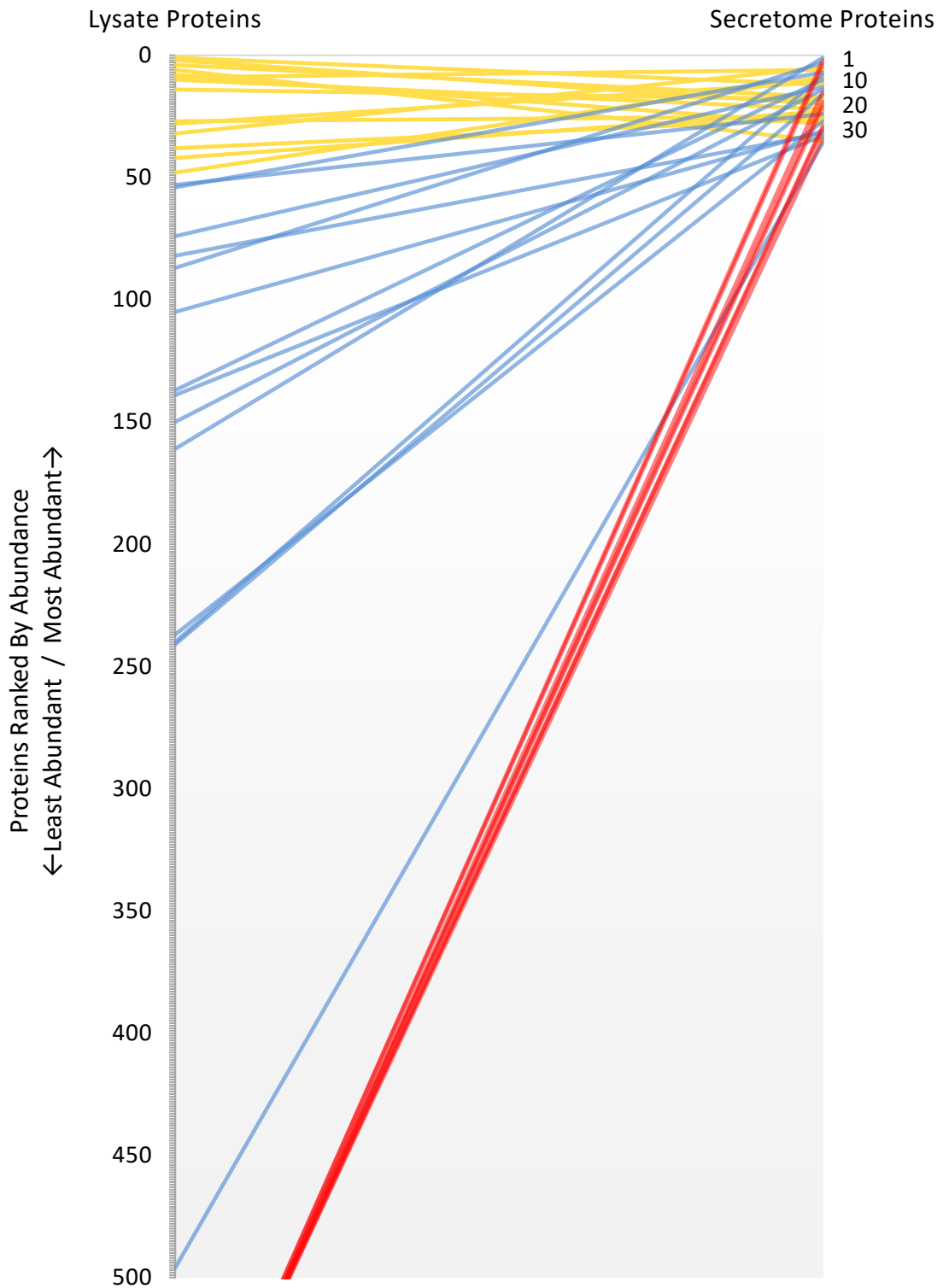


Figure 3-9 *L. mexicana* amastigote whole cell proteins versus secretome proteins arranged in order of decreasing abundance. Tick marks and values from 1 to 497 on the left hand axis denote each protein in the amastigote cell lysate ranked from 1 to 497 in order of decreasing emPAI. Where a line is present, this represents a protein also present in the amastigote secretome. Where there is no line, no corresponding protein was present in the secretome. Proteins identified by LC-MS/MS. Proteins marked by a yellow line are in the top 50 most abundant in the cell lysate, those in blue are enriched in the secretome and less abundant in the lysate. Proteins in red were enriched in the secretome but below the detection limit in the lysate.

3.4 Discussion

3.4.1 Axenic culture systems are advantageous for secretome studies

The complete developmental cycle, including the promastigote and amastigote stages of *Leishmania mexicana* M379 can be cultured axenically (Bates 1994), and for multiple passages. Axenic culture of promastigotes and amastigotes allows confidence in extractions being free from contamination by host or other exogenous proteins. However, these *in vitro* cultures do not fully represent the *in vivo* situation, where promastigotes develop in the sand fly vector and amastigotes within the macrophage host cell, encountering a much more complex and potentially hostile environment than that presented by culture media. The relative contributions of host and parasite activities to the outcome of the interaction are challenging to disentangle and there is obvious potential in the study of axenic parasite systems to reveal the input from the parasite. Model systems for axenic culture *in vitro* are regularly used for many different cell types and are very amenable to secretome studies. Subsequent analyses and conclusions from *in vitro* studies employing these methods generate greater insight into mechanisms employed by the parasite and can highlight leads that can be followed up at the individual protein level using *in vivo* methods.

As outlined previously, serum and other undefined supplements added to axenic culture systems can present problems with batch variability, reproducibility and highly abundant serum proteins which mask the proteins of interest. To combat this, we have chosen a method of secretome collection in serum-free medium. We assessed the use of serum-free base media for short incubations, and defined NM (Nayak *et al.* 2018) to allow longer serum-free incubations. NM was found to be good for increasing the protein yield for the promastigote secretome (Appendix 1), however this media is not yet applicable to amastigote culture. Therefore, for comparison and conclusions to be drawn between both lifecycle stages both methods were kept similar using a 4 hour incubation in serum-free base media. The number of parasites per secretion assay was increased to approximately 10^9 parasites to increase the protein yield due to the short incubation times.

3.4.2 Secretion and isolation processes

During the secretion process, viability monitoring is important to show that cell viability is maintained during transfer to and incubation in different media. Experiments described here show cell viability to be maintained *in vitro* in the employed culture medium. Amastigote viability was also demonstrated in various media, complete growth medium (cSDM), serum-free medium (sfSDM), water or PBS, using the alamar blue viability reagent. The alamar blue assay is routinely used for evaluation of growth and viability of kinetoplastids in response to drug treatment (Räz *et al.* 1997). Blue resazurin dye is reduced by mitochondrial NADH into resorufin, a pink coloured product which fluoresces with an excitation wavelength of 530 nm and with an emission wavelength of 590 nm. The assay can also be measured colorimetrically at 570 nm. However, even with the presence of individual controls for each of the medium types, the differing compositions of the media caused too much variability in the fluorescence readings to quantify the viability of the amastigotes directly after the incubations. Serum in the medium has been reported to cause some quenching of the fluorescence and therefore it is best to have the same medium composition for all samples and controls (Page *et al.* 1993). An incubation and transformation assay (Jain *et al.* 2012) was therefore employed to quantify the viability of the parasites after incubation in the various media. The methods were adapted from Jain *et al.* (2012) by starting with the incubation of axenic amastigotes in the various media, then live amastigotes were differentiated back to promastigotes by temperature and pH change using cHOM. The addition of alamar blue reagent thereafter displayed the presence of metabolically active cells by production of a coloured and fluorescent product. Cells incubated in a non-isotonic control for four hours showed no metabolism of the substrate, whereas those in control media (cSDM), experimental media (sfSDM) and isotonic nutrient-deprived control (PBS) displayed significantly increased metabolism. No significant difference in cell viability was observed between sfSDM and cSDM after four hours of incubation. Results also showed no significant difference in cell viability between cSDM and PBS. However, this assay only takes cell death into account and does not account for cell stress or any other factors. We sought to maintain the cell culture environment as closely as possible and minimise stress as far as possible, so for this reason we chose to continue using the

same media for secretome collection with the only difference being the removal of serum.

There is little benefit to monitoring cell viability during the secretion process if incidental lysis is to occur during the isolation process. Therefore, to maintain cell integrity while separating the parasites from the spent medium, the parasites were separated from the supernatant using progressive centrifugation, starting relatively slowly and increasing in speed at each stage with the supernatant from the previous stage. This approach ensured the parasites were pelleted in a manner that would avoid crushing and mechanical lysis, followed thereafter by pelleting any remaining cell debris. The supernatant was removed carefully at each stage. At this point other studies (Hassani *et al.* 2011, 2014) have used 0.22 or 0.45 μm filters to ensure complete sterility, however we have opted not to use this method in the standard process to minimise loss of protein, as demonstrated in Figure 3-6a.

3.4.3 Overcoming challenges of secretome extraction

An overlooked problem with secretome studies is in the concentration of the dilute protein solutions. Protein recovery from culture media can present various challenges such as co-precipitation of culture media salts or poor yields at low protein concentrations (Chevallet *et al.* 2007). Various protocols were therefore compared to extract the secreted proteins from the media: acetone precipitation, carrier-assisted TCA precipitation and molecular weight cut-off (MWCO) filters. Methods such as dye-binding precipitation with pyrogallol red, used in previous *Leishmania* secretome analyses (Silverman *et al.* 2008), were not evaluated due to previous evidence of poor recovery of acidic proteins and glycoproteins (Marshall & Williams 1996). The first method investigated was acetone precipitation. Addition of acetone and other organic solvents to aqueous protein solutions precipitates the protein by reducing the polarity of the solution and decreasing the solubility of the proteins (Goldring 2015). We tested the efficacy of the acetone precipitation protocol against a carrier-assisted TCA precipitation method and found acetone precipitation to be the least effective for this type of sample (Figure 3-3). Additionally, this method requires the addition of four times the sample volume of acetone in order to create the conditions. As large culture volumes are required to isolate adequate concentrations of secreted protein, acetone

precipitation, alongside other organic solvents such as methanol precipitation where nine volumes of methanol are required, were deemed to be unsuitable from a practical perspective. Carrier-assisted precipitation is specifically designed to improve the precipitation and recovery of proteins from dilute solutions (Chevallet *et al.* 2007). It functions to bind to the protein in solution and precipitate the carrier along with the protein. The carrier is then washed off during subsequent steps. In our hands, this method did improve the recovery of the secreted proteins, but only incrementally (Figure 3-3). Finally, centrifugal filters with a 10 kDa molecular weight cut-off (MWCO) were tested. This method proved the most effective at concentrating and recovering the secreted proteins from the culture media. An additional benefit of a 10kDa filter concentration step is the removal of any contaminating salts, nutrients and peptides from the spent media. The amastigote culture media SDM contains a yeastolate extract which may contain peptides (Thermo Fisher Scientific n.d.). However, as part of the yeastolate production process it is sterilised by passing through a 10kDa filter before its addition to the medium, therefore the yeastolate only contains supplements smaller than 10kDa (SAFC Biosciences 2006). We are retaining anything larger than 10kDa on the filter as our sample.

Improvement of the amastigote secretome was achieved with higher concentrations of protease inhibitors, crucially E64 and EDTA, for the inhibition of cysteine proteases (Barrett *et al.* 1982) and metalloproteases (Woessner 1999). There are known to be abundant cysteine proteases (Mottram *et al.* 1998) and metalloproteases (Cuervo *et al.* 2006) in *Leishmania*. In addition, proteases in general are more abundant in amastigotes (Pupkis & Coombs 1984). Moving from a standard working concentration of all protease inhibitors to using a fivefold increased concentration for the amastigote samples, generated greater secretome coverage. Addition of RIPA buffer would act to lyse exosomes but also act to denature the proteases in the solution.

One of the major challenges was working with low concentrations of protein, even after extraction and concentration down to small volumes. Both in the collection and concentration of the samples, and in obtaining an accurate estimate of protein concentration from low amounts of protein. Most conventional protein assays such as the Bradford assay or to BCA assay are confounded by many of the components

of protein buffers, such as the detergents in Laemmli and lysis buffers, free amino acids such as cysteine in culture media, or reducing agents such as DTT. Many different assays were tested and subsequently the detergent-compatible protein assay reagent (BioRad) was chosen. This was coupled with a method using the Nanodrop spectrophotometer, to avoid consumption of up to 40% of the sample using the standard microplate method (Methods 2.6). The resulting total secretome yield for both cell types was an interesting observation as promastigotes were found to secrete fivefold more protein per cell than amastigotes. Promastigotes are much larger than amastigotes, but in stationary phase they are only around double the size (Bates 1994), not fivefold larger. We can therefore reinforce the observation that amastigotes are more metabolically quiescent than promastigotes (Jara *et al.* 2017; Saunders *et al.* 2014).

3.4.4 Protein identification and validation

Visualisation of the electrophoretic profiles of the secretome samples was improved using silver staining. In contrast, other methods included radioisotope labelling and using known counts/min to run on the gel to overcome problems with protein assays, and for gel visualisation (Chenik *et al.* 2006; Silverman *et al.* 2008). However, these methods are costly, time consuming and require expertise in use of radioisotopes. Resolution of the differences between lysate and secretome was increased by additionally performing 2D electrophoresis. Comparison of the secretome and lysate showed clear, qualitative differences between the two fractions (Chapter 4, Figure 4-2).

Analysis of blank serum-free base media appeared to yield a significant hit to a *Leishmania* protein. However, upon closer inspection the same query matched a trypsin autolysis peptide in the contaminants database (Table 3-9). Thus, this was concluded to be a spurious match by chance to a *Leishmania* peptide and the identification was excluded from the significant hits in the *Leishmania* secretome.

Table 3-9 Spectral query that was matched to the mass and fragmentation of two different peptides.

Trypsin-Sus scrofa(Pig).

Query	Observed	Mr(expt)	Mr(calc)	Delta	Miss	Score	Expect	Rank	Unique	Peptide
877	421.7720	841.5294	841.5022	0.0273	0	36	0.00023	1	U	R.VATVSLPR.S

LmxM.31.1700

Query	Observed	Mr(expt)	Mr(calc)	Delta	Miss	Score	Expect	Rank	Unique	Peptide
877	421.7720	841.5294	841.4658	0.0637	0	32	0.017	1	U	K.AVEAVTPR.L

Comparison of estimated protein abundance in the experimentally determined proteome to the parasite secretome illustrates that the proteins that are common to both the lysate and secretome are not simply a fraction of the most abundant in the lysate. Additionally, there are abundant lysate proteins that do not appear in the secretome. Only one previous study in *Leishmania* has reported the percentage of proteins shared between the secretome and control proteome, at 52%, with the overlap between the secretome and control proteome observed to be higher than this in stationary phase cultures than procyclic promastigote cultures (Santarém *et al.* 2013b). It is important to note that some abundant proteins in the lysate are present in the secretome. They have not, however, been discounted from the secretome analyses in the following chapters of this thesis, as they could play important roles in the natural environment of the parasite.

As further validation of the collective isolation of secreted proteins, between 45 and 86% of the promastigote proteins identified in this study can be observed in other *Leishmania* secretome studies, supporting their identification as secreted proteins, which are presented and discussed in Chapter 4 of this thesis.

Although we show the presence of many low abundance proteins in the secretome, there are still some proteins which have been identified as secreted by *L. mexicana* in individual studies, which do not appear in the secretome presented here. Often, these proteins are identified by highly sensitive immunological methods such as ELISA or Western blot, or by activity assays. It is clear that, although we have eliminated abundant serum proteins, many abundant proteins in the secretome are still masking those that are secreted at low abundance. Improvements to MS identification are always sought after to improve dynamic range. Further separation of the secretome prior to MS, such as using strong cation exchange (SCX) chromatography before C18 liquid chromatography could improve this.

3.5 Summary

The final technique and methodologies presented here for the isolation and extraction of the *Leishmania* secretome can be used to study the secretome of the promastigote and amastigote life-cycle stages. Further development was the inclusion of exosomes by lysing, showing all secreted proteins as one data set. There are several advantages of the techniques employed here for the collection of the secretome, including being able to study promastigotes and amastigotes *in vitro* in parallel with direct comparison, and free from host interactions and contamination. However, there are disadvantages such as lack of *in vivo* stimuli which may affect the secretome obtained.

We aimed to implement and optimise a method for the secretome extraction and collection from *L. mexicana*, which we have shown here. We have evaluated and adapted current methods for the secretome extraction from *Leishmania* promastigotes and applied them to the study of *L. mexicana* promastigote and amastigote cultures, with the aim that these secretome extraction methods will allow us to obtain a global secretome from which the promastigote and amastigote life cycle stages and their survival mechanisms can be investigated. We have taken into account a number of complications and considerations such as parasite viability and protein concentration methods, which have been addressed and provide a basis and methodology for a comparative study of the *L. mexicana* promastigote and amastigote secretomes. The flow-chart below in Figure 3-10 summarises the final methodology used for subsequent studies presented in this thesis, a method for the analysis of the secretome providing insight into disease virulence and parasite pathogenicity.

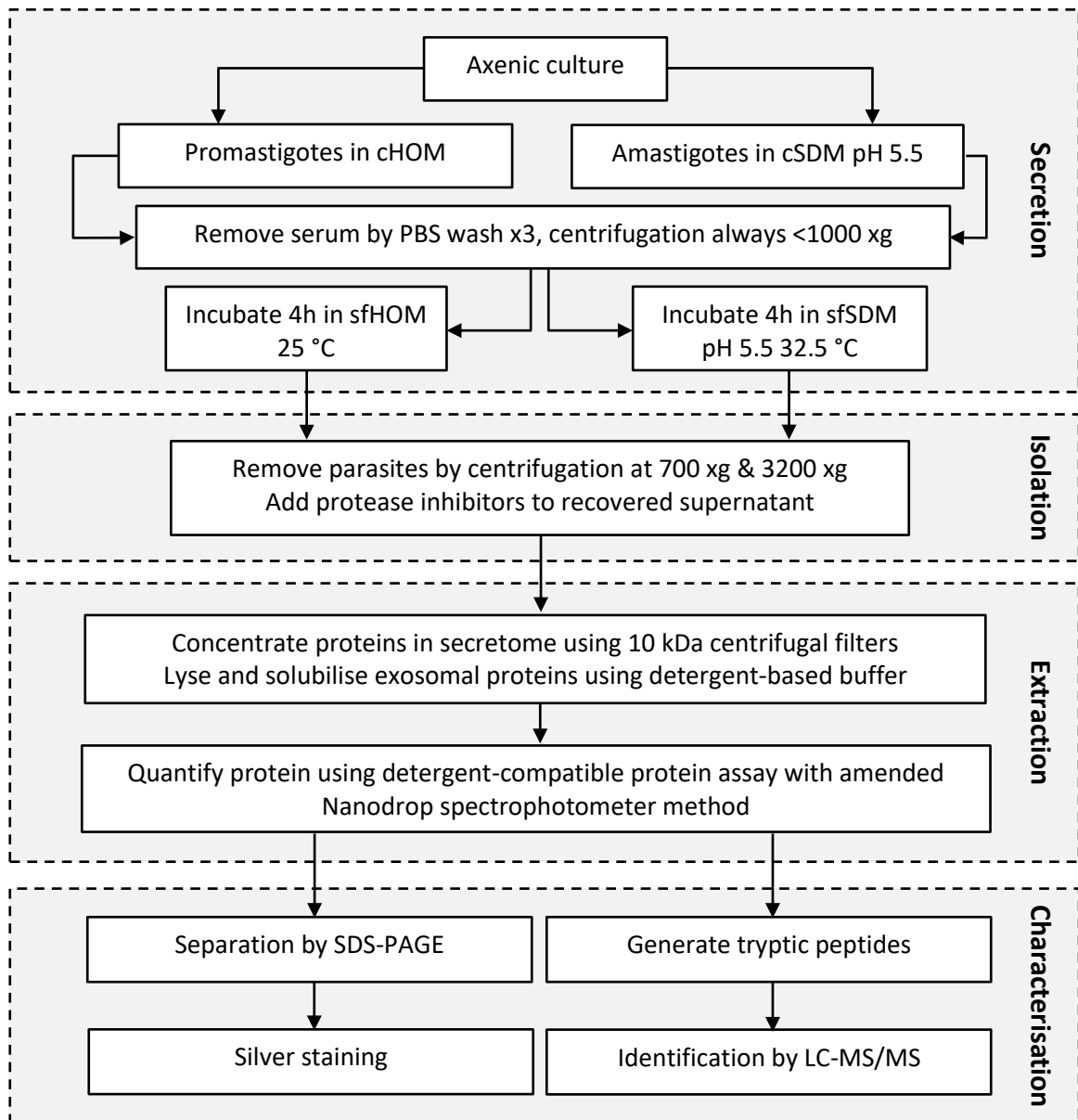


Figure 3-10 Flow chart summarising the method implemented for the study of the *L. mexicana* promastigote and amastigote secretome.

Chapter 4 Characterisation and comparison of the *L. mexicana* promastigote and amastigote secretome

4.1 Introduction

Here, the secretome of the different lifecycle stages of the *Leishmania mexicana* parasite, promastigote and amastigote, will be investigated in more detail. The parasites are only introduced to the body at the vector bite location, but the immune system cannot control and defend against the infection. Macrophages phagocytose the parasites in human tissue, as they would with any microbe or foreign organism to remove these pathogens from the tissue. However, the *Leishmania* parasites can instead differentiate into an intracellular form and thrive in this environment within the macrophage. This is likely to involve modification of the intracellular macrophage niche to allow the parasite to develop and differentiate. We hypothesise, with the emergence of supporting evidence, that *Leishmania* employ secreted molecules to achieve this.

By growing the parasites in an environment that mimics their natural host environment, like that in the phagolysosome, but free of other cell types, we can sample and collect proteins it secretes, as discussed in Chapter 3. With the application of proteomics, we can then characterise the secretome. We can investigate differences in secreted effectors between life cycle stages to deduce their mechanisms of survival, from combating the challenges presented by the macrophage, including reactive oxygen species (ROS) and hydrolytic enzymes, to acquiring nutrient and modulating host cell gene expression. Crucially, processes that are essential for parasite survival present attractive targets for therapeutic intervention.

4.1.1 Secreted proteins play a key role in the virulence of parasites

Intercellular communication is essential for biological interaction, whether within a multicellular organism or between microbes and their hosts. The parasite secretome has been attributed several roles involved in disease progression and virulence, with diverse parasites shown to employ this mechanism including protozoa, nematodes and trematodes. The role of secreted proteins in establishing and mediating host:microbe interactions is challenging to assess *in vitro*, especially for intracellular pathogens.

Protozoa such as Kinetoplastids and Apicomplexans have been found to secrete proteins into their extracellular environment, and furthermore, they play a role in the pathogenicity of the parasite (Mantel & Marti 2014). A number of excreted and secreted proteins from trypanosome procyclic forms have been implicated in disease progression and parasite survival (Atyame Nten *et al.* 2010). Further work in trypanosomes highlighted the important role the secretome plays in trypanosome infections, specifically *T. cruzi* secreted proteins (Bautista-López *et al.* 2016; Watanabe Costa *et al.* 2016). Outlined in Chapter 3, there are a number of studies which have begun to unravel the *Leishmania* secretome (Braga *et al.* 2014; Chenik *et al.* 2006; Cuervo *et al.* 2009; Hassani *et al.* 2011; Santarém *et al.* 2013b; Silverman *et al.* 2008). Of those that have investigated the host cell response to the secretome, effects such as promotion of Th2 polarisation (Silverman *et al.* 2010b), cleavage and activation of host protein tyrosine phosphatases and inhibition of nitric oxide production (Hassani *et al.* 2011) were observed. Apicomplexan parasites have specialised secretory organelles, namely micronemes, rhoptries and dense granules. These have been shown to play a major role in invasion, remodelling of the host cell and immune evasion. In *Plasmodium* these proteins have been extensively characterised (Soni *et al.* 2016). In *Toxoplasma* dense granule proteins have been shown to modulate the parasite niche in the host, providing mechanisms for nutrient acquisition by the parasite in the parasitophorous vacuole (Gold *et al.* 2015). These parasites can also induce the secretion of proteins from their host cells to trigger strong immune responses from surrounding cells. Infection with *Plasmodium* induces secretion of extracellular vesicles from erythrocytes, which would otherwise be unable to produce vesicles due to a lack of exocytosis machinery (Mantel 2013).

4.1.2 Parasites can alter their secretome to adapt to different environments and stresses

Many different parasite species, including *Leishmania*, face a range of environments and challenges that they must overcome in a bid to survive. These include contrasting environments in multiple hosts or migrating to different cell types in the body, for example switching between high nutrient and low nutrient environments or between environments with differing pH.

As well as utilising a secretome for the establishment of disease, different life-cycle stages of parasites use the secretome for niche modification depending on the host that they are infecting. Sotillo *et al.*, present a study which shows differences in the proteome between different developmental stages of *Nippostrongylus* (Sotillo *et al.* 2014). This highlights that parasites are known to alter and adapt their secretome in response to changing conditions and lifecycle stage. For example, only 8 proteins were found in common between the secretory products of *N. brasiliensis* L3 larvae and adult worms, which inhabit distinct anatomical niches (Sotillo *et al.* 2014). This differed from *S. ratti* larval stages and adults which can both reside in the intestine, and had over 50% of their secretome in common between stages (Soblik *et al.* 2011). Alteration of protein secretion and vesicle cargo with life cycle stage is also observed in bacteria, for example *Bacillus subtilis* (Kim *et al.* 2014). 193 proteins were identified in the extracellular vesicles of sporulating and vegetative cells. 61 were found to be significantly more abundant in EV of sporulating cells, and 62 proteins were more abundant in EV shed by vegetative cells (Kim *et al.* 2014).

Stage-specific protein secretion also occurs in protozoa such as *Trypanosoma*, showing that they alter their secretome in response to environment and their life cycle stage. Stage-specific cargo of extracellular vesicles from epimastigote and metacyclic trypomastigote *T. cruzi* was identified, and found to contain both qualitatively and quantitatively different proteins (Bayer-Santos *et al.* 2012). These observations led to the hypothesis that as *Leishmania* inhabit distinct environments, the secretion of proteins may change to adapt to different stresses. Differences in secreted proteins have been discovered between procyclic and metacyclic promastigotes of *L. infantum*, with overrepresentation of proteins with metabolic function in the procyclic secretome and overrepresentation of proteins with functions in folding and degradation, proteasome, and spliceosome in the metacyclic secretome (Santarém *et al.* 2013b). We therefore aim to extend these analyses to amastigotes.

4.1.3 Secreted proteins are major drug targets and vaccine candidates

Understanding the way a parasite interacts with its host and vector gives us insight into the mechanisms, biological functions, biochemical reactions and

immunological process that will give protection to the host against the pathogen. To make advances in the development of new drugs and vaccines, parasite components that are required for survival need to be identified and characterised so that drugs may rationally be designed to target these effectors or their mechanisms of action. The accessibility and importance of the secretome to the parasite renders these proteins attractive targets for intervention, furthermore, secreted proteins have been revealed to be highly effective drug targets. A study of the properties of 148 existing drug target proteins and 3000 non-drug target proteins led to the conclusions that drug targets tend to be found in membranes or extracellularly; are more likely to be enzymes, particularly oxidoreductases or transferases; are secreted; and have long lifetimes, shown by the presence of glycosylation (Bakheet & Doig 2009).

There are also many studies into the secretome of pathogens that have led to the creation of effective vaccines against these pathogens. Many currently and widely used vaccines against bacterial and viral pathogens are derived from secreted proteins. An agricultural vaccine against *E. coli* is based on a Type III secreted protein of the bacterium (Vogstad *et al.* 2013). Successful protein vaccines against human disease include the Hepatitis B vaccine, *Haemophilus* PS-protein vaccine, Meningococcal group B vaccines, Pertussis vaccine and Pneumococcus vaccine (Siegrist 2013). In bacterial pathogens, several other experimental and *in silico* approaches recognised secreted proteins as potential vaccine candidates. Anchorless surface proteins have been identified as a group A strep vaccine candidate (Henningham *et al.* 2012). Screening of non-classically secreted proteins as vaccine candidates in *Brucella*, an intracellular pathogen of phagocytes, resulted in the creation of a multipeptide vaccine using multiple secreted protein epitopes (Vishnu *et al.* 2017). Furthermore, *Haemophilus* secreted proteins induce a Th1 response, therefore highlighting potential vaccine candidates from secretome studies (Li *et al.* 2015).

Potential vaccine candidates were also found in the extracellular vesicles of the parasite *Schistosoma mansoni*, the causative agent of schistosomiasis, which were subsequently used to trial protein vaccines in animal models and were found to be efficacious (Sotillo *et al.* 2016). Using *in silico* reverse-vaccinology, non-classically secreted proteins were identified as possible vaccine candidates. However, no

vaccines are currently licensed for use in humans against parasites. Several vaccines for human schistosomiasis are under development and have been progressed to Phase I, II or III clinical trials: for example Bilhvax, an *S. haematobium* 28-kD glutathione S-transferase (rSh28GST) (Riveau *et al.* 2018); Sm 14, an *S. mansoni* 14-kDa fatty acid-binding protein (Santini-Oliveira *et al.* 2016); and Sm-TSP-2, an *S. mansoni* 9-kDa surface tetraspanin (Merrifield *et al.* 2016). An Sm-p80 based vaccine is also in preparation for clinical trials against schistosomiasis (Siddiqui & Siddiqui 2017). Several *Leishmania* protein vaccine candidates have also begun phase I or II trials in human subjects, namely LEISH-F1 (Nascimento *et al.* 2010), LEISH-F3 (ClinicalTrials.gov 2012) and Leish-111f, which has completed phase I and II trials in humans (Coler *et al.* 2007).

Finally, there are several benefits to developing, producing and utilising a protein or subunit vaccine over live attenuated vaccines. These include limitations of vaccine preparation when producing live attenuated vaccines which involves using a pathogen directly. A serious consideration is the safety aspect of potentially inducing and causing infection when using live attenuated vaccines, which is far less likely with a protein or subunit vaccine. There are also increased logistical and infrastructure requirements for live attenuated vaccines compared to a protein or subunit vaccine, including increases in transport and storage costs. Understanding the secretome of the *Leishmania* parasite will lead to a greater understanding of the survival mechanisms and host:parasite interaction of this parasite, providing the information for and potentially leading to the discovery of a novel drug targets and vaccine candidates.

4.2 Aims and Hypotheses

Here, we present a study characterising and comparing the secretome of the promastigote and amastigote stages of the parasite. Evidence points to the secretion of proteins by *Leishmania* which may be used to create an environment that is required for their successful growth, however in-depth analysis and profiling of the differences between the two secretomes including conclusions on the role these secreted proteins have in disease is yet to be achieved.

The main aim of this study was to present a comprehensive characterisation of the proteins secreted by the two major life cycle stages of *L. mexicana*, promastigotes and amastigotes, and to compare the two.

- We hypothesise that both promastigotes and amastigotes secrete proteins into their extracellular environment
- We hypothesise that *L. mexicana* parasites alter their secretome throughout their life cycle

4.3 Results

Comparative secretome analyses between promastigote- and amastigote-stage parasites were conducted visually, by SDS-PAGE and by using different gel staining methods and 2D separation methods to determine differences in protein properties and modifications; and using shotgun LC-MS/MS to determine differences in protein identities, and the predicted properties thereof.

4.3.1 Promastigote and amastigote secretomes display visually distinct electrophoretic profiles

The secretome collected from *L. mexicana* promastigotes and amastigotes in axenic culture was first separated by SDS-PAGE and silver stained to reveal differences in electrophoretic profile between the two life cycle stages. Figure 4-1 shows the electrophoretic profiles of the secretome of both promastigotes and amastigotes. There are many more protein bands visible in the promastigote secretome compared to the amastigote. Additionally, the most abundant band in the amastigote secretome, at around 63kDa, is considerably reduced in the promastigote samples and difficult to distinguish. The most abundant bands in the promastigote samples, occurring between 70 and 97 kDa are not visible at all in the amastigote samples.

Analysis of the lysate and secretome of the two life cycle stages by 2D-GE show both a difference between the profiles of the cellular and secreted proteins, and clear stage-specific differences between the secreted proteins (Figure 4-2). Similar to the 1D gel profiles (Figure 4-1), there are two main molecular weight areas where the most abundant proteins are in the 2D amastigote secretome, indicated by arrows (Figure 4-2d). Given that these are 12% gels and in the absence of a molecular weight marker on the 2D gels, we can postulate these may be 55-65kDa and 20-30kDa by comparison to a commercial SDS-PAGE migration chart (Appendix 2). The presence of multiple spots in the charge-based first dimension separation, but all at the same molecular weight, suggests post translational modifications of the proteins in the secretome.

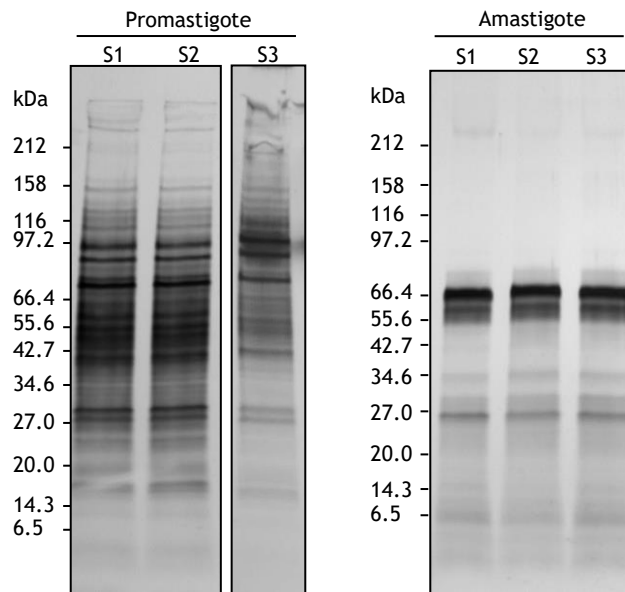


Figure 4-1 Secretome from *L. mexicana* promastigotes and amastigotes. Secreted proteins from conditioned axenic culture supernatant separated on 4-20% SDS-PAGE and silver stained. MW marker used was NEB broad range (2-212 kDa). S1/S2/S3 indicates biological repeat.

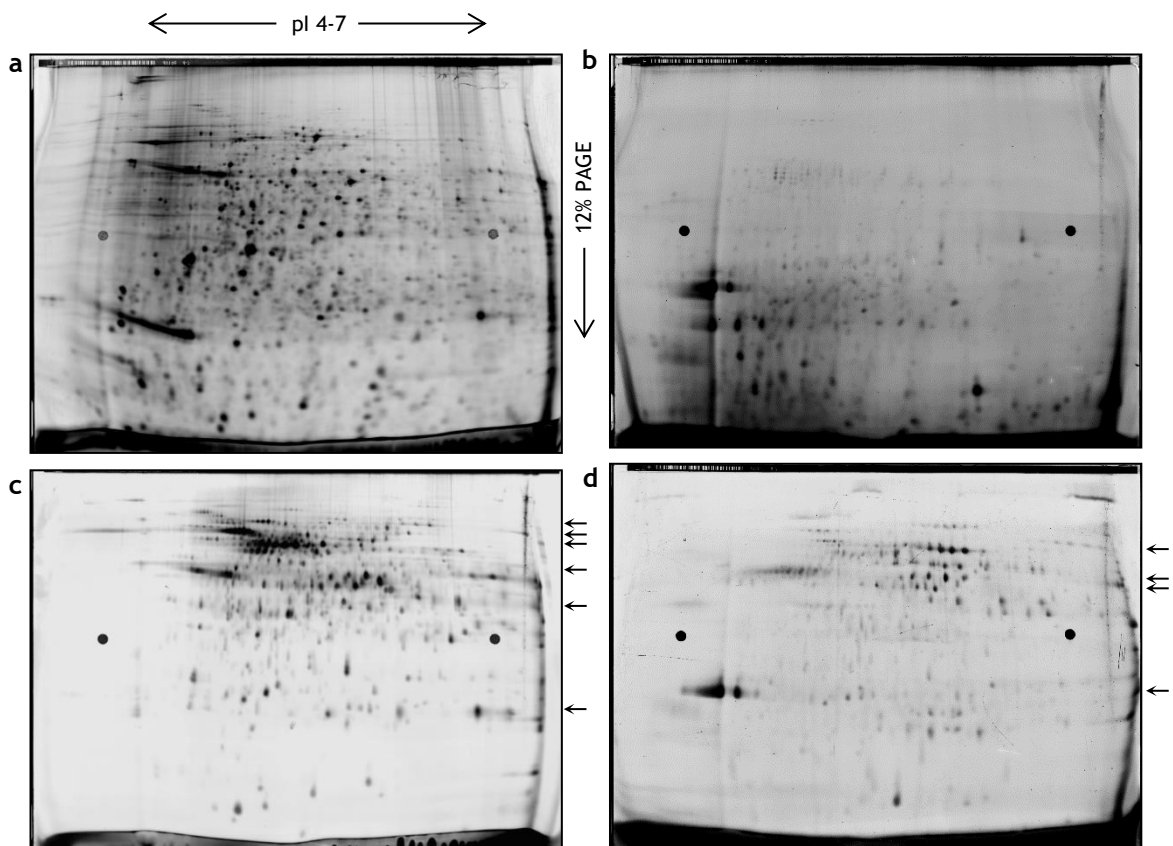


Figure 4-2 2-dimensional SDS-PAGE of *L. mexicana* protein samples. **a**, Promastigote cell lysate, **b** amastigote cell lysate, **c**, promastigote secretome, **d**, amastigote secretome. Separation in the first dimension by isoelectric focusing with non-linear pH range 4-7, followed by electrophoresis through a 12% polyacrylamide gel. 50 μ g total protein loaded, labelled with Cy3 and imaged using the Typhoon imager with 532 nm laser and Cy3 emission filter.

4.3.2 Amastigote secretome has different physical properties compared to the promastigote secretome

Amastigotes appear to have an insoluble fraction in their secretome. It becomes visible after freeze-thawing of the conditioned medium as a precipitate in the recovered supernatant. After centrifugation the insoluble component forms a white pellet (Figure 4-3 c + d). This phenomenon is not due to a component of the medium or the added protease inhibitors as both solutions were treated in the same way as the conditioned medium but did not give the same result (Figure 4-3 a + b). Harsher solubilisation was attempted with RIPA buffer, but the material was not solubilised. The white pellet was not easily solubilised in SDS buffer, RIPA buffer or by raising the pH using Tris-HCl pH 8.0. The pellet was resuspended (but not solubilised) in SDT buffer and subjected to trypsin digestion using the FASP protocol. The proteins identified are listed below (Table 4-1). Only 6 proteins were identified above the confidence threshold of $P < 0.05$ and with a Mascot score of > 30 (see Methods 2.14 for scoring system). These included a superoxide dismutase, cathepsin L-like protease, a glycosomal carboxykinase and a putative Dopey N-terminal protein.

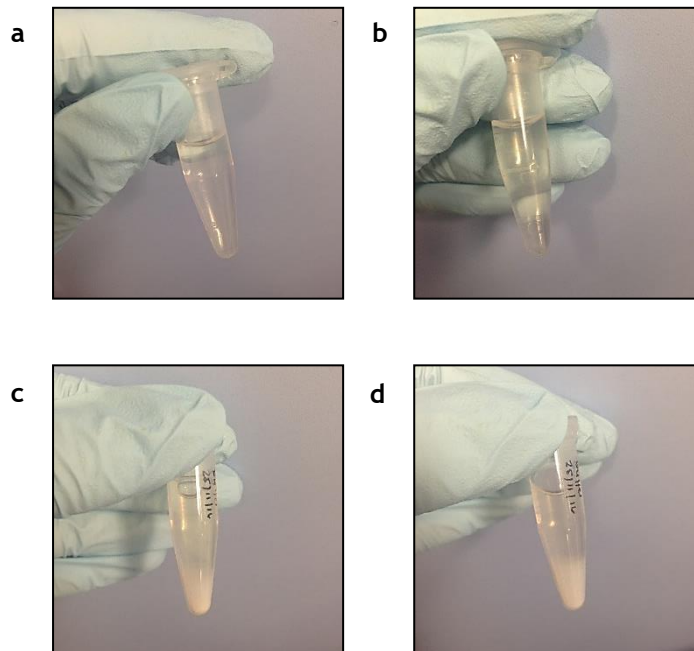


Figure 4-3 The *L. mexicana* amastigote secretome contains an insoluble component. (a), Schneider's Drosophila medium (SDM) pH 5.5 after freezing and thawing, (b), SDM pH 5.5 + protease inhibitors after freezing and thawing, (c,d), two repeats of amastigote-conditioned serum-free SDM + protease inhibitors after freezing and thawing. Prior to freezing no precipitate was visible.

Table 4-1 Proteins from the insoluble component of the *L. mexicana* amastigote secretome. Insoluble pellet was suspended in SDT buffer and transferred to a FASP column for trypsin digestion. Resulting peptides were analysed by LC-MS/MS.

GeneDB Accession	Protein Description	Score	Mass	PSMs	Sequences	Coverage (%)	emPAI
LmxM.31.1820	iron superoxide dismutase, putative	103	21994	4	1	7.2	0.18
LmxM.08.1030 OR 1040 OR 1070	cathepsin L-like protease, putative	144	25997	2	1	4.2	0.15
LmxM.27.1805	Phosphoenolpyruvate carboxykinase [ATP], glycosomal	79	58770	4	2	4.8	0.14
LmxM.08.1171	beta tubulin	117	50319	3	1	2.7	0.08
LmxM.34.1830	hypothetical protein, conserved	36	82713	2	1	1.8	0.05
LmxM.31.3410	Dopey, N-terminal, putative	32	298446	3	1	0.4	0.01

Amastigotes also secrete a heavily glycosylated high molecular weight (HMW) secretome component. This is not visible in the amastigote lysate or the promastigote secretome or lysate. It is very heavily glycosylated as it does not appear at a high concentration in the Coomassie or silver stained gel but stains very strongly in the PAS-stained gel (Figure 4-4). As a reference, the concentration of the positive control glycosylated protein loaded was 5 μ g. This is likely to be the abundantly secreted glycoprotein, aPPG, which when run without deglycosylation by hydrolysis was found at >200 kDa (Ilg *et al.* 1998). A similar double band is visible in the promastigote cell lysate stained with CBB and very faintly in the PAS-stained secretome.

When the amastigote secretome sample is filtered through a 0.22 μ m filter a large proportion of the ~60-65 kDa band is removed. Other bands, including the HMW bands that remain in the stacking gel, are still present (Chapter 3, Figure 3-6a).

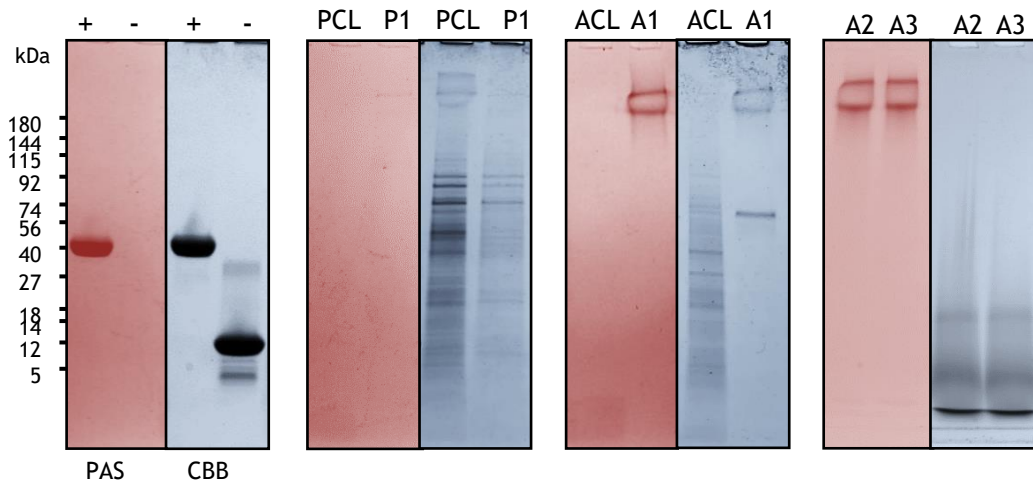


Figure 4-4 Staining of glyco-moieties on *L. mexicana* protein samples. + Positive glycosylated control = horseradish peroxidase, negative non-glycosylated control = soybean trypsin inhibitor. Cell lysate (CL) and replicates of secretome samples (S1-3) from *L. mexicana* promastigotes (P) and amastigotes (A) separated on 4-20% SDS-PAGE and stained for glycoprotein with a periodic acid schiff (PAS) stain. False coloured for clarity; red indicates PAS staining. blue indicates Coomassie staining (CBB). Coomassie staining was performed after PAS for all gels except amastigote S2/3 where the samples were run and stained on separate gels.

4.3.3 Mass spectrometry of culture supernatant reveals the *L. mexicana* secretome

Table 4-2 shows the secreted proteins identified by mass spectrometry in at least three biological repeats of promastigote secretome collection, and Table 4-3 shows the secreted proteins identified by mass spectrometry in at least three biological repeats of amastigote axenic secretome collection. Stringent inclusion criteria were applied to these secretomes. Identifications in each biological repeat must meet a minimum Mascot score of 30 for identity and the threshold for false discovery was set to less than 5%. Proteins must be identified in three or more independent experiments for inclusion in the final list of secreted proteins. Using these criteria, 256 promastigote secreted proteins were identified and 36 amastigote secreted proteins.

Table 4-2 Secreted proteins of *L. mexicana promastigotes*. Proteins identified in three or more biological repeats. Scoring scheme, mascot score >30, see methods for complete settings. Accession numbers from TriTrypDB, peptide spectral matches (PSMs), sequences indicate number of different peptide sequences that the PSMs matched to, estimation of protein abundance = exponentially modified protein abundance index (emPAI) (Ishihama *et al.* 2005).

Accession	Description	Mascot Score	Mass [kDa]	PSMs	Sequences	Coverage (%)	emPAI
LmxM.36.6480	histidine secretory acid phosphatase, putative	1276	127.5	53	18	17.890625	4.946
LmxM.23.1020	hypothetical protein, unknown function	174	12.5	17	8	66.666667	4.623
LmxM.23.1580	nucleoside 2-deoxyribosyltransferase, putative	245	16.9	10	5	59.354839	4.623
LmxM.36.3910	S-adenosylhomocysteine hydrolase	618	47.8	37	19	51.029748	4.012
LmxM.28.2770	heat-shock protein hsp70, putative	1416	71.2	77	28	44.495413	3.711
LmxM.34.2220	kinetoplastid membrane protein-11	97	11.2	10	6	36.956522	3.642
LmxM.25.0910	cyclophilin a, putative	155	18.8	14	6	42.372881	3.394
LmxM.14.1160	enolase	775	46.1	39	18	53.146853	3.184
LmxM.32.0312	heat shock protein 83-1	866	80.5	65	31	41.940086	3.042
LmxM.08.1171	beta tubulin	491	49.7	25	12	34.988713	2.631
LmxM.36.0180	elongation factor 2	926	94	63	32	48.52071	2.511
LmxM.09.0910 OR 0930	calmodulin, putative	190	16.8	12	7	48.993289	2.455
LmxM.17.0080 OR 0085	elongation factor 1-alpha	457	49.2	34	17	40.089087	2.35
LmxM.09.0891	polyubiquitin, putative	169	14.6	12	6	43.75	1.929
LmxM.32.2540	metallo-peptidase, Clan MA(E) Family M32	433	56.9	40	21	44.488978	1.929
LmxM.31.2950	nucleoside diphosphate kinase b	210	16.7	10	5	43.708609	1.894
LmxM.08_29.1160	tryparedoxin 1, putative	160	16.6	9	5	40.689655	1.848
LmxM.17.1220	histone H2B	188	11.9	10	5	45.794393	1.848
LmxM.20.1280	calpain-like cysteine peptidase, putative	157	16.9	8	4	36.423841	1.848
LmxM.36.1100	ribosomal protein L24, putative	83	14.6	5	2	16.129032	1.683
LmxM.25.0720	eukaryotic initiation factor 5a, putative	140	17.8	15	6	41.566265	1.61
LmxM.31.1820	iron superoxide dismutase, putative	102	21.7	10	5	20	1.61
LmxM.13.0280	alpha tubulin	541	60.1	23	12	28.467153	1.512
LmxM.20.1310	small myristoylated protein 1	69	15	6	4	22.900763	1.512
LmxM.34.3230	cystathione gamma lyase, putative	419	44.4	21	7	20.97561	1.462

Accession	Description	Mascot Score	Mass [kDa]	PSMs	Sequences	Coverage (%)	emPAI
LmxM.36.1430	translation elongation factor 1-beta, putative	243	22.9	11	6	26.442308	1.448
LmxM.10.0470	GP63, leishmanolysin	449	63.6	22	14	25.581395	1.39
LmxM.14.0190	hypothetical protein, conserved	88	22.3	9	6	33.668342	1.371
LmxM.29.3340	60S ribosomal protein L9, putative	191	21.5	12	6	35.263158	1.371
LmxM.36.3760	60S ribosomal protein L10a, putative	206	24.6	13	7	29.439252	1.336
LmxM.02.0550	hypothetical protein, unknown function	94	17.6	7	4	34.969325	1.31
LmxM.23.0200	endoribonuclease L-PSP (pb5), putative	226	16.8	8	4	24.539877	1.31
LmxM.13.0570	40S ribosomal protein S12, putative	143	15.6	10	5	28.368794	1.276
LmxM.16.1430	Paraflagellar rod protein 2	448	68.6	29	18	40.066778	1.219
LmxM.15.1040 OR 1160	tryparedoxin peroxidase	173	22.2	8	4	21.105528	1.154
LmxM.16.0230	protein tyrosine phosphatase-like protein	152	19.4	7	4	25.714286	1.154
LmxM.33.0840	translation elongation factor 1-beta, putative	264	34.1	13	8	29.283489	1.154
LmxM.11.0630	metallo-peptidase, Clan MF, Family M17	294	56.9	19	9	22.803738	1.106
LmxM.09.0970	elongation factor-1 gamma	152	46.2	15	9	26.237624	1.096
LmxM.34.0820	aspartate aminotransferase, putative	238	46.2	15	9	15.533981	1.043
LmxM.11.1190	40S ribosomal protein S15A, putative	83	14.7	8	4	23.846154	1.031
LmxM.22.1410	centrin-4, putative	36	16.4	6	4	36.91275	1.031
LmxM.08_29.1750	paraflagellar rod protein 1D, putative	401	68.9	26	13	23.529412	1.024
LmxM.16.0760	transaldolase, putative	272	37	18	10	36.666667	1.009
LmxM.14.0850 OR 0851	small myristoylated protein 3, putative / cysteine peptidase, Clan CA, family C2, putative	129	12.9	6	3	26.086957	0.995
LmxM.23.0110	mannose-1-phosphate guanyltransferase	121	41.5	13	8	24.274406	0.978
LmxM.34.0020	pyruvate kinase	205	28.7	10	5	15.969582	0.968
LmxM.05.0960	metallo-peptidase, Clan M-, Family M49	515	75.7	27	15	28.718704	0.954
LmxM.14.0130	nucleoside hydrolase-like protein	163	39.2	11	6	24.715909	0.905
LmxM.36.1940	inosine-guanosine transporter	367	54.2	15	8	17.43487	0.887
LmxM.05.0350	trypanothione reductase	236	53.1	17	9	20.366599	0.874
LmxM.36.1960	phosphomannomutase, putative	184	28.1	12	6	22.267206	0.874
LmxM.36.6290	glucose transporter 2	191	61.1	10	5	13.227513	0.874

Accession	Description	Mascot Score	Mass [kDa]	PSMs	Sequences	Coverage (%)	emPAI
LmxM.24.2060	transketolase, putative	330	71.8	19	11	18.181818	0.855
LmxM.08_29.1090	ribosomal protein L1a, putative	84	47.6	12	8	20.506912	0.848
LmxM.29.2980	glyceraldehyde 3-phosphate dehydrogenase, glycosomal	257	39.1	15	6	19.390582	0.848
LmxM.22.1360	farnesyl pyrophosphate synthase, putative	206	41.1	10	6	17.955801	0.823
LmxM.28.2740a	hypothetical protein	264	34.4	15	6	24.038462	0.823
LmxM.30.0010	5-methyltetrahydropteroyltriglutamate-homocysteinemethyltransferase, putative	295	86.1	24	13	15.844156	0.817
LmxM.34.2350	aminopeptidase P, putative	298	53.7	17	8	15.495868	0.812
LmxM.36.2950	succinyl-CoA ligase [GDP-forming] beta-chain, putative	71	44.1	12	8	21.549637	0.812
LmxM.18.1370	heat shock protein, putative	512	91.9	26	15	23.08627	0.795
LmxM.14.0310	proteasome alpha 3 subunit, putative	115	32.2	9	6	25.614035	0.778
LmxM.15.0950	40S ribosomal protein S3, putative	182	24.5	11	6	28.310502	0.778
LmxM.18.1520	P-type H ⁺ -ATPase, putative	406	107.4	28	15	16.837782	0.778
LmxM.21.1700	proteasome alpha 2 subunit, putative	224	25.1	8	4	23.809524	0.778
LmxM.21.1830	proteasome subunit alpha type-5, putative	161	26.8	8	5	21.721311	0.778
LmxM.34.0030	pyruvate kinase, putative	329	54	14	9	25.702811	0.778
LmxM.34.3800	60S ribosomal protein L23, putative	70	14.9	5	3	17.266187	0.778
LmxM.26.2680	hypothetical protein, unknown function	208	40.9	11	6	18.832891	0.738
LmxM.01.0770	Eukaryotic initiation factor 4A-1	207	51.1	15	8	20.833333	0.719
LmxM.24.0761	malic enzyme	250	62.5	15	8	14.535902	0.719
LmxM.26.0890	40S ribosomal protein S16, putative	103	16.7	8	4	22.818792	0.719
LmxM.30.1440c	hypothetical protein	61	46	6	3	8.5585586	0.701
LmxM.36.6650	2,3-bisphosphoglycerate-independent phosphoglyceratemutase	472	60.8	16	9	21.699819	0.701
LmxM.05.0830	methylthioadenosine phosphorylase, putative	114	33.3	10	5	18.300654	0.688
LmxM.11.0240	proteasome alpha 7 subunit, putative	117	27.8	8	5	19.433198	0.688
LmxM.16.0540	aspartate carbamoyltransferase, putative	111	35.4	8	5	23.547401	0.688
LmxM.26.1570	thimet oligopeptidase, putative	257	77	19	10	17.518248	0.677
LmxM.24.0850	triosephosphate isomerase	214	27	8	4	17.928287	0.668
LmxM.08_29.2800	inosine-adenosine-guanosine-nucleosidehydrolase, putative	77	36.4	8	5	18.618619	0.65

Accession	Description	Mascot Score	Mass [kDa]	PSMs	Sequences	Coverage (%)	emPAI
LmxM.27.1390	hypothetical protein	83	34.6	10	5	9.3167702	0.65
LmxM.32.1035	hypothetical protein, conserved	104	19	5	3	23.163842	0.638
LmxM.23.1220	T-complex protein 1, gamma subunit, putative	216	60.2	17	10	20.145191	0.632
LmxM.27.0190	proteasome alpha 7 subunit, putative	141	25.6	6	4	18.067227	0.624
LmxM.04.0950	hypothetical protein	193	24.5	10	4	23.474178	0.585
LmxM.15.0200	60S ribosomal protein L13a, putative	70	25.5	9	5	20.720721	0.585
LmxM.21.0730	60S ribosomal protein L36, putative	41	11.9	3	2	21.90476	0.585
LmxM.21.1550	40S ribosomal protein S11, putative	79	16.3	5	3	21.276596	0.585
LmxM.23.0360	NADP-dependent alcohol dehydrogenase, putative	119	38.5	8	5	14.204545	0.585
LmxM.29.0880	adenosine kinase, putative	119	37.2	7	4	14.782609	0.585
LmxM.29.2850	hypothetical protein, conserved	43	13.1	3	2	19.13043	0.585
LmxM.29.3650	ribosomal protein L15, putative	86	24.4	8	4	16.666667	0.585
LmxM.15.1010	glutamate dehydrogenase	519	114.6	31	17	19.27237	0.562
LmxM.36.1600	proteasome subunit alpha type-1, putative	83	29.7	7	4	13.636364	0.551
LmxM.13.0560	60S ribosomal protein L18, putative	118	22.1	5	2	11.111111	0.54
LmxM.34.0750	proteasome activator protein pa26, putative	35	24.9	7	4	11.73913	0.52
LmxM.36.4170	oxidoreductase, putative	100	36.1	5	4	22.647059	0.52
LmxM.10.0390	GP63, leishmanolysin	256	63.8	11	7	13.621262	0.512
LmxM.01.0520	long-chain-fatty-acid-CoA ligase, putative	122	77.5	13	8	11.468531	0.492
LmxM.31.3270	chaperonin alpha subunit, putative	272	59.2	15	8	14.835165	0.492
LmxM.19.0160	metallo-peptidase, Clan MG, Family M24	105	42.4	8	5	14.210526	0.487
LmxM.03.0440	60S acidic ribosomal protein P2, putative	33	11	2	1	14.54545	0.468
LmxM.23.0040	tryparedoxin peroxidase	91	25.4	4	3	12.831858	0.468
LmxM.27.0760	ras-related protein RAB1A, putative	56	22.2	5	4	21	0.468
LmxM.29.3500	S-adenosylmethionine synthetase	115	43.1	8	5	12.755102	0.468
LmxM.33.2580	ALBA-domain protein 3	85	22.6	6	3	22.439024	0.468
LmxM.33.4340	20s proteasome beta 7 subunit, (putative)	103	24.6	5	3	16.363636	0.468
LmxM.36.3590	cysteine synthase, putative	143	35.4	8	4	16.216216	0.468
LmxM.28.2910	glutamate dehydrogenase, putative	144	49	9	6	13.938053	0.453

Accession	Description	Mascot Score	Mass [kDa]	PSMs	Sequences	Coverage (%)	emPAI
LmxM.04.1230	actin	139	42.1	7	4	15.957447	0.445
LmxM.30.2600	calreticulin, putative	43	44.7	4	4	7.575758	0.445
LmxM.25.2010	2,4-dihydroxyhept-2-ene-1,7-dioic acid aldolase, putative	80	30.3	5	3	13.620072	0.438
LmxM.29.2490	heat shock 70-related protein 1, mitochondrial precursor, putative	336	72.5	15	8	16.516517	0.438
LmxM.34.3840	proteasome beta 2 subunit, putative	79	27.5	4	3	12.992126	0.438
LmxM.08_29.1720	histone H2A, putative	49	14	4	2	12.121212	0.425
LmxM.09.0770	oligopeptidase b	272	83.5	15	8	15.731874	0.425
LmxM.11.0820	hypothetical protein, conserved	196	37.4	5	3	16.617211	0.413
LmxM.26.2710	glutamate 5-kinase, putative	58	29.1	5	3	13.257576	0.413
LmxM.12.0030	proteasome beta-1 subunit, putative	216	30.5	6	3	14.487633	0.389
LmxM.23.0840	hypothetical protein, unknown function	150	57	8	4	5.5028463	0.389
LmxM.24.1500	IgE-dependent histamine-releasing factor, putative	147	31.1	5	3	16.666667	0.389
LmxM.29.2580	reticulon domain protein, 22 kDa potentially aggravating protein (paple22)	39	22.2	3	2	10.6599	0.389
LmxM.34.1880	60S ribosomal protein L5, putative	198	34	9	5	14.754098	0.389
LmxM.36.0940	40S ribosomal protein S18, putative	39	17.4	3	1	6.535948	0.389
LmxM.24.2080	40S ribosomal protein S8, putative	89	24.7	6	3	14.678899	0.369
LmxM.30.2150	prostaglandin f2-alpha synthase	48	31.8	4	3	14.084507	0.369
LmxM.02.0740	peptidyl dipeptidase, putative	144	76.6	8	6	9.7345133	0.359
LmxM.20.1180	calpain-like cysteine peptidase	158	103.5	11	6	8.137045	0.359
LmxM.04.0190	surface antigen-like protein	224	74.1	7	5	9.0267983	0.354
LmxM.30.2310	3'-nucleotidase/nuclease	90	41.6	6	3	7.6719577	0.35
LmxM.36.2590	membrane-bound acid phosphatase 2, putative	121	62.6	8	5	8.7565674	0.343
LmxM.11.1130	60S ribosomal protein L28, putative	41	16.2	4	2	12.2449	0.334
LmxM.15.1450	proliferative cell nuclear antigen (PCNA), putative	61	32.4	6	3	8.8737201	0.334
LmxM.16.0530	dihydroorotate dehydrogenase, putative	75	33.8	3	2	5.7507987	0.334
LmxM.17.0735	lysine decarboxylase-like protein	79	35.3	5	3	9.3167702	0.334
LmxM.19.0570	hypothetical protein, conserved	98	57.5	6	3	5.019305	0.334
LmxM.25.0490	RNA-binding protein, putative, UPB1	36	19.9	2	1	4.597701	0.334

Accession	Description	Mascot Score	Mass [kDa]	PSMs	Sequences	Coverage (%)	emPAI
LmxM.31.3130	ribosomal protein L3, putative	39	47.6	7	4	11.45585	0.334
LmxM.32.0610	paraflagellar rod component, putative	32	14.2	2	1	8.8	0.334
LmxM.32.3150	40S ribosomal protein S13, putative	59	17.5	3	2	10.596026	0.334
LmxM.36.2020 OR 2030	chaperonin HSP60, mitochondrial precursor	250	59.6	11	6	12.566372	0.334
LmxM.08.0290	iron superoxide dismutase A, mitochondrial	42	26.5	4	2	10.43478	0.311
LmxM.16.0460	60S ribosomal protein L21, putative	105	18	3	2	15.09434	0.311
LmxM.36.1370	Valosin-containing protein, putative	146	86.8	12	7	10.063694	0.308
LmxM.06.0410	60S ribosomal protein L19, putative	73	28.2	6	3	13.360324	0.304
LmxM.33.0140	malate dehydrogenase	139	33.7	6	3	12.025316	0.304
LmxM.07.0680	40S ribosomal protein S9, putative	66	22.1	3	2	9.5238095	0.292
LmxM.07.1000	RNA binding protein-like protein	70	38.5	4	2	6.557377	0.292
LmxM.14.1360	myo-inositol-1-phosphate synthase	111	58.2	6	4	8.365019	0.292
LmxM.21.1552	ATP-dependent RNA helicase SUB2, putative	133	49.4	7	4	8.9655172	0.292
LmxM.30.0440	hypothetical protein	89	79.8	8	6	12.569061	0.292
LmxM.34.1230	short chain dehydrogenase, putative	41	28.1	4	2	7.086614	0.292
LmxM.04.0320	hypothetical protein	85	44.3	5	3	8.0200501	0.28
LmxM.12.1130	NADH:flavin oxidoreductase/NADH oxidase, putative	93	41.4	5	3	8.59375	0.28
LmxM.36.1260	fructose-1,6-bisphosphate aldolase	38	40.8	5	3	7.54717	0.28
LmxM.22.1520	40S ribosomal protein L14, putative	89	20	4	2	11.428571	0.274
LmxM.31.0430	60S ribosomal protein L17, putative	48	19.1	3	2	9.6385542	0.274
LmxM.32.1330	glutamine aminotransferase, putative	103	46.1	6	3	7.0048309	0.269
LmxM.18.0510	aconitase, putative	217	97.4	12	7	9.1517857	0.267
LmxM.12.0630	alanine aminotransferase, putative	158	54.9	6	4	10.060362	0.266
LmxM.04.1030	hypothetical protein	54	21.3	2	1	4.639175	0.259
LmxM.19.0850	ATG8/AUT7/APG8/PAZ2, putative	70	12.8	2	1	9.6	0.259
LmxM.22.1460	i/6 autoantigen-like protein	55	22.9	4	2	13.72549	0.259
LmxM.24.1770	inhibitor of cysteine peptidase	43	12.7	2	1	16.81416	0.259
LmxM.36.2360	tyrosine aminotransferase, putative	51	49.5	3	2	9.5982143	0.259
LmxM.11.0100	seryl-tRNA synthetase	62	52.9	7	4	7.1729958	0.252

Accession	Description	Mascot Score	Mass [kDa]	PSMs	Sequences	Coverage (%)	emPAI
LmxM.21.0540	Lupus La protein homolog, putative	118	37.2	6	2	10.619469	0.25
LmxM.34.0400	40S ribosomal protein S3A, putative	111	30	4	2	11.742424	0.245
LmxM.08.1030a	hypothetical protein	139	57.5	6	3	6.1913696	0.241
LmxM.32.2300	udp-glc 4'-epimerase, putative	99	43.5	5	3	8.6956522	0.241
LmxM.15.1230	nucleoside transporter 1, putative	89	54.1	3	2	4.2769857	0.233
LmxM.27.1730	hypothetical protein, conserved	86	37.8	2	2	6.1764706	0.233
LmxM.29.0850	surface protein amastin, putative	52	21.1	2	1	5.0505051	0.233
LmxM.36.3770	transcription factor btf3, putative	78	11.6	1	1	15.53398	0.233
LmxM.36.6910	T-complex protein 1, theta subunit, putative	124	58.2	6	4	8.3798883	0.227
LmxM.19.0440	nucleosome assembly protein, putative	52	39.8	3	2	5.9659091	0.222
LmxM.36.3210	14-3-3 protein 1, putative	152	29.7	4	2	13.178295	0.222
LmxM.08_29.0060	tryptophanyl-tRNA synthetase, putative	50	45.3	4	3	7.0707071	0.218
LmxM.27.1805	Phosphoenolpyruvate carboxykinase [ATP], glycosomal	115	58.4	4	3	7.8095238	0.218
LmxM.29.2740	TPR domain protein, conserved	92	45.1	6	3	8.4577114	0.218
LmxM.21.1090	T-complex protein 1, delta subunit, putative	108	59.7	7	4	6.3520871	0.216
LmxM.25.0820	hypothetical protein, conserved	41	14.7	1	1	7.874016	0.212
LmxM.13.1220	40S ribosomal protein S4, putative	69	47.3	5	3	7.6744186	0.205
LmxM.20.0110	phosphoglycerate kinase B, cytosolic	58	44.8	4	3	9.8321343	0.205
LmxM.29.0460	aspartyl-tRNA synthetase, putative	105	62.3	8	4	6.7272727	0.198
LmxM.34.3340	6-phosphogluconate dehydrogenase, decarboxylating, putative	95	52.1	6	3	7.0981211	0.194
LmxM.36.6940	protein disulfide isomerase 2	67	52.2	6	3	7.6109937	0.194
LmxM.10.0290	isocitrate dehydrogenase [NADP], mitochondrial precursor, putative	83	48.4	5	3	6.4367816	0.189
LmxM.11.0350	14-3-3 protein 2, putative	57	29.1	4	2	6.3241107	0.186
LmxM.25.1120	aldehyde dehydrogenase, mitochondrial precursor	91	54.2	6	3	5.01002	0.184
LmxM.22.0460	40S ribosomal protein S15, putative	34	17.4	1	1	10.52632	0.179
LmxM.13.0090	metallo-peptidase, Clan MA(E) Family M32	86	57.2	6	3	5.7654076	0.174
LmxM.24.2050	60S ribosomal protein L26, putative	42	16.2	2	1	6.293706	0.166
LmxM.07.0510	60S ribosomal protein L7a, putative	69	33.8	3	2	6.3545151	0.155

Accession	Description	Mascot Score	Mass [kDa]	PSMs	Sequences	Coverage (%)	emPAI
LmxM.19.1420	cysteine peptidase A (CPA)	50	38.7	2	1	3.6723164	0.155
LmxM.34.3700	glycosomal membrane protein	45	24.9	2	1	3.555556	0.155
LmxM.36.0250	eukaryotic translation initiation factor 3 subunit l	56	62.7	5	3	4.5955882	0.155
LmxM.08_29.1500	hypothetical protein, conserved	43	73.5	3	2	4.315476	0.15
LmxM.26.2700	6-phosphogluconolactonase	40	28.4	2	1	3.745318	0.145
LmxM.36.6750	prolyl endopeptidase	34	77.9	5	3	6.743185	0.145
LmxM.26.1960	hypothetical protein, conserved	94	89.4	7	4	5.4931336	0.143
LmxM.33.2820	regulatory subunit of protein kinase a-like protein	97	71.7	5	3	5.2631579	0.142
LmxM.12.0400	3'-nucleotidase/nuclease, putative	49	41	2	1	2.6246719	0.136
LmxM.18.0680	citrate synthase, putative	48	52.2	4	2	3.4042553	0.136
LmxM.23.1480	hypothetical protein, conserved	52	27.3	2	1	3.265306	0.136
LmxM.24.2110	3-hydroxy-3-methylglutaryl-CoA synthase, putative	33	55.3	3	2	2.794411	0.136
LmxM.26.1380	prefoldin-like protein	74	22.2	2	1	6.185567	0.136
LmxM.06.0140	proteasome beta 6 subunit, putative	37	27.9	2	1	4.048583	0.129
LmxM.08_29.1960	fumarate hydratase, putative	87	24.5	2	1	5.4794521	0.129
LmxM.29.0180	2-hydroxy-3-oxopropionate reductase, putative	72	31	2	1	7.0234114	0.129
LmxM.36.5100	hypothetical protein, conserved	81	105.8	4	3	4.4715447	0.129
LmxM.15.0440b	hypothetical protein	67	73.3	4	3	10.502283	0.12
LmxM.34.0640	beta-fructofuranosidase-like protein	71	121.1	5	3	3.9233577	0.118
LmxM.27.1310	arginyl-tRNA synthetase, putative	42	78	5	3	4.624277	0.114
LmxM.34.0500 OR 0500a OR 0520b	proteophosphoglycan ppg3, putative	145	121456	8	4	3.5	0.11
LmxM.34.3860	T-complex protein 1, eta subunit, putative	44	61.7	3	2	5.087719	0.11
LmxM.17.0010	eukaryotic translation initiation factor 3 subunit a	41	87.6	5	3	4.521964	0.107
LmxM.32.3070partial	hypothetical protein	110	96.4	5	2	12.735327	0.107
LmxM.30.2080	hypothetical protein, conserved	57	87.1	4	2	3.9653036	0.105
LmxM.26.1240	heat shock protein 70-related protein	70	70.6	2	2	6.0842434	0.099
LmxM.27.1870	trypanothione synthetase	97	74.4	4	2	3.9877301	0.099
LmxM.31.0400	ATP-dependent RNA helicase HEL67	84	67.7	3	2	3.2154341	0.099

Accession	Description	Mascot Score	Mass [kDa]	PSMs	Sequences	Coverage (%)	emPAI
LmxM.27.1300	hypothetical protein, conserved	61	60	3	2	4.9149338	0.094
LmxM.19.1160	hypothetical protein, conserved	38	41.3	2	1	5.149051	0.093
LmxM.31.0840	hypothetical protein, conserved	86	56.7	2	1	3.0828516	0.093
LmxM.22.1290	ribonucleoside-diphosphate reductase small chain, putative	50	44.4	2	1	3.3163265	0.089
LmxM.18.1380	pyruvate dehydrogenase E1 component alpha subunit, putative	48	42.7	2	1	2.9100529	0.08
LmxM.16.1010	hypothetical protein, conserved	68	104.8	3	2	3.4267913	0.077
LmxM.25.0750	protein phosphatase, putative	37	45.2	2	1	2.463054	0.077
LmxM.32.2270	hypothetical protein, conserved	32	83.3	3	2	51.04809	0.073
LmxM.25.1170	ATP synthase subunit beta, mitochondrial, putative	55	56.2	1	1	2.285714	0.07
LmxM.08.1100	hypothetical protein, conserved	58	42.2	2	1	6.027397	0.068
LmxM.12.1090	promastigote surface antigen protein PSA	39	55.4	2	1	2.140078	0.068
LmxM.13.0160	protein kinase A regulatory subunit	30	56.3	2	1	1.590457	0.066
LmxM.22.1540	alanyl-tRNA synthetase, putative	83	106.1	4	2	1.7671518	0.061
LmxM.36.5620	isoleucyl-tRNA synthetase, putative	57	125.7	5	3	2.1838035	0.056
LmxM.15.0230	lysyl-tRNA synthetase, putative	42	67.1	1	1	1.365188	0.054
LmxM.23.0540	acetyl-CoA synthetase, putative	68	79.2	2	1	1.2622721	0.051
LmxM.30.0930	sodium stibogluconate resistance protein, putative	33	68.4	2	1	1.127214	0.051
LmxM.27.1260	T-complex protein 1, beta subunit, putative	31	57.7	1	1	3.780718	0.05
LmxM.21.0810	methionyl-tRNA synthetase, putative	38	83.8	2	1	1.07095	0.044
LmxM.33.0080	glucose-6-phosphate dehydrogenase	49	63.7	2	2	4.8042705	0.044
LmxM.31.2150	hypothetical protein, conserved	49	117.4	2	1	0.9242144	0.042
LmxM.12.0250	cysteinyl-tRNA synthetase, putative	66	88.4	2	1	1.2755102	0.041
LmxM.36.6980	eukaryotic translation initiation factor 3 subunit c	81	81.7	2	1	1.9178082	0.04
LmxM.11.1170	eukaryotic release factor 3, putative	34	84.7	2	1	0.912647	0.038
LmxM.08_29.2200	dynammin-1-like protein	33	76.9	1	1	1.157742	0.036
LmxM.30.3090	peptidase, putative	33	118.6	1	1	1.203704	0.036
LmxM.34.1410	threonyl-tRNA synthetase, putative	70	89.7	2	1	1.3977128	0.036
LmxM.34.3100	ATP-dependent RNA helicase, putative	45	100.8	2	1	1.4038877	0.032
LmxM.13.1100	leucyl-tRNA synthetase, putative	53	121.9	2	1	0.8372093	0.03

Accession	Description	Mascot Score	Mass [kDa]	PSMs	Sequences	Coverage (%)	emPAI
LmxM.34.2080	calcium motive p-type ATPase, putative	43	133.8	2	1	1.469388	0.029
LmxM.31.2270	membrane associated protein-like protein	45	163.8	2	1	12.90102	0.019
LmxM.27.0500	cysteine peptidase, Clan CA, family C2, putative	128	653.7	5	4	1.2167565	0.018
LmxM.14.1120	kinesin K39, putative	86	297.4	3	2	17.574164	0.016

Table 4-3 Secreted proteins of *L. mexicana* amastigotes. Proteins identified in three or more biological repeats. Scoring scheme, mascot score >30, see methods for complete settings. Accession numbers from TriTrypDB, peptide spectral matches (PSMs), sequences indicate number of different peptide sequences that the PSMs matched to. Estimation of protein abundance by the exponentially modified protein abundance index (emPAI).

Accession	Protein description	Mascot Score	Mass [kDa]	PSMs	Sequences	Coverage (%)	emPAI
LmxM.10.0460	GP63, leishmanolysin	810	69.6	34	15	25.2	2.2
LmxM.10.0465	GP63, leishmanolysin	651	69	31	14	23.1	2.2
LmxM.24.0850	triosephosphate isomerase	299	27	15	9	40.2	2.2
LmxM.29.1510	p1/s1 nuclease	200	35.2	11	7	21.2	2.0
LmxM.09.0891	polyubiquitin, putative	203	14.6	9	6	46.1	1.9
LmxM.31.2950 OR 2951	nucleoside diphosphate kinase b	196	16.7	9	6	50.3	1.9
LmxM.09.1490	cytochrome b5-like protein, putative	115	12.9	6	3	46.2	1.7
LmxM.08.1030a	hypothetical protein [cysteine protease, putative]	345	57.5	23	10	20.6	1.5
LmxM.16.1310	cytochrome c, putative	97	12.2	5	4	29.2	1.5
LmxM.08_29.0867	guanine deaminase, putative	316	49.1	11	7	20.3	1.4
LmxM.15.1040	tryparedoxin peroxidase	208	22.2	8	4	23.6	1.2
LmxM.09.0910, 0920 OR 0930	calmodulin, putative	140	16.8	4	3	30.2	0.7

Accession	Protein description	Mascot Score	Mass [kDa]	PSMs	Sequences	Coverage (%)	emPAI
LmxM.23.0040	tryparedoxin peroxidase	138	25.4	7	3	19.9	0.7
LmxM.29.0970	p22 protein precursor, putative	118	25.8	4	4	19.3	0.7
LmxM.08.1040 OR 1070partial	hypothetical protein [cysteine protease, putative]	323	55.5	15	4	13.3	0.62
LmxM.17.0360	cytidine deaminase-like protein	107	19.3	4	3	16.5	0.6
LmxM.28.2770	heat-shock protein hsp70, putative	300	71.2	17	10	17.7	0.6
LmxM.29.2490	heat shock 70-related protein 1, mitochondrial precursor, putative	260	72.5	18	12	10.1	0.6
LmxM.32.1750	macrophage migration inhibitory factor-like protein	60	12.7	2	2	13.3	0.6
LmxM.08_29.1160	tryparedoxin 1, putative	39	16.6	3	2	13.8	0.5
LmxM.30.1900, 2030 OR 36.3530partial	ubiquitin-fusion protein	68	14.96	2	1	12.5	0.36
LmxM.29.2550	heat shock 70-related protein 1, mitochondrial precursor, putative	252	71.34	16	4	6.9	0.3
LmxM.33.0140	malate dehydrogenase	169	33.7	5	2	8.2	0.3
LmxM.28.1200	luminal binding protein 1 (BiP), putative	106	71.7	5	4	5.5	0.2
LmxM.28.2910	glutamate dehydrogenase, putative	100	49	5	3	10.8	0.2
LmxM.29.2980	glyceraldehyde 3-phosphate dehydrogenase, glycosomal	32	39.1	2	2	7.2	0.2
LmxM.31.0840	hypothetical protein, conserved	51	56.7	3	2	5.2	0.2
LmxM.36.2020	chaperonin HSP60, mitochondrial precursor	73	60.3	4	4	5.7	0.2
LmxM.07.0990	nucleolar RNA-binding protein, putative	31	36.3	1	1	2.9	0.1
LmxM.14.0310	proteasome alpha 3 subunit, putative	44	32.2	1	1	3.5	0.1
LmxM.26.0660	protein disulfide isomerase, putative	30	40.9	1	1	1.8	0.1
LmxM.26.1960	hypothetical protein, conserved	111	89.4	5	3	5.5	0.1
LmxM.36.3990	ATP-dependent protease subunit HslV, putative	52	24.7	1	1	5.3	0.1
LmxM.27.0240	kinetoplast-associated protein-like protein	67	145.6	2	1	81.7	0.0
LmxM.32.0312	heat shock protein 83-1	52	80.5	2	1	1.7	0.0
LmxM.33.3230	hypothetical protein, conserved	37	243.7	2	1	0.3	0.0

4.3.4 Comparative analyses of the predicted properties of *Leishmania* secreted proteins

The predicted properties of the secretome from each of the life cycle stages also show overall differences, summarised in Table 4-4. 9.8% of the proteins in the promastigote secretome were predicted to contain a signal peptide directing the protein to the classical secretion pathway, and 20.7% were predicted to be non-classically secreted, using the SignalP and SecretomeP algorithms, respectively. Whereas 13.9% of amastigote secretome proteins are predicted to contain a signal peptide and a further 33.3% are predicted to be non-classically secreted. If we compare this to the total percentage of classically and non-classically secreted proteins predicted in the whole cell proteome for promastigotes and amastigotes, this is only 6.9% SigP Pro and 13.5 % SigP Ama%, respectively (Supplementary Data I).

Gene ontology (GO) functions were assigned to the proteins in the promastigote and amastigote secretome (Figure 4-5 a, b). The most abundant functions in the promastigote secretome were ribosomal-associated proteins, protein degradation, carbohydrate metabolism and protein biosynthesis. The most abundant functions in the amastigote secretome were protein degradation, redox and chaperones/stress induced proteins.

Proteins extracted from parasites and identified by LC-MS/MS were searched against the *L. mexicana* genome database at TriTrypDB.org and exported with their predicted isoelectric points. Figure 4-6 shows the percentages of proteins with specific predicted pI in the experimental proteome and secretome of promastigotes and amastigotes. The mean isoelectric point is recorded in brackets next to the key. When the predicted isoelectric points of the secretome and proteome proteins are investigated on a pH by pH basis there appears to be a shift in the pI of the amastigote secretome proteins to a more basic pI between 7 and 9.

Table 4-4 Predicted molecular properties of proteins secreted from *L. mexicana* promastigotes and amastigotes. Predictions of protein size, pI and number of trans-membrane domains were exported from the *L. mexicana* annotated genome database at tritrypdb.org. Signal peptide predictions were made using the online SignalP server, and the online SecretomeP server was used to predict non-classical secretion, found at cbs.dtu.dk/services/SignalP/ and cbs.dtu.dk/services/SecretomeP/, respectively.

	Promastigote	Amastigote
Total number of reproducible secretome proteins	256	36
Proteins with TM Domains	10.9%	22.22%
Proteins with Predicted Signal Peptide	9.8%	13.9%
Proteins Predicted as Non-Classically Secreted	20.7%	33.3%
Average Isoelectric Point	6.82	6.61
Average Molecular Weight	51,090	49,750
Average Protein Length	462.3	455.5

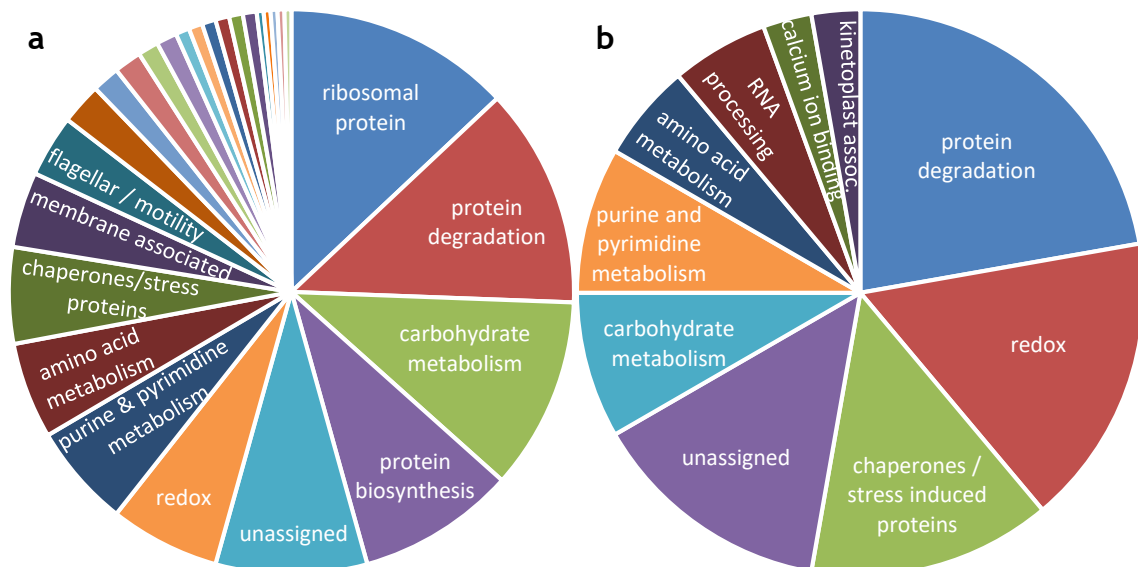


Figure 4-5 Gene ontology (GO) of the promastigote (a) and amastigote (b) secretome. Percentages assigned by number of different proteins with function, does not take protein abundance into account. Not accounting for proteins which can fit into multiple categories.

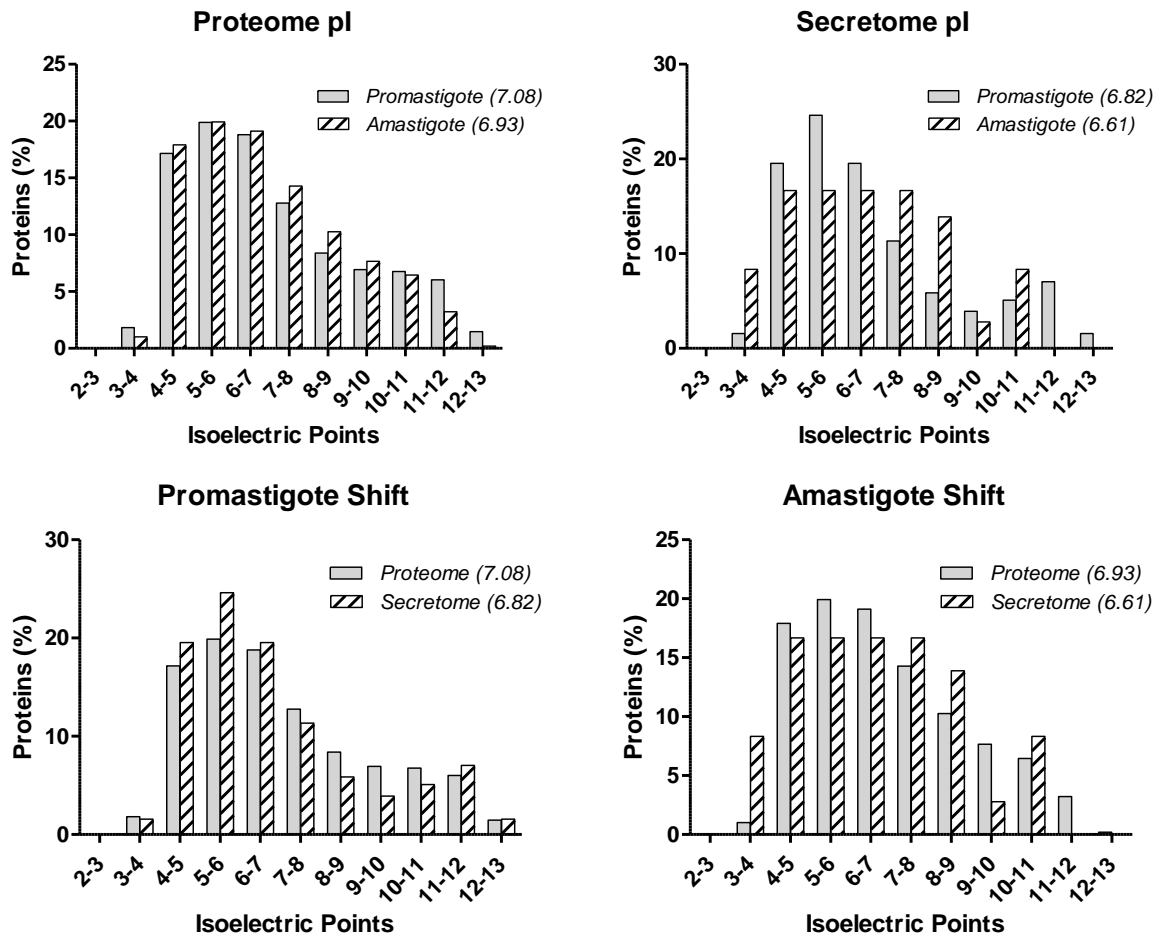


Figure 4-6 Predicted isoelectric point of *L. mexicana* promastigote and amastigote proteins from the proteome and the secretome. Proteins from the experimental proteome and secretome of both promastigotes and amastigotes were grouped according to their predicted isoelectric point assigned on TriTrypDB.

4.3.5 Validation and experimentation using Western Blot

Figure 4-7a shows Western blot testing of the antibodies for the promastigote and amastigote cell lysate proteins. In addition to providing a positive control for the antibody response to *L. mexicana* proteins, these show interesting stage-dependent differences between the life cycle stages. GP63 is recognised in both promastigotes and amastigotes using polyclonal antisera raised against GP63, but is not recognised in amastigotes with a monoclonal antibody to GP63 raised against promastigote purified GP63, demonstrating stage-dependent isoforms of GP63 in *L. mexicana*. Enolase (ENO) shows the presence of a common band at ~44 kDa, but multiple stage-specific differences at 22-25 kDa and 74-92 kDa. Similar stage-dependent differences are observed for glutamate dehydrogenase (GDH). B-tubulin antibody clone KMX detected β -tubulin in promastigotes but not in amastigotes. And as expected and demonstrated previously (Nugent *et al.* 2004), amastigote-specific antigens cysteine protease and HASPB were only detected in the amastigote cell lysate.

Figure 4-7b shows Western blotting demonstrating the presence of proteins identified in the secretome by MS. In the absence of any proteins equivalent to housekeeping genes in the secretome, equal sample loading has been shown by silver staining of the same samples. Secretory acid phosphatase and enolase, which were not identified in the amastigote secretome by MS, were also not detected in the amastigote secretome by Western blot. GP63 was detected in both the promastigote and amastigote secretome, consistent with the MS findings. Oligopeptidase B (OPB) was identified in some but not three or more replicates of the secretome using MS and was therefore not included in the amastigote secretome list for further analysis. However, the results of the Western blot clearly show the presence of OPB in all three replicates of the amastigote secretome.

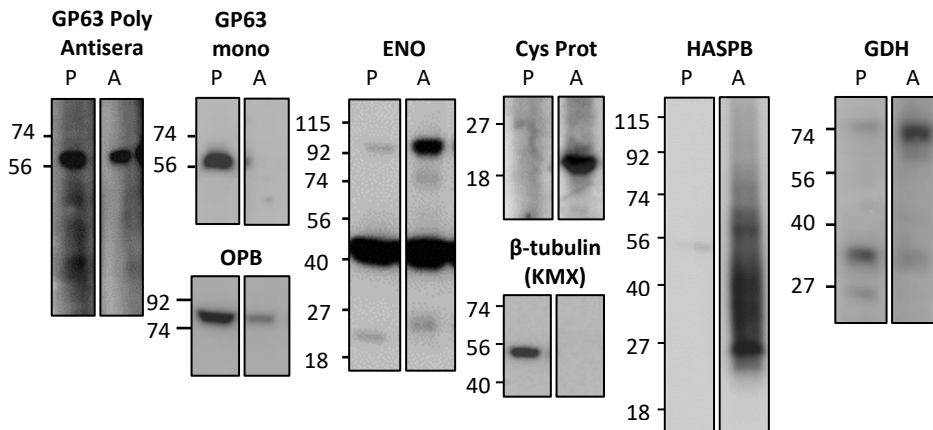
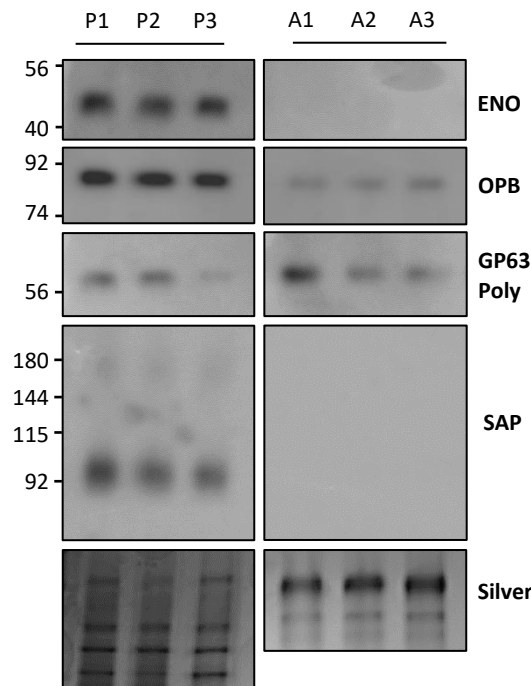
a Parasite lysate**b Parasite secretome**

Figure 4-7 Western blots of *L. mexicana* parasite lysates (a) and secreted proteins (b). a. 10 μ g of promastigote and amastigote lysate, separated by SDS-PAGE and blotted on PVDF membrane, were probed with polyclonal or monoclonal antibodies to glycoprotein 63 (GP63), oligopeptidase b (OPB), enolase (ENO), cysteine protease (Cys Prot), β -tubulin clone KMX, hydrophilic acylated surface protein B (HASPB), and glutamate dehydrogenase (GDH). b. To test the antibodies against *Leishmania* proteins and determine total cell differences between promastigotes and amastigotes. 0.4 μ g of promastigote and amastigote secretome, equivalent to secretion from approx. 10^7 promastigotes and 5×10^7 amastigotes, were blotted with the above antibodies and additional secretory acid phosphatase (SAP) antibody. Sample loading is shown by silver staining.

4.4 Discussion

4.4.1 The *Leishmania* secretome

Previously characterised *Leishmania* secreted proteins such as histidine secretory acid phosphatase (SAP) (Ilg *et al.* 1991), GP63 (Gómez *et al.* 2009a), PPGs (Peters *et al.* 1997b), and iron superoxide dismutase (Marín *et al.* 2007) were identified within the isolated promastigote secretome presented here. Figure 4-8 shows the number of proteins in common with this study and the others. 80.5% of the Hamilton secretome has been previously identified in other published *Leishmania* promastigote secretomes with 65% in two or more other published secretomes. 75% of the amastigote secretome has been identified in other published *Leishmania* promastigote secretomes, with only 54% of amastigote secretome found in two or more published promastigote secretomes. This is the first study to report the secreted proteome of *Leishmania* amastigotes.

Paape *et al.* identified 67 potential amastigote secreted proteins from the supernatant of a FACS analysis when amastigotes were sorted from macrophage cell debris and lysed cells (Paape *et al.* 2010). They identified 67 proteins in this fraction, however, only 3 proteins are in common between these data and the amastigote secretome presented here (Figure 4-9). While this was an interesting additional analysis by Paape *et al.* to ensure fuller coverage of the amastigote proteome, the supernatant was likely contaminated with proteins from parasite and host cell lysis and thus would not accurately represent an amastigote secretome.

In addition to the proteins which have been previously observed in promastigote secretome studies, there were other proteins of interest identified here which have not previously been described as secreted, and which may therefore be novel secreted proteins. Here, 19.5% of the protein identifications were unique to the Hamilton promastigote secretome (excluding hypothetical proteins) and 25% were unique to the amastigote secretome.

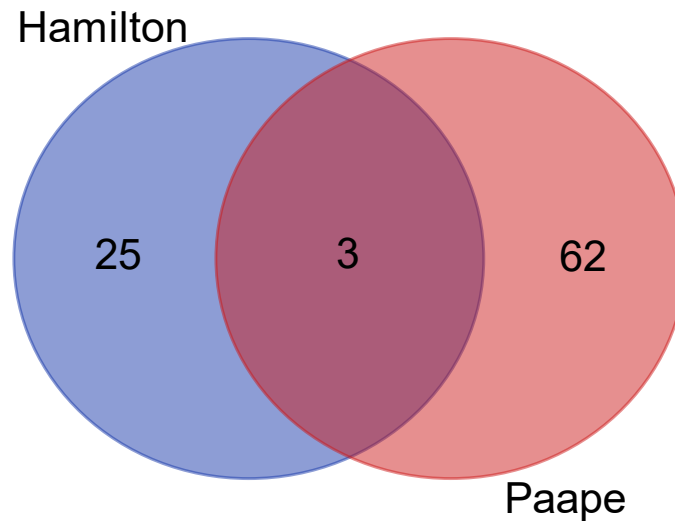


Figure 4-9 Venn diagram showing common identifications between *L. mexicana* amastigote putatively secreted proteins Excluding hypothetical proteins. Proteins identified from culture supernatant of axenic amastigotes (Hamilton) or from the supernatant of FACS-sorted amastigotes isolated from macrophages (Paape *et al.* 2010).

Using the putative annotations of the proteins identified we can infer possible roles in niche modification, such as involvement in alternative activation of macrophages or inhibition of apoptosis in macrophages. These processes have been observed in *Leishmania* infection (Kamir *et al.* 2008; Lisi *et al.* 2005; Moore & Matlashewski 1994; Ruhland *et al.* 2007), but the mechanisms not deduced. Secreted proteins are also known to play roles in the inactivation of macrophage transcription factors (Contreras *et al.* 2010) and altering the nucleopore complex in the host macrophage (Isnard *et al.* 2015).

Molecular chaperones calreticulin and protein disulphide isomerase were both found in the promastigote secretome and have been shown to be involved in the control of protein secretion in *L. donovani* (Duncan *et al.* 2011).

90.2% of the promastigote secretome and 86.1% of the amastigote secretome did not contain a classical signal peptide, suggesting alternative secretion pathways including the presence of nonclassical secretory signals or release from the parasite via exosomes (Nickel & Rabouille 2009). Indeed, some putative exosomal proteins, such as Rab1A, and membrane proteins were identified in the promastigote secretome (Simpson *et al.* 2008). This was not to the extent that other studies have observed (Silverman *et al.* 2008) as orthologues to proteins from the endosomal sorting complexes required for transport (ESCRT) pathway (Schmidt & Teis 2012) were not identified here. These have previously been found in other studies in

Leishmania, albeit in low abundance before vesicle purification (Silverman *et al.* 2008, 2010a). However, by comparison to the analyses performed by Silverman *et al.* (2008), we found that of the proteins identified in the *L. donovani* secretome as vesicle-associated, using the exosomal proteins of B lymphocytes, dendritic cells and adipocytes, 67% were also present in our promastigote secretome (Appendix 3).

4.4.2 Comparison of promastigote and amastigote secretome

As we can see from the summary of the properties of the promastigote and amastigote secretome (Table 4-4), *L. mexicana* amastigotes secrete qualitatively and quantitatively different proteins to promastigotes, likely reflecting their adaptation to different environments within the host.

Here, the discovery of proteins detected in promastigotes but not amastigotes, or vice versa, provides validation on the differences between promastigotes and axenic amastigotes. One such example is the detection of secretory acid phosphatase only in promastigote samples. It is known that amastigotes do not produce a secretory acid phosphatase (Menz *et al.* 1991). Antibody to promastigote soluble acid phosphatase did not precipitate any enzyme activity from lysed amastigotes or amastigote culture supernatant (Menz *et al.* 1991). Secretory acid phosphatase was found to be the most abundant protein secreted by promastigotes in this study but was not detected in the secretome of amastigotes by MS or by Western blot.

The total numbers of proteins identified for each of the two life cycle stages differs greatly. 256 proteins were identified in the promastigote secretome, with only 36 proteins in the amastigote secretome. It is unclear if this is a technical effect or a reflection of reduced secretion in amastigotes. The evidence points to a combination of the two. In terms of total secreted protein isolated from promastigotes and amastigotes, we have shown that promastigotes secrete approximately five times more protein per cell than amastigotes. This of course will, in part, be due to the smaller size of the amastigotes at approximately 4 μm compared to late-log and stationary phase promastigotes at between 7.5 and 8 μm (Bates 1994). We increased the numbers of amastigotes per secretion assay to

account for this, but as this is only a two-fold reduction in size this does not fully account for the observed reduced secretion in amastigotes. The reduction in secretion could therefore also be explained by the slower growth rate of amastigotes and their adoption of a stringent metabolic state (Saunders *et al.* 2014), thus longer incubation time may be required to give a fuller picture of amastigote secretion.

Nevertheless, we have shown by Western blot of OPB that proteins which were not identified in all replicates of the amastigote secretome by MS were indeed present in all three replicates, detectable by specific antibodies. This demonstrates the variability in the identification of low-abundance proteins by MS particularly in protocols where only the three most abundant peptides are selected from the survey scan for fragmentation. Due to the length of this investigation and the optimisation steps involved, the corresponding mass spectrometry equipment and protocols had been changed and improved over the course of the investigation. Due to time constraints and limited sample availability, not all replicates were analysed using the latest method (2.13) which selects the top 20 most abundant peptides per scan for fragmentation. This could therefore account for some of the discrepancy. Finally, an increase in glycosylation of amastigote PPG and potentially other proteins, demonstrated here (Figure 4-4) and by others (Peters *et al.* 1997a), may prevent the efficient trypsin digestion of the proteins to the appropriate peptides for database matching. A deglycosylation step in the amastigote secretome isolation protocol could therefore be added to investigate this.

The predicted isoelectric point (pI) of many of the amastigote secreted proteins has shifted towards a more basic pH than that of the promastigote, away from a pI of between 4 and 6 (Figure 4-6). Proteins are least soluble in solutions which are the pH of their isoelectric point. Thus, this could indicate an increase in the solubility of amastigote secreted proteins at acidic pH, correlating with the acidic environment of the parasitophorous vacuole of pH 5 (Antoine *et al.* 1998), into which these proteins are delivered by intracellular amastigotes. This observation is supported by the comparison of the secretome protein profiles in 2-dimensional electrophoresis (Figure 4-2).

We also observed differences in physical properties of the secretome. When isolating the amastigote secretome we observed a viscous 'gel' like substance in the sample pellet after precipitation. This property is commonly observed in preparations of glycoproteins or mucins (Davies *et al.* 2012; Davies & Carlstedt 2000). An insoluble component was also observed in the amastigote secretome after freezing. It is not known where the insoluble component originated from but it is unique to amastigote-conditioned medium as the phenomenon did not occur in cSDM alone or in cSDM with the addition of protease inhibitors. A similar phenomenon occurs in urinary samples, where a precipitate is formed after freezing (Saetun *et al.* 2009). These were characterised as calcium crystals and calcium oxalate, with the addition of CaCl₂ found to increase sediment formation. This is an interesting observation as amastigote media, cSDM, contains calcium in the form of CaCl₂, whereas HOMEM does not. Saetun and colleagues also note that the sedimentation entrapped a considerable amount of protein, and if discarded severely diminished the total protein content of the samples (Saetun *et al.* 2009). This may provide an explanation for the reduced protein concentration in the amastigote samples when compared to the promastigote samples. Proteomic analysis of the precipitate, however, was inconclusive as it showed the presence of only a few peptides, most of which matched to proteins already identified in the amastigote secretome. These observations require further investigation as this is a significant difference between the promastigote and amastigote secretome. Chelation of calcium by amastigotes may be a potent virulence mechanism used by the parasite, as dysfunctions in infected host cells have been previously related to abnormal intracellular Ca²⁺ homeostasis (Olivier 1996). Indeed, macrophages infected with *Leishmania major* amastigotes were shown to contain approximately 40% more intracellular calcium than uninfected cells. This was attributed to the strong calcium-binding capacity of an amastigote 'excreted factor', as the effect could be replicated using other cell types coated with excreted factor (Eilam *et al.* 1985). Taken together, we can postulate that amastigote excreted factor may be binding calcium in the media and precipitating upon freezing. This excreted factor may be the abundant amastigote PPG (aPPG) which may be difficult to identify in proteomic analyses, as discussed below.

4.4.3 Predicted functions and categories of secreted proteins

i. Glycoproteins

Leishmania are known to express multiple proteophosphoglycans (PPGs). Promastigote PPG 2 (pPPG2) is a glycoisoform of amastigote PPG (aPPG), with the same protein backbone but different glycosylation (Klein *et al.* 1999). Due to the different ultrastructure of the protein it was found to be smaller than the aPPG, eluting from a Superose 6 gel filtration column between 300 and 500 kDa (Klein *et al.* 1999). Promastigotes also express a filamentous PPG (fPPG). When staining for glyco-moieties in the SDS-PAGE gel, two high molecular weight glycosylated bands were observed in the amastigote secretome (Figure 4-4). This is likely to be the abundant aPPG. The level of glycosylation of amastigote aPPG may be responsible for the concentration visualised in the gel which exceeds any other component of the secretome. The *ppg2* gene encodes the common backbone of aPPG and pPPG2 secreted by amastigotes and promastigotes, respectively. Amastigotes and promastigotes exhibit stage-specific phosphoglycosylation patterns. The serine-rich repeats in the sequence are targets for Ser phosphoglycosylation in *Leishmania mexicana* (Gopfert *et al.* 1999). However, the level of glycoprotein staining observed in promastigotes was much less than in amastigotes. This could be due to the small amounts of secretome proteins loaded onto the gels, with amastigote staining visible due to extensive glycosylation of aPPG.

This same result was not seen in the LC-MS/MS amastigote secretome potentially due to extensive glycosylation. Abundant glycoproteins were identified by MS in the secretome of the promastigotes, but not seen in amastigotes. There are two main reasons this is thought to occur. Ilg *et al.* observed a reduction or absence of aPPG in cultured amastigotes whereas aPPG was identified in *ex-vivo* parasites. In this case the authors suggest that the synthesis of aPPG may rely on signals from the macrophage, and therefore they did not see it in the supernatant of axenic parasites (Ilg *et al.* 1998). However, we observe the presence of a high molecular weight and heavily glycosylated protein by SDS-PAGE. Therefore it is likely that in a mass spectrometry analysis of the protein as opposed to the glyco moieties, the extensive and branched glycosylation on the aPPG could be preventing the action of trypsin by steric hindrance thereby preventing the production of the unique tryptic peptides necessary for sequence matching and identification (Aebischer *et*

al. 1999; Yang *et al.* 2017). As discussed above it is possible that aPPG is analogous to amastigote 'excreted factor' and forms the precipitate observed in the thawed secretome.

Secretory acid phosphatase (SAP) is another well-known *Leishmania* glycoprotein (Ilg *et al.* 1991). A previous publication has shown that *L. mexicana* SAP appears in two distinct bands for SAP1 and SAP2, at ~95 and >180 kDa, respectively (Klein *et al.* 1999). Results presented here are consistent with this when analysing the secretome from Western Blotting. Whereas, fPPG was located in the stacking gel which also correlates with findings presented herein. Furthermore, PPG has been shown to form a gel in concentrated solutions (Ilg *et al.* 1995), which was further observed here during the preparation of the amastigote secretome. In addition this was proteinase resistant (Ilg *et al.* 1995). It was been described that secreted aPPG causes vacuole formation in macrophages (Peters *et al.* 1997b), an example of niche modification.

Searching in Mascot for glycan modifications is very new and involves creating a custom database of your organism of interest with multiple glycan modifications. A method for this has now been designed but the field is still in its infancy (Bollineni *et al.* 2018). It may be possible to add extra modifications and missed cleavages to the amastigote secretome mascot search to look for glycosylated peptides, however this would require extensive data analysis and constitutes future development and work.

ii. **GP63 in amastigotes**

It is shown here that GP63 is an abundant component of the amastigote secretome. This initially appears surprising given that surface-bound and released GP63 is more often associated with promastigotes, however there is abundant evidence of stage-specific isoforms and localisation of GP63. Amastigote GP63 could not be surface-labelled to the same extent as promastigote GP63 and lacked a PI membrane anchor. In addition, the majority of the GP63 in the amastigote localised to the flagellar pocket (Medina-Acosta *et al.* 1989; Paape *et al.* 2008). Nugent *et al.* used a monoclonal antibody to promastigote GP63 which did not recognise amastigote GP63. In this study, monoclonal GP63 antibody did not recognise GP63 in amastigotes, but polyclonal antisera did recognise a protein in amastigotes and

promastigotes showing that there is a fundamental difference in epitope and different forms are expressed in these cells. This may give an indication as to why GP63 appears to be the most abundant secreted protein in amastigotes where it was previously not associated with amastigotes. Also there is different electrophoretic mobility between amastigote and promastigote GP63 (Chaudhuri *et al.* 1989). Amastigote GP63 was found in the soluble fraction of the lysate but not the membrane fraction as with promastigotes and appeared at higher apparent molecular weight than its promastigote counterpart (Bahr *et al.* 1993). Transcripts of the large GP63 gene family were found to be differentially processed in promastigotes and amastigotes (Frommel *et al.* 1990; Medina-Acosta *et al.* 1989), and later it was discovered that these are encoded by different members of the GP63 gene family in promastigotes and amastigotes (Medina-Acosta *et al.* 1993).

We also postulate that the ~66.4 kDa band seen in amastigotes is a form of GP63 and is possibly found in secreted vesicles. This is because when the amastigote secretome is filtered through a 0.22 µm membrane before detergent extraction and SDS-PAGE, the intensity of the 66.4 kDa band decreases, but the intensity of other bands do not, including high molecular weight bands. Presence of a 66 kDa GP63 has been observed before in amastigotes but not in promastigotes (Hsiao 2008). Secretion of GP63 by amastigotes as well as promastigotes is further substantiated by the identification of GP63 in the secreted exosomes of *Leishmania*-infected macrophages (Hassani & Olivier 2013). Parasite-derived GP63 was found in these host exosomes demonstrating active transfer of GP63 from intracellular parasites into the host cell. It is well established that GP63 is a major virulence factor in *Leishmania* promastigotes (Contreras *et al.* 2010; Gómez *et al.* 2009a; Hassani *et al.* 2014) and it will be interesting to extend these findings to amastigotes.

iii. Secretion of antioxidants

Phagocytes employ the production of reactive oxygen species including oxygen radicals, superoxide, and hydrogen peroxide, as a mechanism of immune attack against parasites (Castro *et al.* 2017; Van Assche *et al.* 2011). In defence, many parasites, including *Leishmania*, employ counter-mechanisms and implement pathways to counteract the host's immune attack. This includes the expression of antioxidants, for example: superoxide dismutases (SODs), catalases, glutathione

and thioredoxin peroxidases, and peroxiredoxins. In helminths, secreted antioxidant enzymes include *B. malayi* glutathione peroxidase and SOD (Bennuru *et al.* 2009). Another example is thioredoxin peroxidase from *F. hepatica*, which is further implicated in the alternative activation of macrophages (Donnelly *et al.* 2005).

Antioxidants secreted from *Leishmania* are also likely to be involved in intracellular survival of the parasite, such as iron superoxide dismutase, providing protection from oxidative burst during phagocytosis and from intracellular free radical attack (Castro *et al.* 2017; Van Assche *et al.* 2011). Iron superoxide dismutase has previously been shown to be a key player in the survival of *Leishmania* within the macrophage, detoxifying reactive superoxide radicals produced by activated macrophages (Ghosh *et al.* 2003). Tryparedoxin peroxidase has also been shown to protect the parasite from peroxide-induced damage (Castro *et al.* 2002). Another secreted protein which putatively interacts with the antioxidant network is cystathionine gamma lyase (CGL) (Giordana *et al.* 2014). *T. cruzi* CGL has been shown to establish interactions with proteins in the complex system involved in maintaining the cellular redox status, such as tryparedoxin 1 (Piñeyro *et al.* 2011).

Here, we observe the secretion of a host of antioxidants from both promastigotes and amastigotes. Namely tryparedoxin 1 and two tryparedoxin peroxidases, in promastigotes and amastigotes, in addition to iron superoxide dismutases, trypanothione reductase, oxidoreductase and cystathione gamma lyase in promastigotes.

iv. Nutrient salvage

A functional category which is important in parasite survival in order to preserve and maintain parasite growth is nutrient acquisition. Endoribonuclease, an enzyme implicated in this category has been previously shown to be secreted by *Leishmania* promastigotes (Silverman *et al.* 2008). Our findings are consistent with this. Nucleases are an important addition when discussing parasite intracellular survival. Nucleases may aid in purine salvage which is essential for *Leishmania* survival because they are incapable of *de novo* purine synthesis. We also observe that a p1/s1 nuclease is one of the main proteins secreted by amastigotes.

Extracellular 3'-nucleotidase was also detected in the promastigote secretome. This enzyme is known to be expressed on the surface of *Leishmania* (Dwyer & Gottlieb 1984) where it can specifically cleave DNA and RNA into nucleotides and phosphate (Guimarães-Costa *et al.* 2014). Furthermore its role in evasion of the immune response has been demonstrated, as it mediates parasite escape from neutrophil extracellular traps (NETs) (Guimarães-Costa *et al.* 2014).

v. **Proteases**

Oligopeptidase B is involved in secreted serine protease activity. Parasite proteases are thought to mediate intracellular survival, through proteolytic activities against degradative enzymes found in phagolysosomes. Cysteine proteases are one of the most abundant proteins in the amastigote secretome. Another hypothesised role for parasite proteases is through degradation of major histocompatibility complex class I and II molecules, for example by cysteine proteases (De Souza Leao *et al.* 1995).

vi. **Moonlighting proteins and other secreted proteins of interest**

Many of the proteins secreted by *Leishmania*, and in fact many other organisms, appear to already have defined roles in the cell. However, they consistently appear in the secretome of these organisms, and are now considered 'moonlighting' proteins. The expression 'moonlighting proteins' was established as a term when the phenomenon was reviewed by C. Jeffery in 1999 for proteins that perform multiple functions (Jeffery 1999). Some groups of these proteins have been extensively studied and reviewed for a number of organisms such as the glycolytic enzymes of parasites (Gómez-Arreaza *et al.* 2014), and bacteria (Henderson & Martin 2011). Other proteins were found to have many different functions in pathogenic protozoa, fungi and multicellular parasites (Karkowska-Kuleta & Kozik 2014).

Several molecular chaperones are present in the secretome of both promastigotes and amastigotes, listed in Table 4-5. 5.5% of the promastigote secretome was composed of molecular chaperones and 19.4% of the amastigote secretome. Bacterial molecular chaperones have been found to modulate phagocyte function (Henderson & Martin 2011).

Table 4-5 Molecular chaperone proteins present in the *L. mexicana* promastigote and amastigote secretome.

Promastigote Secretome	
GeneDB Accession	Protein Description
LmxM.30.2600	calreticulin, putative
LmxM.31.3270	chaperonin alpha subunit, putative
LmxM.36.2020 OR 2030	chaperonin HSP60, mitochondrial precursor
LmxM.29.2490	heat shock 70-related protein 1, mitochondrial precursor, putative
LmxM.26.1240	heat shock protein 70-related protein
LmxM.32.0312	heat shock protein 83-1
LmxM.18.1370	heat shock protein, putative
LmxM.28.2770	heat-shock protein hsp70, putative
LmxM.36.6940	protein disulfide isomerase 2
LmxM.27.1260	T-complex protein 1, beta subunit, putative
LmxM.21.1090	T-complex protein 1, delta subunit, putative
LmxM.34.3860	T-complex protein 1, eta subunit, putative
LmxM.23.1220	T-complex protein 1, gamma subunit, putative
LmxM.36.6910	T-complex protein 1, theta subunit, putative
Amastigote Secretome	
GeneDB Accession	Protein Description
LmxM.36.2020	chaperonin HSP60, mitochondrial precursor
LmxM.29.2490	heat shock 70-related protein 1, mitochondrial precursor, putative
LmxM.29.2550	heat shock 70-related protein 1, mitochondrial precursor, putative
LmxM.32.0312	heat shock protein 83-1
LmxM.28.2770	heat-shock protein hsp70, putative
LmxM.28.1200	luminal binding protein 1 (BiP), putative
LmxM.26.0660	protein disulfide isomerase, putative

Nucleoside-diphosphate kinases are enzymes that catalyze the exchange of phosphate groups between different nucleoside diphosphates. However, in addition to its house-keeping functions, *Leishmania*-released nucleoside diphosphate kinase has been shown to prevent ATP-mediated cytolysis of macrophages (Kolli *et al.* 2008).

Enolase, found here to be secreted by *Leishmania*, is also secreted by many pathogenic microorganisms. Enolase is known to be associated to the external surface of the *Leishmania* parasite and in this location, does not appear to have enzymatic activity (Avilán *et al.* 2011). Extracellular enolase functions as a plasminogen-binding protein (Figuera *et al.* 2013). Plasminogen/plasmin binding is involved in several processes such as degradation of fibrin and other extracellular matrix proteins. Acquisition of this host protease allows pathogens to invade and disseminate in the host. In *L. mexicana*, plasminogen and plasmin bind to both the promastigote and amastigote forms. *In vivo*, host fibrin could provide a barrier which could limit the interaction between parasites and macrophages, limiting the

invasion and dissemination of the parasites. Parasite surface-bound plasmin could therefore break down this fibrin (Gómez-Arreaza *et al.* 2014).

Macrophage migration inhibitory factor (MIF) is a cytokine homologue, and highly enriched in amastigote secretome as it was below the detection limit in our amastigote whole cell proteome. MIF mRNA was also previously found to be more abundant in amastigotes than promastigotes (Leifso *et al.* 2007). Multiple protozoan parasites express MIF homologues that play a role in pathogenesis and immune evasion, such as *E. histolytica* (Ngobeni *et al.* 2017), *Plasmodium spp.* (Shao *et al.* 2008; Sun *et al.* 2012; Zhang *et al.* 2012), *T. gondii* (Sommerville *et al.* 2013), *Leishmania* (Holowka *et al.* 2016; Kamir *et al.* 2008; Richardson *et al.* 2009), *T. vaginalis* (Twu *et al.* 2014) and various helminths (Falcone *et al.* 2001; Sharma *et al.* 2012; Wang *et al.* 2017; Wu *et al.* 2003; Younis *et al.* 2012; Zang *et al.* 2002). The importance of MIF in the host:parasite interaction was investigated using macrophage exosomes collected from noninfected cells (NILX), *Leishmania*-infected cells (LEISHX), and LPS-stimulated cells (LPSX). These were used to stimulate naïve macrophages and the responding differentially regulated genes were assessed (Hassani & Olivier 2013). Stimulation with LPSX induced a substantial downregulation of MIF in the naïve macrophages, which was not induced by exposure to LEISHX (Hassani & Olivier 2013). The mechanisms responsible for these effects in the host cells have not been deduced, but suggest the importance of MIF in the host:parasite interaction in *Leishmania* infection.

4.5 Summary

We hypothesised that both promastigotes and amastigotes secrete proteins into their extracellular environment and we have subsequently shown that this is the case having successfully isolated and characterised a secretome from both life cycle stages of the parasite.

We also hypothesised that *L. mexicana* parasites change their secretome in response to their changing environments encountered their life cycle. We have shown here through proteomic analysis that the secretome differs between the life cycle stages.

Through analysis of predicted protein function and comparison to other known parasite virulence factors, we postulate that these secreted proteins play a role in the virulence of the parasite in the host and in parasite survival in a variety of broad functional categories: nutrient acquisition, antioxidant function, signalling disruption and directing the host immune response to the parasite's advantage.

Leishmania parasites cause debilitating disease and any further work into their mechanisms of disease bring us closer to understanding the parasite and potentially allowing the development of a novel treatment strategy or vaccine.

**Chapter 5 Application of secretomics
to *Leishmania* parasites
with differing phenotypes**

5.1 Introduction

As discussed previously, the secretome of *Leishmania* parasites has been implicated in the pathology of Leishmaniasis (Diniz Atayde *et al.* 2016). Previous results presented in this thesis have detailed and provided new insight into the composition of the *Leishmania mexicana* secretome throughout the life cycle. However, to gain further insight into the biological role of *Leishmania* secreted proteins, parasite lines expressing different disease phenotypes with regards to host cell infection and disease outcome were chosen to initiate a comparative proteomic analysis of the secretome under differing conditions. These include an attenuated strain of *Leishmania mexicana*, able to be cultured as promastigotes and amastigotes. In addition, parasite isolates from six Colombian patients were sourced, three of which exhibited chronic infection, and three exhibiting a self-healing infection.

5.1.1 Quantitative Proteomics Methods

Quantitative proteomic analyses can be performed using several methods which fall into two main categories, label-free quantitation (Wong & Cagney 2010) and chemical labelling techniques, which use stable isotopes to differentially label the samples. Chemical labelling of proteins can be performed metabolically, using Stable Isotope Labelling by Amino acids in Cell culture (SILAC), commonly employing ^{13}C -lysine and ^{13}C -arginine (Ong & Mann 2007). Alternatively, labelling of proteins or peptides takes place after extraction from the organism or cells of interest, by chemical incorporation of stable isotopes. Multiple techniques are available, for example isotope-coded affinity tags (ICAT) (Gygi *et al.* 1999), using dimethyl labelling (DiMe) (Hsu *et al.* 2003), or isobaric tags, utilised in isobaric tag for relative and absolute quantitation (iTRAQ) (Ross *et al.* 2004) and tandem mass tagging (TMT) (Thompson *et al.* 2003).

In this study we performed TMT⁶ labelling. TMT⁶ employs six isobaric tags, which are reporter tags of the same nominal mass but with discrete stable isotope incorporation positions, pictured in Figure 5-1. The tags are attached via amide linkages to peptides in trypsin-digested samples. After labelling, the six different samples can be combined and analysed together by LC-MS/MS. Each tag releases a unique reporter ion in MS/MS, enabling relative quantitation for peptides derived

from each of the 6 samples. Figure 5-2 shows a schematic of the TMT labelling process.

SILAC is not a suitable approach for the study on *Leishmania* presented here. This is because previous studies of *Leishmania* have shown that the parasites are difficult to label metabolically, and the approach takes many passages in culture to achieve high incorporation of the label (Ong & Mann 2007). This is unsuitable for field samples such as patient isolates of *L. panamensis*, as extended culture *in vitro* could cause these cells to adapt metabolically and genetically, and subsequently lose their disease phenotype. TMT labelling is performed after isolation and digestion of the samples therefore the cultures can be treated the same way as they were in earlier studies presented previously in this thesis, thus providing method consistency and reproducibility. The reaction also allows multiplex experimental design, reducing run-to-run variation which can complicate label-free quantitation.

a

Figure has been removed due to Copyright restrictions.

b

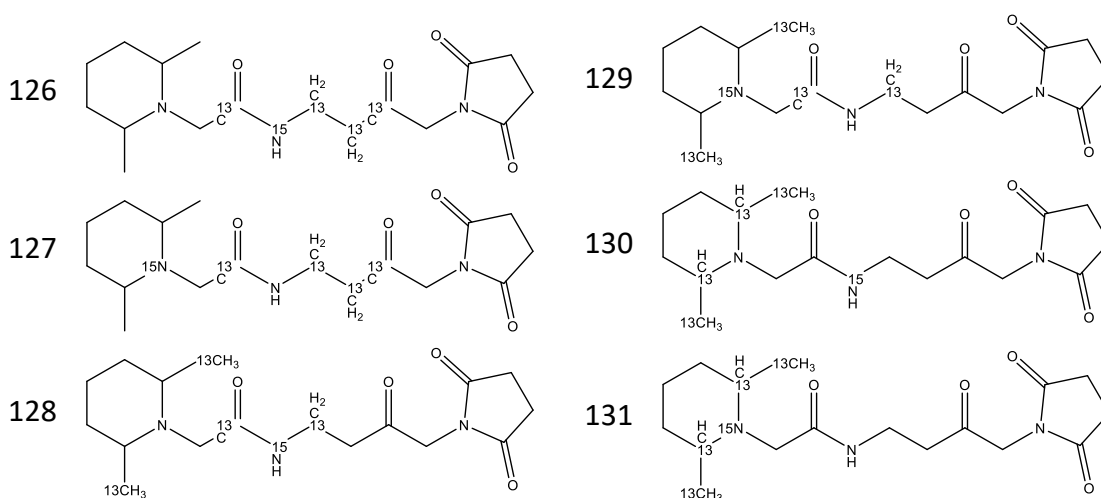


Figure 5-1 Diagram depicting the structural chemistry of Thermo Scientific Tandem Mass Tags (TMT™) (a) The general composition of each tag, containing a mass reporter, a linker which is cleavable by fragmentation with higher energy collision dissociation (HCD), a region to normalise the

mass to make all six tags equal, and an amine-reactive group to bind to the peptide. (b) The TMT 6-plex kit contains tags with mass reporters ranging from an m/z of 126 to 131. (Adapted from Thermo Scientific TMTsixplex™ webpage found at: thermofisher.com/order/catalog/product/90061)

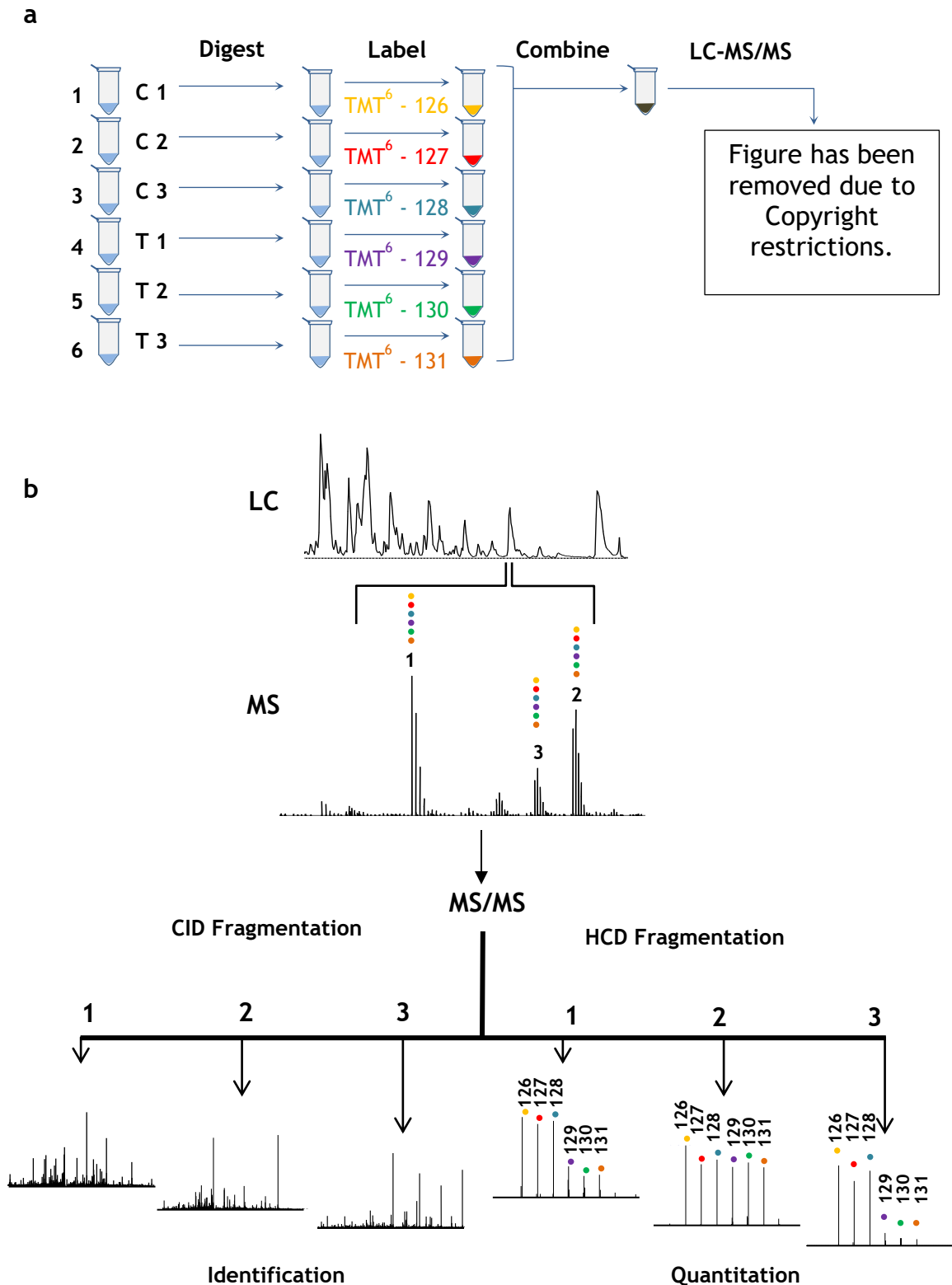


Figure 5-2 Schematic of the quantitative Tandem Mass Tagging (TMT™) process from sample preparation to mass spectrometry analysis. (a) Six protein samples, for example control (C) and treatment (T), are processed by denaturing, reducing, alkylating and trypsin digesting. Resulting tryptic peptides are then tagged and the six differentially labelled samples combined to be analysed by LC-

MS/MS in one run. (b) The top three precursor ions from the MS scan are selected for fragmentation by collision induced dissociation (CID) for peptide identification and by higher energy collision dissociation (HCD) for reporter ion quantitation.

5.1.2 Quantitative proteomics data analysis

Numerous studies have applied quantitative analyses to the study of large proteome data sets. Two approaches utilised in previously published studies were identified as appropriate software packages for the study presented here. The first is Proteome Discoverer™ (Thermo Fisher Scientific), for processing of the raw MS data to annotate and quantitate the peptides and the reporter tags. Followed by an adapted “Linear Models for Microarray Data” (LIMMA) model (D’Angelo *et al.* 2017; Kammers *et al.* 2015), to statistically test the differential abundance of the proteins identified in Proteome Discoverer.

Proteome Discoverer allows for the identification and quantitation of proteins in complex biological samples. The software first takes the spectrum files generated by the mass spectrometer in .RAW format and processes these in one of two ways. 1. Spectrum selector and Mascot nodes are used to map and identify peptides from the raw spectra, and 2. the Reporter Ions Quantifier node is used to analyse the spectra in the region of the mass tag (Figure 5-3a). The MSF files generated by the Mascot node are then used in the consensus workflow (Figure 5-3b). This workflow groups, validates and filters the peptides and subsequently assigns them to proteins.

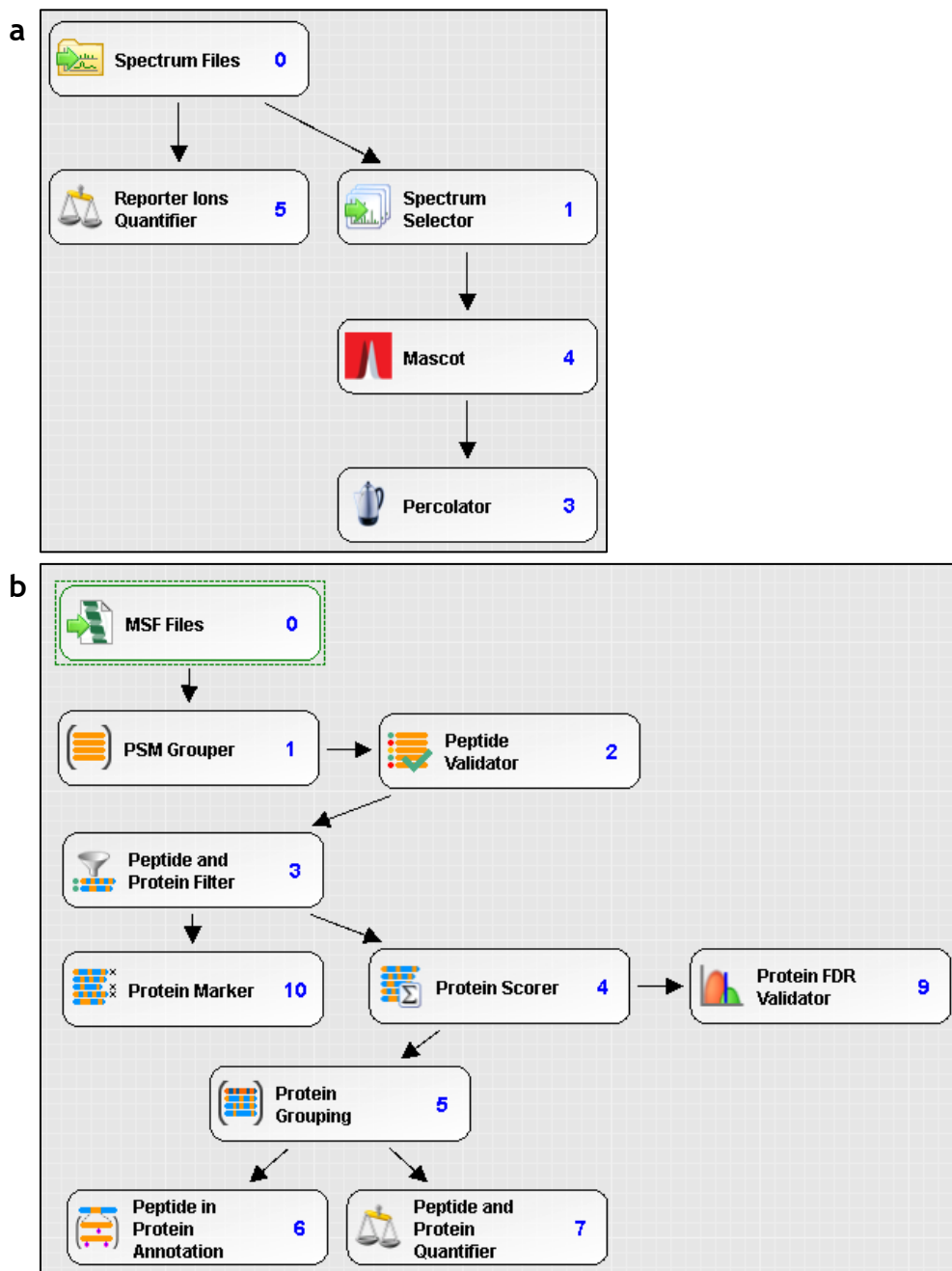


Figure 5-3 Proteome Discoverer™ Software processing and consensus workflows. (a) The Processing Workflow contains nodes to extract the data from the spectrum files for peptide matching and reporter ion-based quantification. (b) The Consensus Workflow contains nodes for enhanced annotation and quantitative analysis of the identifications from the previous workflow.

Identification and quantitation of the proteins in the secretome was then followed by statistical testing and data visualisation in R (Ver 3.5.1). Differential abundance of proteins in a secretome can be tested for statistical significance using a method modified from an approach commonly used in gene expression analysis, LIMMA (Linear Models for Microarray Data) as demonstrated and reviewed by Kammers *et al.* (2015) and presented as a freely available software vignette (Kammers *et al.*

2015). One of the main advantages of this method is it allows for biological variances to be handled with a more realistic distribution, as opposed to assuming constant variance. Traditional methods using two-sample t-tests assume constant variance across the data range. As genes, or in this case proteins, that display large fold change between samples also tend to have higher sample variance, this can result in proteins with large fold changes being declared less significant than proteins with smaller fold changes and lower sample variance, particularly when the number of samples is small. LIMMA uses an empirical Bayes method which calculates a pooled estimate of variance across samples and shrinks the variance of individual proteins towards this estimate. Used in conjunction with a moderated t-test, this technique for accommodating realistic biological variance greatly increases the inferential power of the model, increasing confidence in fold changes and resulting in fewer false positives (Smyth 2004).

D'Angelo *et al.* (2017) evaluated several statistical models, including LIMMA, for quantitative proteomics data using TMT-tagged test data. They created simulated proteomic data sets using known concentrations of proteins and also using a spike-in method. They then analysed the data sets using a general linear model (GLM), LIMMA, and mixed models, while also varying the method of normalisation. LIMMA was concluded to be their preferential method over GLM and mixed models for TMT-based quantitative proteomics (D'Angelo *et al.* 2017).

Here, we successfully applied previously established methods to relevant clinical isolates and obtained secretome profiles for each of the 6 parasite isolates, three from patients with chronic infection and three from patients with self-healing infections. Furthermore, using a quantitative proteomic approach we have compared the relative abundances of these secreted proteins between the two groups and found significant upregulation and downregulation of several proteins in the secretome of parasites from chronic infections, compared to self-healing infections.

5.1.3 Attenuated *L. mexicana* parasites and clinical isolates of *L. panamensis*

To initiate a comparative analysis, a virulence-attenuated cell line which does not divide in host cells or in mice was sourced. The attenuated parasites are taken up by host macrophages but do not sustain an infection, as shown in Figure 5-4a (Daneshvar *et al.* 2003a). Additionally, these parasites no longer sustain an infection in mice and can be utilised to sensitize mice to *L. mexicana* and produce an immune response when infected with wild type parasites thereafter (Figure 5-4b) (Daneshvar *et al.* 2003b, 2003a). This approach is being used to develop an attenuated vaccine in trials with *L. infantum* species (Daneshvar *et al.* 2014). The *L. mexicana* version is compared here to the wild type to look for differences in the secreted protein profile. We hypothesise that the differences in the parasites' virulence phenotype in the host cell may, in part, be due to differing secreted proteins. Any changes identified would give us an indication as to the functionality of the secretome in virulence.

a

b

Figure has been removed due to Copyright restrictions.

Figure 5-4 Virulence of *L. mexicana* wild type (WT) and attenuated (H-line) parasites and efficacy of the H-line as a vaccine in mice. (a) Percentage of infected bone marrow-derived macrophages after exposure to stationary-phase WT or attenuated promastigotes. (b) Lesion size after infection with WT *L. mexicana* in BALB/c mice vaccinated with stationary-phase promastigotes of *L. mexicana* H-line ($n=14$). Data from (Daneshvar *et al.* 2003a).

The second phenotypic comparison was from parasites isolated from patients with cutaneous Leishmaniasis (CL) in Colombia. Parasites were isolated from three different patients presenting with self-healing CL and from three different patients with chronic CL. CL in Colombia is mainly caused by parasites of the subgenus *L. (Viannia)*, and within this subgenus the species *L. (V) panamensis* is one of the more predominant species in Colombia (Alvar *et al.* 2012). CL can have varied disease outcomes from asymptomatic infections and infections that cause lesions that self-heal, to chronic and exacerbated disease. Chronic disease caused by *L. panamensis*

is refractory to chemotherapy and characterised by a high degree of inflammation and few parasites at the lesion site (Navas *et al.* 2014). Early expression of chemokines and their receptors by the host cell is modulated upon infection by *Leishmania*, which results in recruitment of host cells to the site. This is thought to cause the uncontrolled immunopathology (Navas *et al.* 2014). Rather than being an effect of immune variation between individuals, this effect on host cell chemokine response was shown to be parasite-mediated in *L. braziliensis* infection by researchers who showed that two distinct isolates of the same species could produce different chemokine stimulatory responses in the host cell (Teixeira *et al.* 2005). We hypothesise that parasites of the same species isolated from patients with chronic disease and patients with self-healing disease would have different secretome profiles, which leads to this modulation of the immune response. We aim to examine the secretion of proteins by *L. panamensis* parasites isolated from patients with chronic and with self-healing disease in collaboration with CIDEIM (Cali, Colombia), to identify mechanisms by which the parasites may be driving the divergent outcomes of this disease. If hyperactivation of the immune response was found to be parasite-mediated, therapeutic intervention targeting the responsible parasite factors could allow clearing of the infection to prevent chronic disease.

5.2 Aims and hypotheses

The overall aim was to take the methods developed in research presented in previous chapters in this thesis, for isolating and analysing the secretome of *Leishmania* parasites, and apply them to an attenuated *L. mexicana* parasite line and to clinical parasite isolates, obtained in collaboration with a Colombian research and treatment centre.

The aim of the *L. mexicana* analyses were to investigate the role of the secretome in the establishment of infection and parasite survival inside the host cell. We hypothesised that there would be a significant difference in the parasite secretome between wild type and attenuated *L. mexicana* promastigotes and amastigotes.

The aim of the secretome analysis was to investigate the potential functional role of the *Leishmania panamensis* secretome in the outcome of the disease. The comparative analyses were as follows:

- Parasites from three different patients with chronic cutaneous *Leishmaniasis* VS parasites from three different patients with self-healing cutaneous *Leishmaniasis*.
- The study also looked at differences in parasite incubation temperature, at 25°C VS 34°C, to mimic the temperature stimulus upon entry to the skin during infection.

We hypothesised that there would be a significant difference in the parasite secretome between isolates from chronic cutaneous *Leishmaniasis* compared to isolates from self-healing cutaneous *Leishmaniasis*. We also hypothesised that a change in temperature would alter the parasite secretome.

5.3 Results

To further investigate the *Leishmania* secretome, comparative proteomic analyses were employed on parasites with differing growth and disease phenotypes, to search for secreted proteins with potential roles in parasite survival in the host cell and in chronicity of the disease.

5.3.1 Growth and morphology of *L. mexicana* wild type and attenuated parasites

The first cell line used for the comparative secretome analyses was an attenuated line of *L. mexicana*, known as the H-line (Daneshvar *et al.* 2003a, 2003b). This line was generated by repeated sub-passage in the presence of gentamicin, and confirmed as attenuated by infection of primary mouse macrophages, where no parasite proliferation was observed in the host cell (Daneshvar *et al.* 2003a).

We observed no difference in the axenic growth of H-line promastigotes compared to that of wild type parasites freshly isolated from mice, passage 2 (WT), or wild type parasites after repeated sub-passage without gentamicin (HWT) (Figure 5-5a). All three parasite lines display logarithmic growth over 72 h between 1×10^5 and 1×10^7 cells/ml and enter late-logarithmic and stationary phases thereafter, slowly increasing to a maximum of 2×10^7 cells/ml before plateauing. As amastigotes, there is some delay in the growth of the H-line, but both H and HWT cell lines reach a maximum density exceeding 10^7 cells/ml over 150 to 200 h, with the H-line taking approximately 48 h longer to reach this density (Figure 5-5b).

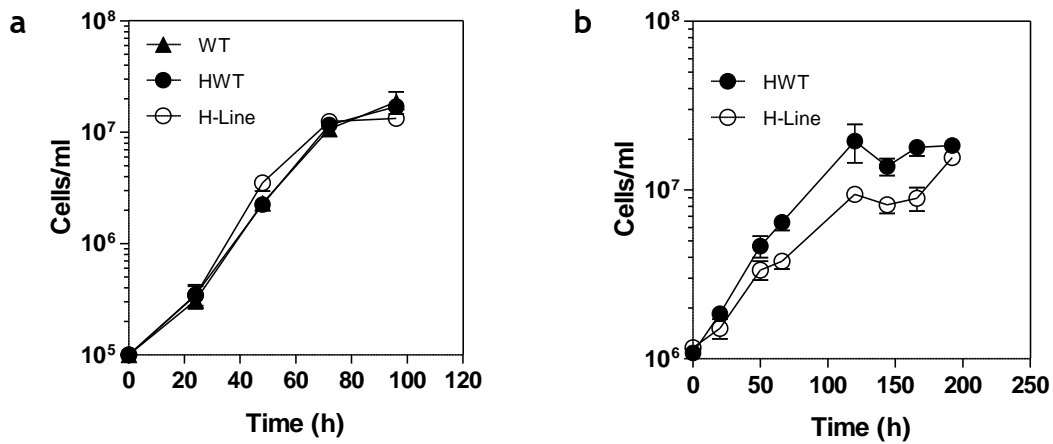


Figure 5-5 Growth of wild type and attenuated *L. mexicana* promastigotes and amastigotes *in vitro*. Promastigotes (a) and amastigotes (b) were cultured in complete HOMEM and SDM, respectively, and aliquots removed every 24h for counting using a haemocytometer. WT – wild type parasites maintained between 4 – 15 passages, HWT – wild type parasites maintained to the same passage number as the attenuated cells, H-line – parasites attenuated by repeated culture in complete medium with gentamicin. $n = 3$.

With regards to parasite morphology, there are some differences in stationary phase promastigotes as shown in Figure 5-6a-c, with the average cell length and width significantly larger in the H-line, with the average length increasing from 10 μm to 14 μm , and the average width increasing from 1.1 μm to 1.9 μm . No significant difference in flagellum length was observed between the cell lines. Both cell types successfully differentiate to amastigotes and divide and grow as axenic amastigotes (Figure 5-5b). There appeared to be a delay in the differentiation to amastigotes in the H-line as the cells were still significantly different from the wild-type in length and width at day 1 after amastigote induction (Figure 5-6d,e). However, after 48 h the cell sizes of both parasite lines had reduced, indicating a complete morphological change to amastigotes (Figure 5-6f-i).

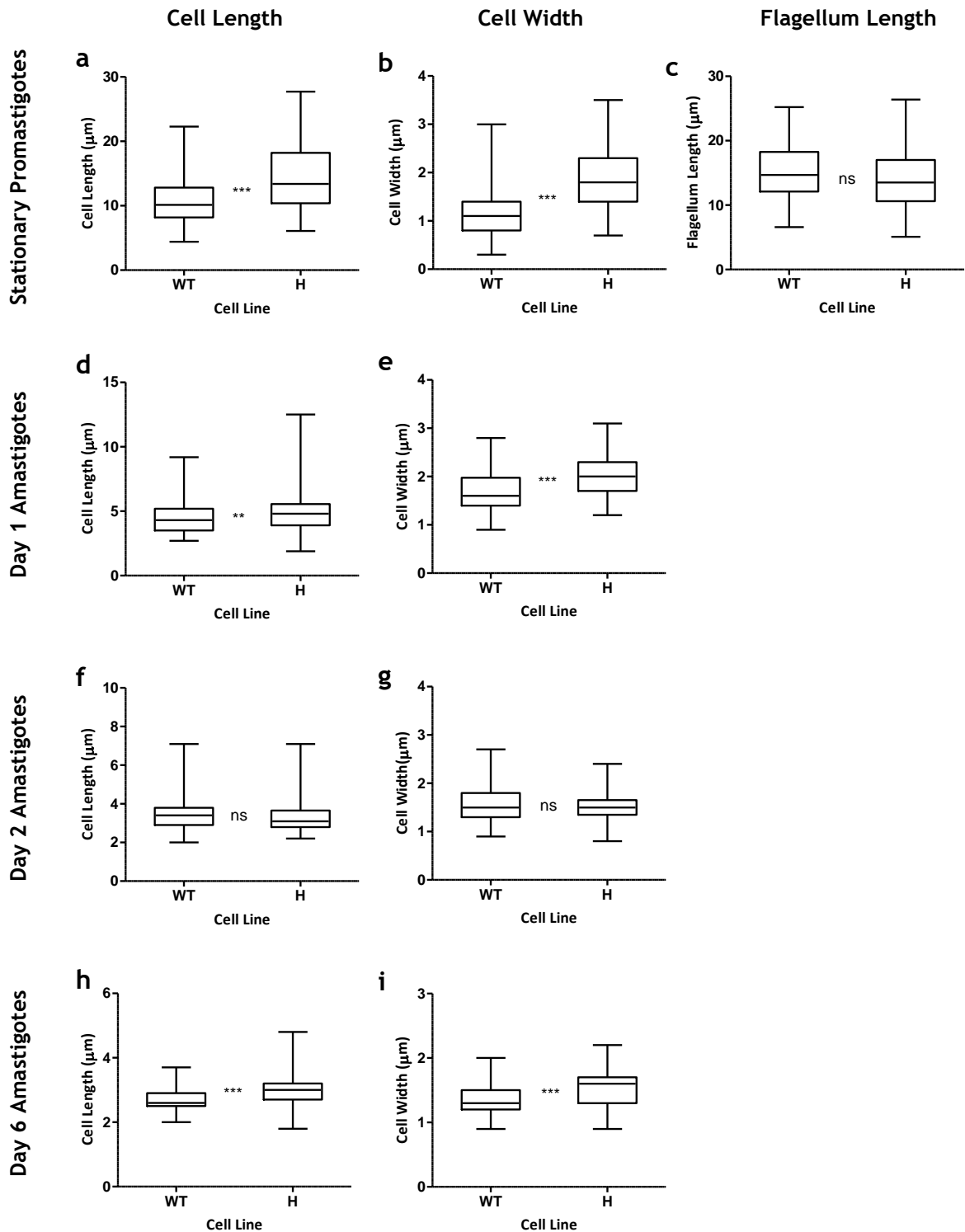


Figure 5-6 Measurements of *L. mexicana* wild type (WT) and attenuated (H) parasites during axenic growth. Stationary phase promastigotes, cultured in complete HOMEM, were sampled at a density of 1.4×10^7 cells/ml and air dried on slides, fixed and giemsa stained (a, b, c). These stationary cultures were then used to start amastigote cultures in complete SDM, pH 5.5, at a starting density of 1×10^6 cells/ml. Samples were taken at 24 h (Day1) (d, e), 48 h (Day2) (f, g) and 144 h (Day6) (h, i) and stained as above. Measurements were made using Fiji image analysis software. Graphs and analysis of significance were made using GraphPad Prism. Box plot whiskers denote min to max values. Means were compared using a two-tailed T-test with Welch's correction for unequal variance *** $P = < 0.0001$, ** $P = 0.003$, ns = not significant. $n = 100$ cells imaged and measured per condition.

5.3.2 Secretome collection and visualisation from *L. mexicana* wild type and attenuated parasites

The successful differentiation and growth of both parasite lines as axenic amastigotes allowed for the parasite-only secretome to be isolated and analysed from both WT and H-line promastigotes and amastigotes and analysed using direct comparative approaches.

Visualising the profiles of the secreted proteins isolated from the axenic culture supernatants by SDS-PAGE and using densitometry analysis to plot and overlap the profiles showed good sample reproducibility, both for the WT and H-line promastigotes (Figure 5-7a,b) and for WT amastigotes (Figure 5-8a). H-line amastigotes displayed a more variable secretome (Figure 5-8b).

Overlaying and taking the average of the densitometry plots of the WT and H-line secretomes showed distinct secretome profiles for the promastigote stages (Figure 5-7c). At least 8 or more bands showed differences in density of more than 2-fold. In contrast, the comparison of the amastigote secretome profiles showed minimal differences between the two cell lines, with the differential peak at ~40 kDa only present in one of three H-line replicates (Figure 5-8c).

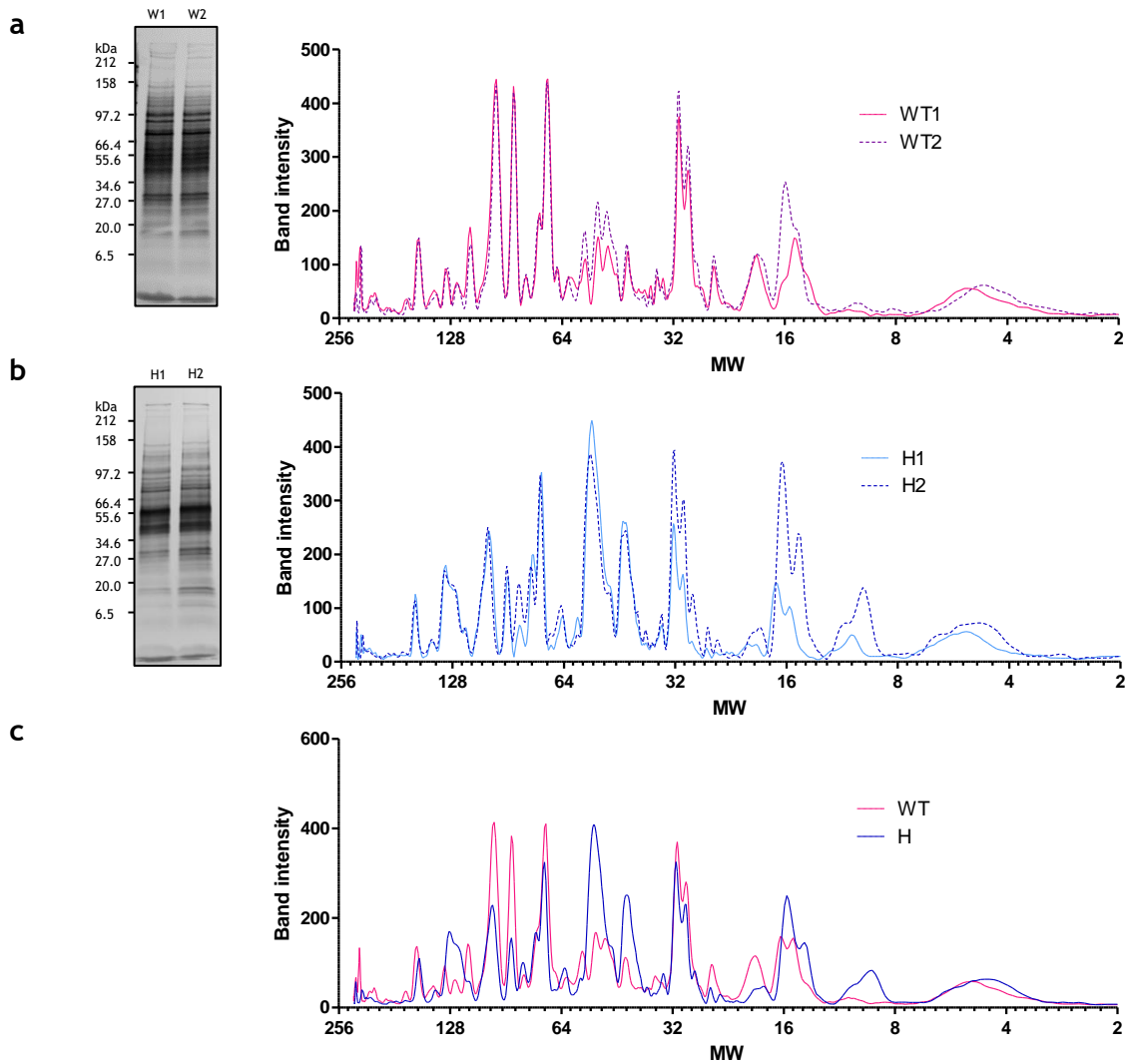


Figure 5-7 Densitometry profile plots of the *L. mexicana* promastigote secretome. Secreted proteins collected from the supernatant of wild type (W) and attenuated (H) axenic cultures were separated by SDS-PAGE and stained with silver stain. Densitometry analysis was performed using ImageJ and plotted and overlaid using GraphPad Prism. Replicates of W (a) and H (b) parasite secretome were compared to investigate their reproducibility, and representative lanes of W and H were compared (c) to illustrate any visible differences.

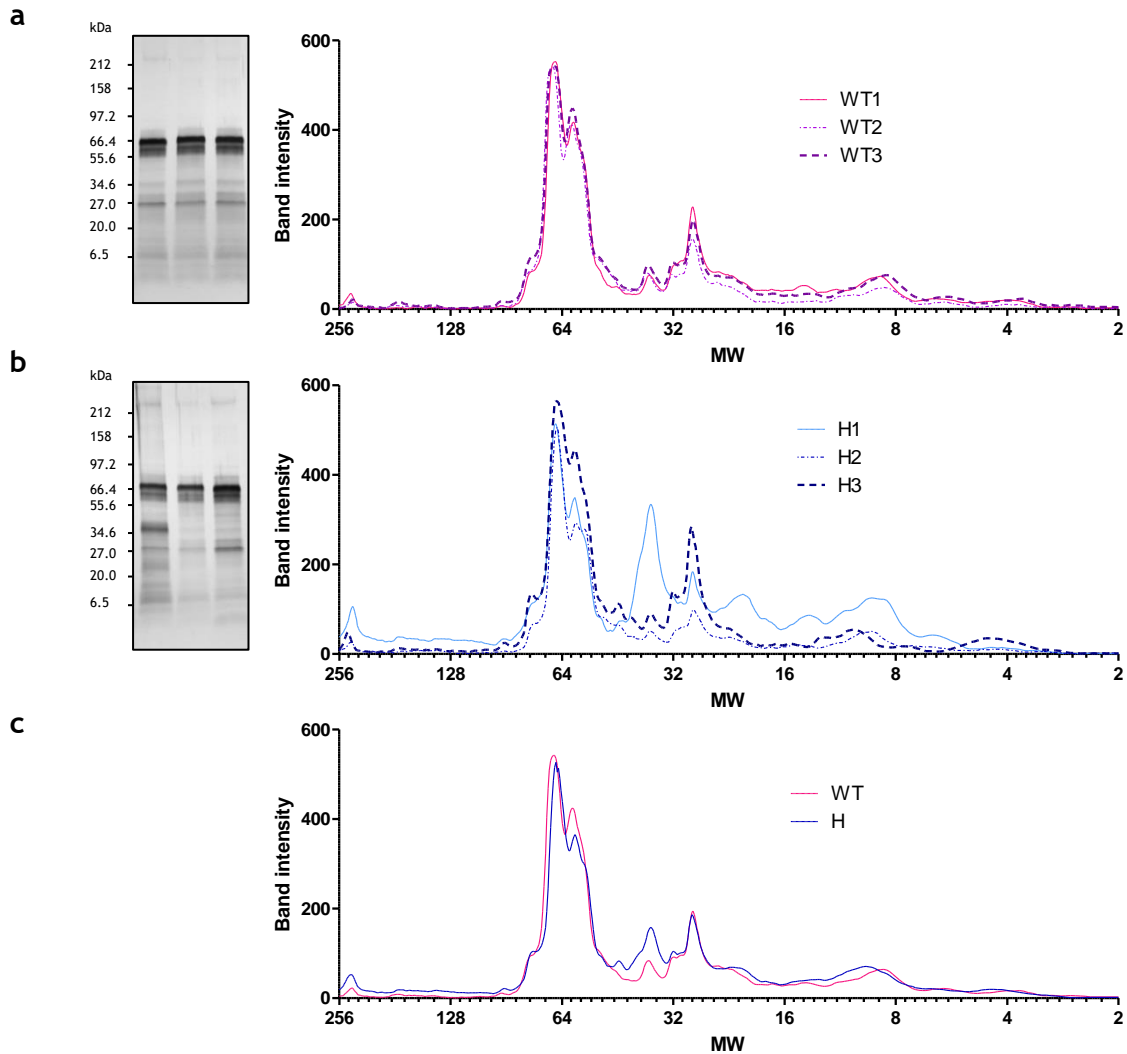


Figure 5-8 Densitometry profile plots of the *L. mexicana* amastigote secretome. Secreted proteins collected from the supernatant of wild type (W) and attenuated (H) axenic cultures was separated by SDS-PAGE and stained with silver stain. Densitometry analysis was performed using ImageJ and graphed using GraphPad Prism. Replicates of W (a) and H (b) parasite secretome were compared to investigate their reproducibility, and an average of the densitometry values of W and H were compared (c) to illustrate any visible differences.

Difference gel electrophoresis (DiGE) was used to further separate and increase the resolution of the visual secretome comparisons (Figure 5-9). The WT and H secretome samples were differentially labelled with spectrally distinct Cy3 and Cy5 dyes, respectively, combined, then separated in two dimensions. This allowed for co-migration of the proteins in both samples under identical conditions (Westermeyer *et al.* 2008). Clear differences were again observed in the promastigote secretome, both in isoelectric point of the proteins and in molecular weight (Figure 5-9a). Subtle differences in the molecular weight of some proteins

are visible, not only indicating alterations in protein expression, but also in protein isoforms and post-translational modifications. As before, fewer differences are observed in the amastigote secretome between WT and H than the promastigote (Figure 5-9b). However, with the increased resolution some changes are evident that could not be observed in the 1D gel separation.

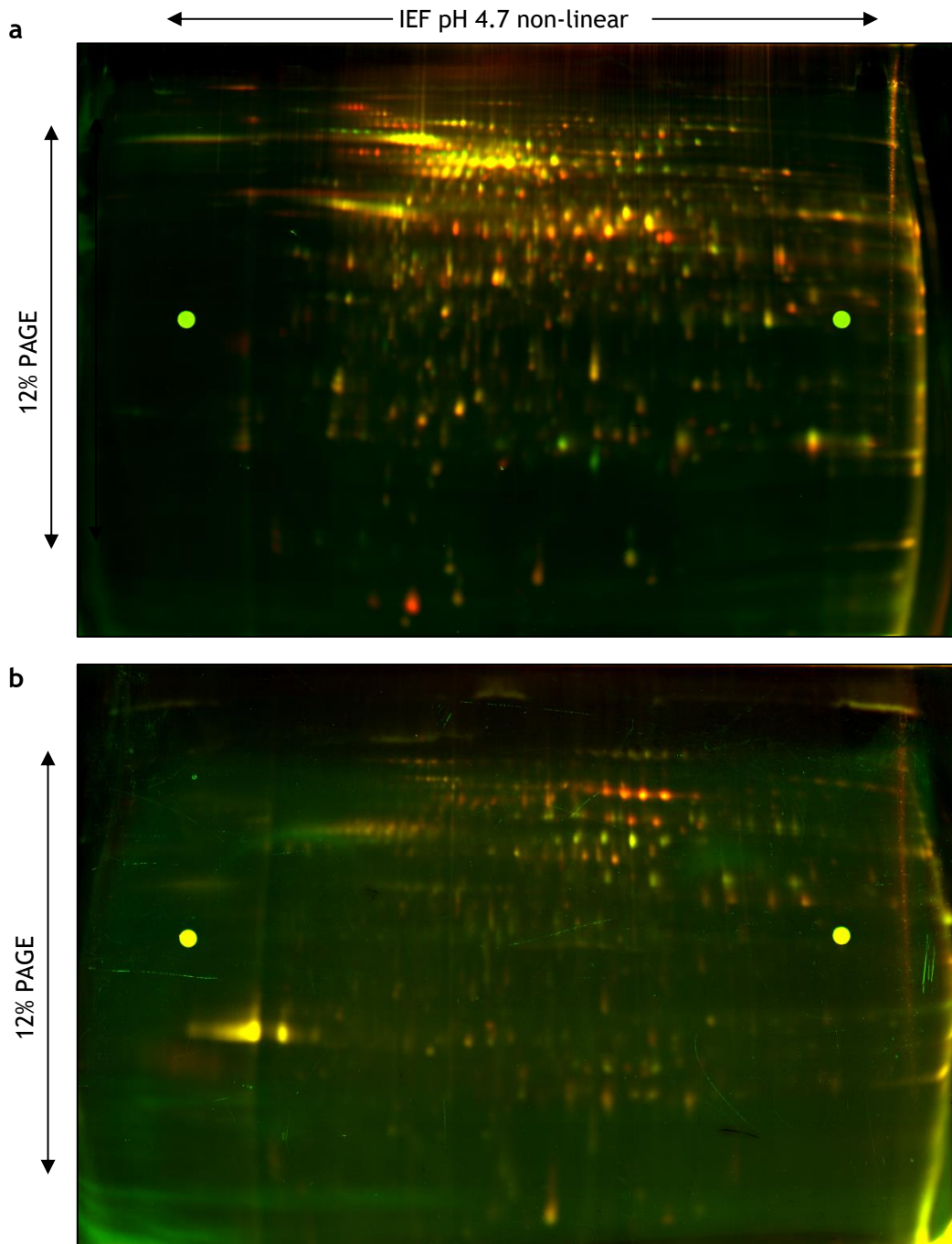


Figure 5-9 *L. mexicana* secretome proteins separated by 2-dimensional electrophoresis. Promastigote secretome (a) and amastigote secretome (b) from wild type and attenuated parasites were differentially labelled with Cy3 and Cy5 dyes before combining and separating in two dimensions. 2-dimensional separation, first by isoelectric focusing (IEF) within pH range 4-7, followed by electrophoresis through a 12% polyacrylamide gel.

5.3.3 Quantitative analysis of the *L. mexicana* WT and attenuated parasite secretome using isobaric peptide tagging

The comparison of *L. mexicana* WT and attenuated parasite secretomes was studied by using LC-MS/MS to identify the proteins and employing isobaric peptide tagging to quantitate the proteins. The tryptic peptides from each secretome sample were differentially labelled before combining and analysing by LC-MS/MS. Using clustering analysis on the full list of promastigote protein identifications and their corresponding quantitation values (Figure 5-10) we can see that the three biological repeats of WT and H samples cluster together and shows that the secretomes of the two cell lines are quantitatively distinct. Repeat 3, labelled with 128 and 131 for WT and H cell line, respectively, clusters slightly further from repeats 1 and 2 for both cell lines. This cluster, along with the clustering of up- and downregulated proteins, was then used to create the heat map depicted in Figure 5-11. This heat map shows a visual representation of both the level of change in abundance and the reproducibility of the biological replicates. A total of 52 proteins were reproducibly up- or downregulated in each of the three replicates from both cell lines, with a p-value of ≤ 0.05 , and exhibiting a fold change of $\geq \pm 1.5$. Each protein is assigned a colour based on the scale of Euclidean distance.

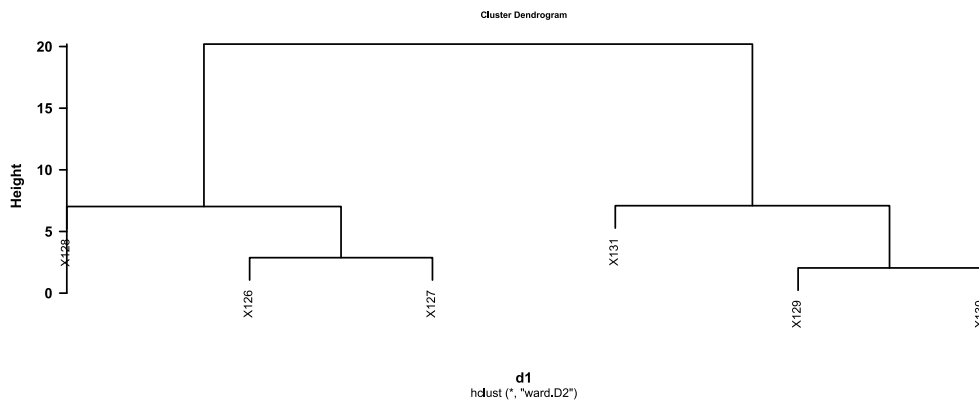


Figure 5-10 Cluster dendrogram of *L. mexicana* promastigote quantitative secretome data. - Created in RStudio using Euclidean distance to show the similarity or dissimilarity between observations. The replicates for each of the two sample types cluster together. Labels X126-X131 denote the quantitation channels for each TMT reporter tag. X126-128 are wild type samples 1-3 and X129-131 are attenuated samples 1-3.

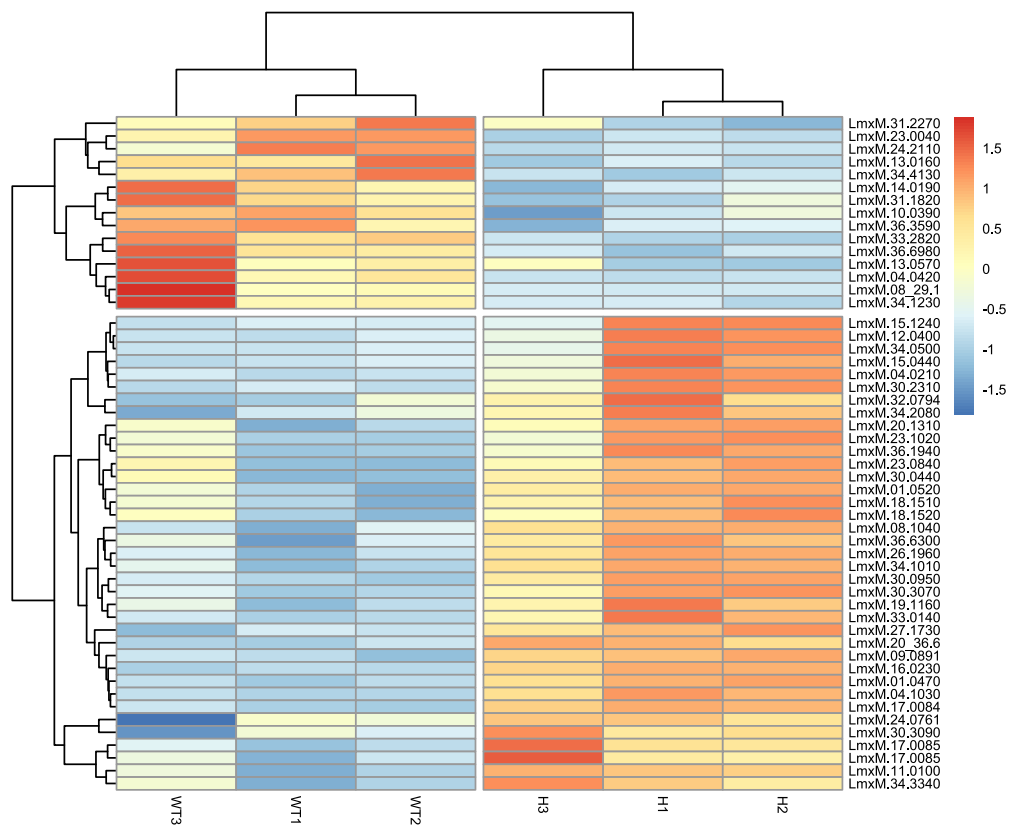


Figure 5-11 Heat map of quantitative differences between secreted proteins of *L. mexicana* promastigote wild type and attenuated cell lines. Colour denotes value assigned to distance. Columns are the samples and rows are the quantitated proteins. $-\log_{10}p\text{-value} = 1.3$ (0.05) and \log_2FC of 0.58 (1.5).

The volcano plot in Figure 5-12a shows the level of up- or downregulation of all the secreted proteins in the promastigote secretome for the WT and H line parasites against the p-value for reproducibility of the replicates. The proteins marked in red indicate proteins with a p-value of ≤ 0.05 over three biological repeats from each cell line and with a fold change in abundance of ≥ 1.5 fold. In the plot depicted in Figure 5-12a, the *ordinary* p-values from individual *t*-tests are used to plot the data, with a total of 42 proteins above the significance thresholds. In Figure 5-12b, an alternative method of significance estimation has been used and the resulting *modified* p-values used to plot the data. Using this method, a total of 52 proteins were found to change reproducibly between the secretomes of the two parasite lines. Table 5-1 contains the descriptions of each of the proteins.

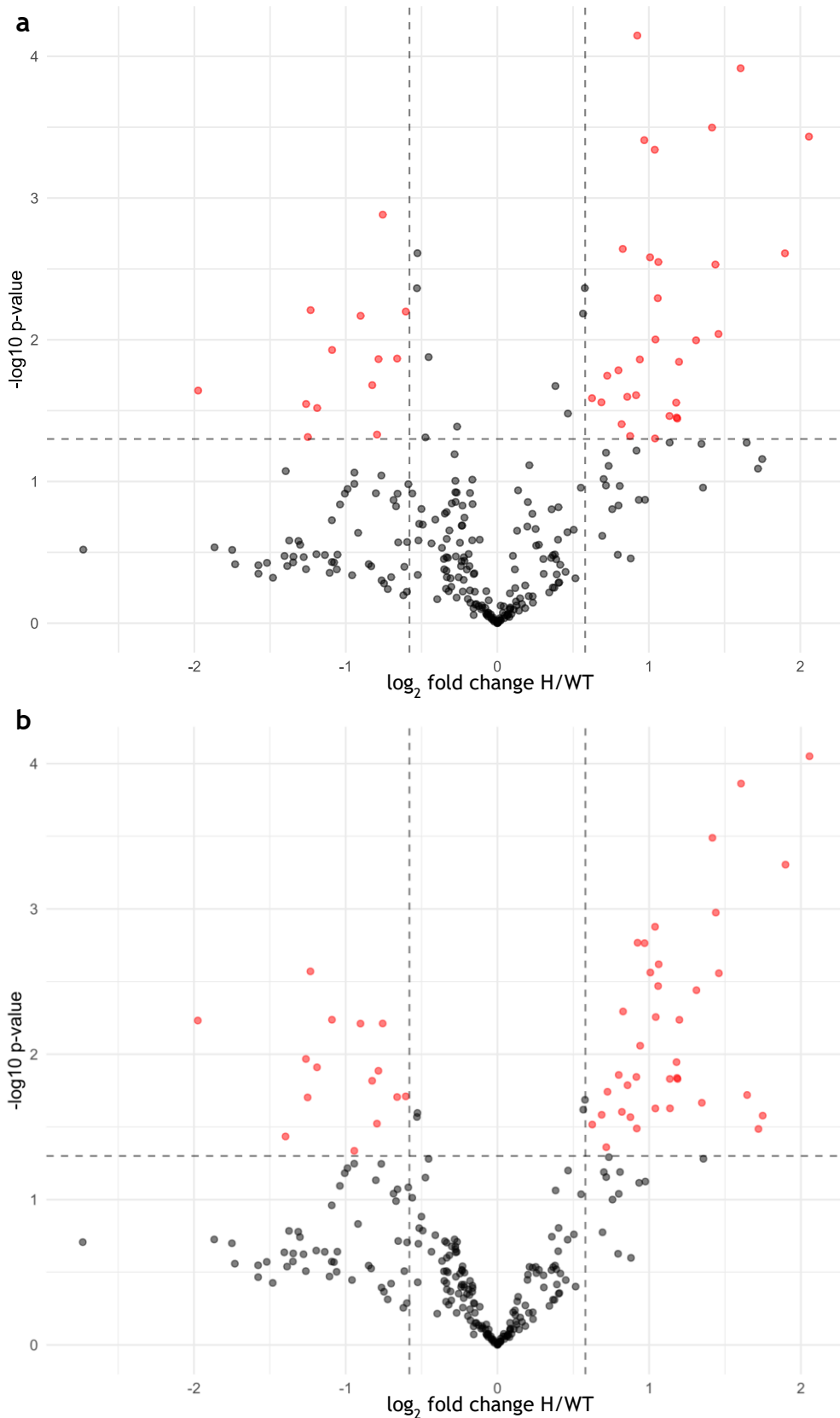


Figure 5-12 Volcano plots of 6-plex TMT™ quantitation of *L. mexicana* promastigote secretome from wild type (WT) and attenuated (H) parasites. (a) Volcano plot of the fold change of each protein in WT and H samples against the p-values of the sample variability using standard t-tests. (b) Reanalysis of p-values using Kammers et al. (D'Angelo *et al.* 2017; Kammers *et al.* 2015) method of using moderated *t*-statistics from the empirical Bayes procedure LIMMA. Statistical testing performed and figures made in RStudio. -log₁₀ p-value cut off of ≥1.3 (≤0.05), log₂FC of ±0.58 (FC 1.5).

Performing clustering analysis on the amastigote protein identifications and their corresponding quantitation values (Figure 5-13), we can see that the three biological repeats of the WT and H cell line samples cluster together. In contrast, comparing the promastigote and amastigote clustering analysis, the height of the cluster for amastigote samples, which relates to the Euclidean distance or similarity of the values, is much smaller than that of the promastigote samples, shrinking from a range of 0-20 shown in Figure 5-10 to 0.5-3.5 shown in Figure 5-13. This suggests that although the amastigote WT and H-line samples do show enough differences to cluster separately, they are not as different as the promastigote samples. This cluster, along with clustering of up- and downregulated proteins, were then used to create the heat map in Figure 5-14 which shows a visual representation of both the level of change in abundance and the reproducibility of the biological replicates. Only two proteins were found to be reproducibly up or downregulated between the cell lines, with a p-value of ≤ 0.05 , and exhibiting a fold change of $\geq \pm 1.5$. Each protein is assigned a colour based on the scale of Euclidean distance.

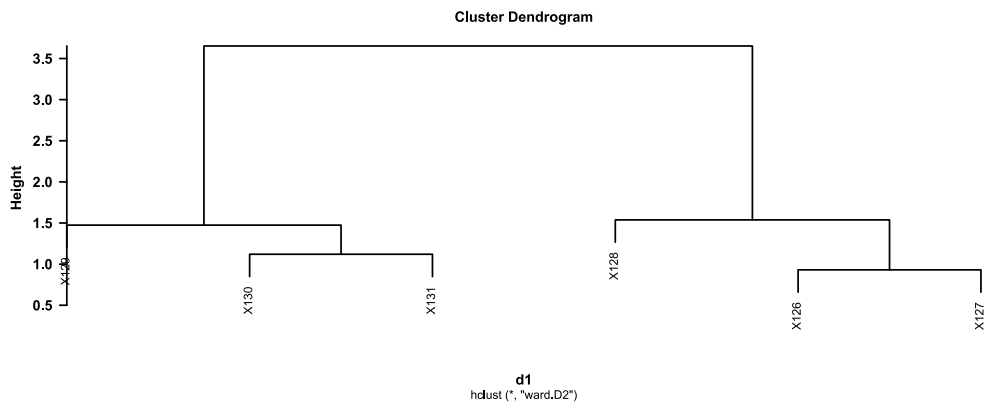


Figure 5-13 Cluster dendrogram of *L. mexicana* amastigote quantitative secretome data Created in RStudio using Euclidean distance to show the similarity or dissimilarity between observations. The replicates for each of the two sample types cluster together. Labels X126-X131 denote the quantitation channels for each TMT reporter tag. X126-128 are wild type samples 1-3 and X129-131 are attenuated samples 1-3.

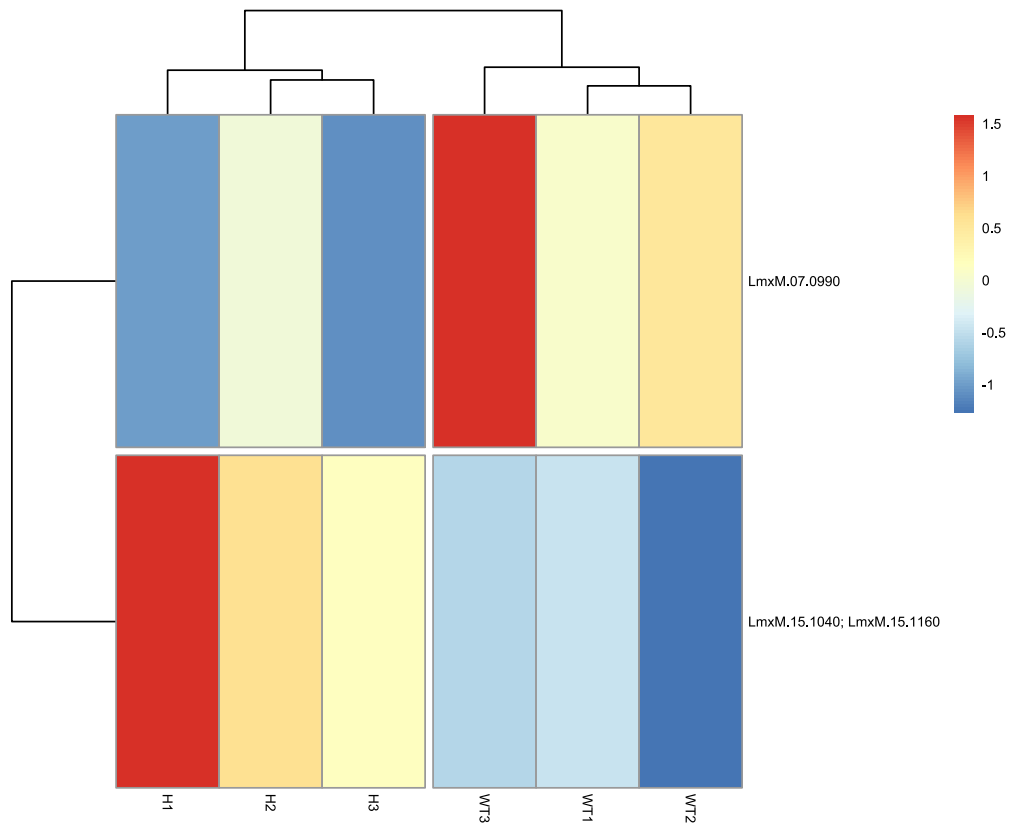


Figure 5-14 Heat map of quantitative differences between secreted proteins of *L. mexicana* amastigote wild type and attenuated cell lines. Colour denotes value assigned to distance. Columns are the samples and rows are the quantitated proteins. $-\log_{10}p = 1.3$ (0.05) and \log_2FC of 0.58 (1.5).

The volcano plot in Figure 5-15a shows the level of up- or downregulation of all the secreted proteins in the amastigote secretome for WT and H line parasites, against the p-value for reproducibility of the replicates. The proteins marked in red indicate proteins with a p-value of ≤ 0.05 over three biological repeats from each cell line and with a fold change in abundance of ≥ 1.5 fold. In plot Figure 5-15a, the *ordinary* p-values from individual *t*-tests are used to plot the data, with one protein above the significance thresholds. In the plot depicted in Figure 5-15b, an alternative method of significance estimation has been used and the resulting *modified* p-values used to plot the data. Using this method, two proteins were above the significance thresholds. Table 5-2 contains the names of the two proteins.

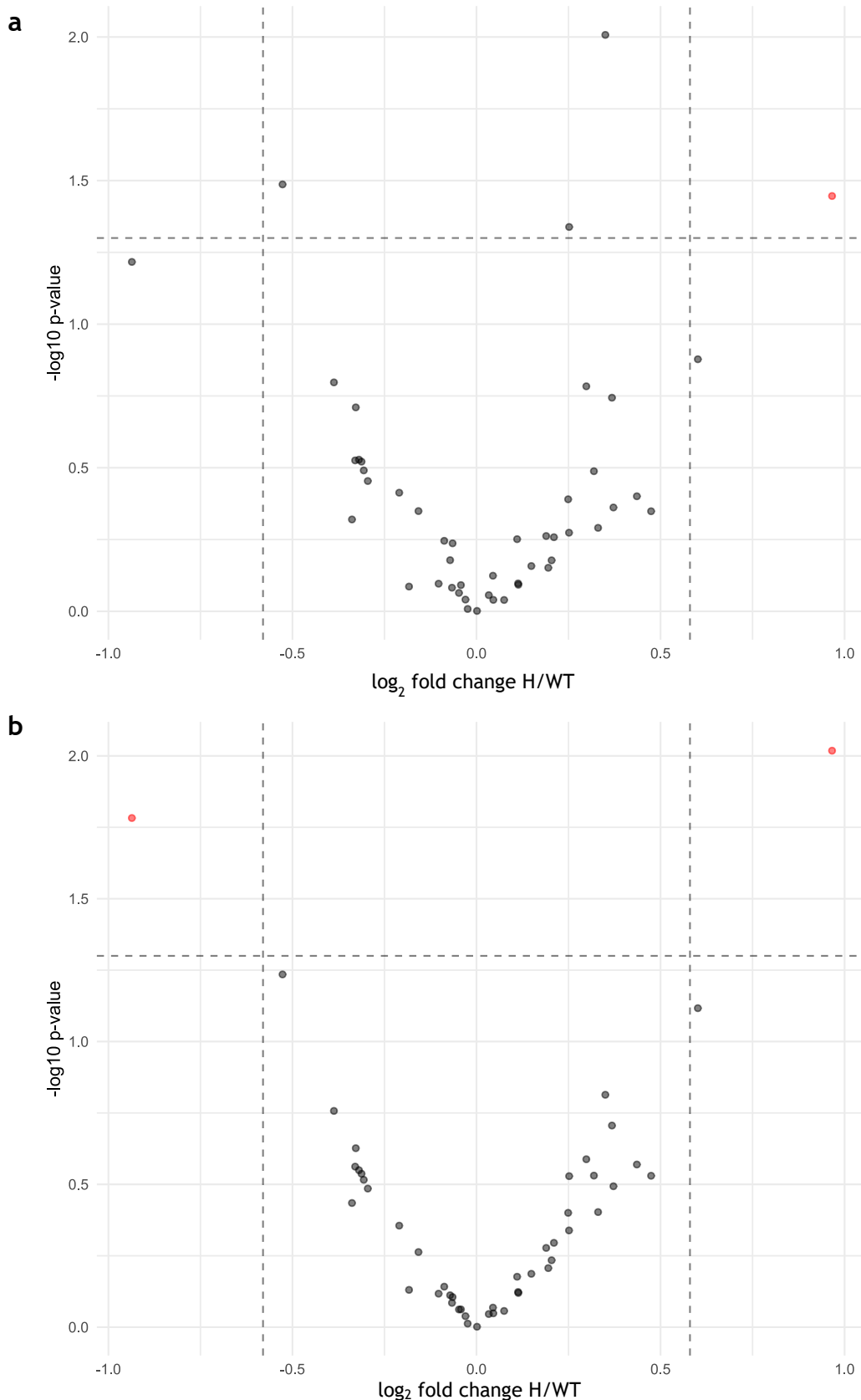


Figure 5-15 Volcano plots of 6-plex TMT™ quantitation of *L. mexicana* amastigote secretome from wild type (WT) and attenuated (H) parasites. (a) Volcano plot of the fold change of each protein in WT and H samples against the p-values of the sample variability using standard t-tests. (b) Reanalysis of p-values using Kammers *et al.* (D'Angelo *et al.* 2017; Kammers *et al.* 2015) method of using moderated *t*-statistics from the empirical Bayes procedure LIMMA. Statistical testing performed and figures made in RStudio. -log₁₀ p-value cut off of ≥1.3 (≤0.05), log₂ FC of ±0.58 (FC 1.5).

Table 5-1 *L. mexicana* promastigote secretome proteins significantly up- or down-regulated in attenuated parasites compared to wild-type.
ProTMT - sigtable_kammod 0.58, 1.3

Accession	Description	Log ₂ FC	FC	p-value
LmxM.04.1030	COPI associated protein, putative	2.056667	4.16024	8.91E-05
LmxM.30.0950	hypothetical protein (sodium stibogluconate resistance protein, putative)	1.898667	3.728684	0.000496
LmxM.34.0500	proteophosphoglycan ppg3, putative	1.748333	3.359702	0.026442
LmxM.15.1240	nucleoside transporter 1, putative	1.720333	3.295125	0.032675
LmxM.36.1940	inosine-guanosine transporter	1.645667	3.128924	0.019077
LmxM.17.0084	elongation factor 1-alpha	1.605667	3.043364	0.000137
LmxM.17.0085	elongation factor 1-alpha	1.459667	2.750448	0.00277
LmxM.27.1730	Flabarin, putative	1.439333	2.711955	0.00106
LmxM.20_36.6480a	hypothetical protein (histidine secretory acid phosphatase, paralogue)	1.417	2.670297	0.000324
LmxM.23.1020	hypothetical protein, unknown function	1.347333	2.544414	0.021558
LmxM.30.3070	ferrous iron transport protein	1.311667	2.482281	0.003627
LmxM.36.6300	glucose transporter 1	1.199333	2.296335	0.005797
LmxM.04.0210	surface antigen-like protein	1.187667	2.27784	0.014788
LmxM.20.1310	polyubiquitin, putative	1.183667	2.271534	0.014547
LmxM.30.2310	3'-nucleotidase/nuclease	1.180333	2.266291	0.011325
LmxM.12.0400	3'-nucleotidase/nuclease, putative	1.137333	2.19974	0.023561
LmxM.17.0085	P-type H ⁺ -ATPase, putative	1.136333	2.198216	0.014775
LmxM.08.1040	hypothetical protein	1.062667	2.088789	0.002404
LmxM.11.0100	seryl-tRNA synthetase	1.059	2.083487	0.003393
LmxM.33.0140	malate dehydrogenase	1.043667	2.06146	0.005545
LmxM.15.0440	tb-292 membrane associated protein-like protein	1.041	2.057653	0.023591
LmxM.01.0470	fatty acyl CoA syntetase 1, putative	1.039	2.054803	0.001327
LmxM.34.1010	casein kinase, putative	1.008	2.011121	0.002739
LmxM.09.0891	polyubiquitin, putative	0.97	1.958841	0.001721
LmxM.01.0520	long-chain-fatty-acid-CoA ligase, putative	0.940667	1.919415	0.008733
LmxM.16.0230	protein tyrosine phosphatase-like protein	0.923667	1.89693	0.001709
LmxM.23.0840	hypothetical protein, unknown function	0.918333	1.889931	0.032427
LmxM.34.2080	calcium motive p-type ATPase, putative	0.915667	1.886441	0.014332
LmxM.18.1520	hypothetical protein, conserved	0.876333	1.835704	0.027104
LmxM.18.1510	P-type H ⁺ -ATPase, putative	0.857667	1.812105	0.016324
LmxM.26.1960	hypothetical protein, conserved	0.828	1.775223	0.005078
LmxM.30.0440	cytoskeleton-associated protein CAP5.5, putative	0.820333	1.765814	0.024928
LmxM.19.1160	small myristoylated protein 1	0.799333	1.740297	0.013879
LmxM.34.3340	6-phosphogluconate dehydrogenase, decarboxylating, putative	0.725333	1.653283	0.018112
LmxM.24.0761	malic enzyme	0.717333	1.64414	0.043628
LmxM.30.3090	peptidase, putative	0.687	1.609932	0.026089
LmxM.32.0794	beta tubulin	0.625	1.542211	0.03045

Accession	Description	Log ₂ FC	FC	p-value
LmxM.13.0160	protein kinase A regulatory subunit	-0.60433	1.520276	0.019488
LmxM.36.3590	cysteine synthase, putative	-0.66133	1.581544	0.019688
LmxM.33.2820	regulatory subunit of protein kinase a-like protein	-0.75633	1.689192	0.006143
LmxM.36.6980	eukaryotic translation initiation factor 3 subunit c	-0.78433	1.722296	0.013003
LmxM.31.2270	membrane associated protein-like protein	-0.794	1.733875	0.030022
LmxM.14.0190	Thioredoxin-like, putative	-0.82567	1.772354	0.015225
LmxM.34.4130	polyadenylate-binding protein 2	-0.90267	1.869518	0.006154
LmxM.08_29.1750	paraflagellar rod protein 1D, putative	-0.94333	1.922966	0.046177
LmxM.10.0390	GP63, leishmanolysin	-1.09067	2.129724	0.005788
LmxM.24.2110	3-hydroxy-3-methylglutaryl-CoA synthase, putative	-1.18933	2.280473	0.012294
LmxM.23.0040	tryparedoxin peroxidase	-1.23267	2.35001	0.002691
LmxM.34.1230	short chain dehydrogenase, putative	-1.251	2.380063	0.01981
LmxM.04.0420	Tetratricopeptide repeat, putative	-1.26233	2.398834	0.010782
LmxM.13.0570	40S ribosomal protein S12, putative	-1.39667	2.632925	0.036789
LmxM.31.1820	iron superoxide dismutase, putative	-1.97467	3.930374	0.005858

Table 5-2 *L. mexicana* amastigote secretome proteins significantly up- or down-regulated in attenuated parasites compared to wild-type.AmaTMT.
Kammersmod, sigtable 0.58, 1.3

Accession	Description	Log ₂ FC	FC	p-value
LmxM.15.1040;	tryparedoxin peroxidase	0.966	1.953417	0.009588
LmxM.15.1160			1.913658	0.016499
LmxM.07.0990	nucleolar RNA-binding protein, putative	-0.93633	1.913658	0.016499

5.3.4 Secreted protein identities and quantitation are validated by immunodetection

The identities of a selection of the secreted proteins identified by LC-MS/MS were validated by immunoblotting with antibodies raised against *Leishmania* proteins. The quantitation could also be validated for a proportion of the proteins for which *Leishmania*-specific antibodies could be obtained. Figure 5-16 shows the quantitation values for each protein in each of the 6 samples and the corresponding Western blot of the same samples separated by SDS-PAGE including; Oligopeptidase B (OPB), enolase (ENO), secretory acid phosphatase (SAP), glycoprotein 63/leishmanolysin (GP63). A silver stained gel has been included to serve as the loading control in the absence of any known constitutively secreted proteins across the two cell types.

In most cases there appears to be an anomaly with the TMT quantitation of W3 - tag 128. The quantitation of the other samples and reporter tags correlates well and the quantitation looks accurate except for W3-tag 128. Re-analysis of the fold change and significance excluding reporter ion 128 could be performed to study this anomaly, however due to time constraints and sample availability this was not performed.

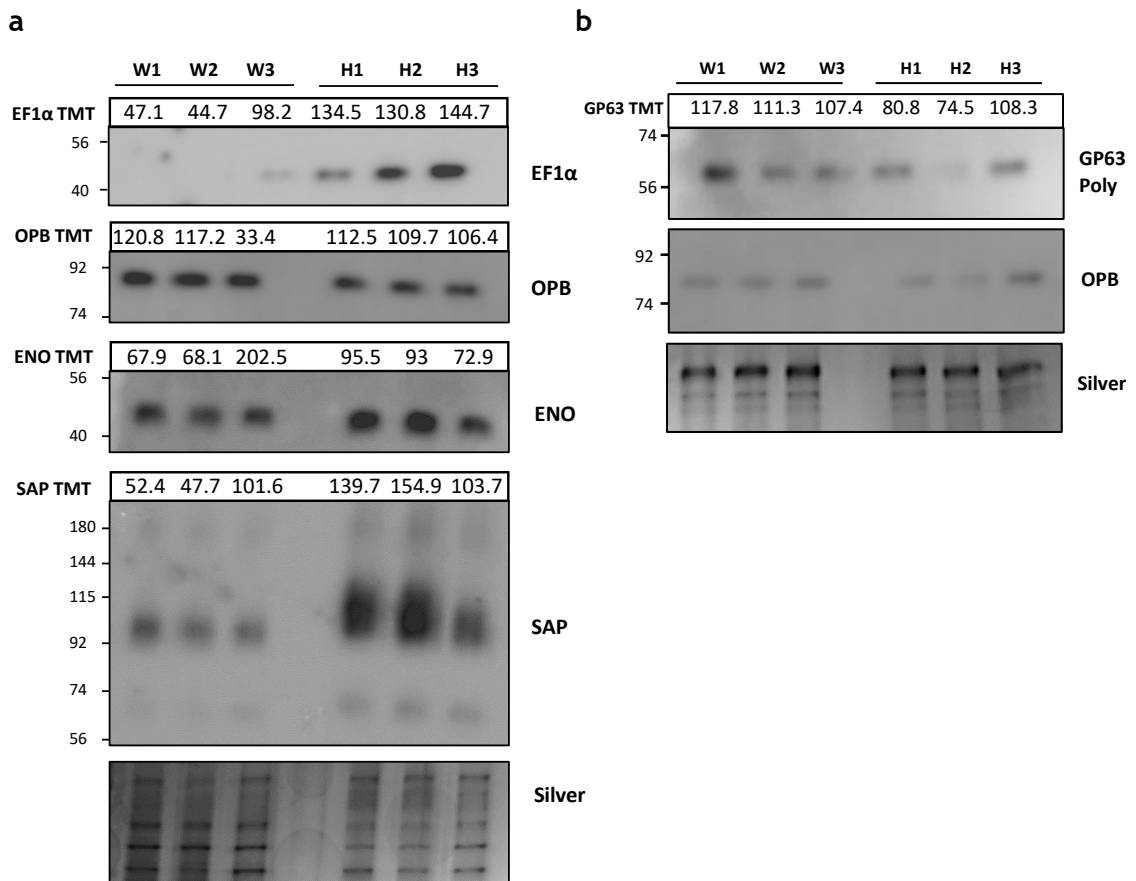


Figure 5-16 Western blots of *L. mexicana* secreted proteins paired with quantitation values from the same samples analysed by LC-MS/MS. (a) Promastigote secretome probed with antibodies to oligopeptidase b (OPB), enolase (ENO) and secretory acid phosphatase (SAP). Quantitative measurements of proteins from analysis of TMT-labelled peptides from the secreted proteome, quantified using Proteome Discoverer, are shown above the immunoblots. (b) Amastigote secretome probed with antisera to glycoprotein 63 (GP63) and oligopeptidase b (OPB). OPB was not detected in the TMT-labelled MS analysis therefore quantitation values are not shown. Sample loading is shown by silver staining.

5.3.5 Secretome collection and visualisation from *L. panamensis* parasites causing chronic and self-healing disease

L. panamensis parasites were isolated from three patients with chronic cutaneous lesions (Chr) and from three patients with self-healing cutaneous lesions (SH). The parasites were cultured axenically at 25°C in serum-supplemented RPMI 1640 media to obtain high numbers of parasites that were then incubated in a serum-free medium to collect the secretome (samples from the parasites of each disease phenotype will be denoted as Chr / SH). This collection was performed at both 25°C and 34°C, to evaluate if a temperature increase would alter the secretome, as this mimics the parasites' entry to the skin. The secretome was then analysed

by SDS-PAGE and mass spectrometry, using the TMT™ kit from Thermo Fisher to label tryptic peptides with isobaric tags.

To assess and minimize contamination with proteins released through cell lysis, the viability of the parasites was monitored before and after incubation in serum-free collection medium. The typical viability of the *L. panamensis* field isolates lies at around 70% in culture which is much lower than the laboratory strains of *L. mexicana* which are typically >95% viable in culture. This complicates the secretome analysis as there is a higher chance of products of cell lysis being present in the secretome. However, lower cell viabilities of between 60-80% remained consistent between the 6 isolates both before and after incubation in secretome collection medium, therefore a comparative analysis could be performed between the samples whilst also making use of a control cell lysate proteome.

Table 5-3 *L. panamensis* promastigote cell viability *in vitro*. Cell viabilities were measured before incubation, when the cells were in normal culture in cRPMI at 25°C, and after four-hour incubations in sfRPMI at the temperatures stated. Measured by counting with trypan blue and motility assessment. *n*=2 for samples with SD.

Sample	Before Incubation		After 4h at 25°C		After 4h at 34°C	
	Viable %	SD	Viable %	SD	Viable %	SD
[SH] A1	80.72	-	85.5	-	88.3	-
[SH] A2	85.95	±9.26	81.15	±3.04	83.15	±0.21
[SH] A3	79.65	±1.91	71.75	±2.47	76.4	±7.07
[Chr] B1	88.5	±0.71	90.85	±5.87	87.1	±5.51
[Chr] B2	63.5	±4.95	61	±5.66	57.5	±2.12
[Chr] B3	63	-	71	-	63.5	-

From the mass spectrometry data of the control whole cell proteome compared to the secretome, enrichment of secreted proteins was evident from the observation that 11% of proteins in the secretome were too rare to be identified at all in the control proteome (Figure 5-17). This was due to the limitation of dynamic range in the mass spectrometer.

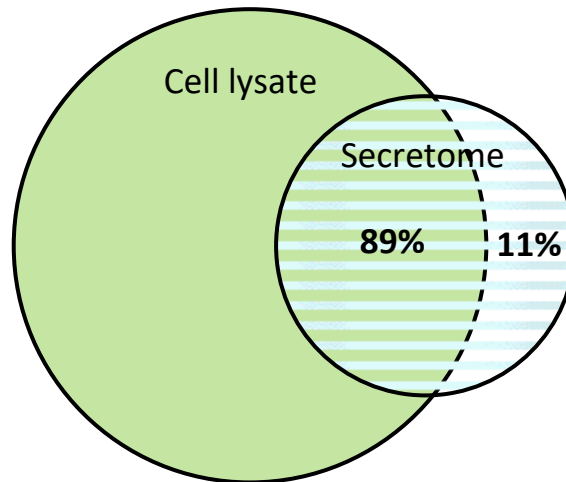


Figure 5-17 *L. panamensis* cell lysate proteome and secretome comparison

Proteome and secretome obtained by LC-MS/MS and protein identifications from Mascot compared using Excel. Overlap indicates proteins present in both samples.

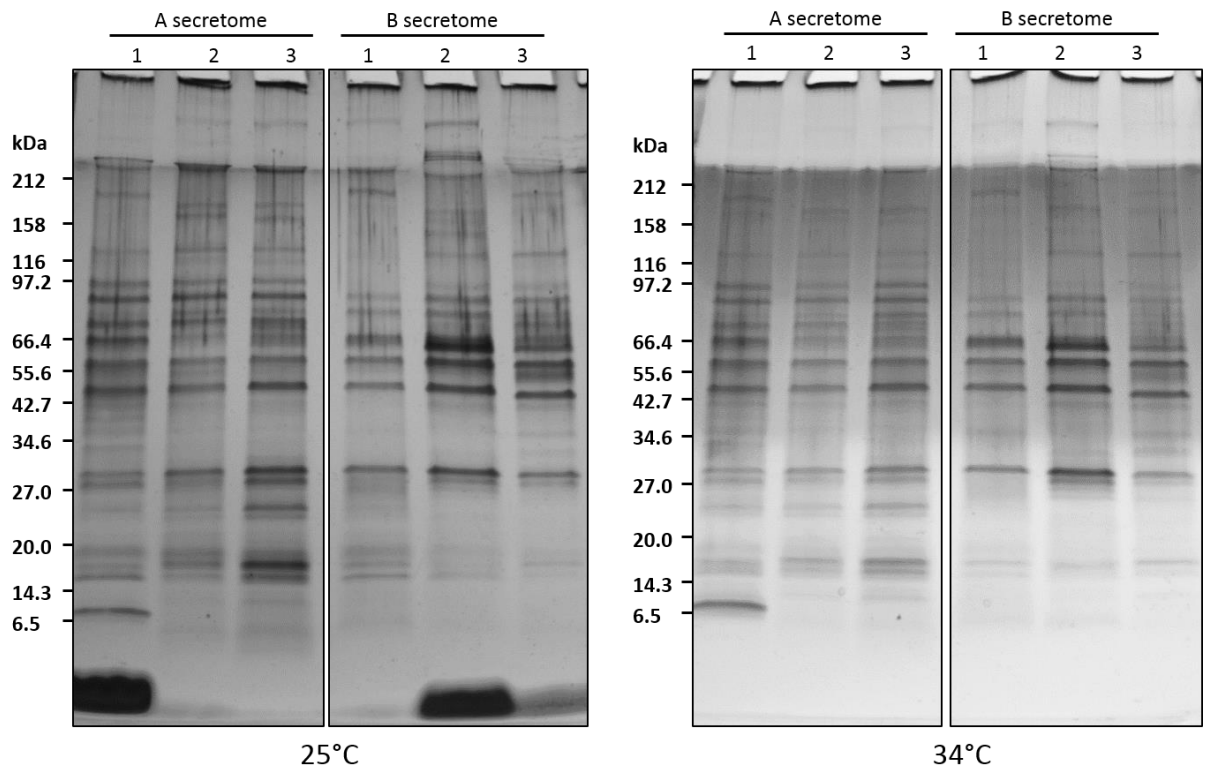


Figure 5-18 SDS-PAGE separation of *L. panamensis* promastigote secretome. 0.13 μ g of each secretome sample was loaded per lane of a 4-20% polyacrylamide gel and silver stained. A secretome isolated from parasites from self-healing infections, B secretome isolated from parasites from chronic infections.

Using SDS-PAGE and silver staining, reproducible visual differences between secreted proteins in the self-healing and chronic groups are clear (Figure 5-18). These differences were investigated in more detail by aligning the profiles of each lane in graphical format (Figure 5-19) where proteins 1 and 6 - 10 were visible as being more abundant in Chr and 2-5 and 11 - 15 are noticeably downregulated in the Chr. A similar pattern is evident in the secretome samples from the 34°C incubation (Figure 5-20), where the central bands 6 & 7 are upregulated in Chr

and bands 8 & 9 are downregulated in Chr. No striking differences were observed at this stage between the secretome of parasites incubated at 25 and 34 °C.

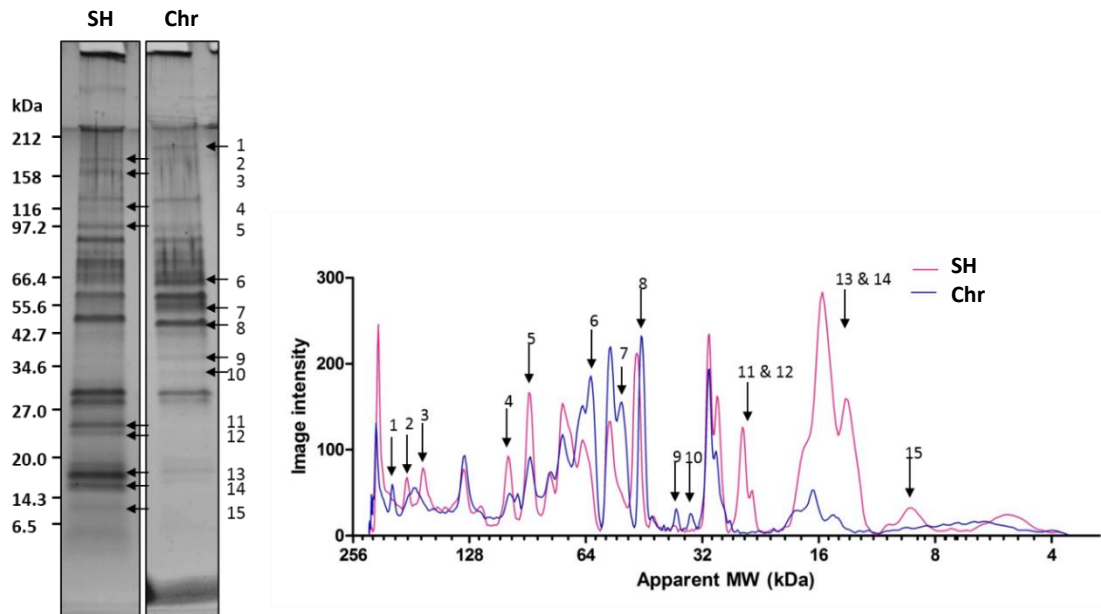


Figure 5-19 Lane profiling of *L. panamensis* 25°C secretome. A representative lane from each group was selected and the band intensities profiled using ImageJ software and plotted using Prism.

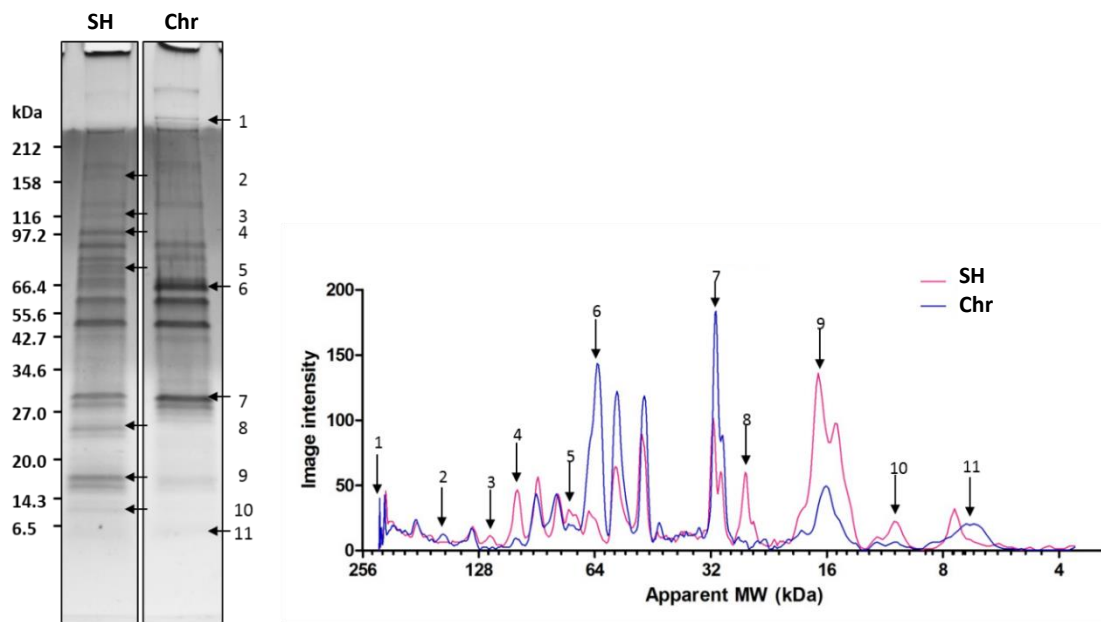


Figure 5-20 Lane profiling of *L. panamensis* 34°C secretome. One lane from each group was selected and the band intensities profiled using ImageJ software and plotted using Prism.

5.3.6 Quantitative analysis of the *L. panamensis* secretome using isobaric peptide tagging

After visual confirmation of the integrity of the samples and the identification of differences between the groups, TMT labelling was used for relative quantitation to determine the differences in protein abundance between the parasites of the two disease outcomes. The full list of protein identifications and quantitation for the *L. panamensis* promastigotes can be found in Supplementary Data II.

Using clustering analysis on the full list of protein identifications and their corresponding quantitation values, the three biological replicates of **Chr** and **SH** samples cluster together and shows that the secretomes of the two cells lines are quantitatively distinct for both 25°C and 34°C secretome collection (Figure 5-21, Figure 5-23). The heat maps in Figure 5-22 and Figure 5-24 demonstrate both the level of change in abundance and the reproducibility of the biological replicates for the 25°C and 34°C samples, respectively. A total of 12 proteins were reproducibly up or down-regulated with a p-value of ≤ 0.05 , and exhibiting a fold change of $\geq \pm 1.5$ in the 25°C samples (Figure 5-22). A total of 16 proteins were reproducibly up or down-regulated with a p-value of ≤ 0.05 , and exhibiting a fold change of $\geq \pm 1.5$ in the 34°C samples (Figure 5-24). Each protein is assigned a colour based on the scale of Euclidean distance.

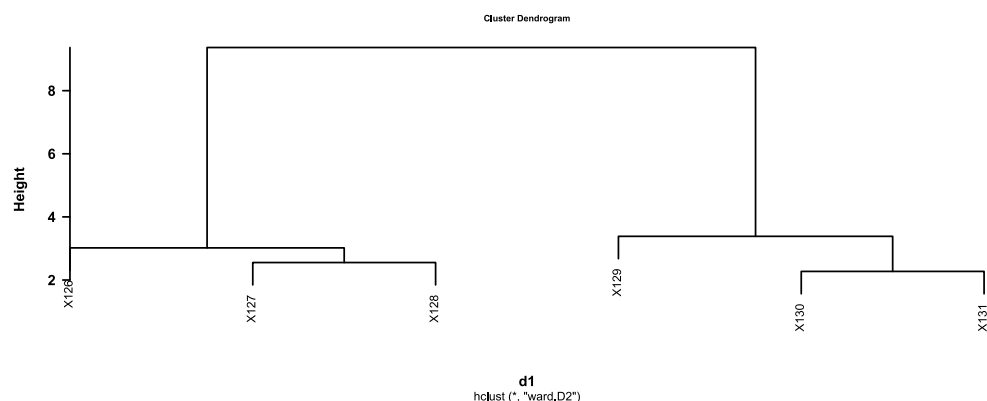


Figure 5-21 Cluster dendrogram of *L. panamensis* promastigote quantitative 25°C secretome data comparing replicates collected from self-healing parasites and from chronic parasites. Created in RStudio using Euclidean distance to show the similarity or dissimilarity between observations. The replicates for each of the two sample types cluster together. Labels X126-X131 denote the quantitation channels for each TMT reporter tag. X126-128 are self-healing samples 1-3 and X129-131 are chronic samples 1-3. *L. panamensis* 25°C self-healing vs chronic 0.58 1.3.

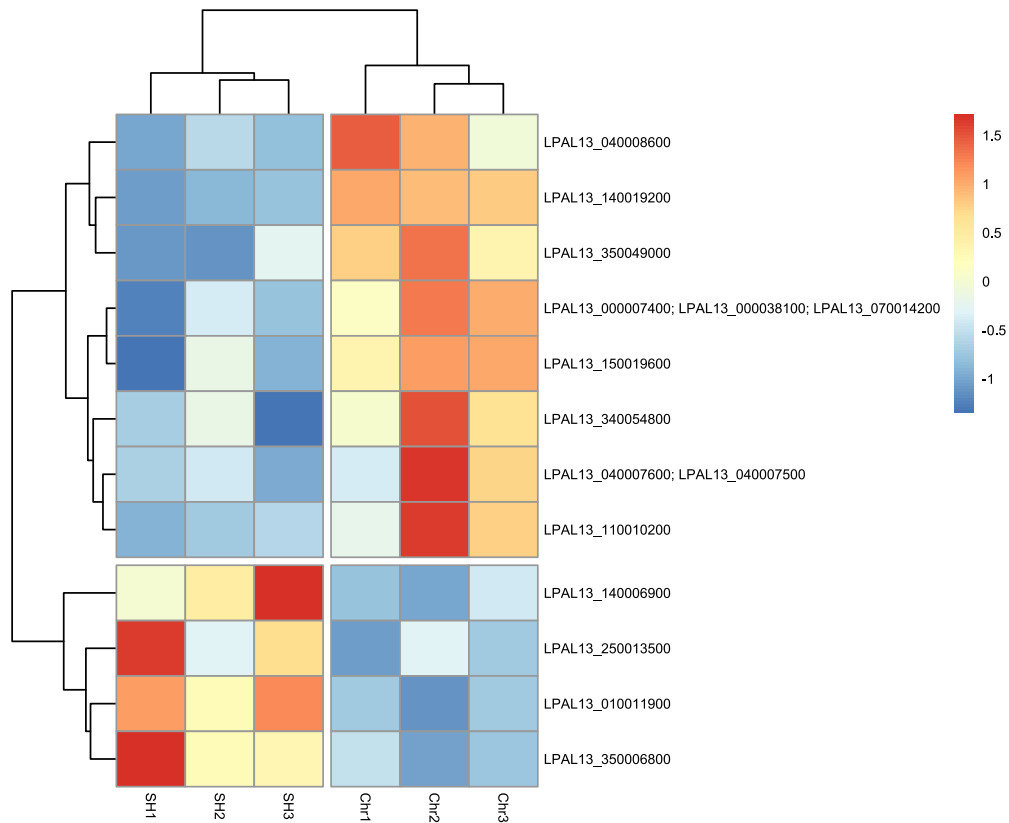


Figure 5-22 Heat map of quantitative differences between secreted proteins of *L. panamensis* parasites causing self-healing and chronic disease, collected at 25°C. Colour denotes value assigned to distance. Columns are the samples and rows are the quantitated proteins *L. panamensis* 25°C self-healing vs chronic 0.58 1.3.

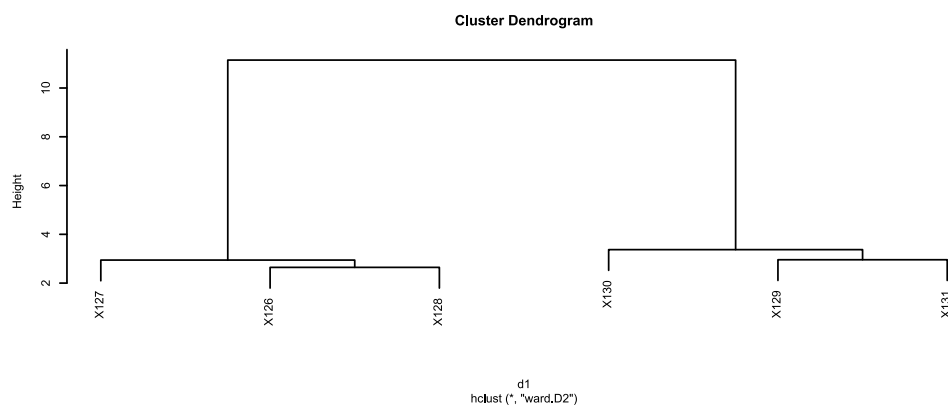


Figure 5-23 Cluster dendrogram of *L. panamensis* promastigote quantitative 34°C secretome data comparing replicates collected from self-healing parasites and from chronic parasites. Created in RStudio using Euclidean distance to show the similarity or dissimilarity between observations. The replicates for each of the two sample types cluster together. Labels X126-X131 denote the quantitation channels for each TMT reporter tag. X126-128 are self-healing samples 1-3 and X129-131 are chronic samples 1-3 *L. pan.* 34°C Chr/SH 0.58 1.3.

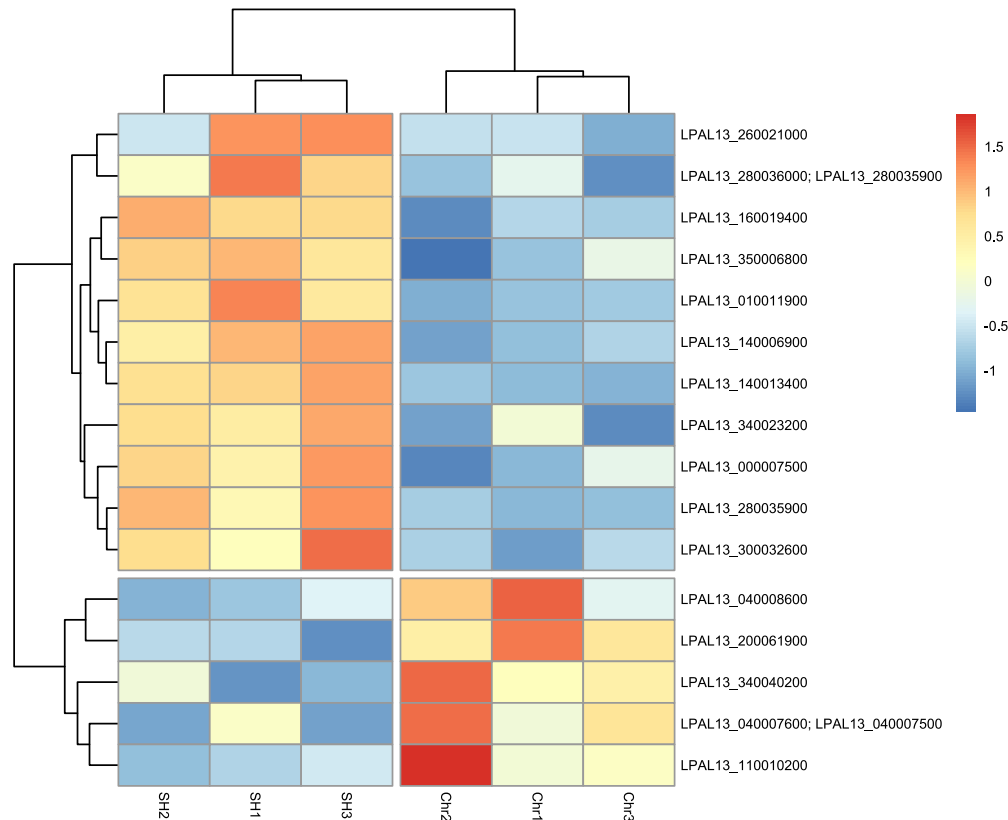


Figure 5-24 Heat map of quantitative differences between secreted proteins of *L. panamensis* parasites causing self-healing and chronic disease, collected at 34°C. Colour denotes value assigned to distance. Columns are the samples and rows are the quantitated proteins *L. pan.* 34°C Chr/SH 0.58 1.3.

Figure 5-25 shows the spread of all the confidently identified proteins over the three biological repeats with the differences in abundance shown between chronic and self-healing patients. Figure 5-26 shows the same for 34°C. In each of the data sets there are around 10 proteins reliably up or downregulated in chronic compared to self-healing. Table 5-4 shows the data/detail of the secreted proteins from parasites incubated at 25°C identified by LC-MS/MS with a differential abundance ratio of over or under 0.58 or -0.58, respectively.

Table 5-5 shows the secretome from parasites incubated at 34°C, and selected with the same criteria. Temperature does not appear to play a major role in altering the content of the secretome as there were very few differences between the two sample sets.

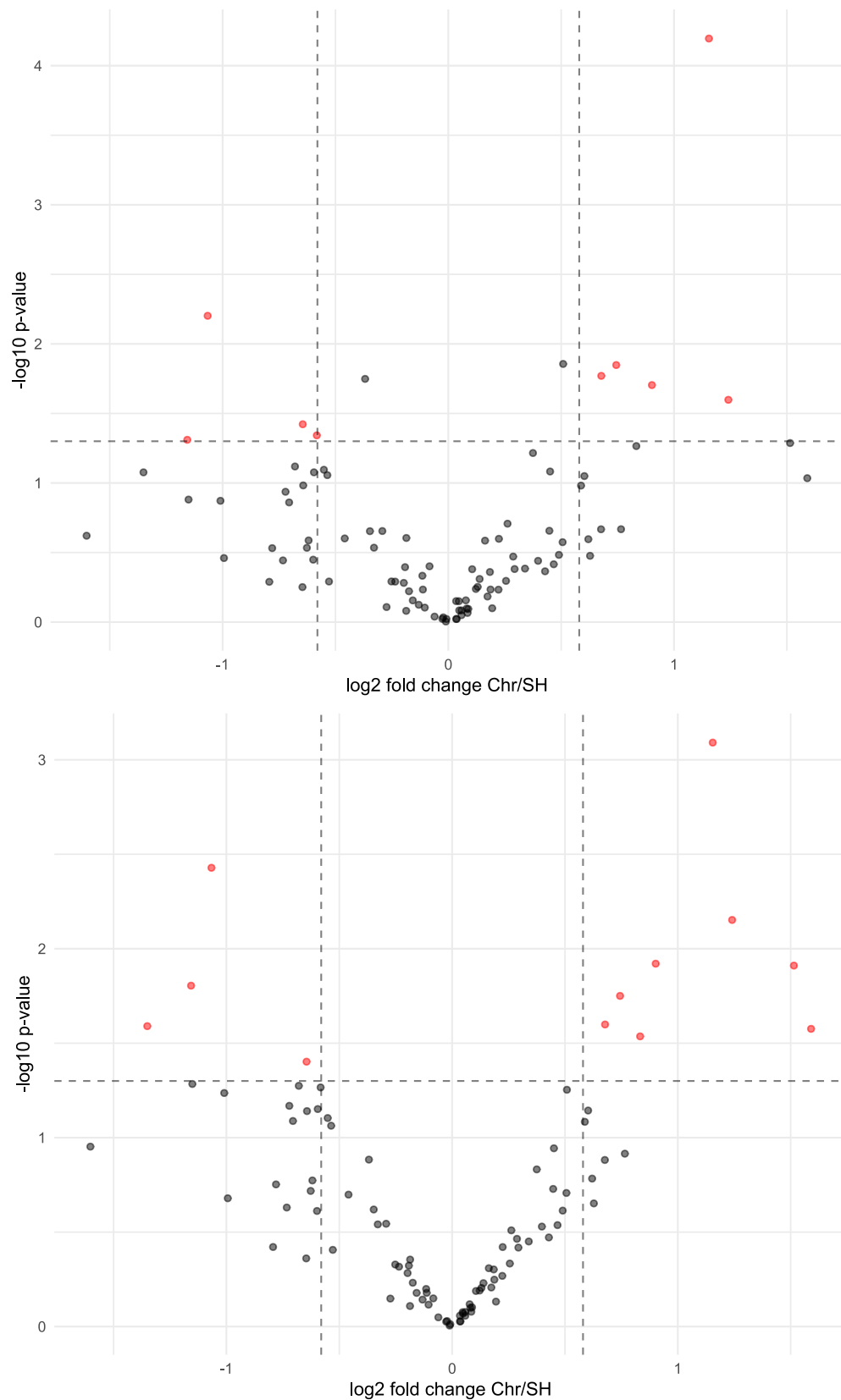


Figure 5-25 Volcano plots of 6-plex TMT™ quantitation of *L. panamensis* promastigote secretome collected from Chronic (Chr) and Self-healing (SH) disease-causing parasites at 25°C. (a) Volcano plot of the fold change of each protein in Chr and SH samples against the p-values of the sample variability using standard *t*-tests. (b) Reanalysis of p-values using Kammers *et al.* (D'Angelo *et al.* 2017; Kammers *et al.* 2015) method of using moderated *t*-statistics from the empirical Bayes procedure LIMMA. Statistical testing performed and figures made in RStudio. *L. panamensis* secretome 25°C volcano plot ord (top) and modified p-values. $p < 0.05$, FC 1.5 Proteins in red are significantly upregulated or downregulated in chronic secretome compared to self-healing, with a fold change of ± 1.5 and p -value of ≤ 0.05 .

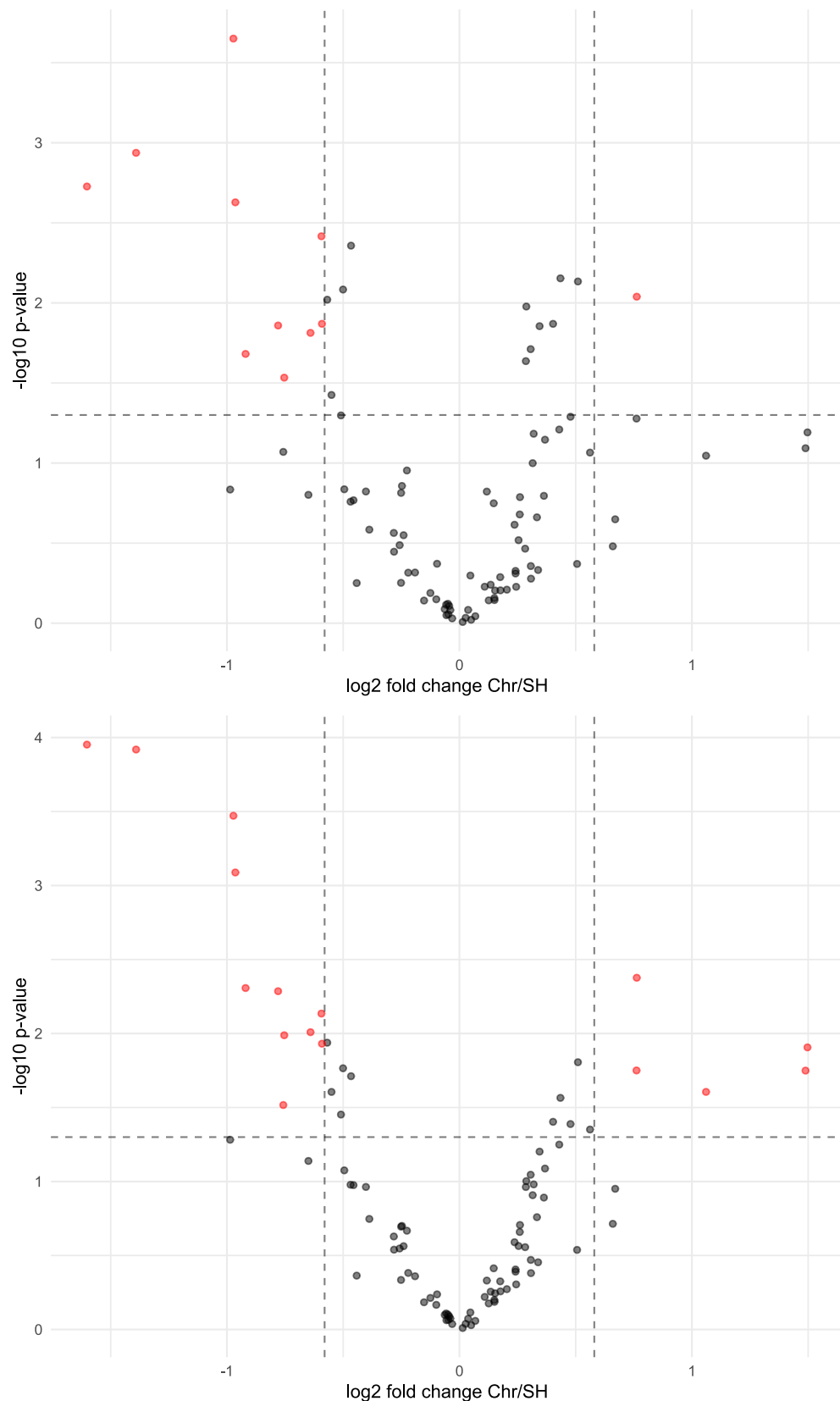


Figure 5-26 Volcano plots of 6-plex TMT™ quantitation of *L. panamensis* promastigote secretome collected from Chronic (Chr) and Self-healing (SH) disease-causing parasites at 34°C. (a) Volcano plot of the fold change of each protein in Chr and SH samples against the p-values of the sample variability using standard t-tests. (b) Reanalysis of p-values using Kammers et al. (D'Angelo et al. 2017; Kammers et al. 2015) method of using moderated *t*-statistics from the empirical Bayes procedure LIMMA. Statistical testing performed and figures made in RStudio. *L. panamensis* secretome 34°C volcano plot ord (top) and modified p-values. $p < 0.05$, FC 1.5 Proteins in red are significantly upregulated or downregulated in chronic secretome compared to self-healing, with a fold change of ± 1.5 and p-value of ≤ 0.05 .

Table 5-4 *L. panamensis* secretome proteins significantly up- or down-regulated in parasites from chronic infection compared to self-healing infection. Incubation at 25C, significant proteins <0.05 pvalue and changing greater than 1.5 fold.

Accession	Description	Log ₂ FC	FC	p-value
LPAL13_040007600; LPAL13_040007500	surface antigen-like protein	1.590333	3.011188451	0.02655
LPAL13_110010200	aminopeptidase, putative	1.514333	2.856667254	0.012281
LPAL13_040008600	beta-fructofuranosidase, putative	1.240667	2.36307759	0.00704
LPAL13_140019200	inositol-3-phosphate synthase	1.154667	2.2263293	0.000811
LPAL13_000007400; LPAL13_000038100;				
LPAL13_070014200	hypothetical protein, conserved	0.902	1.868654694	0.011998
LPAL13_340054800	proteasome alpha 1 subunit, putative	0.833	1.781385801	0.029099
LPAL13_350049000	hs1vu complex proteolytic subunit-like, threonine peptidase, Clan T(1), family T1B	0.744	1.674812975	0.017769
LPAL13_150019600	proliferative cell nuclear antigen (PCNA), putative	0.677667	1.599551009	0.025176
LPAL13_350006800	elongation factor 2	-0.645	1.563739286	0.039623
LPAL13_010011900	eukaryotic initiation factor 4a, putative	-1.06633	2.09409951	0.003728
LPAL13_140006900	Thioredoxin-like, putative	-1.15667	2.229422424	0.015686
LPAL13_250013500	eukaryotic initiation factor 5a, putative	-1.35067	2.550305363	0.025692

Table 5-5 *L. panamensis* secretome proteins significantly up- or down-regulated in parasites from chronic infection compared to self-healing infection. Incubation at 34C significant proteins <0.05 pvalue and changing greater than 1.5 fold.

Accession	Description	Log ₂ FC	FC	p-value
LPAL13_040007600; LPAL13_040007500	surface antigen-like protein	1.488667	2.806295	0.017811
LPAL13_110010200	aminopeptidase, putative	1.060667	2.085895	0.024808
LPAL13_200061900	small myristoylated protein-3, putative	0.762667	1.696624	0.004201
LPAL13_340040200	structural maintenance of chromosome (SMC) family protein, putative	0.761667	1.695448	0.017767
LPAL13_350006800	elongation factor 2	-0.59133	1.506639	0.011721
LPAL13_280035900	heat-shock protein hsp70, putative	-0.59367	1.509077	0.007335
LPAL13_300032600	hypothetical protein, conserved (T. brucei PFR component, putative)	-0.64067	1.559049	0.009798
LPAL13_280036000;				
LPAL13_280035900	heat-shock protein hsp70, putative	-0.75367	1.686073	0.010274
LPAL13_260021000	thimet oligopeptidase, putative	-0.75767	1.690754	0.030429
LPAL13_000007500	paraflagellar rod protein 1D, putative	-0.78	1.717131	0.005178
LPAL13_340023200	60S ribosomal protein L5, putative	-0.92	1.892115	0.00493
LPAL13_010011900	eukaryotic initiation factor 4a, putative	-0.964	1.950711	0.000816
LPAL13_140013400	small myristoylated protein-3, putative	-0.97233	1.962011	0.000338
LPAL13_160019400	paraflagellar rod protein 1D, putative	-1.391	2.622604	0.000121
LPAL13_140006900	Thioredoxin-like, putative	-1.60233	3.03634	0.000112

5.4 Discussion

Further insight into the role proteins play in parasitic diseases is crucial. It is already understood that *Leishmania* parasites secrete numerous proteins which are implicated in the disease pathophysiology (Diniz Atayde *et al.* 2016). Here we present a quantitative study looking at differences in these secreted proteins between different isolates responsible for varying disease phenotypes and provide crucial insight into the roles these may proteins play.

5.4.1 Quantitative analysis using isobaric tags

TMT labelling has been shown to be a valuable tool in quantitative proteome analysis (Ahrné *et al.* 2016; Thompson *et al.* 2003). It allows for the quantitation of proteins in a complex biological sample and when coupled with high resolution mass spectrometry and analytical data analysis software, employing statistical robustness to fold changes and subsequent results, we can gain confidence in our findings and come to novel conclusions, inferring functionality of the role proteins play in disease pathophysiology.

Although a powerful and extremely useful approach, TMT labelling has the disadvantage of ratio distortion with isobaric multiplexing (Ahrné *et al.* 2016). Contaminating tagged ions co-elute or co-fragment with the fragments of interest which adds to the overall intensity of the tag at certain times therefore potentially skewing results and giving false positives. Precursor isolation window widths were therefore set to 1.0 m/z , to obtain the best trade-off between ratio compression and identification, in agreement with previous studies (Ahrné *et al.* 2016; Savitski *et al.* 2011).

5.4.2 Statistical testing for analysis of quantitative proteomic data

It is recognised that detecting statistically significant changes in protein abundance is a fundamental task in quantitative mass spectrometry experiments. This includes analyses and comparisons of treated to untreated cells, wild types to mutants, or samples from diseased and non-diseased subjects. Statistical approaches and analyses of comparative experiments are typically based on standard 2-sample t-tests (Kammers *et al.* 2015). These tests typically analyse and compare the

measured relative or absolute abundances for each peptide or protein across the differing conditions of interest. Small sample sizes, however, encourage uncertainty in the sample variance estimates and can subsequently reduce the power of the analysis. In extreme cases, results can be falsely rejected based on large sample variance or conversely, small fold changes might be accepted and declared statistically significant based on small sample variance (Kammers *et al.* 2015). Statistical models such as the moderated *t*-test have to be applied to take into account higher variance with higher fold changes, thus making these more significant, and lower variance with lower fold changes, thus making these less significant (Smyth 2004). As described in the introduction of this chapter, D'Angelo *et al.* evaluated the application of GLM; LIMMA, which is popular in microarray data analysis but not commonly applied in proteomic analysis; and mixed models, to TMT-tagged proteomic data, and concluded LIMMA to have the best overall statistical properties, regardless of the normalisation method (D'Angelo *et al.* 2017).

We therefore utilised R scripts from (Kammers *et al.* 2015) and used a two-stage analysis, reducing the data to independent summary measures of the proteins and performing the statistical analysis using the independent measures. Here, in a modification to Kammers *et al.* data analysis, proteins identified by only one peptide were retained in the secretome analyses due to the nature of the sample. Not only is the secretome a small fraction of the whole proteome, we are also searching for the presence of rare proteins. We are using data-dependent acquisition (DDA) and therefore will only see the top *n* peptides in any particular scan, therefore rare proteins may only be identifiable by one peptide.

5.4.3 *L. mexicana* attenuated parasites display delayed progression through the life cycle

The first parasite phenotype used in the comparative studies was an attenuated line of *L. mexicana*. These parasites were attenuated under gentamicin pressure *in vitro*, subsequently losing the ability to sustain infection in bone marrow-derived macrophages and to induce cutaneous lesions in BALB/c mice (Daneshvar *et al.* 2003a). However, the mechanism of attenuation is unknown.

Although the growth rates of WT and attenuated (H-line) *L. mexicana* promastigotes were similar in axenic culture, the attenuated parasites exhibited slightly delayed growth as axenic amastigotes. Metacyclogenesis is characterised phenotypically by a reduction in cell length and width (Wheeler *et al.* 2011) therefore we can infer that the H-line are either not undergoing the transformation to metacyclic stage parasites as quickly as the WT or are not transforming as efficiently due to differences in cell size. Consequently, the rate at which the parasites differentiate into amastigotes is also affected, which is evident in the difference in cell size at days 1 and 2 after stimulus, with the H-line displaying slower growth as amastigotes. The major difference between the WT and H-line parasites appears to be at the metacyclic stage. This could indicate that the attenuation occurs in the processes which establish infection. When analysing the secretome samples it is seen that there were far fewer differences between the two cell lines in the amastigote stage.

5.4.4 Comparative analysis of the secretome of *L. mexicana* wild type and attenuated parasites

In addition to gaining insight into the mechanisms of attenuation in the H-line parasites, our aim of this comparative analysis was to reveal secreted proteins with potential roles in the virulence of *L. mexicana*. We undertook a quantitative analysis to not only detect qualitative differences, but to compare the relative abundance of the proteins secreted by these two cell lines.

Unfortunately, due to the low abundance of the secretome and difficulties in collecting large amounts of protein whilst minimising cell stress and inadvertent cell death, the identification of the modulated proteins highlighted in the DiGE analysis was difficult. Normally, a preparative gel is run in parallel to a DiGE gel with a higher amount of protein and no dyes. The spot patterns are then matched between the gels using DeCyder™ software (GE Healthcare), and any protein spots of interest identified in the DiGE gel can be picked from the preparative gel and analysed by mass spectrometry (Westermeier *et al.* 2008). However, insufficient secretome sample was available to run a preparative gel in addition to a DiGE gel. Protein spots of interest were instead picked from the DiGE gel to attempt MS identification, however this was unsuccessful. Thus, a gel-free quantitative approach was undertaken.

We can infer the role of the secretome in cell survival and infection outcome by assigning identified proteins their putative functional role. Additionally, previous studies have implicated several of these proteins in the pathology of the disease. Proteins up or downregulated by ≥ 1.5 were categorised by their putative ontologies which were assigned by their known functional roles according to gene ontology annotations on the TriTryp database (Aslett *et al.* 2010) and to other studies. The ontologies were then grouped by percentage of the secretome with this function and by up or downregulation in the attenuated samples, as shown in Figure 5-27.

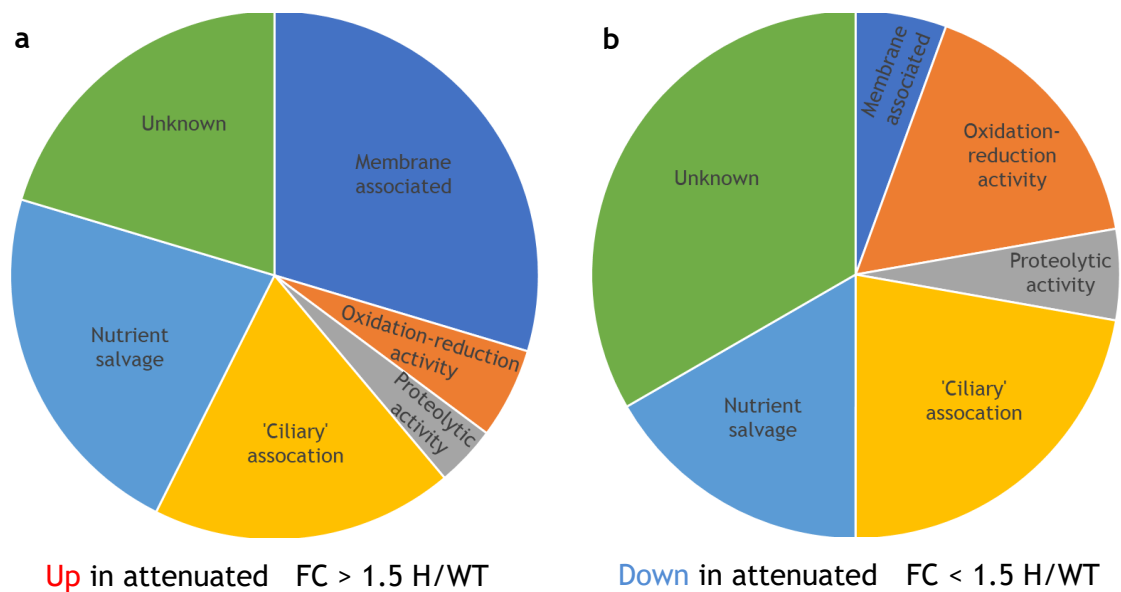


Figure 5-27 Pie chart indicating the percentage of the *L. mexicana* promastigote secretome with certain activity or location associations. (a) Functional categories of proteins upregulated in the secretome of attenuated parasites (H). (b) functional categories of proteins downregulated in attenuated parasites (H) versus wild type (WT).

An increase in proteins associated with vesicle trafficking and membrane proteins was observed in the H-line. This suggests a dysregulation of vesicle trafficking and exosome budding. This is not to say production of vesicles is not associated with virulence, but rather that vesicular dysregulation, in combination with delayed progression through the life cycle, suggests that the attenuated parasites are readily recognised in the host cell and do not have the tools to withstand anti-microbial attack before they can fully differentiate to amastigotes.

In addition, there is a downregulation in secretion of the antioxidants superoxide dismutase, trypanothione peroxidase and thioredoxin-like protein in the H-line compared to wild-type. This is consistent with previous findings by Daneshvar *et al.* who undertook a comparative analysis of the proteome of the WT and H-line.

They found differential expression of a number of isoforms of trypanothione peroxidase, a reduction in trypanothione reductase activity and trypanothione-dependent peroxidase activity in the H-line and significant sensitivity of the H-line to hydrogen peroxide in comparison to the wild type (Daneshvar *et al.* 2012). This demonstrates the crucial role of a strong and immediate antioxidant defence to the survival of *Leishmania* upon entry to the host cell (Mittra *et al.* 2013; Olmo *et al.* 2015). Upregulation of iron superoxide dismutase has also been shown to trigger the differentiation of promastigotes to amastigotes (Mittra *et al.* 2017), therefore a reduction of this protein in attenuated parasites may delay their differentiation to amastigotes.

Crucially, a downregulation in the secretion of GP63 is also observed in the attenuated line. GP63 has been shown to play many roles in the disruption of signalling in the macrophage, as it can gain access to the macrophage cytosol (Gómez *et al.* 2009b). Overall host translation and protein synthesis is downregulated upon infection with *Leishmania* (Jaramillo *et al.* 2011), which occurs through a variety of mechanisms mediated by GP63. For example cleavage of c-Jun, a component of AP-1 transcription factor (Contreras *et al.* 2010); cleavage and thus activation of protein tyrosine phosphatases, preventing JAK-STAT signalling (Gómez *et al.* 2009b); and cleavage of mTOR, which activates the downstream translational repressor 4E-BP1 (Jaramillo *et al.* 2011). Our results further demonstrate the importance of GP63 to the virulence of the parasite in the host as its downregulation appears to be detrimental to the survival of the H-line in the macrophage. Further to the suppression of host translation by GP63, the secretion of a *Leishmania* eukaryotic translation initiation factor (LeTIF) was also downregulated in the H-line. Interestingly, expression of one copy of an *L. infantum* LeTIF in yeast interfered with the translation machinery, resulting in growth inhibition (Barhoumi *et al.* 2006). Therefore secretion of LeTIF may also play a role in disruption of host translation, and therefore parasite virulence.

LeTIF has also been shown to induce the secretion of IL-10 by host cells, directing the immune response towards a Th2, anti-inflammatory response, a response which favours parasite persistence (Carrillo *et al.* 2018). This, coupled with our observation of LeTIF downregulation in the H-line, is consistent with the findings of Daneshvar *et al.*, who found that infection with the H-line directed the immune

system towards a Th1 response in mice (Daneshvar *et al.* 2003b). However, LeTIF can also induce the secretion of IL-12 in addition to IL-10 (Barhoumi *et al.* 2013), IL-12 stimulating a Th1 response, and so the complex interplay between the parasite and host is not altogether straightforward and doubtless relies on the presence of a number of different factors secreted by the parasite.

GP63 has also been implicated in playing a role in exosomal protein sorting in *Leishmania* (Hassani *et al.* 2014). Analysis of exosomes from GP63 knock-out (KO) parasites showed major differences between the proteomic content of KO and WT exosomes. KO exosomes contained higher percentages of hypothetical and transmembrane proteins, with higher percentages of proteins containing putative GP63 cut-sites in the WT exosomes (Hassani *et al.* 2014). Our results are consistent with these findings as the attenuated parasites, which show a downregulation in GP63, also display an increase in the secretion of membrane-associated proteins (Figure 5-27a).

5.4.5 *L. panamensis* secretome

The second phenotype investigated was parasites isolated from patients with chronic (Chr) and self-healing (SH) lesions. These *L. panamensis* parasites were isolated in collaboration with CIDEIM in Cali, Colombia. This comparison was initiated to indicate which proteins in the secretome may play a role in the exacerbation of the disease. For example, causing the excessive inflammation and uncontrolled immunopathology that is typically seen in chronic cutaneous leishmaniasis (Navas *et al.* 2014). The difficulty with the immune responses to *L. panamensis* cutaneous disease is that the traditional Th1/Th2 dichotomy, where upregulation of the Th1 response results in parasite clearing, does not always apply.

From the quantitative proteomic results, in the chronic samples we observe a down-regulation of proteins such as elongation factor 2 and eukaryotic initiation factors 4a and 5a, which have been shown to stimulate a mixed immune response in the host, with stimulation of IL-10 and IL-12 (Barhoumi *et al.* 2013). A down-regulation of receptor activated kinase C is also seen, implicated as an immunomodulatory protein used as a vaccine candidate (Sinha *et al.* 2013).

There is an up-regulation of aminopeptidase and threonine peptidase in the chronic samples, shown to result in exacerbation of the inflammatory response, and enhancement of macrophage phagocytic activity (Goto *et al.* 2011). Up-regulation of surface antigen-like protein is also observed in chronic parasites. Up-regulation of the secretion of SMP-3 is seen in Chr parasites. Little is known about SMP-3 in comparison to SMP-1, which is known to play roles in normal flagellar function (Tull *et al.* 2010), and as a potent plasminogen binding protein found in *Leishmania* extracellular vesicles (Figuera *et al.* 2013). However, reduction of SMP-3, amongst other proteins, was observed in parasites with loss of virulence, implicating this form of SMP as a potential virulence factor (Magalhães *et al.* 2014).

The increase in temperature may trigger degradation of the flagellum, as paraflagellar rod proteins are seen in the secretome of the 34°C parasites but not the 25°C parasites (Suppl II). Few other differences were observed between 25°C and 34°C, with the differentially regulated proteins between Chr/SH remaining constant between the two independent experiments. We therefore reject the hypothesis that temperature alone alters the proteins present in the secretome. This analysis did not take into account the total amount of protein secreted at each of the different temperatures, however. This has been shown previously to affect the amount of protein secreted but not necessarily the protein content (Hassani *et al.* 2011). Therefore, this could be investigated in more detail in future. Another future study looking at environmental factors would be to try a lowered pH as this appeared to have an effect on the secreted proteins when studied in *L. major* (Chenik *et al.* 2006).

5.5 Summary

Here, the overall aim was to take methods developed for isolating and analysing the secretome of *Leishmania* parasites and apply them to an attenuated *L. mexicana* parasite line, and to clinical parasite isolates. We aimed to investigate the role of the secretome in the establishment of infection and parasite survival inside the host cell. We hypothesised that there is a significant difference in the parasite secretome between wild type and attenuated *L. mexicana* promastigotes and amastigotes.

These results highlight significant differences in the parasite secretome between wild type and attenuated *L. mexicana* promastigotes. From the differential regulation of secreted proteins from these two phenotypes we can conclude that secretion of antioxidant protein is important for virulence of the promastigote stage in the host cell. Furthermore, our results further substantiate the role of GP63 as a virulence factor. And may also point to its putative role as a regulator of exosomal cargo.

We aimed to investigate the potential functional role of the *Leishmania panamensis* secretome in the outcome of the disease. Through comparative analyses looking at parasites of the same species that establish different disease phenotypes. We hypothesised that as other studies point to the differing disease outcomes being parasite-mediated, there may be a significant difference in the parasite secretome between isolates from chronic cutaneous *Leishmaniasis* compared to isolates from self-healing cutaneous *Leishmaniasis*. We identified modest but consistent differences in the secretomes of the two isolates. Many of the differentially regulated proteins have little-known functions in the *Leishmania* secretome, particularly in the complex immune responses associated with chronic cutaneous *Leishmaniasis*. However, the upregulation of peptidases in the chronic isolates may play a role in local inflammatory responses.

Here we have provided crucial insight into *Leishmania* survival and further implicated the secretome in virulence and disease progression. *Leishmania* lack an adequate vaccine and leishmaniasis an appropriate treatment therapy. Results here may be used for vaccine targets and provide a basis for future secretome analysis.

Chapter 6 Concluding Remarks

This thesis presents a comprehensive analysis of the secretome of *Leishmania* promastigotes and amastigotes. Here, we demonstrate implementation and testing of a secretome collection method. The method was successfully adapted from previous protocols to the study of promastigotes and amastigotes. Analysis of the secretome compared to the whole cell lysate proteome provided validation and confidence of the method, demonstrating that it is the secretome that has been extracted and analysed. This enabled comparative analyses between the secretome of promastigotes and amastigotes. In addition, we have shown the method to be applicable both to laboratory strains and to clinical isolates, allowing for conclusions in the secretomes role in disease phenotype to be made. Quantitative analyses were implemented for the analysis of wild-type and virulence-attenuated parasites, and to parasites causing chronic and self-healing cutaneous disease in patients.

6.1 Change in environmental niche is accompanied by life cycle progression and alterations to protein secretion

Leishmania inhabit contrasting environments in the insect vector and mammalian host. To cope with challenges of these different conditions the parasite both adapts its form and modifies its niche. We demonstrated that the promastigote secretome contains a myriad of membrane proteins, plasminogen binding proteins, redox proteins and other proteins which appear to have nutritional function. Here, we have shown that amastigotes show an increase in the proportion of protein degradation, redox proteins, and chaperones/stress-induced proteins in their secretome. We have further shown the abundance of GP63 in the amastigote secretome, which is a different form to promastigote GP63. In addition changes in the abundance of MIF are observed.

Studies presented here are focused on *in vitro* cell culture models. Future work is required to improve these models to further mimic *in vivo* conditions but still provide a controlled, defined environment. More information may be gleaned from the addition of factors to the culture which better replicate the stresses

encountered by the amastigotes *in vivo*. For example addition of superoxide or hydrolases may stimulate secretion of proteins in amastigotes, akin to the effects of stimulation by temperature increase in promastigotes (Atayde *et al.* 2015; Hassani *et al.* 2011).

6.2 Changes in secretion are associated with virulence

Developed methods were applied to parasites with differing host morphology and disease phenotypes. This allowed the consolidation of the secretome to a selection of highly influential proteins.

Here, we note a downregulation of antioxidants in virulence-attenuated parasites compared to wild-type parasites, highlighting their role in virulence. Antioxidants including FeSOD, trypanothione peroxidase and thioredoxin-like protein were shown to be down-regulated. The downregulation of GP63, tetratricopeptide repeat protein, translation initiation factor 3 and polyadenylate binding protein 2 are also associated with the loss of virulence. Analysis of the total percentage of up and down regulated proteins grouped together according to functionality reveals functional differences between the secretomes. The largest differences between the up and down regulated proteins have roles in membrane association and oxidation-reduction activity.

Further, we highlight the secretomes role in the exacerbation of inflammatory mediators in chronic disease. Surface antigen-like protein was resolved from analyses presented here and was found to be upregulated in parasites derived from chronic manifestations. In addition, aminopeptidase was too found to be upregulated in the same parasite line. Overall, these results provide evidence and implications for niche modification in disease outcome, inducing disease phenotype through inflammation. Identification of these differentially regulated factors narrows the secretome down to a few key proteins for further study.

First of all, further replicates are required. Results presented here present a relatively small sample set but robust biological replicates were utilised, using parasites isolated from different patients with the same condition. However, technical replicates of the process as a whole would be very valuable in confirming the results presented here and providing method validation. These replicates would

be of particular value due to the difficulties in culturing field isolates. Their viability in axenic culture is lower than that of the laboratory strains. Therefore, additional replicates are required to solidify the inclusion of proteins to the secretome.

6.3 Further analyses of the secretome as a whole

The physical differences between the secretome of promastigotes and amastigotes are intriguing but require further analysis. Further research and analysis into the amastigote secretome further would represent future work here. The observation of a viscous gel-like pellet visible when precipitating the amastigote secretome with organic solvents or TCA and an insoluble component to the amastigote secretome upon freeze-thawing could reveal novel proteins or molecules excreted by *Leishmania*.

Through the use of attenuated parasites and parasites with differing disease phenotypes, we have been able to indicate potential roles for various secreted proteins in the host. As a next step to address the functionality of the secretome, we propose various experiments to investigate the host cell response to the secretome investigating the following. Application of a wild-type secretome could prime host cells and influence the survival of an attenuated parasite. We would investigate how the host cell response differs in response to the secretome from: promastigotes, amastigotes, attenuated cells, chronic disease inducing parasites, and self-healing disease parasites. Analyses could include qPCR array plate looking at cytokine/chemokine response or an ELISA based methodology as previously described (Pollock *et al.* 2003).

In addition, potential exosomal proteins were identified in this study. Therefore, isolation of exosomes using ultracentrifugation and classification of *bona fide* exosomes by electron microscopy, differential digestion using detergents and trypsin, and density gradient purification would corroborate and increase the evidence for the production of exosomes in *Leishmania*. Crucially, this would extend these analyses to the amastigote stage. What is known about the mechanisms of secretion in *Leishmania* is still largely based on confirmation of the presence of secretory organelles and multivesicular bodies (McConville *et al.* 2002).

The processes involved in and the locations of physical egress of exosomes, however, remain to be elucidated. Exosomal release from the flagellar pocket is a previously presented hypothesis in kinetoplastids, with evidence of the production of nanotubes which bud off producing vesicles from *T. brucei* (Szempruch *et al.* 2016b). However, images of *Leishmania* show vesicles budding from or associated with various regions on the cell surface and flagella (Hassani *et al.* 2011). In support of this, our data demonstrate the presence of numerous membrane proteins in the promastigote secretome, both cell body and flagellar membrane-associated. The lack of membrane proteins in the amastigote secretome requires further investigation as this, coupled with the relatively small number of proteins identified in the secretome, could indicate that adjustments are required to the incubation time during the secretion assay.

To summarise, further work into the secretome as a whole and its role in the host cell is required. Here we provide a discovery study looking at the secretome of differing *Leishmania* cell lines and draw initial conclusions of their secretomes role in disease.

6.4 Proposal of protein candidates for further analyses

In addition to characterising the role of the secretome in the cell biology of the parasite, the ultimate goal in this discovery project is the identification of potential candidates for therapeutic intervention or vaccination. Here, we have begun with characterising the secretome as a whole, looking at global analysis of the secretome using shotgun proteomic approaches, then narrowing the proteome down based on functionality using comparative analyses. Based on the comparative analyses and placing in literature, we have identified some promising candidates for further analysis. These proteins would provide the basis of future work to move forward and go on for further analysis.

One methodology that would have been useful in looking at specific protein function is loss-of-function screens using RNA interference (RNAi). Unfortunately, RNAi cannot be used in *L. mexicana* due to the lack of RNAi machinery in this species (Lye *et al.* 2010). Traditional methods of genetic manipulation are time consuming and complicated by multiple gene copies and variable ploidy (Cruz *et*

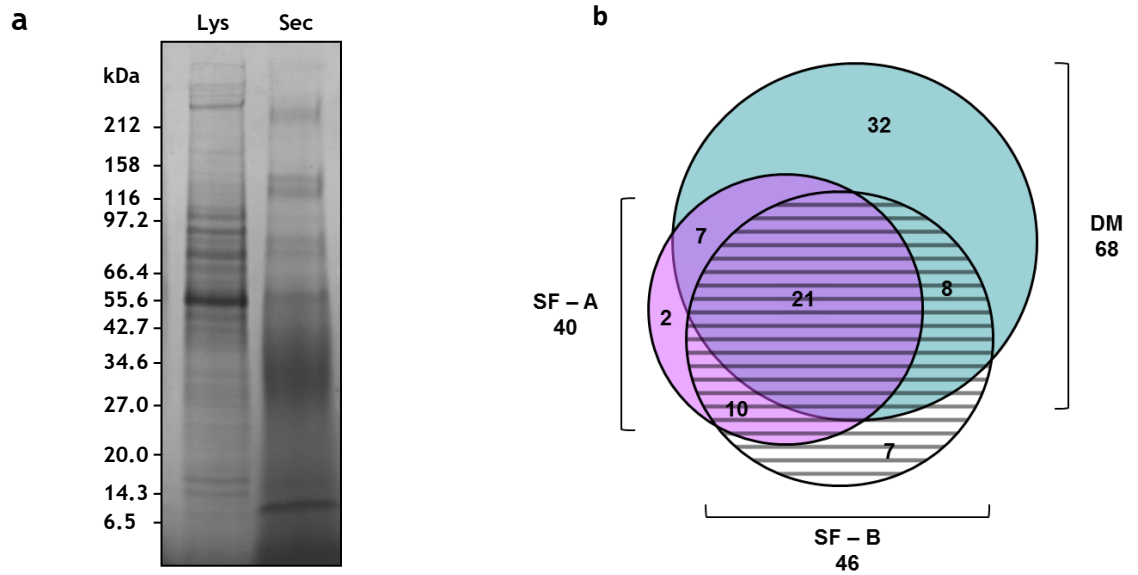
al. 1993). A more suitable method would be the use of the CRISPR-Cas9 system for knock-out or tagging in *Leishmania* described by the Gluenz group (Beneke *et al.* 2017). Knock-out experiments look for the effect on cell survival and differentiation, virulence, and effect on host cell, for example, lesion-forming in the host. Tagging experimental design could include tagging of proteins to identify the localisation to and in exosomes and location within the host cell.

We have identified several secreted proteins as candidates for further analyses. The first is the amastigote-secreted migration inhibition factor homologue (MIF). In addition to its high enrichment in the secretome of amastigotes, MIF has been shown to regulate host immunity to promote parasite persistence in other studies (Holowka *et al.* 2016; Kamir *et al.* 2008). This therefore makes it an attractive candidate for therapeutic intervention.

Further candidates for further analysis include; amastigote GP63, SMP-3, Iron superoxide dismutase, trypanothione peroxidase and thioredoxin-like protein. Amastigote GP63 differs in antibody reactivity to promastigote GP63. Previously discovered to be a major virulence factor in promastigotes, further investigation is required to understand whether this is a major virulence factor in amastigotes. Iron superoxide dismutase, trypanothione peroxidase and thioredoxin-like protein were all upregulated in the secretome of wild-type, virulent parasites compared to avirulent parasites. Superoxide dismutase A (SODA) has been previously demonstrated to be essential for *L. amazonensis* virulence (Mittra *et al.* 2017). SMP-3 is a little-known version of the *Leishmania* SMPs. However, it has been implicated in the virulence of *L. amazonensis* by the observation of its reduction in parasites with loss of virulence (Magalhães *et al.* 2014).

In summary, results presented here implicate a number of candidates for further investigation. Leishmaniasis is a debilitating disease affecting millions world-wide. The lack of a suitable treatment strategy or an appropriate, commercially available vaccine make this disease a research priority. Any research highlighting potential mechanisms into disease virulence and targets for therapeutic intervention or vaccination are a must in order to help combat this disease.

Appendices



Appendix 1 Analysis of the secretome of *L. mexicana* promastigotes cultured in chemically defined medium. (a) Lysate (Lys) and 24h secretome collection (Sec) from *L. mexicana* promastigotes cultured in chemically defined medium run on 4-20% SDS-PAGE and stained with Coomassie. (b) Proteins identified by LC-MS/MS from two serum-free secretome collections (SF-A, SF-B) and defined medium collection (DM). Total proteins numbers are indicated beside sample names.

Figure has been removed due to Copyright restrictions.

Appendix 2 Molecular Weight marker migration chart from abcam Precast Gel SDS-PAGE system. Found at www.abcam.com.

Appendix 3 Microvesicle associations of Leishmania secretome proteins. From (Silverman et al. 2008)

GeneDB Accession No.	Protein Identification	Microvesicle Association	Present in L. mexicana promast. secretome	GeneDB Accession
LmjF36.6910	chaperonin, putative, T-complex protein 1 (theta subunit), putative	AP	Yes	LmxM.36.6910
LmjF28.2860	cytosolic malate dehydrogenase, putative *	AP	Yes	LmxM.33.0140
LmjF33.2550	isocitrate dehydrogenase, putative	AP		
LmjF35.3860	t-complex protein 1, eta subunit, putative	AP	Yes	LmxM.34.3860
LmjF14.1160	enolase	AP	Yes	LmxM.14.1160
LmjF36.2030	chaperonin Hsp60, mitochondrial precursor	AP	Yes	LmxM.36.2030
LmjF23.1220	t-complex protein 1, gamma subunit, putative	AP	Yes	LmxM.23.1220
LmjF36.2020	chaperonin Hsp60, mitochondrial precursor	AP	Yes	LmxM.36.2020
LmjF36.1630	clathrin heavy chain, putative	AP		
LmjF31.1070	biotin/lipoate protein ligase-like protein	AP		
LmjF27.1260	T-complex protein 1, beta subunit, putative	AP	Yes	LmxM.27.1260
LmjF36.1600	proteasome alpha 1 subunit, putative	AP	Yes	LmxM.27.0190
LmjF35.4850	proteasome alpha 1 subunit, putative	AP	Yes	LmxM.11.0240
LmjF32.0230	dynein light chain, flagellar outer arm, putative	AP		
LmjF10.0290	isocitrate dehydrogenase [NADP], mitochondrial precursor, putative	AP	Yes	LmxM.10.0290
LmjF08.0550	translation initiation factor-like protein	AP	Similar	LmxM.33.0840
LmjF01.0410	ribosomal protein S7, putative	AP	Similar	LmxM.31.3130
LmjF32.1000	chaperonin containing t-complex protein, putative	AP	Similar	LmxM.21.1090
LmjF25.1120	aldehyde dehydrogenase, mitochondrial precursor	AP		
LmjF24.2070	40S ribosomal protein S8, putative	AP		
LmjF21.1770	ATP synthase F1 subunit gamma protein, putative	AP		
LmjF35.3060	ubiquitin-activating enzyme E1, putative	AP		
LmjF30.2820	chaperonin HSP60/CNP60, putative	AP, GLY		
LmjF21.1860	beta tubulin	BC	Yes	LmxM.08.1171
LmjF35.0030	pyruvate kinase, putative	BC, AP		
LmjF28.2770	heat-shock protein hsp70, putative	BC, DC, AP		LmxM.28.2770
LmjF26.1240	heat shock protein 70-related protein	BC, DC, AP		LmxM.26.1240
LmjF29.0510	cofilin-like protein	DC		
LmjF11.0350	14-3-3 protein, putative	DC		LmxM.36.3210
LmjF10.0910	small GTP-binding protein Rab11, putative, Rab11 GTPase, putative	DC	Similar	LmxM.27.0760
LmjF15.0010	histone h4	DC		
LmjF01.0770	eukaryotic initiation factor 4a, putative	DC, AP	Yes	LmxM.01.0770
LmjF36.3210	14-3-3 protein-like protein	DC, AP	Yes	LmxM.11.0350
LmjF04.1230	actin	DC, AP	Yes	LmxM.04.1230

List of References

- Aebischer, T., Harbecke, D., & Ilg, T. (1999). Proteophosphoglycan, a major secreted product of intracellular *Leishmania mexicana* amastigotes, is a poor B-cell antigen and does not elicit a specific conventional CD4⁺ T-cell response. *Infection and Immunity*, **67**(10), 5379-5385.
- Ahrné, E., Glatter, T., Viganò, C., Schubert, C. von, Nigg, E. A., & Schmidt, A. (2016). Evaluation and improvement of quantification accuracy in isobaric mass tag based protein quantification experiments. *Journal of Proteome Research*, **15**, 2537-2547.
- Akarid, K., Arnoult, D., Micic-polianski, J., Sif, J., Estaquier, J., & Ameisen, J. (2004). Leishmania major-mediated prevention of programmed cell death induction in infected macrophages is associated with the repression of mitochondrial release of cytochrome c. *Journal of Leukocyte Biology*, **76**, 95-103.
- Alcolea, P. J., Alonso, A., Moreno-Izquierdo, M. A., Degayón, M. A., Moreno, I., & Larraga, V. (2016). Serum Removal from Culture Induces Growth Arrest, Ploidy Alteration, Decrease in Infectivity and Differential Expression of Crucial Genes in *Leishmania infantum* Promastigotes. *Plos One*, **11**(3), e0150172.
- Alexander, J. (1981). *Leishmania mexicana*: Inhibition and stimulation of phagosome–lysosome fusion in infected macrophages. *Experimental Parasitology*, **52**, 261-270.
- Alexander, J., Coombs, G. H., & Mottram, J. C. (1998). *Leishmania mexicana* Cysteine Proteinase-Deficient Mutants Have Attenuated Virulence for Mice and Potentiate a Th1 Response. *The Journal of Immunology*, **161**, 6794-801.
- Ali, K. S., Rees, R. C., Terrell-Nield, C., & Ali, S. a. (2013). Virulence loss and amastigote transformation failure determine host cell responses to *Leishmania mexicana*. *Parasite Immunology*, **35**(12), 441-56.
- Alvar, J., Vélez, I. D., Bern, C., ... den Boer, M. (2012). Leishmaniasis worldwide and global estimates of its incidence. *PloS One*, **7**(5), e35671.
- Ambit, A., Woods, K. L., Cull, B., Coombs, G. H., & Mottram, J. C. (2011). Morphological Events during the Cell Cycle of *Leishmania major*. *EUKARYOTIC CELL*, **10**(11), 1429-1438.
- Anand, S., Samuel, M., Ang, C.-S., Keerthikumar, S., & Mathivanan, S. (2017). Label-Based and Label-Free Strategies for Protein Quantitation. In S. Keerthikumar & S. Mathivanan, eds., *Proteome Bioinformatics*, New York, NY: Springer New York, pp. 31-43.

- Andrei, C., Margiocco, P., Poggi, A., Lotti, L. V, Torrisi, M. R., & Rubartelli, A. (2004). Phospholipases C and A2 control lysosome-mediated IL-1B secretion: Implications for inflammatory processes. *Proc. Natl. Acad. Sci. USA*, **101**(26), 9745-50.
- Antelmann, H., Tjalsma, H., Voigt, B., ... Hecker, M. (2001). A proteomic view on genome-based signal peptide predictions. *Genome Research*, **11**, 1484-1502.
- Antoine, J.-C., Prina, E., Lang, T., & Courret, N. (1998). The biogenesis and properties of the parasitophorous vacuoles that harbour Leishmania in murine macrophages. *Trends in Microbiology*, **6**(10), 392-401.
- Antoine, J., Lang, T., Prina, E., Courret, N., & Hellio, R. (1999). H-2M molecules, like MHC class II molecules, are targeted to parasitophorous vacuoles of Leishmania-infected macrophages and internalized by amastigotes of *L. amazonensis* and *L. mexicana*. *Journal of Cell Science*, **112**, 2559-70.
- Appelberg, R. (2006). Macrophage nutritive antimicrobial mechanisms. *Journal of Leukocyte Biology*, **79**, 1117-1128.
- Aslett, M., Aurrecochea, C., Berriman, M., ... Wang, H. (2010). TriTrypDB: a functional genomic resource for the Trypanosomatidae. *Nucleic Acids Research*, **38**(suppl_1), D457-D462.
- Atayde, V. D., Aslan, H., Townsend, S., Hassani, K., Kamhawi, S., & Olivier, M. (2015). Exosome Secretion by the Parasitic Protozoan Leishmania within the Sand Fly Midgut. *Cell Reports*, **13**(5), 957-967.
- Atyame Nten, C. M., Sommerer, N., Rofidal, V., ... Geiger, A. (2010). Excreted/secreted proteins from trypanosome procyclic strains. *Journal of Biomedicine and Biotechnology*, **2010**, 1-8.
- Avilán, L., Gualdrón-López, M., Quiñones, W., ... Concepción, J. L. (2011). Enolase: A key player in the metabolism and a probable virulence factor of trypanosomatid parasites - Perspectives for its use as a therapeutic target. *Enzyme Research*, **2011**(1). doi:10.4061/2011/932549
- Bahl, S., Parashar, S., Malhotra, H., Raje, M., & Mukhopadhyay, A. (2015). Functional characterization of monomeric GTPase Rab1 in the secretory pathway of Leishmania. *Journal of Biological Chemistry*. doi:10.1074/jbc.M115.670018
- Bakheet, T. M., & Doig, A. J. (2009). Properties and identification of human protein drug targets. *Bioinformatics*, **25**(4), 451-457.
- Barhoumi, M., Meddeb-Garnaoui, A., Tanner, N. K., Banroques, J., Kaabi, B., & Guizani, I. (2013).

- DEAD-box proteins, like *Leishmania* eIF4A, modulate interleukin (IL)-12, IL-10 and tumour necrosis factor- α production by human monocytes. *Parasite Immunology*, **35**(5-6), 194-199.
- Barhoumi, M., Tanner, N. K., Banroques, J., Linder, P., & Guizani, I. (2006). *Leishmania infantum* LeIF protein is an ATP-dependent RNA helicase and an eIF4A-like factor that inhibits translation in yeast. *FEBS Journal*, **273**(22), 5086-5100.
- Barrett, A. J., Kembhavi, A. A., Brown, M. A., ... Hanadat, K. (1982). *L-trans-Epoxy succinyl-leucylamido(4-guanidino)butane (E-64) and its analogues as inhibitors of cysteine proteinases including cathepsins B, H and L*. *Biochem. J*, Vol. 201. Retrieved from <https://www.ncbi.nlm.nih.gov/pmc/articles/PMC1163625/pdf/biochemj00384-0189.pdf>
- Bates, P. A. (1994). Complete developmental cycle of *Leishmania mexicana* in axenic culture. *Parasitology*, **108**(1), 1-9.
- Bates, P. a. (2007). Transmission of *Leishmania* metacyclic promastigotes by phlebotomine sand flies. *International Journal for Parasitology*, **37**(10), 1097-106.
- Bates, P. a, Robertson, C. D., Tetley, L., & Coombs, G. H. (1992). Axenic cultivation and characterization of *Leishmania mexicana* amastigote-like forms. *Parasitology*, **105** (Pt 2, 193-202.
- Bautista-López, N. L., Ndao, M., Camargo, F. V., ... Jardim, A. (2016). Characterization and diagnostic application of *Trypanosoma cruzi* trypomastigote excreted-secreted antigens shed in extracellular vesicles released from infected mammalian cells. *Journal of Clinical Microbiology*, (December), JCM.01649-16.
- Bayer-Santos, E., Aguilar-Bonavides, C., Rodrigues, S. P., ... Almeida, I. C. (2012). Proteomic Analysis of *Trypanosoma cruzi* Secretome: Characterization of Two Populations of Extracellular Vesicles and Soluble Proteins. doi:10.1021/pr300947g
- Ben-Othman, R., Flannery, A. R., Miguel, D. C., Ward, D. M., Kaplan, J., & Andrews, N. W. (2014). *Leishmania*-mediated inhibition of iron export promotes parasite replication in macrophages. *PLoS Pathogens*, **10**(1), e1003901.
- Beneke, T., Madden, R., Makin, L., Valli, J., Sunter, J., & Gluenz, E. (2017). A CRISPR Cas9 high-throughput genome editing toolkit for kinetoplastids. *Royal Society Open Science*, **4**, 170095.
- Bennuru, S., Semnani, R., Meng, Z., Ribeiro, J. M. C., Veenstra, T. D., & Nutman, T. B. (2009). *Brugia malayi* Excreted/Secreted Proteins at the Host/Parasite Interface: Stage- and Gender-

- Specific Proteomic Profiling. *PLoS Neglected Tropical Diseases*, **3**(4), e410.
- BLUM, J. J., & OPPERDOES, F. R. (1994). Secretion of Sucrase by *Leishmania donovani*. *The Journal of Eukaryotic Microbiology*, **41**(3), 228-231.
- Bollineni, R. C., Koehler, C. J., Gislefoss, R. E., Anonsen, J. H., & Thiede, B. (2018). Large-scale intact glycopeptide identification by Mascot database search. *Scientific Reports*, **8**(1), 1-13.
- Braga, M. S., Neves, L. X., Campos, J. M., ... Castro-Borges, W. (2014). Shotgun proteomics to unravel the complexity of the *Leishmania infantum* exoproteome and the relative abundance of its constituents. *Molecular and Biochemical Parasitology*, **195**(1), 43-53.
- Brittingham, A., Morrison, C. J., McMaster, W. R., McGwire, B. S., Chang, K. P., & Mosser, D. M. (1995). Role of the *Leishmania* surface protease gp63 in complement fixation, cell adhesion, and resistance to complement-mediated lysis. *Journal of Immunology (Baltimore, Md. : 1950)*, **155**(6), 3102-11.
- Broedel Jr., S. E., & Papciak, S. M. (2003). The Case for Serum-Free Media. *Biopharm International*, **1**, 56-58.
- Burchmore, R. J. S., & Barrett, M. P. (2001). Life in vacuoles--nutrient acquisition by *Leishmania* amastigotes. *International Journal for Parasitology*, **31**(12), 1311-20.
- Burchmore, R. J. S., & Hart, D. T. (1995). Glucose transport in amastigotes and promastigotes of *Leishmania mexicana mexicana*. *Molecular and Biochemical Parasitology*, **74**(1), 77-86.
- Burchmore, R. J. S., Rodriguez-contreras, D., McBride, K., ... Merkel, P. (2003). Genetic characterization of glucose transporter function in *Leishmania mexicana*. *Proceedings of the National Academy of Sciences*, **100**(7), 3901-3906.
- Carrillo, E., Hilda Straus, A., Iborra, S., ... Oswaldo Cruz-FIOCRUZ, F. (2018). Analysis of the Antigenic and Prophylactic Properties of the *Leishmania* Translation Initiation Factors eIF2 and eIF2B in Natural and Experimental Leishmaniasis. *Front. Cell. Infect. Microbiol*, **8**, 112.
- Castro, H., Duarte, M., & Tomás, A. M. (2017). The Redox Metabolism and Oxidative Stress in *Leishmania* as a Crossroads for the Lethal Effect of Drugs. In *Drug Discovery for Leishmaniasis*, pp. 316-347.
- Castro, H., Sousa, C., Santos, M., Cordeiro-da-Silva, A., Flohé, L., & Tomás, A. M. (2002). Complementary antioxidant defense by cytoplasmic and mitochondrial peroxiredoxins in *Leishmania infantum*. *Free Radical Biology and Medicine*, **33**(11), 1552-1562.

- Cecílio, P., Pérez-Cabezas, B., Santarém, N., Maciel, J., Rodrigues, V., & Cordeiro-da-Silva, A. (2014). Deception and manipulation: the arms of leishmania, a successful parasite. *Frontiers in Immunology*, *5*(October), 480.
- Chaudhuri, G., Chaudhuri, M., Pan, A. A., & Chang, K.-P. (1989). Surface Acid Proteinase (gp63) of *Leishmania mexicana*. *The Journal of Biological Chemistry*, *264*(13), 7483-89.
- Chenik, M., Lakhal, S., Ben Khalef, N., Zribi, L., Louzir, H., & Dellagi, K. (2006). Approaches for the identification of potential excreted/secreted proteins of *Leishmania major* parasites. *Parasitology*, *132*(4), 493-509.
- Chevallet, M., Diemer, H., Van Dorssealer, A., Villiers, C., & Rabilloud, T. (2007). Toward a better analysis of secreted proteins: The example of the myeloid cells secretome. *Proteomics*, *7*(11), 1757-1770.
- Clayton, C. E. (2002). Life without transcriptional control? From fly to man and back again. *The EMBO Journal*, *21*(8), 1881-88.
- ClinicalTrials.gov. (2012). *A Phase 1 Clinical Trial to Evaluate the Safety, Tolerability, and Immunogenicity of the Vaccine Candidates LEISH-F3 + GLA-SE, LEISH-F3 + MPL-SE, and LEISH-F3 + SE in Healthy Adult Subjects NCT01751048*.
- Coler, R. N., Goto, Y., Bogatzki, L., Raman, V., & Reed, S. G. (2007). Leish-111f, a recombinant polyprotein vaccine that protects against visceral leishmaniasis by elicitation of CD4+T cells. *Infection and Immunity*, *75*(9), 4648-4654.
- Contreras, I., Gómez, M. A., Nguyen, O., Shio, M. T., McMaster, R. W., & Olivier, M. (2010). *Leishmania*-induced inactivation of the macrophage transcription Factor AP-1 Is Mediated by the Parasite Metalloprotease GP63. *PLoS Pathogens*, *6*(10). doi:10.1371/journal.ppat.1001148
- Cottrell, J. S. (2011). Protein identification using MS/MS data. *Journal of Proteomics*, *74*(10), 1842-1851.
- Courret, N., Fréhel, C., Gouhier, N., ... Antoine, J.-C. (2002). Biogenesis of *Leishmania*-harbouring parasitophorous vacuoles following phagocytosis of the metacyclic promastigote or amastigote stages of the parasites. *Journal of Cell Science*, *115*(11), 2303-16.
- Cruz, A. K., Titus, R., & Beverley, S. M. (1993). Plasticity in chromosome number and testing of essential genes in *Leishmania* by targeting. *Proc. Natl. Acad. Sci. USA*, *90*, 1599-1603.
- Cuervo, P., De Jesus, J. B., Saboia-Vahia, L., Mendonça-Lima, L., Domont, G. B., & Cupolillo, E.

- (2009). Proteomic characterization of the released/secreted proteins of *Leishmania* (Viannia) *braziliensis* promastigotes. *Journal of Proteomics*, **73**(1), 79-92.
- Cuervo, P., Sabóia-Vahia, L., Costa Silva-Filho, F., Fernandes, O., Cupolillo, E., & De Jesus, J. B. (2006). A zymographic study of metalloprotease activities in extracts and extracellular secretions of *Leishmania* (Viannia) *braziliensis* strains. *Parasitology*, **132**(Pt 2), 177-185.
- D'Angelo, G., Chaerkady, R., Yu, W., ... Yang, H. (2017). Statistical Models for the Analysis of Isobaric Tags Multiplexed Quantitative Proteomics. *Journal of Proteome Research*, **16**(9), 3124-3136.
- Daneshvar, H., Coombs, G. H., Hagan, P., & Phillips, R. S. (2003a). *Leishmania mexicana* and *Leishmania major*: attenuation of wild-type parasites and vaccination with the attenuated lines. *The Journal of Infectious Diseases*, **187**(10), 1662-1668.
- Daneshvar, H., Hagan, P., & Phillips, R. S. (2003b). *Leishmania mexicana* H-line attenuated under pressure of gentamicin, potentiates a Th1 response and control of cutaneous leishmaniasis in BALB/c mice. *Parasite Immunology*, **25**(11-12), 589-596.
- Daneshvar, H., Namazi, M. J., Kamiabi, H., Burchmore, R. J. S., Cleaveland, S., & Phillips, R. S. (2014). Gentamicin-attenuated *Leishmania infantum* vaccine: protection of dogs against canine visceral leishmaniasis in endemic area of southeast of Iran. *PLoS Neglected Tropical Diseases*, **8**(4), e2757.
- Daneshvar, H., Wyllie, S., Phillips, R. S., Hagan, P., & Burchmore, R. J. S. (2012). Comparative proteomics profiling of a gentamicin-attenuated *Leishmania infantum* cell line identifies key changes in parasite thiol-redox metabolism. *Journal of Proteomics*, **75**(5), 1463-71.
- Davidson, R. N., Di Martino, L., Gradoni, L., ... Cascio, A. (1994). Liposomal amphotericin B (AmBisome) in Mediterranean visceral leishmaniasis: a multi-centre trial. *The Quarterly Journal of Medicine*, **87**(2), 75-81.
- Davies, J. R., & Carlstedt, I. (2000). Isolation of Large Gel-Forming Mucins. In A. P. Corfield, ed., *Glycoprotein Methods and Protocols, Methods in Molecular Biology, Volume 125*, Humana Press. Retrieved from <https://link.springer.com/content/pdf/10.1385%2F1-59259-048-9%3A003.pdf>
- Davies, J. R., Wickström, C., & Thornton, D. J. (2012). Gel-Forming and Cell-Associated Mucins: Preparation for Structural and Functional Studies. In M. McGuckin & D. Thornton, eds., *Mucins, Methods in Molecular Biology, Volume 842*, Humana Press. doi:10.1007/978-1-61779-513-8_2

- de Menezes, J. P. B., Guedes, C. E. S., Petersen, A. L. de O. A., Fraga, D. B. M., & Veras, P. S. T. (2015). Advances in Development of New Treatment for Leishmaniasis. *BioMed Research International*, **Article ID**, 11.
- De Paula Lima, C. V, Batista, M., Kugeratski, F. G., ... Marchini, F. K. (2014). LM14 defined medium enables continuous growth of *Trypanosoma cruzi*. *BMC Microbiology*, **14**(238), 1-8.
- De Souza Leao, S., Lang, T., Prina, E., Hellio, R., & Antoine, J. (1995). Intracellular *Leishmania amazonensis* amastigotes internalize and degrade MHC class II molecules of their host cells. *Journal of Cell Science*, **108**, 3219-3231.
- Dean, P., Major, P., Nakjang, S., Hirt, R. P., & Embley, T. M. (2014). Transport proteins of parasitic protists and their role in nutrient salvage. *Frontiers in Plant Science*, **5**(April), 153.
- Delahunty, C., & Yates III, J. R. (2005). Protein identification using 2D-LC-MS/MS. *Methods*, **35**, 248-255.
- Denise, H., McNeil, K., Brooks, D. R., Alexander, J., Coombs, G. H., & Mottram, J. C. (2003). Expression of Multiple CPB Genes Encoding Cysteine Proteases Is Required for *Leishmania mexicana* Virulence In Vivo. *Infection and Immunity*, **71**(6), 3190-3195.
- Denny, P., Gokool, S., Russell, D. G., Field, M., & Smith, D. F. (2000). Acylation-dependent protein export in *Leishmania*. *Journal of Biological Chemistry*, **275**(15), 11017-11025.
- Diniz Atayde, V., Hassani, K., Da Silva, A., ... Olivier, M. (2016). *Leishmania* exosomes and other virulence factors: Impact on innate immune response and macrophage functions. *Cellular Immunology*, **309**, 7-18.
- Doerr, A. (2015). DIA mass spectrometry. *Nature Publishing Group*, **12**(1), 35.
- Donnelly, S., O'Neill, S. M., Sekiya, M., Mulcahy, G., & Dalton, J. P. (2005). Thioredoxin peroxidase secreted by *Fasciola hepatica* induces the alternative activation of macrophages. *Infection and Immunity*, **73**(1), 166-73.
- Donovan, M. J., Maciuba, B. Z., Mahan, C. E., & McDowell, M. A. (2009). *Leishmania* infection inhibits cycloheximide-induced macrophage apoptosis in a strain-dependent manner. *Experimental Parasitology*, **123**(1), 58-64.
- Duncan, R., Gannavaram, S., Dey, R., Debrabant, A., Lakhal-Naouar, I., & Nakhasi, H. L. (2011). Identification and characterization of genes involved in *leishmania* pathogenesis: the potential for drug target selection. *Molecular Biology International*, **2011**, 428486.

- Dwivedi, P., Alam, S. I., & Tomar, R. S. (2016). Secretome, surfome and immunome: emerging approaches for the discovery of new vaccine candidates against bacterial infections. *World Journal of Microbiology and Biotechnology*, **32**(9), 155.
- Dwyer, D. M., & Gottlieb, M. (1984). SURFACE MEMBRANE LOCALIZATION OF 3'- AND 5'-NUCLEOTIDASE ACTIVITIES IN LEISHMANIA DONOVANI PROMASTIGOTES. *Molecular and Biochemical Parasitology*, **10**, 139-150.
- Dyballa, N., & Metzger, S. (2009). Fast and sensitive colloidal coomassie G-250 staining for proteins in polyacrylamide gels. *Journal of Visualized Experiments : JoVE*, **30**(1431).
- Eichelbaum, K., & Krijgsveld, J. (2014). Combining Pulsed SILAC Labeling and Click-Chemistry for Quantitative Secretome Analysis. In A. I. Ivanov, ed., *Exocytosis and Endocytosis*, 2nd edn, Vol. 1174, New York, NY: Springer, pp. 101-114.
- Eilam, Y., El-On, J., & Spira, D. T. (1985). *Leishmania major: Excreted Factor, Calcium Ions, and the Survival of Amastigotes*. *Experimental parasitology*, Vol. 59.
- Esch, K. J., & Petersen, C. A. (2013). Transmission and epidemiology of zoonotic protozoal diseases of companion animals. *Clinical Microbiology Reviews*, **26**(1), 58-85.
- Falcone, F. H., Loke, P., Zang, X., MacDonald, A. S., Maizels, R. M., & Allen, J. E. (2001). A *Brugia malayi* homolog of macrophage migration inhibitory factor reveals an important link between macrophages and eosinophil recruitment during nematode infection. *The Journal of Immunology*, **167**, 5348-5354.
- Figuera, L., Acosta, H., Gómez-Arreaza, A., ... Avilán, L. (2013). Plasminogen binding proteins in secreted membrane vesicles of *Leishmania mexicana*. *Molecular and Biochemical Parasitology*, **187**(1), 14-20.
- Flannagan, R. S., Jaumouille, V., & Grinstein, S. (2012). The Cell Biology of Phagocytosis. *Annual Review of Pathology: Mechanisms of Disease*, **7**, 61-98.
- Frommel, T. O., Button, L. L., Fujikura, Y., & McMaster, R. W. (1990). The major surface glycoprotein (GP63) is present in both life stages of *Leishmania*. *Molecular and Biochemical Parasitology*, **38**(1), 25-32.
- Gaur, U., Roberts, S. C., Dalvi, R. P., Corraliza, I., Ullman, B., & Wilson, M. E. (2007). An Effect of Parasite-Encoded Arginase on the Outcome of Murine Cutaneous Leishmaniasis. *The Journal of Immunology*, **179**(12), 8446-8453.

- Ghosh, S., Goswami, S., & Adhya, S. (2003). Role of superoxide dismutase in survival of *Leishmania* within the macrophage. *Biochemical Journal*, **369**(3), 447-452.
- Giordana, L., Mantilla, B. S., Santana, M., Silber, A. M., & Nowicki, C. (2014). Cystathionine γ -lyase, an Enzyme Related to the Reverse Transsulfuration Pathway, is Functional in *Leishmania* spp. *Journal of Eukaryotic Microbiology*, **61**(2), 204-213.
- Glaser, T. A., Baatz, J. E., Kreishman, G. P., & Mukkada, A. J. (1988). pH homeostasis in *Leishmania donovani* amastigotes and promastigotes. *Proc. Natl. Acad. Sci. USA*, **85**, 7602-7606.
- Gold, D. A., Kaplan, A. D., Lis, A., ... Saeij, J. P. J. (2015). The *Toxoplasma* dense granule proteins GRA17 and GRA23 mediate the movement of small molecules between the host and the parasitophorous vacuole. *Cell Host and Microbe*, **17**(5), 642-652.
- Goldring, J. P. D. (2015). Methods to Concentrate Proteins for Protein Isolation, Proteomic, and Peptidomic Evaluation. In B. T. Kurien & R. H. Scofield, eds., *Detection of Blotted Proteins: Methods and Protocols*, New York, NY: Springer New York, pp. 5-18.
- Goldston, A. M., Sharma, A. I., Paul, K. S., & Engman, D. M. (2014). Acylation in trypanosomatids: an essential process and potential drug target. *Trends in Parasitology*, **30**(7). doi:10.1016/j.pt.2014.05.003
- Gómez-Arreaza, A., Acosta, H., Quiñones, W., Concepción, J. L., Michels, P. A. M., & Avilán, L. (2014). Extracellular functions of glycolytic enzymes of parasites: Unpredicted use of ancient proteins. *Molecular and Biochemical Parasitology*, **193**(2), 75-81.
- Gómez, M. A., Contreras, I., Hallé, M., Tremblay, M. L., McMaster, R. W., & Olivier, M. (2009a). *Leishmania* GP63 alters host signaling through cleavage-activated protein tyrosine phosphatases. *Science Signaling*, **2**(90), ra58.
- Gómez, M. A., Contreras, I., Hallé, M., Tremblay, M. L., McMaster, R. W., & Olivier, M. (2009b). *Leishmania* GP63 alters host signaling through cleavage-activated protein tyrosine phosphatases. *Science Signaling*, **2**(90), ra58.
- Gopfert, U., Goehring, N., Klein, C., & Ilg, T. (1999). Molecular cloning and characterization of the *Leishmania mexicana* ppg2 gene encoding the proteophosphoglycans aPPG and pPPG2 that are secreted by amastigotes and promastigotes. *Biochemical Journal*, **344**, 787-795.
- Goto, Y., Ogawa, K., Hattori, A., & Tsujimoto, M. (2011). Secretion of Endoplasmic Reticulum Aminopeptidase 1 Is Involved in the Activation of Macrophages Induced by Lipopolysaccharide and Interferon- γ . *Journal of Biological Chemistry*, **286**(24), 21906-21914.

- Goundry, A., Romano, A., Paula A Lima, A. C., Mottram, J. C., & Myburgh, E. (2018). Inhibitor of serine peptidase 2 enhances *Leishmania major* survival in the skin through control of monocytes and monocyte-derived cells. *FASEB Journal*, **32**, 1315-27.
- Green, S. J., Meltzer, M. S., Hibbs, J. B., & Nacy, C. A. (1990). Activated macrophages destroy intracellular *Leishmania major* amastigotes by an L-arginine-dependent killing mechanism. *The Journal of Immunology*, **144**(1), 278-283.
- Guimarães-Costa, A. B., DeSouza-Vieira, T. S., Paletta-Silva, R., Freitas-Mesquita, A. L., Meyer-Fernandes, J. R., & Saraiva, E. M. (2014). 3'-Nucleotidase/Nuclease Activity Allows *Leishmania* Parasites To Escape Killing by Neutrophil Extracellular Traps. *Infection and Immunity*, **82**(4), 1732-1740.
- Gupta, N., Goyal, N., & Rastogi, A. K. (2001). In vitro cultivation and characterization of axenic amastigotes of *Leishmania*. *Trends in Parasitology*, **17**(3), 150-153.
- Gygi, S. P., Rist, B., Gerber, S. A., Turecek, F., Gelb, M. H., & Aebersold, R. (1999). Quantitative analysis of complex protein mixtures using isotope-coded affinity tags. *Nature Biotechnology*, **17**(10), 994-999.
- Hakimi, M.-A., & Bougdour, A. (2015). *Toxoplasma* 's ways of manipulating the host transcriptome via secreted effectors. *Current Opinion in Microbiology*, **26**, 24-31.
- Hart, D. T., & Coombs, G. H. (1982). *Leishmania mexicana*: Energy metabolism of amastigotes and promastigotes. *Experimental Parasitology*, **54**, 397-409.
- Hassan, H., & Coombs, G. H. (1987). Phosphomonoesterases of *Leishmania mexicana mexicana* and other flagellates. *Molecular and Biochemical Parasitology*, **23**(3), 285-96.
- Hassani, K., Antoniak, E., Jardim, A., & Olivier, M. (2011). Temperature-induced protein secretion by *Leishmania mexicana* modulates macrophage signalling and function. *PLoS One*, **6**(5), e18724.
- Hassani, K., & Olivier, M. (2013). Immunomodulatory Impact of *Leishmania*-Induced Macrophage Exosomes: A Comparative Proteomic and Functional Analysis. *PLoS Neglected Tropical Diseases*, **7**(5), e2185.
- Hassani, K., Shio, M. T., Martel, C., Faubert, D., & Olivier, M. (2014). Absence of metalloprotease GP63 alters the protein content of *leishmania* exosomes. *PLoS ONE*, **9**(4). doi:10.1371/journal.pone.0095007

- Henderson, B., & Martin, A. (2011). Bacterial virulence in the moonlight: Multitasking bacterial moonlighting proteins are virulence determinants in infectious disease. *Infection and Immunity*, **79**(9), 3476-3491.
- Henningham, A., Chiarot, E., Gillen, C. M., ... Walker, M. J. (2012). Conserved anchorless surface proteins as group A streptococcal vaccine candidates. *Journal of Molecular Medicine*, **90**(10), 1197-1207.
- Hewitson, J. P., Ivens, A., H Marcus, Y., ... Maizels, R. M. (2013). Secretion of Protective Antigens by Tissue-Stage Nematode Larvae Revealed by Proteomic Analysis and Vaccination-Induced Sterile Immunity. *PLoS Pathogens*, **9**(8). doi:10.1371/journal.ppat.1003492
- Hine, R., & Martin, E. (Eds.). (2015). *A Dictionary of Biology*, Oxford University Press. doi:10.1093/acref/9780198714378.001.0001
- Holm, Å., Tejle, K., Magnusson, K.-E., Descoteaux, A., & Rasmusson, B. (2001). Leishmania donovani lipophosphoglycan causes periphagosomal actin accumulation: correlation with impaired translocation of PKC α and defective. *Cellular Microbiology*, **3**(7), 439-447.
- Holowka, T., Castilho, T. M., Garcia, A. B., Sun, T., McMahon-Pratt, D., & Bucala, R. (2016). Leishmania-encoded orthologs of macrophage migration inhibitory factor regulate host immunity to promote parasite persistence. *FASEB Journal*, **30**, 1-17.
- Hsu, J.-L., Huang, S.-Y., Chow, N.-H., & Chen, S.-H. (2003). Stable-Isotope Dimethyl Labeling for Quantitative Proteomics. *Analytical Chemistry*, **75**, 6843-6852.
- Huang, H., Kawamata, T., Horie, T., ... Fukusaki, E. (2015). Bulk RNA degradation by nitrogen starvation-induced autophagy in yeast. *The EMBO Journal*, **34**(2), 154-168.
- Huynh, C., & Andrews, N. W. (2008). Iron acquisition within host cells and the pathogenicity of Leishmania. *Cellular Microbiology*, **10**(2), 293-300.
- Ilg, T. (2000a). Lipophosphoglycan is not required for infection of macrophages or mice by Leishmania mexicana. *The EMBO Journal*, **19**(9), 1953-62.
- Ilg, T. (2000b). Proteophosphoglycans of Leishmania. *Parasitology Today*, **16**(11), 489-497.
- Ilg, T., Craik, D., Currie, G., Multhaup, G., & Bacic, A. (1998). Stage-specific Proteophosphoglycan from Leishmania mexicana Amastigotes. *The Journal of Biological Chemistry*, **273**(22), 13509-13523.

- Ilg, T., Stierhof, Y. D., Craik, D., Simpson, R., Handman, E., & Bacic, A. (1996). Purification and Structural Characterization of a Filamentous, Mucin-like Proteophosphoglycan Secreted by Leishmania Parasites. *Journal of Biological Chemistry*, **271**(35), 21583-21596.
- Ilg, T., Stierhof, Y. D., Etges, R., Adrian, M., Harbecke, D., & Overath, P. (1991). Secreted acid phosphatase of *Leishmania mexicana*: a filamentous phosphoglycoprotein polymer. *Proc. Natl. Acad. Sci. USA*, **88**, 8774-8778.
- Ilg, T., Stierhof, Y. D., McConville, M. J., & Overath, P. (1995). Purification, partial characterization and immunolocalization of a proteophosphoglycan secreted by *Leishmania mexicana* amastigotes. *European Journal of Cell Biology*, **66**(2), 205-15.
- Ishihama, Y., Oda, Y., Tabata, T., ... Mann, M. (2005). Exponentially Modified Protein Abundance Index (emPAI) for Estimation of Absolute Protein Amount in Proteomics by the Number of Sequenced Peptides per Protein. *Molecular & Cellular Proteomics*, **4**(9), 1265-1272.
- Isnard, A., Christian, J. G., Kodiha, M., Stochaj, U., McMaster, R. W., & Olivier, M. (2015). Impact of *Leishmania* Infection on Host Macrophage Nuclear Physiology and Nucleopore Complex Integrity. *PLOS Pathogens*, **11**(3), e1004776.
- Jacobson, R. L., & Schlein, Y. (2001). *Phlebotomus papatasi* and *Leishmania major* parasites express α -amylase and α -glucosidase. *Acta Tropica*, Vol. 78. Retrieved from www.parasitology-online.com
- Jain, S. K., Sahu, R., Walker, L. A., & Tekwani, B. L. (2012). A Parasite Rescue and Transformation Assay for Antileishmanial Screening Against Intracellular *Leishmania donovani* Amastigotes in THP1 Human Acute Monocytic Leukemia Cell Line. *J. Vis. Exp.*, (70), 4054.
- Jara, M., Berg, M., Caljon, G., ... Arevalo, J. (2017). Macromolecular biosynthetic parameters and metabolic profile in different life stages of *Leishmania braziliensis*: Amastigotes as a functionally less active stage. *PLoS One*, **12**(7), e0180532.
- Jaramillo, M., Gómez, M. A., Larsson, O., ... Sonenberg, N. (2011). *Leishmania* repression of host translation through mTOR cleavage is required for parasite survival and infection. *Cell Host and Microbe*, **9**(4), 331-41.
- Jeffery, C. J. (1999). Moonlighting proteins. *Trends in Biochemical Sciences*, **24**(1), 8-11.
- Joshi, M. B., & Dwyer, D. M. (2007). Molecular and functional analyses of a novel class I secretory nuclease from the human pathogen, *Leishmania donovani*. *The Journal of Biological Chemistry*, **282**(13), 10079-95.

- Joshi, M. B., Rogers, M. E., Shakarian, A. M., ... Dwyer, D. M. (2005). Molecular characterization, expression, and in vivo analysis of LmexCht1: the chitinase of the human pathogen, *Leishmania mexicana*. *The Journal of Biological Chemistry*, **280**(5), 3847-61.
- Kamir, D., Zierow, S., Leng, L., ... Bucala, R. (2008). A *Leishmania* Ortholog of Macrophage Migration Inhibitory Factor Modulates Host Macrophage Responses. *The Journal of Immunology*, **180**(12), 8250-8261.
- Kammers, K., Cole, R. N., Tiengwe, C., & Ruczinski, I. (2015). Detecting significant changes in protein abundance. *EuPA Open Proteomics*, **7**, 11-19.
- Karkowska-Kuleta, J., & Kozik, A. (2014). Moonlighting proteins as virulence factors of pathogenic fungi, parasitic protozoa and multicellular parasites. *Molecular Oral Microbiology*, **29**(6), 270-283.
- Karpievitch, Y. V., Polpitiya, A. D., Anderson, G. A., Smith, R. D., & Dabney, A. R. (2010). Liquid chromatography mass spectrometry-based proteomics: Biological and technological aspects. *Annals of Applied Statistics*, **4**(4), 1797-1823.
- Kedzierski, L., Zhu, Y., & Handman, E. (2006). *Leishmania* vaccines: progress and problems. *Parasitology*, **133**, S87-D112.
- Khanra, S., Sarraf, N. R., Das, A. K., Roy, S., & Manna, M. (2017). Miltefosine Resistant Field Isolate From Indian Kala-Azar Patient Shows Similar Phenotype in Experimental Infection. *Scientific Reports*, **7**(1), 10330.
- Kim, Y., Edwards, N., & Fenselau, C. (2014). Extracellular vesicle proteomes reflect developmental phases of *Bacillus subtilis*. *Clinical Proteomics*, **13**, 6.
- Klein, C., Göpfert, U., Goehring, N., Stierhof, Y. D., & Ilg, T. (1999). Proteophosphoglycans of *Leishmania mexicana*. Identification, purification, structural and ultrastructural characterization of the secreted promastigote proteophosphoglycan pPPG2, a stage-specific glycoisoform of amastigote aPPG. *The Biochemical Journal*, **344 Pt 3**, 775-786.
- Kolli, B. K., Kostal, J., Zaborina, O., Chakrabarty, A. M., & Chang, K.-P. (2008). *Leishmania*-released nucleoside diphosphate kinase prevents ATP-mediated cytolysis of macrophages. *Molecular and Biochemical Parasitology*, **158**(2), 163-75.
- Kuhn, P.-H., Koroniak, K., Hognl, S., ... Lichtenthaler, S. F. (2012). Secretome protein enrichment identifies physiological BACE1 protease substrates in neurons. *The EMBO Journal*, **31**(14), 3157-3168.

- Laemmli, U. K. (1970). Cleavage of Structural Proteins during the Assembly of the Head of Bacteriophage T4. *Nature*, **227**(5259), 680-685.
- Lambertz, U., Silverman, J. M., Nandan, D., ... Reiner, N. E. (2012). Secreted virulence factors and immune evasion in visceral leishmaniasis. *Journal of Leukocyte Biology*, **91**(6), 887-99.
- Larson, C. L., Beare, P. A., Voth, D. E., ... Heinzen, R. A. (2015). Coxiella burnetii Effector Proteins That Localize to the Parasitophorous Vacuole Membrane Promote Intracellular Replication. *Infection and Immunity*, **83**(2), 661-670.
- Leifso, K., Cohen-Freue, G., Dogra, N., Murray, A., & McMaster, R. W. (2007). Genomic and proteomic expression analysis of Leishmania promastigote and amastigote life stages: the Leishmania genome is constitutively expressed. *Molecular and Biochemical Parasitology*, **152**(1), 35-46.
- Lerm, M., Holm, Å., Seiron, Å., Sarndahl, E., Magnusson, K.-E., & Rasmusson, B. (2006). Leishmania donovani requires functional Cdc42 and Rac1 to prevent phagosomal maturation. *Infection and Immunity*, **74**(5), 2613-2618.
- Li, M., Song, S., Yang, D., Li, C., & Li, G. (2015). Identification of secreted proteins as novel antigenic vaccine candidates of Haemophilus parasuis serovar 5. *Vaccine*, **33**(14), 1695-1701.
- Lin, Q., Tan, H. T., Lim, H. S. R., & Chung, M. C. M. (2013). Sieving through the cancer secretome. *Biochimica et Biophysica Acta*, **1834**(11), 2360-71.
- Lisi, S., Sisto, M., Acquafredda, A., ... Panaro, M. (2005). Infection with Leishmania infantum Inhibits actinomycin D-induced apoptosis of human monocytic cell line U-937. *The Journal of Eukaryotic Microbiology*, **52**(3), 211-7.
- Lodge, R., & Descoteaux, A. (2005). Leishmania donovani promastigotes induce periphagosomal F-actin accumulation through retention of the GTPase Cdc42. *Cellular Microbiology*, **7**(11), 1647-58.
- Lodge, R., Diallo, T. O., & Descoteaux, A. (2006). Leishmania donovani lipophosphoglycan blocks NADPH oxidase assembly at the phagosome membrane. *Cellular Microbiology*, **8**(12), 1922-31.
- Lye, L.-F., Owens, K., Shi, H., ... Beverley, S. M. (2010). Retention and Loss of RNA Interference Pathways in Trypanosomatid Protozoans. *PLOS Pathogens*, **6**(10), e1001161.
- MacKenzie, A., Wilson, H. L., Kiss-Toth, E., Dower, S. K., North, R. A., & Surprenant, A. (2001). Rapid Secretion of Interleukin-1beta by Microvesicle Shedding. *Immunity*, **8**, 825-35.

- Magalhães, R. D. M., Duarte, M. C., Mattos, E. C., ... Coelho, E. A. F. (2014). Identification of Differentially Expressed Proteins from *Leishmania amazonensis* Associated with the Loss of Virulence of the Parasites. *PLoS Neglected Tropical Diseases*, **8**(4), e2764.
- Makridakis, M., & Vlahou, A. (2010). Secretome proteomics for discovery of cancer biomarkers. *Journal of Proteomics*, **73**(12), 2291-2305.
- Mallinson, D. J., & Coombs, G. H. (1989). Biochemical characteristics of the metacyclic forms of *Leishmania major* and *L. mexicana mexicana*. *Parasitology*, **98**, 7-15.
- Manske, C., & Hilbi, H. (2014). Metabolism of the vacuolar pathogen *Legionella* and implications for virulence. *Frontiers in Cellular and Infection Microbiology*, **4**(September), 125.
- Mantel, P.-Y., & Marti, M. (2014). The role of extracellular vesicles in *Plasmodium* and other protozoan parasites. *Cellular Microbiology*, **16**(3), 344-354.
- Marín, C., Longoni, S. S., Mateo, H., ... Sánchez-Moreno, M. (2007). The use of an excreted superoxide dismutase in an ELISA and Western blotting for the diagnosis of *Leishmania (Leishmania) infantum* naturally infected dogs. *Parasitology Research*, **101**, 801-8.
- Marshall, T., & Williams, K. (1996). Two-dimensional electrophoresis of human urinary proteins following concentration by dye precipitation. *Electrophoresis*, **17**(7), 1265-1272.
- Matallana-Surget, S., Leroy, B., & Wattiez, R. (2010). Shotgun proteomics: concept, key points and data mining. *Expert Review of Proteomics*, **7**(1), 5-7.
- McConville, M. J., & Blackwell, J. M. (1991). Developmental Changes in the Glycosylated Phosphatidylinositols of *Leishmania donovani*. *The Journal of Biological Chemistry*, **266**(23), 15170-15179.
- McConville, M. J., de Souza, D., Saunders, E. C., Likic, V. a, & Naderer, T. (2007). Living in a phagolysosome; metabolism of *Leishmania* amastigotes. *Trends in Parasitology*, **23**(8), 368-75.
- McConville, M. J., Mullin, K. A., Ilgoutz, S. C., & Teasdale, R. D. (2002). Secretory Pathway of Trypanosomatid Parasites. *Microbiology and Molecular Biology Reviews*, **66**(1), 122-154.
- McConville, M. J., & Naderer, T. (2011). Metabolic pathways required for the intracellular survival of *Leishmania*. *Annual Review of Microbiology*, **65**, 543-61.
- Medina-Acosta, E., Karess, R. E., & Russell, D. G. (1993). *Structurally distinct genes for the surface*

- protease of Leishmania mexicana are developmentally regulated. Molecular and Biochemical Parasitology*, Vol. 57.
- Medina-Acosta, E., Karess, R. E., Schwartz, H., & Russell, D. G. (1989). The promastigote surface protease (gp63) of *Leishmania* is expressed but differentially processed and localized in the amastigote stage. *Molecular and Biochemical Parasitology*, **37**(2), 263-273.
- Menz, B., Winter, G., Ilg, T., Lottspeich, F., & Overath, P. (1991). Purification and characterization of a membrane-bound acid phosphatase of *Leishmania mexicana*. *Molecular and Biochemical Parasitology*, **47**(1), 101-108.
- Merrifield, M., Hotez, P. J., Beaumier, C. M., ... Bottazzi, M. E. (2016). Advancing a vaccine to prevent human schistosomiasis. *Vaccine*, **34**(26), 2988-2991.
- Mitra, B., Cortez, M., Haydock, A., Ramasamy, G., Myler, P. J., & Andrews, N. W. (2013). Iron uptake controls the generation of *Leishmania* infective forms through regulation of ROS levels. *The Journal of Experimental Medicine*, **210**(2), 401-416.
- Mitra, B., Laranjeira-Silva, M. F., Miguel, D. C., Perrone Bezerra De Menezes, J., & Andrews, N. W. (2017). The iron-dependent mitochondrial superoxide dismutase SODA promotes *Leishmania* virulence. *Journal of Biological Chemistry*, **292**(29), 12324-12338.
- Moore, K., & Matlashewski, G. (1994). Intracellular infection by *Leishmania donovani* inhibits macrophage apoptosis. *The Journal of Immunology*, **152**(19), 2930-37.
- Moradin, N., & Descoteaux, A. (2012). *Leishmania* promastigotes: building a safe niche within macrophages. *Frontiers in Cellular and Infection Microbiology*, **2**(September), 121.
- Mottram, J. C., Brooks, D. R., & Coombs, G. H. (1998). Roles of cysteine proteinases of trypanosomes and *Leishmania* in host-parasite interactions. *Current Opinion in Microbiology*, **1**(4), 455-460.
- Mottram, J. C., Coombs, G. H., & Alexander, J. (2004). Cysteine peptidases as virulence factors of *Leishmania*. *Current Opinion in Microbiology*, **7**(4), 375-381.
- Naderer, T., & McConville, M. J. (2008). The *Leishmania*-macrophage interaction: a metabolic perspective. *Cellular Microbiology*, **10**(2), 301-8.
- Nascimento, E., Fernandes, D. F., Vieira, E. P., ... Piazza, F. M. (2010). A clinical trial to evaluate the safety and immunogenicity of the LEISH-F1 + MPL-SE vaccine when used in combination with meglumine antimoniate for the treatment of cutaneous leishmaniasis. *Vaccine*, **28**(40),

6581-6587.

- Navas, A., Vargas, D. A., Freudzon, M., McMahon-Pratt, D., Saravia, N. G., & Gómez, M. A. (2014). Chronicity of dermal leishmaniasis caused by *Leishmania panamensis* is associated with parasite-mediated induction of chemokine gene expression. *Infection and Immunity*, **82**(7), 2872-2880.
- Nayak, A., Akpunarlieva, S., Barrett, M., & Burchmore, R. J. S. (2018). A defined medium for *Leishmania* culture allows definition of essential amino acids. *Experimental Parasitology*, **185**, 39-52.
- Ngô, H. M., Hoppe, H. C., & Joiner, K. A. (2000). Differential sorting and post-secretory targeting of proteins in parasitic invasion. *Trends in Cell Biology*, **10**, 67-72.
- Ngobeni, R., Abhyankar, M. M., Jiang, N. M., ... Moonah, S. N. (2017). Entamoeba histolytica-Encoded Homolog of Macrophage Migration Inhibitory Factor Contributes to Mucosal Inflammation during Amebic Colitis. *The Journal of Infectious Diseases*, **215**(8), 1294-1302.
- Nickel, W., & Rabouille, C. (2009). Mechanisms of regulated unconventional protein secretion. *Nature Reviews Molecular Cell Biology*, **10**, 148-56.
- Nielsen, H. (2017). Predicting Secretory Proteins with SignalP. *Methods in Molecular Biology (Clifton, N.J.)*, **1611**, 59-73.
- Nugent, P. G., Karsani, S. a, Wait, R., Tempero, J., & Smith, D. F. (2004). Proteomic analysis of *Leishmania mexicana* differentiation. *Molecular and Biochemical Parasitology*, **136**(1), 51-62.
- O'Farrell, P. H. (1975). High Resolution Two-Dimensional Electrophoresis of Proteins. *The Journal of Biological Chemistry*, **250**(10), 4007-4021.
- Olivier, M. (1996). Modulation of host cell intracellular Ca²⁺. *Parasitology Today (Personal Ed.)*, **12**(4), 145-50.
- Olmo, F., Urbanová, K., Rosales, M. J., Martín-Escolano, R., Sánchez-Moreno, M., & Marín, C. (2015). An invitro iron superoxide dismutase inhibitor decreases the parasitemia levels of *Trypanosoma cruzi* in BALB/c mouse model during acute phase. *International Journal for Parasitology: Drugs and Drug Resistance*, **5**(3), 110-116.
- Ong, S.-E., & Mann, M. (2007). A practical recipe for stable isotope labeling by amino acids in cell culture (SILAC). *Nature Protocols*, **1**(6), 2650-2660.

- Overath, P., Stierhof, Y. D., & Wiese, M. (1997). Endocytosis and secretion in trypanosomatid parasites—tumultuous traffic in a pocket. *Trends in Cell Biology*, **7**, 27-33.
- Paape, D., Barrios-Llerena, M. E., Le Bihan, T., Mackay, L., & Aebischer, T. (2010). Gel free analysis of the proteome of intracellular *Leishmania mexicana*. *Molecular and Biochemical Parasitology*, **169**(2), 108-14.
- Paape, D., Lippuner, C., Schmid, M., ... Aebischer, T. (2008). Transgenic, fluorescent *Leishmania mexicana* allow direct analysis of the proteome of intracellular amastigotes. *Molecular & Cellular Proteomics : MCP*, **7**(9), 1688-701.
- Page, B., Page, M., & Noel, C. (1993). A NEW FLUOROMETRIC ASSAY FOR CYTOTOXICITY MEASUREMENTS IN-VITRO. *International Journal of Oncology*, **3**(3), 473-476.
- Peters, C., Kawakami, M., Kaul, M., Ilg, T., Overath, P., & Aebischer, T. (1997a). Secreted proteophosphoglycan of *Leishmania mexicana* amastigotes activates complement by triggering the mannan binding lectin pathway. *European Journal of Immunology*, **27**(10), 2666-2672.
- Peters, C., Stierhof, Y. D., & Ilg, T. (1997b). Proteophosphoglycan secreted by *Leishmania mexicana* amastigotes causes vacuole formation in macrophages. *Infection and Immunity*, **65**(2), 783-786.
- Peysseon, F., Launay, G., Lisacek, F., Duclos, B., & Ricard-Blum, S. (2013). Comparative analysis of *Leishmania* exoproteomes: implication for host-pathogen interactions. *Biochimica et Biophysica Acta*, **1834**(12), 2653-62.
- Pimenta, P., & de Souza, W. (1985). Fine structure and cytochemistry of the endoplasmic reticulum and its association with the plasma membrane of *Leishmania mexicana amazonensis*. *Journal of Submicroscopic Cytology*, **17**(3), 413-9.
- Piñeyro, M. D., Parodi-Talice, A., Portela, M., Arias, D. G., Guerrero, S. A., & Robello, C. (2011). Molecular characterization and interactome analysis of *Trypanosoma cruzi* Tryparedoxin 1. *Journal of Proteomics*, **74**(9), 1683-1692.
- Podinovskaia, M., & Descoteaux, A. (2015). *Leishmania* and the macrophage: a multifaceted interaction. *Future Microbiology*, **10**(1), 111-29.
- Pollock, K. G. J., McNeil, K. S., Mottram, J. C., ... Alexander, J. (2003). The *Leishmania mexicana* Cysteine Protease, CPB2.8, Induces Potent Th2 Responses. *The Journal of Immunology*, **170**, 1746-53.

- Prajapati, V. K., Awasthi, K., Gautam, S., ... Sundar, S. (2011). Targeted killing of *Leishmania donovani* in vivo and in vitro with amphotericin B attached to functionalized carbon nanotubes. *Journal of Antimicrobial Chemotherapy*, **66**, 874-879.
- Pupkis, M. F., & Coombs, G. H. (1984). Purification and characterization of proteolytic enzymes of *Leishmania mexicana mexicana* amastigotes and promastigotes. *Journal of General Microbiology*, **130**(9), 2375-83.
- Raposo, G., & Stoorvogel, W. (2013). Extracellular vesicles: exosomes, microvesicles, and friends. *The Journal of Cell Biology*, **200**(4), 373-83.
- Rätz, B., Iten, M., Grether-Bühler, Y., Kaminsky, R., & Brun, R. (1997). The Alamar Blue® assay to determine drug sensitivity of African trypanosomes (*T.b. rhodesiense* and *T.b. gambiense*) in vitro. *Acta Tropica*, **68**(2), 139-147.
- Richardson, J. M., Morrison, L. S., Bland, N. D., ... Walkinshaw, M. D. (2009). Structures of *Leishmania major* orthologues of macrophage migration inhibitory factor. *Biochemical and Biophysical Research Communications*, **380**, 442-448.
- Riveau, G., Schacht, A.-M., Dompnier, J.-P., ... Capron, A. (2018). Safety and efficacy of the rSh28GST urinary schistosomiasis vaccine: A phase 3 randomized, controlled trial in Senegalese children. *PLOS Neglected Tropical Diseases*, **12**(12), e0006968.
- Rogers, M. E., Chance, M. L., & Bates, P. A. (2002). The role of promastigote secretory gel in the origin and transmission of the infective stage of *Leishmania mexicana* by the sandfly *Lutzomyia longipalpis*. *Parasitology*, **124**(5), 495-507.
- Rogers, M. E., Kropf, P., Choi, B.-S., ... Müller, I. (2009). Proteophosphoglycans Regurgitated by *Leishmania*-Infected Sand Flies Target the L-Arginine Metabolism of Host Macrophages to Promote Parasite Survival. *PLoS Pathogens*, **5**(8), e1000555.
- Ross, P. L., Huang, Y. N., Marchese, J. N., ... Pappin, D. J. (2004). Multiplexed Protein Quantitation in *Saccharomyces cerevisiae* Using Amine-reactive Isobaric Tagging Reagents. *Molecular & Cellular Proteomics*, **3**, 1154-1169.
- Ruhland, A., Leal, N., & Kima, P. E. (2007). *Leishmania* promastigotes activate PI3K/Akt signalling to confer host cell resistance to apoptosis. *Cellular Microbiology*, **9**(1), 84-96.
- Russell, D. G., Xu, S., & Chakraborty, P. (1992). Intracellular trafficking and the parasitophorous vacuole of *Leishmania mexicana*-infected macrophages. *Journal of Cell Science*, **103**, 1193-1210.

- Saetun, P., Semangoen, T., & Thongboonkerd, V. (2009). Characterizations of urinary sediments precipitated after freezing and their effects on urinary protein and chemical analyses. *American Journal of Physiology. Renal Physiology*, **296**(6), F1346-54.
- SAFC Biosciences. (2006). *Yeastolate UF Solution 50X*. Retrieved from https://www.sigmaaldrich.com/content/dam/sigmaaldrich/docs/Sigma/Product_Information_Sheet/p58902.pdf
- Sansom, F. M., Tang, L., Ralton, J. E., Saunders, E. C., Naderer, T., & McConville, M. J. (2013). Leishmania major methionine sulfoxide reductase A is required for resistance to oxidative stress and efficient replication in macrophages. *PLoS One*, **8**(2), e56064.
- Santarém, N., Cunha, J., Silvestre, R., ... Cordeiro-da-Silva, A. (2013a). The impact of distinct culture media in Leishmania infantum biology and infectivity. *Parasitology*, **141**(2), 192-205.
- Santarém, N., Racine, G., Silvestre, R., Cordeiro-da-Silva, A., & Ouellette, M. (2013b). Exoproteome dynamics in Leishmania infantum. *Journal of Proteomics*, **84**, 106-18.
- Santini-Oliveira, M., Coler, R. N., Parra, J., ... Tendler, M. (2016). Schistosomiasis vaccine candidate Sm14/GLA-SE: Phase 1 safety and immunogenicity clinical trial in healthy, male adults. *Vaccine*, **34**(4), 586-594.
- Saunders, E. C., Ng, W. W., Kloehn, J., Chambers, J. M., Ng, M., & McConville, M. J. (2014). Induction of a Stringent Metabolic Response in Intracellular Stages of Leishmania mexicana Leads to Increased Dependence on Mitochondrial Metabolism. *PLoS Pathogens*, **10**(1). doi:10.1371/journal.ppat.1003888
- Savitski, M. M., Sweetman, G., Askenazi, M., ... Bantscheff, M. (2011). Delayed Fragmentation and Optimized Isolation Width Settings for Improvement of Protein Identification and Accuracy of Isobaric Mass Tag Quantification on Orbitrap-Type Mass Spectrometers. *Anal. Chem*, **83**, 8959-8967.
- Schaible, U., Schlesinger, P., Steinberg, T. H., Mangel, W. F., Kobayashi, T., & Russell, D. G. (1999). Parasitophorous vacuoles of Leishmania mexicana acquire macromolecules from the host cell cytosol via two independent routes. *Journal of Cell Science*, **112**, 681-693.
- Schmidt, O., & Teis, D. (2012). The ESCRT machinery. *Current Biology*, **22**(4), R116-R120.
- Scianimanico, S., Desrosiers, M., Dermine, J.-F., Meresse, S., Descoteaux, A., & Desjardins, M. (1999). Impaired recruitment of the small GTPase rab7 correlates with the inhibition of phagosome maturation by Leishmania donovani promastigotes. *Cellular Microbiology*, **1**(1),

19-32.

- Secundino, N., Eger-Mangrich, I., Braga, E., Santoro, M. M., & Pimenta, P. (2005). *Lutzomyia longipalpis* peritrophic matrix: formation, structure, and chemical composition. *Journal of Medical Entomology*, **42**(6), 928-938.
- Shakarian, A. M., McGugan, G. C., Joshi, M. B., ... Dwyer, D. M. (2010). Identification, characterization, and expression of a unique secretory lipase from the human pathogen *Leishmania donovani*. *Molecular and Cellular Biochemistry*, **341**(1-2), 17-31.
- Shao, D., Han, Z., Lin, Y., ... Wang, H. (2008). Detection of *Plasmodium falciparum* derived macrophage migration inhibitory factor homologue in the sera of malaria patients. *Acta Tropica*, **106**, 9-15.
- Sharma, R., Hoti, S. L., Meena, R. L., Vasuki, V., Sankari, T., & Kaliraj, P. (2012). Molecular and functional characterization of macrophage migration inhibitory factor (MIF) homolog of human from lymphatic filarial parasite *Wuchereria bancrofti*. *Parasitology Research*, **111**, 2035-2047.
- Sibley, D. L., Charron, A., Håkansson, S., & Mordue, D. (2013). Invasion and Intracellular Survival by *Toxoplasma*. In *Madame Curie Bioscience Database [Internet]*, Austin (TX): Landes Bioscience. Retrieved from <https://www.ncbi.nlm.nih.gov/books/NBK6450/?report=reader>
- Siddiqui, A. A., & Siddiqui, S. Z. (2017). Sm-p80-Based Schistosomiasis Vaccine: Preparation for Human Clinical Trials. *Trends in Parasitology*, **33**(3), 194-201.
- Siegrist, C.-A. (2013). Vaccine Immunology. In S. A. Plotkin, W. A. Orenstein, & P. A. Offit, eds., *Vaccines*, 6th Editio, W. B. Saunders, pp. 14-32.
- Silverman, J. M., Chan, S. K., Robinson, D. P., ... Reiner, N. E. (2008). Proteomic analysis of the secretome of *Leishmania donovani*. *Genome Biology*, **9**(2), R35.
- Silverman, J. M., Clos, J., De'Oliveira, C. C., ... Reiner, N. E. (2010a). An exosome-based secretion pathway is responsible for protein export from *Leishmania* and communication with macrophages. *Journal of Cell Science*, **123**(Pt 6), 842-52.
- Silverman, J. M., Clos, J., Horakova, E., ... Reiner, N. E. (2010b). *Leishmania* Exosomes Modulate Innate and Adaptive Immune Responses through Effects on Monocytes and Dendritic Cells. *Journal of Immunology*, **185**, 5011-5022.
- Silverman, J. M., & Reiner, N. E. (2012). *Leishmania* exosomes deliver preemptive strikes to create an environment permissive for early infection. *Frontiers in Cellular and Infection*

Microbiology, 1, 1-8.

Simpson, R. J., Jensen, S. S., & Lim, J. W. E. (2008). Proteomic profiling of exosomes: Current perspectives. *Proteomics*, 8, 4083-4099.

Singh, R., Kaushik, S., Wang, Y., ... Czaja, M. J. (2009). Autophagy regulates lipid metabolism. *Nature*, 458(7242), 1131-5.

Sinha, S., Kumar, A., & Sundaram, S. (2013). A comprehensive analysis of LACK (Leishmania homologue of receptors for activated C kinase) in the context of Visceral Leishmaniasis. *Bioinformatics*, 9(16), 832-7.

Smyth, G. K. (2004). Linear Models and Empirical Bayes Methods for Assessing Differential Expression in Microarray Experiments. *Statistical Applications in Genetics and Molecular Biology*, 3(1), Article 3.

Soblik, H., Elshazly Younis, A., Mitreva, M., ... Brattig, N. W. (2011). Life Cycle Stage-resolved Proteomic Analysis of the Excretome/Secretome from *Strongyloides ratti*-Identification of Stage-specific Proteases. *Molecular & Cellular Proteomics*, 10, 1-16.

Sommerville, C., Richardson, J. M., Williams, R. A. M., ... Henriquez, F. L. (2013). Biochemical and Immunological Characterization of *Toxoplasma gondii* Macrophage Migration Inhibitory Factor. *The Journal of Biological Chemistry*, 288(18), 12733-12741.

Soni, R., Sharma, D., & Bhatt, T. K. (2016). Plasmodium falciparum Secretome in Erythrocyte and Beyond. *Frontiers in Microbiology*, 7, 194.

Sotillo, J., Pearson, M., Potriquet, J., ... Loukas, A. (2016). Extracellular vesicles secreted by *Schistosoma mansoni* contain protein vaccine candidates. *International Journal for Parasitology*, 46(1), 1-5.

Sotillo, J., Sanchez-Flores, A., Cantacessi, C., ... Loukas, A. (2014). Secreted proteomes of different developmental stages of the gastrointestinal nematode *Nippostrongylus brasiliensis*. *Molecular & Cellular Proteomics : MCP*, 13(10), 2736-51.

Stegmayer, C., Kehlenbach, A., Tournaviti, S., ... Nickel, W. (2005). Direct transport across the plasma membrane of mammalian cells of *Leishmania* HASPB as revealed by a CHO export mutant. *Journal of Cell Science*, 118(Pt 3), 517-27.

Stein, A. (2007). Decreasing variability in your cell culture. *BioTechniques*, 43(2), 228-229.

- Stierhof, Y. D., Ilg, T., Russell, D. G., Hohenberg, H., & Overath, P. (1994). Characterization of Polymer Release from the Flagellar Pocket of *Leishmania mexicana* Promastigotes. *The Journal of Cell Biology*, **125**(2), 321-331.
- Sun, T., Holowka, T., Song, Y., ... Bucala, R. (2012). A Plasmodium-encoded cytokine suppresses T-cell immunity during malaria. *Proceedings of the National Academy of Sciences*, **109**(31), E2117-E2126.
- Sunter, J. D., & Gull, K. (2017). Shape, form, function and *Leishmania* pathogenicity: from textbook descriptions to biological understanding. *Open Biology*, **7**, 170165.
- Szempruch, A. J., Dennison, L., Kieft, R., Harrington, J. M., & Hajduk, S. L. (2016a). Sending a message: extracellular vesicles of pathogenic protozoan parasites. *Nature Reviews Microbiology*, **14**(11), 669-675.
- Szempruch, A. J., Sykes, S. E., Almeida, I. C., Hajduk, S. L., & Harrington Correspondence, J. M. (2016b). Extracellular Vesicles from *Trypanosoma brucei* Mediate Virulence Factor Transfer and Cause Host Anemia. *Cell*, **164**, 246-257.
- Teixeira, M. J., Fernandes, J. D., Teixeira, C. R., ... Barral, A. (2005). Distinct *Leishmania braziliensis* isolates induce different paces of chemokine expression patterns. *Infection and Immunity*, **73**(2), 1191-1195.
- Thermo Fisher Scientific. (n.d.). 11720 - Schneider's *Drosophila* Medium - UK. Retrieved December 7, 2018, from <https://www.thermofisher.com/uk/en/home/technical-resources/media-formulation.124.html>
- Thompson, A., Scha, rgen, Kuhn, K., ... Hamon, C. (2003). Tandem Mass Tags: A Novel Quantification Strategy for Comparative Analysis of Complex Protein Mixtures by MS/MS. doi:10.1021/ac0262560
- Tjalsma, H., Bolhuis, A., Jongbloed, J. D. H., Bron, S., & Maarten van Dijl, J. (2000). Signal peptide-dependent protein transport in *Bacillus subtilis*: a genome-based survey of the secretome. *Microbiology and Molecular Biology Reviews*, **64**(3), 515-547.
- Tull, D., Naderer, T., Spurck, T., ... McConville, M. J. (2010). Membrane protein SMP-1 is required for normal flagellum function in *Leishmania*. *Journal of Cell Science*, **123**(Pt 4), 544-54.
- Twu, O., Dessí, D., Vu, A., ... Johnson, P. J. (2014). *Trichomonas vaginalis* homolog of macrophage migration inhibitory factor induces prostate cell growth, invasiveness, and inflammatory responses. *Proc. Natl. Acad. Sci. USA*, **111**(22), 8179-8184.

- Ueno, N., & Wilson, M. E. (2012). Receptor-mediated phagocytosis of Leishmania: implications for intracellular survival. *Trends in Parasitology*, **28**(8), 335-344.
- Ünlü', M., Morgan', M. E., & Minden', J. S. (1997). Difference gel electrophoresis: A single gel method for detecting changes in protein extracts. *Electrophoresis*, **18**(11), 2071-2077.
- Utzinger, J., Becker, S. L., Knopp, S., ... Hatz, C. F. (2012). Neglected tropical diseases: diagnosis, clinical management, treatment and control. *Swiss Medical Weekly*, **142**(November), w13727.
- Van Assche, T., Deschacht, M., da Luz, R. A. I., Maes, L., & Cos, P. (2011). Leishmania-macrophage interactions: Insights into the redox biology. *Free Radical Biology and Medicine*, **51**(2), 337-351.
- van der Valk, J., Bieback, K., Buta, C., ... Gstraunthaler, G. (2018). Fetal Bovine Serum (FBS): Past - Present - Future. *ALTEX*, **35**(1), 99-118.
- van der Valk, J., Brunner, D., De Smet, K., ... Gstraunthaler, G. (2010). Optimization of chemically defined cell culture media - Replacing fetal bovine serum in mammalian in vitro methods. *Toxicology in Vitro*, **24**(4), 1053-1063.
- Vinet, A. F., Fukuda, M., Turco, S. J., & Descoteaux, A. (2009). The Leishmania donovani lipophosphoglycan excludes the vesicular proton-ATPase from phagosomes by impairing the recruitment of synaptotagmin V. *PLoS Pathogens*, **5**(10), e1000628.
- Vishnu, U. S., Sankarasubramanian, J., Gunasekaran, P., & Rajendhran, J. (2017). Identification of potential antigens from non-classically secreted proteins and designing novel multipeptide vaccine candidate against Brucella melitensis through reverse vaccinology and immunoinformatics approach. *Infection, Genetics and Evolution*, **55**(July), 151-158.
- Vogstad, A. R., Moxley, R. A., Erickson, G. E., Klopfenstein, T. J., & Smith, D. R. (2013). Assessment of Heterogeneity of Efficacy of a Three-Dose Regimen of a Type III Secreted Protein Vaccine for Reducing STEC O157 in Feces of Feedlot Cattle. *Foodborne Pathogens and Disease*, **10**(8), 678-683.
- W.H.O. (2010). *Control of the leishmaniasis*. WHO Technical Report Series, Vol. 949, Geneva. Retrieved from <http://www.pubmedcentral.nih.gov/articlerender.fcgi?artid=3307017&tool=pmcentrez&rendertype=abstract>
- W.H.O. (2017). *Global leishmaniasis update, 2006-2015: a turning point in leishmaniasis surveillance*. Weekly Epidemiological Record, Vol. 92, Geneva.

- W.H.O. (2018). Global leishmaniasis surveillance update, 1998-2016. *Weekly Epidemiology Record*, **40**(93), 521-540.
- Wagner, D., Maser, J., Lai, B., ... Bermudez, L. E. (2005). Elemental Analysis of Mycobacterium avium-, Mycobacterium tuberculosis-, and Mycobacterium smegmatis-Containing Phagosomes Indicates Pathogen-Induced Microenvironments within the Host Cell's Endosomal System. *The Journal of Immunology*, **174**(3), 1491-1500.
- Wang, Y., Lu, M., Wang, S., ... Li, X. (2017). Characterization of a secreted macrophage migration inhibitory factor homologue of the parasitic nematode Haemonchus Contortus acting at the parasite-host cell interface. *Oncotarget*, **8**(25), 40052-40064.
- Watanabe Costa, R., da Silveira, J. F., & Bahia, D. (2016). Interactions between Trypanosoma cruzi secreted proteins and host cell signaling pathways. *Frontiers in Microbiology*, **7**(MAR), 1-9.
- Weidberg, H., Shvets, E., & Elazar, Z. (2011). Biogenesis and cargo selectivity of autophagosomes. *Annual Review of Biochemistry*, **80**, 125-56.
- Wenzel, U. A., Bank, E., Florian, C., ... van Zandbergen, G. (2012). Leishmania major parasite stage-dependent host cell invasion and immune evasion. *FASEB Journal*, **26**(1), 29-39.
- Westermeier, R., Naven, T., & Hopker, H.-R. (2008). *Proteomics in Practice - A guide to successful experimental design*, 2nd edn, Weinheim: Wiley-VCH.
- Wheeler, R. J., Gluenz, E., & Gull, K. (2011). The cell cycle of Leishmania: morphogenetic events and their implications for parasite biology. *Molecular Microbiology*, **79**(3), 647-62.
- Winberg, M. E., Holm, A., Särndahl, E., ... Lerm, M. (2009). Leishmania donovani lipophosphoglycan inhibits phagosomal maturation via action on membrane rafts. *Microbes and Infection / Institut Pasteur*, **11**(2), 215-22.
- Woessner, J. F. (1999). Matrix Metalloproteinase Inhibition: From The Jurassic To The Third Millennium. *Annals of the New York Academy of Sciences*, **878**, 388-403.
- Wolters, D. A., Washburn, M. P., & Yates III, J. R. (2001). An Automated Multidimensional Protein Identification Technology for Shotgun Proteomics. *Analytical Chemistry*, **73**(23), 5683-5690.
- Wong, J. W. H., & Cagney, G. (2010). An Overview of Label-Free Quantitation Methods in Proteomics by Mass Spectrometry. In S. J. Hubbard & A. R. Jones, eds., *Proteome Bioinformatics*, Totowa, NJ: Humana Press, pp. 273-283.

- Wu, Z., Boonmars, T., Nagano, I., Nakada, T., & Takahashi, Y. (2003). MOLECULAR EXPRESSION AND CHARACTERIZATION OF A HOMOLOGUE OF HOST CYTOKINE MACROPHAGE MIGRATION INHIBITORY FACTOR FROM TRICHINELLA SPP. *Journal of Parasitology*, **89**(3), 507-515.
- Xue, H., Lu, B., & Lai, M. (2008). The cancer secretome: a reservoir of biomarkers. *Journal of Translational Medicine*, **6**, 52.
- Yang, Y., Franc, V., & Heck, A. J. R. (2017). Glycoproteomics: A Balance between High-Throughput and In-Depth Analysis. *Trends in Biotechnology*, **35**(7), 598-609.
- Younis, A. E., Soblik, H., Ajonina-Ekoti, I., ... Brattig, N. W. (2012). Characterization of a secreted macrophage migration inhibitory factor homologue of the parasitic nematode *Strongyloides* acting at the parasite-host cell interface. *Microbes and Infection*, **14**, 279-289.
- Zang, X., Taylor, P., Wang, J. M., ... Maizels, R. M. (2002). Homologues of Human Macrophage Migration Inhibitory Factor from a Parasitic Nematode. *The Journal of Biological Chemistry*, **277**(46), 44261-44267.
- Zehe, C., Engling, A., Wegehingel, S., Schafer, T., & Nickel, W. (2006). Cell-surface heparan sulfate proteoglycans are essential components of the unconventional export machinery of FGF-2. *Proc. Natl. Acad. Sci. USA*, **103**(42), 15479-84.
- Zhang, M., Chen, L., Wang, S., & Wang, T. (2009). Rab7: roles in membrane trafficking and disease. *Bioscience Reports*, **29**(3), 193-209.
- Zhang, Y., Miura, K., Li, J., ... Long, C. (2012). Macrophage migration inhibitory factor homolog from *Plasmodium yoelii* modulates monocyte recruitment and activation in spleen during infection. *Parasitology Research*, **110**, 1755-1763.
- Zilberstein, D., & Shapira, M. (1994). The role of pH and temperature in the development of *Leishmania* parasites. *Annual Reviews Microbiology*, **48**, 449-70.